



THE HONG KONG
POLYTECHNIC UNIVERSITY

香港理工大學

Pao Yue-kong Library

包玉剛圖書館

Copyright Undertaking

This thesis is protected by copyright, with all rights reserved.

By reading and using the thesis, the reader understands and agrees to the following terms:

1. The reader will abide by the rules and legal ordinances governing copyright regarding the use of the thesis.
2. The reader will use the thesis for the purpose of research or private study only and not for distribution or further reproduction or any other purpose.
3. The reader agrees to indemnify and hold the University harmless from and against any loss, damage, cost, liability or expenses arising from copyright infringement or unauthorized usage.

IMPORTANT

If you have reasons to believe that any materials in this thesis are deemed not suitable to be distributed in this form, or a copyright owner having difficulty with the material being included in our database, please contact lbsys@polyu.edu.hk providing details. The Library will look into your claim and consider taking remedial action upon receipt of the written requests.

**A STUDY OF TRACE METAL CONTAMINATION IN
DIFFERENT URBAN TERRESTRIAL COMPARTMENTS IN
HONG KONG AND GUANGZHOU**

LIANG SIYUAN

PhD

The Hong Kong Polytechnic University

2019

The Hong Kong Polytechnic University

Department of Civil and Environmental Engineering

**A Study of Trace Metal Contamination in Different Urban
Terrestrial Compartments in Hong Kong and Guangzhou**

Liang Siyuan

**A thesis submitted in partial fulfilment of the requirements for the
degree of Doctor of Philosophy**

November/2018

CERTIFICATE OF ORIGINALITY

I hereby declare that this thesis is my own work and that, to the best of my knowledge and belief, it reproduces no material previously published or written, nor material that has been accepted for the award of any other degree or diploma, except where due acknowledgement has been made in the text.

_____ (Signed)

Siyuan LIANG (Name of student)

Abstract

Trace metal contamination in urban terrestrial environments is a major environmental problem throughout the world, due to its harmful implications on human health. This research aims to conduct a multi-compartmental environmental investigation on trace metal distribution in urban environments of Hong Kong and Guangzhou, focusing on: (1) soil geochemical signature of urbanization and industrialization in the two cities; (2) quantitative source contributions of trace metals in soils, road dust, and foliar dust, and comparison of their suitability for monitoring urban contamination conditions in a typical megacity; and (3) chemical partitioning of trace metals in various particle size fractions of soil dust, associations of trace metals between soil dust and other types of dust, and potential health risks.

Firstly, the vertical and horizontal distribution patterns of trace metals in urban soils were compared between Hong Kong and Guangzhou. Slightly lower trace metal concentrations and higher Pb isotopic compositions ($^{206}\text{Pb}/^{207}\text{Pb}$) of surface soils (0 to 3 cm) compared to top soils (0 to 15 cm) were found in Hong Kong, possibly due to the temporally decrease of anthropogenic deposition and a downward migration of trace metals in urban soils. Higher trace metal concentrations and lower Pb isotopic compositions ($^{206}\text{Pb}/^{207}\text{Pb}$) in surface soils than top soils were observed in Guangzhou, consistent with the temporally increase of trace metal inputs in soils. The remarkable hotspots of trace metals in urban soils were mainly attributed to industrial and traffic sources in these two cities.

Secondly, a multi-compartmental investigation of trace metal contamination was conducted in the urban environment of Guangzhou. Lead isotopic data and modeling (Absolute Principal Component Scores-Multiple Linear Regression, APCS-MLR) results identified industrial and traffic emissions as the major sources of trace metals in urban soils, road dust, and foliar dust. Spatial distribution patterns implied that Cu in road dust was a good indicator for traffic contamination, particularly influenced by traffic volume and vehicle speed. Lead and Zn in

foliar dust indicated the industrial contamination, which decreased from the emission source (*e.g.*, power plant and steel factory) to the surrounding environment.

Finally, the chemical partitioning of trace metals in soil dust was studied. Trace metal concentrations were inversely associated with particle sizes in soil dust of Guangzhou and Hong Kong. Source apportionment and chemical composition of trace metals illustrated the important influence of anthropogenic particles, as well as Mn/Fe oxides and organic complexes, on the metal accumulation in fine particles of soil dust. Results of Pb isotopes and the comparison of temporal trace metal variations indicated the similar metal sources and potential metal exchange between fine soil dust particles and other types of dust (*e.g.*, fine road dust and respirable suspended particles (PM₁₀)). Health risks posed by trace metals elevated with decreasing soil particle sizes. 53% and 100% of the soil dust <10 µm in Hong Kong showed a probability of noncarcinogenic hazard and a nonnegligible carcinogenic risk, respectively. Thus, the re-suspension of soil dust should be paid more attention to control health risks caused by trace metal contamination in urban environments.

Acknowledgement

First and most importantly, I would like to express my deepest gratitude to my supervisor, Professor Xiangdong LI, for leading, teaching and helping me to achieve one of the most important milestones in my life. His tremendous insights, his immense dedication to research, his attention to detail, and his high standards for research quality have marked not only my research work but also my personality and I take a lot of it with me.

During my PhD study at the Hong Kong Polytechnic University, I have met a number of people that have helped me in different ways throughout my research work. I would like express a very special gratitude to Dr. Jinli CUI, Dr. Xiangyang BI, and Dr. Xiaosan LUO, for their valuable help in my research. I would like to thank Dr. Lili MING, Dr. Yanping ZHAO, Dr. Nan XIANG, Ms. Jiawen XIE, Dr. Baowei CHEN, Dr. Ling JIN, Dr. Long CANG, Dr. Runsheng YIN, Dr. Haijian BING, Dr. Linchuan FANG, Dr. Jianteng SUN, and Dr. Mei MENG, for their kind help and support during my study life. In addition, I would like to thank Mr. W.S. LAM, Ms. Carman IP, and Ms. Chloe TANG for their help on laboratory work.

Last but not least, I am grateful to my parents, my husband, and my baby boy, for their selfless love and great support.

Table of Contents

The Hong Kong Polytechnic University	I
CERTIFICATE OF ORIGINALITY	I
Abstract	II
Acknowledgement.....	IV
Table of Contents	V
List of Figures	IX
List of Tables	XVI
Chapter 1 Introduction	1
1.1 Background	2
1.2 Objectives.....	5
1.3 Scope of work.....	6
1.4 Organization of thesis.....	6
Chapter 2 Literature Review	8
2.1 Urban environment.....	8
2.2 Trace metals	8
2.3 Trace metals in urban soils.....	9
2.3.1 Urban soils.....	9
2.3.2 Trace metals in urban soils.....	10
2.3.3 Behavior of trace metals in soils	10
2.3.4 Trace metal sources in urban soils.....	13
2.3.4.1 Lithogenic sources.....	16
2.3.4.2 Anthropogenic sources	16
2.3.4.3 Source identification.....	18
2.4 Trace metals in road dust.....	19
2.5 Trace metals in plant and foliar dust	21
2.6 Potential health risks of trace metals in urban environments	22
2.7 Research emphasis on trace metal contamination in urban environments	25

2.7.1	Trace metal contamination in urban soils at a city scale	25
2.7.2	Trace metal contamination in multiple environmental compartments	26
2.7.3	Trace metal distribution in urban soils as a function of particle size	28
2.8	Summary and outlook	30
Chapter 3	Methodology	32
3.1	Study region and sample collection.....	32
3.1.1	Hong Kong	32
3.1.2	Guangzhou	33
3.2	Sample collection	34
3.2.1	Urban soil collection	34
3.2.2	Soil dust collection.....	35
3.2.3	Multi-compartments collection	38
3.3	Sample preparation.....	40
3.4	Analytical methods.....	40
3.4.1	Total digestion.....	40
3.4.2	Sequential extraction	41
3.4.3	Bioaccessibility	42
3.4.4	Lead isotopic composition analysis.....	42
3.4.5	Total carbon and total organic carbon in solids.....	42
3.4.6	X-ray powder diffraction.....	43
3.4.7	Scanning electron microscopy-energy dispersive X-ray spectroscopy	43
3.5	Statistical analysis	44
3.5.1	Calculation of trace metal concentrations in foliar dust.....	44
3.5.2	Enrichment factor.....	45
3.5.3	Multivariate statistical analysis	45
3.5.4	Geostatistical analysis	47
Chapter 4	Soil Geochemical Signature of Urbanization and Industrialization: A Regional Comparison between Hong Kong and Guangzhou	48
4.1	General soil properties	48
4.2	Trace metal concentrations in urban soils	50

4.3	Lead isotopic compositions	56
4.4	Vertical distribution of trace metals	62
4.5	Horizontal distribution of trace metals	65
4.5.1	Trace metal distribution in urban soils of Hong Kong	66
4.5.2	Trace metal distribution in urban soils of Guangzhou	67
4.5.3	Comparison between Hong Kong and Guangzhou	68
4.6	Summary	73
Chapter 5 Characterization, Source Apportionment, and Geochemical Interactions of Trace Metals in Soils, Road Dust, Plants, and Foliar Dust of an Urban Environment: Indicators for Urban Contamination		
5.1	Trace metal concentrations in different urban compartments	76
5.1.1	Urban soil	76
5.1.2	Road dust.....	77
5.1.3	Plants and foliar dust	79
5.2	Spatial distribution of trace metals in surface soil, road dust, foliar dust, and tree leaves.....	86
5.3	Source identification by Pb isotopic compositions.....	93
5.4	Source apportionment using APCS-MLR and its spatial variations	99
5.5	Geochemical cycling of trace metals in soil, road dust, and foliar dust in urban environment	111
5.6	Summary	113
Chapter 6 Chemical Partitioning of Trace Metals in Various Particle Size Fractions of Urban Soil Dust and Road Dust, and its Implication to Health Risk Assessment		
6.1	General properties of bulk soil, soil dust and road dust	116
6.2	Metal concentrations in soil dust, bulk soil, and road dust.....	123
6.2.1	Trace metal concentrations in bulk soil dust and soil.....	123
6.2.2	Trace metal concentrations in different particle size fractions of soil dust ...	124
6.2.3	Trace metal concentrations in different particle size fractions of road dust..	125
6.3	Lead isotopic compositions in soil dust and road dust.....	131
6.4	Trace metal speciation in soil dust	139
6.4.1	Sequential extraction of trace metals in soil dust	139

6.4.2	Lead isotopic compositions of extracted Pb in soil dust	140
6.5	Association of trace metals between soil dust and atmospheric particulate matters	142
6.5.1	Trace metal accumulation in the finest soil dust particles (<10 µm) and comparison with PM ₁₀	143
6.5.2	Re-suspension of fine particles of soil dust.....	144
6.6	Trace metal bioaccessibility and human health risks	147
6.6.1	Trace metal bioaccessibility	147
6.6.2	Human health risk assessment.....	149
6.6.2.1	Human health risk assessment of trace metals in soil dust incorporating bioaccessibility	149
6.6.2.2	Human health risk assessment of trace metals in soil dust <10µm in Hong Kong.....	152
6.7	Summary	157
Chapter 7	Conclusions and Recommendation	159
7.1	Summary of major scientific findings	159
7.2	Limitations and future research.....	161
References	163
Publications from the Research Project.....		187
Database of Original Results from All Experiments in the Study.....		188

List of Figures

Figure 1.1 Flowchart of the thesis	7
Figure 3.1 Geographical locations of Hong Kong and Guangzhou.	32
Figure 3.2 Sampling locations of urban soils in Hong Kong.	35
Figure 3.3 Sampling locations of urban soils in Guangzhou. Samples collected from Guangzhou city center area were used for comparison with Hong Kong.	35
Figure 3.4 Soil and road dust sampling device.	36
Figure 3.5 Sampling locations of soil dust (n=30, including 14 non-roadside sites and 16 roadside sites) and road dust (n=16, corresponding to the roadside sites of soil dust) in Hong Kong. Detail information is listed in the Appendix.	37
Figure 3.6 Sampling locations of soil dust (n=7) and road dust (n=7) in Guangzhou. Detail information is listed in the Appendix.	38
Figure 3.7 Sampling locations of road dust (n=178) and tree leaf (n=160) in Guangzhou. Detail information is listed in the Appendix.	39
Figure 4.1 The XRD pattern of selected soil samples of two cities. (a:Hong Kong; b: Guangzhou).....	49
Figure 4.2 Temporal variation of trace metal concentrations in urban soils of Hong Kong (a) and Guangzhou (b).....	56
Figure 4.3 Lead isotopic compositions ($^{206}\text{Pb}/^{207}\text{Pb}$ vs $^{208}\text{Pb}/^{207}\text{Pb}$) of urban soils in Hong Kong (a) and Guangzhou (b) and other environmental samples. Detail information is listed in Table 4.7 and Table 4.8.....	61
Figure 4.4 Surface accumulation factor (SAF,%) of urban soils in Hong Kong and Guangzhou.	65
Figure 4.5 Comparison of Pb isotopic compositions ($^{206}\text{Pb}/^{207}\text{Pb}$) of surface and top soils in Hong Kong and Guangzhou. The error bars denote 1 SD.....	65

Figure 4.6 Trace metal distribution in surface soils of Hong Kong. The hot spots were circled with red in (e).	72
Figure 4.7 Trace metal distribution in top soils of Hong Kong.	72
Figure 4.8 Trace metal distribution in surface soils of Guangzhou.	73
Figure 4.9 Trace metal distribution in top soils of Guangzhou.....	73
Figure 5.1 Distribution of trace metal concentrations (mg kg^{-1}) of environmental compartments in different urban land use areas with the sample numbers listed below the x-axis. The box represents the data between the 25 th and 75 th percentiles. The horizontal line inside the box indicates the median data. The small square indicates the mean data. The whiskers (error bars) above and below the box indicate the 95 th and 5 th percentiles. The asterisks indicate the 1 st and 99 th percentile.....	83
Figure 5.2 Impact of traffic volume on trace metal distribution in road dust with the sample numbers listed below the x-axis. Traffic flow of 104 roadside sampling sites (excluded industrial sites) were identified based on the traffic volume plotted by Guangzhou Transport Planning Research Institute (2012). The bars were defined (from the bottom) as the 1 st percentile, 5 th , percentile, 25 th percentile, median, mean (the square), 75 th percentile, 95 th percentile and 99 th percentile.	84
Figure 5.3 Impact of traffic speed on trace metal distribution in road dust with the sample numbers listed below the x-axis. Traffic flow of 104 roadside sampling sites (excluded industrial sites) were identified based on the vehicle speed plotted by Guangzhou Transport Planning Research Institute (2012). 22 samples collected near intersections were used for comparison. The bars were defined (from the bottom) as the 1 st percentile, 5 th , percentile, 25 th percentile, median, mean (the square), 75 th percentile, 95 th percentile and 99 th percentile.	85
Figure 5.4 Impact of the steel factory (a-b) and power plant (c-d) on the Pb and Zn concentrations in the foliar dust. The x-axis indicates increasing distance from the industrial source. Pearson's r and p values were listed in the figure.	86
Figure 5.5 Distribution of trace metals (mg kg^{-1}) in surface soil.	88
Figure 5.6 Distribution of trace metals (mg kg^{-1}) in road dust.....	89

Figure 5.7 Distribution of trace metals (mg kg ⁻¹) in washed tree leaves.....	90
Figure 5.8 Distribution of trace metals (mg kg ⁻¹) in foliar dust.	91
Figure 5.9 Distribution of major traffic network with traffic volume in Guangzhou urban area in 2012 (Guangzhou Transport Planning Research Institute, 2012). Traffic volume indicated from yellow to red lines approximated to <1000, 1000–2250, 2250–3500, 3500–4750, and >4750 PCU h ⁻¹ . The sampling area of the present study was within the black rectangle.....	92
Figure 5.10 Distribution of major traffic network with traffic speed in Guangzhou urban area in 2012 (Guangzhou Transport Planning Research Institute, 2012). Traffic speed indicated by red, purple, blue, dark green, and light green lines approximated to ≤15, 15–30, 30–45, 45–60, and ≥60 km h ⁻¹ . The sampling area of the present study was within the black rectangle. Roads with lowest traffic speed (≤15 km h ⁻¹) were concentrated in the area circled with red.	92
Figure 5.11 Lead isotopic compositions (²⁰⁶ Pb/ ²⁰⁷ Pb vs. ²⁰⁸ Pb/ ²⁰⁷ Pb) of different urban compartments. Data of Pb sources were all included in (a) for comparison. All data in the dashed rectangle of (a) are enlarged to (b). Detail information is listed in Table 5.5 and Table 4.8.....	98
Figure 5.12 ²⁰⁸ Pb/ ²⁰⁷ Pb and ²⁰⁶ Pb/ ²⁰⁷ Pb ratios vs. Pb concentration in surface soil and road dust. The curve lines are the Polynomial fitting results (<i>Radj. 2</i> of ²⁰⁶ Pb/ ²⁰⁷ Pb and ²⁰⁸ Pb/ ²⁰⁷ Pb in surface soil equal to 0.63 and 0.66, respectively; <i>Radj. 2</i> of ²⁰⁶ Pb/ ²⁰⁷ Pb and ²⁰⁸ Pb/ ²⁰⁷ Pb in road dust equal to 0.58, and 0.87, respectively).	99
Figure 5.13 The spatial distribution maps of robust factor scores interpolated by ordinary kriging. (a) factor 1 of surface soils primarily representing Cr, Ni, and Mn; (b) factor 2 of surface soils primarily representing Cu, Pb and Zn; (c) factor 3 of surface soils primarily representing Co, Al, and Fe; (d) factor 1 of road dust primarily representing Co, Cr, Pb, Zn, Fe, and Mn; (e) factor 2 of road dust primarily representing Cu and Ni; and (f) factor 3 of road dust primarily representing Al; (g) factor 1 of foliar dust primarily representing Al, Fe, and Pb; (h) factor 2 of foliar dust primarily representing Cu, Zn and Cr; and (i) factor 3 of foliar dust primarily representing Co and Ni. The area with highest population density (Guangzhou Transport Planning Research Institute, 2012) and dense traffic	

network (Figure 5.10) was circled in red in (e) and sampling sites next to overpasses were marked with red dots in (h).	108
Figure 5.14 Spatial variation of contributions from industrial and agricultural sources (PC1) to Cu (a), Pb (b), and Zn (c); traffic and industrial sources (PC2) to Cu (d), Pb (e), and Zn (f); and geogenic sources (PC3) to Cu (g), Pb (h), and Zn (i) in surface soils.....	109
Figure 5.15 Spatial variation of the contribution from traffic sources (PC2) to Pb (a) and Zn (b), industrial/traffic sources (PC1) to Pb (d) and Zn (e), and geogenic sources (PC3) to Pb (f) and Zn (g) in road dust. PC1 and PC3 were not independent variable for Cu concentration in the APCS-MLR modeling of road dust. c (Cu) is the product of the Cu concentration and the corresponding absolute factor score of PC2.....	110
Figure 5.16 Spatial variation of contributions from industrial sources (PC1) to Cu (a), Pb (b), and Zn (c); traffic sources (PC2) to Cu (d), Pb (e), and Zn (f); and geogenic sources (PC3) to Cu (g), Pb (h), and Zn (i) in foliar dust. Sampling sites next to overpasses were marked with red dots in (d-f).....	111
Figure 5.17 Scheme for trace metal sources and cycling in urban compartments including surface soil, road dust, and foliar dust in the megacity Guangzhou. The arrows indicate the transport of trace metals from sources, such as lithogenic sources, industrial emission/coal combustion, traffic exhaust/industrial transport, orchard activity, atmospheric deposition, particle re-suspension from surface soil and road dust, and other anthropogenic sources. The numbers are the ranges of certain sources contributing to the trace metals in each terrestrial urban compartment obtained using APCS-MLR modeling.	113
Figure 6.1 Particle size distribution in soil dust and bulk surface soils of Hong Kong (a, n=5) and Guangzhou (b, n=7). The error bars represent 1 SD.....	120
Figure 6.2 The XRD pattern of selected soil dust samples collected from two cities...120	
Figure 6.3 SEM photomicrographs and EDX analyses of selected soil dust samples in Hong Kong. a: K-feldspar; b: quartz; c: feldspars; d: tire debris.	121

Figure 6.4 SEM photomicrographs and EDX analyses of selected soil dust samples in Guangzhou. a: K-feldspar; b: quartz; c, d: fly ash.....	122
Figure 6.5 The XRD pattern of selected road dust samples (50-99 μm fraction) collected from two cities.	122
Figure 6.6 SEM photomicrographs and EDX analyses of selected road dust samples in Hong Kong. a and b: tire debris; c: soil particle.....	123
Figure 6.7 SEM photomicrographs and EDX analyses of selected road dust samples in Guangzhou. a and b: tire debris; c: soil particle.	123
Figure 6.8 Trace metal concentrations in bulk soil dust, surface soils and top soils of Hong Kong (a, n=30) and Guangzhou (b, n=7). The bars were defined (from the bottom) as the 1 st percentile, 5 th , percentile, 25 th percentile, median, mean (the square), 75 th percentile, 95 th percentile and 99 th percentile.	129
Figure 6.9 Metal distribution in different particle size fractions of soil dust in Hong Kong. n=30; The bars were defined (from the bottom) as the 1 st percentile, 5 th , percentile, 25 th percentile, median, mean (the square), 75 th percentile, 95 th percentile and 99 th percentile.	129
Figure 6.10 Metal distribution in different particle size fractions of soil dust in Guangzhou. n=7; The bars were defined (from the bottom) as the 1 st percentile, 5 th , percentile, 25 th percentile, median, mean (the square), 75 th percentile, 95 th percentile and 99 th percentile.	130
Figure 6.11 Trace metal distribution in different particle size fractions of road dust in Hong Kong. n=16; The bars were defined (from the bottom) as the 1 st percentile, 5 th , percentile, 25 th percentile, median, mean (the square), 75 th percentile, 95 th percentile and 99 th percentile.	130
Figure 6.12 Trace metal distribution in different particle size fractions of road dust in Guangzhou. n=7; The bars were defined (from the bottom) as the 1 st percentile, 5 th , percentile, 25 th percentile, median, mean (the square), 75 th percentile, 95 th percentile and 99 th percentile.	131

Figure 6.13 Lead isotopic compositions ($^{206}\text{Pb}/^{207}\text{Pb}$ vs $^{208}\text{Pb}/^{207}\text{Pb}$) in soil dust, soils, road dust and some Pb sources. The references of Pb sources were listed in Table 4.8 of Chapter Four.	136
Figure 6.14 Distribution of Pb isotopic compositions ($^{206}\text{Pb}/^{207}\text{Pb}$) in different particle size fractions of soil dust from selected sampling sites in Hong Kong. The error bars represent 1 SD.	137
Figure 6.15 Distribution of Pb isotopic compositions ($^{206}\text{Pb}/^{207}\text{Pb}$) in different particle size fractions of soil dust from selected sampling sites in Guangzhou. The error bars represent 1 SD.	137
Figure 6.16 Distribution of Pb isotopic compositions ($^{206}\text{Pb}/^{207}\text{Pb}$) in different particle size fractions of soil dust and road dust incorporating the fraction of $<10\ \mu\text{m}$ in Hong Kong. The error bars represent 1 SD.	138
Figure 6.17 Distribution of Pb isotopic compositions ($^{206}\text{Pb}/^{207}\text{Pb}$) in different particle size fractions of soil dust and road dust in Guangzhou. The error bars represent 1 SD.	138
Figure 6.18 Trace metal proportion (%) of different soil dust particle size fractions extracted from BCR analysis in Hong Kong (a, n=24) and Guangzhou (b, n=8). 141	
Figure 6.19 Trace metal concentrations of different soil dust particle size fractions in Hong Kong (a, n=24) and Guangzhou (b, n=8, Because only two groups of soil dust in Guangzhou were selected for the BCR extraction, no error bar was available) extracted from BCR analysis.	141
Figure 6.20 Distribution of BCR extracted Pb isotopic compositions ($^{206}\text{Pb}/^{207}\text{Pb}$) in different particle size fractions of soil dust. The error bars represent the standard deviation.	142
Figure 6.21 Trace metal distribution among different particle size fractions of soil dust incorporating with the fractions of $<10\ \mu\text{m}$ in Hong Kong. The dash lines indicated the background concentrations of Hong Kong soil (Zhang et al., 2007).....	147
Figure 6.22 Bioaccessibility of trace metals among different particle size fractions in Hong Kong (n=7) and Guangzhou (n=6). The bars were defined (from the bottom)	

as minimum, 25th percentile, median, mean (the square), 75th percentile, and maximum.148

Figure 6.23 Hazard Quotient (HQ) of metals incorporating bioaccessibility in Hong Kong (a, n=7) and Guangzhou (b, n=6). The bars were defined (from the bottom) as minimum, 25th percentile, median, mean (the square), 75th percentile, and maximum.155

Figure 6.24 Hazard Quotient (HQ) and Hazard Index (HI) of trace metals in soil dust < 10 μ m in Hong Kong through various exposure pathways (ingestion, inhalation, dermal) for children. (a) HQ of combined metals through the three pathways and the overall HI; (b) HQ of each metal through ingestion; (c) HQ of each metal through inhalation; (d) HQ of each metal through dermal contact. Data above the red line indicates the probability of adverse health effects. The bars were defined (from the bottom) as minimum, 25th percentile, median, mean (the square), 75th percentile, and maximum.156

Figure 6.25 Carcinogenic risks of trace metals in soil dust < 10 μ m in Hong Kong through various exposure pathways (ingestion, inhalation, dermal) and the overall risks (RISK) for adult. Data above the red line indicates unacceptable carcinogenic risk; data within the red line and blue line indicates nonnegligible but acceptable carcinogenic risk; and data below the blue line indicates negligible carcinogenic risk. The bars were defined (from the bottom) as minimum, 25th percentile, median, mean (the square), 75th percentile, and maximum.157

List of Tables

Table 2.1 Trace metal concentrations in soils and Earth crust ^a	14
Table 2.2 Trace metal concentrations in soils of various regions (mean, mg kg ⁻¹).....	15
Table 2.3 Decay process of ²³⁸ U, ²³⁵ U, and ²³² Th and their half-lives (Faure, 1977).....	19
Table 2.4 Trace metal concentrations in road dust from various regions (mg kg ⁻¹).....	21
Table 4.1 Physicochemical properties of soil samples from Hong Kong and Guangzhou.	49
Table 4.2 Metal concentrations (mg kg ⁻¹) of urban soils in Hong Kong.....	53
Table 4.3 Metal concentrations (mg kg ⁻¹) of urban soils in Guangzhou.	53
Table 4.4 Trace metal concentrations (mg kg ⁻¹) in backgrounds and guidelines.....	54
Table 4.5 Temporal variations of trace metal concentrations (mean, mg kg ⁻¹) in urban soils of Hong Kong and Guangzhou.	54
Table 4.6 Regional comparison of trace metal concentrations (mg kg ⁻¹) in urban soils.	55
Table 4.7 The Pb isotopic compositions and Pb concentrations of urban soils in Hong Kong and Guangzhou.....	58
Table 4.8 The Pb isotopic compositions of natural and anthropogenic sources of Hong Kong and Guangzhou.....	59
Table 4.9 Surface accumulation factors (SAFs, %) of urban soils in Hong Kong and Guangzhou.	64
Table 4.10 Historical development of Guangzhou and Hong Kong.	64
Table 4.11 Correlation matrix for trace metals in urban soils of Hong Kong.....	70
Table 4.12 Correlation matrix for trace metals in urban soils of Guangzhou.	70
Table 4.13 Theoretical semivariogram models of predication.....	71

Table 5.1 Trace metal concentrations (mg kg^{-1}) in different compartments.	80
Table 5.2 Trace metal concentrations (mg kg^{-1}) in standards, backgrounds, and some environmental samples.	81
Table 5.3 Correlation matrix for trace metals in each compartment.	82
Table 5.4 Washing efficiency (%) of tree leaves.	82
Table 5.5 Summary of Pb isotopic compositions and corresponding Pb concentrations.	96
Table 5.6 Cumulative variance of PCA results.	104
Table 5.7 Rotated component matrix of PCA analysis.	104
Table 5.8 Contribution (%) of each source for trace metals in urban soils, road dust, and foliar dust.	105
Table 5.9 Trace metal enrichment factors (EFs) of urban soils and road dust.	106
Table 5.10 Anthropogenic contribution (PC1+PC2, mean) to Cu, Pb and Zn concentrations in urban soils obtained using APCS-MLR modeling.	107
Table 5.11 The stepwise linear regression models of log(metal concentration) against log(TOC), log(Mn concentration), log(Fe concentration), and soil pH.	107
Table 6.1 Physicochemical properties and characteristic of soil dust samples from two cities.	119
Table 6.2 Summary of trace metal concentrations (mg kg^{-1}) in soil dust, urban soils, road dust, and backgrounds (mean \pm standard deviation) in Hong Kong.	127
Table 6.3 Summary of trace metal concentrations (mg kg^{-1}) in soil dust, urban soils, road dust, and backgrounds (mean \pm standard deviation) in Guangzhou.	128
Table 6.4 The Pb isotopic compositions and Pb concentrations of soil dust in Hong Kong.	133
Table 6.5 The Pb isotopic compositions and Pb concentrations of road dust in Hong Kong.	134

Table 6.6 The Pb isotopic compositions and Pb concentrations of soil dust and road dust in Guangzhou.	135
Table 6.7 Pearson correlation coefficients of total metal concentrations (mg kg ⁻¹) in different particle size fractions as related to the sequentially extracted fractions (mg kg ⁻¹) in soil dust samples collected from Hong Kong (n=24) and Guangzhou (n=8).	141
Table 6.8 Trace metal concentrations in soil particles finer than 10 µm and PM ₁₀ in Urban Hong Kong.	146
Table 6.9 Information of soil dust particles finer than 10 µm.	146
Table 6.10 The stepwise linear regression models to estimate the bioaccessible metals (n=18).	149
Table 6.11 Parameters for risk assessment calculation (USDOE, 2011; USEPA, 2011).	155

Chapter 1 Introduction

The expansion of urban areas is causing a wide range of social and environmental problems and has become a major concern for urban planners and policy makers in the world. In China, urbanization started some decades ago, as a result of the government's land reform (Cabral et al., 2013). In the process of urbanization, trace metal contaminants from industrial operations, traffic emissions, municipal waste disposal, and other anthropogenic activities, directly or indirectly cause contamination to urban environments. From a health perspective, trace metal contamination from urbanization and industrialization may cause several adverse human health effects.

Urban soil is an important compartment in urban environments, extremely essential to biodiversity preservation and city landscape. Urban soils are subject to continuous accumulation of contaminants from either localized or diffuse sources. Whilst polluting activities may be currently reduced, a legacy of contamination can remain in soils for tens, hundreds or even thousands of years (Johnson et al., 2011). In China, contamination caused by trace metals and metalloids including As, Cd, Cr, Cu, Hg, Pb, Ni, and Zn, accounted for 82.4% of the soils classified as being contaminated (The Ministry of Environmental Protection, 2014). Such trace metal contaminants in soils may act as a source of further contamination in urban environments and pose a potential threat to human health. Furthermore, plant surface and road surface are important receptors of metal-enriched particulates and dust in urban environments. The metal-enriched particulates and dust deposited on plant and road surface, often remain relatively mobile and tend to disperse by wind, rain, and surface runoff (Wong et al., 2006). Eventually, trace metals released from numerous anthropogenic sources can be deposited in various terrestrial compartments, resulting in trace metal contamination in urban environments. Understanding the sources and the transport pathways of trace metals in terrestrial compartments at a city scale is critical for

urban environmental management and contamination control. It is thus the soil and its nearby compartments in urban environments that are the principal environmental compartments studied in this thesis.

1.1 Background

The Pearl River Delta (PRD) region is situated in the southern part of China. It is one of the most developed and densely populated areas in China. The regional integration of the PRD and Hong Kong was initiated in 1978. Since the 1980s, Hong Kong manufacturing investment moved to the PRD. This market-led integration between the PRD and Hong Kong, labeled as “front shop, back factory” model, was market-driven based on the cultural affinity, geographical proximity, and personal connections of businesses (Yang, 2004). After the establishment of the Closer Economic Partnership Arrangement (CEPA) between mainland China and Hong Kong in 2003, it turned to a new style of economic integration based on emerging institutional arrangements and governmental involvement between the PRD and Hong Kong (Yang, 2004). In addition to cross-border investment and trade of goods, the economic integration between the PRD and Hong Kong nowadays also involves the cross-border movement of residents, tourists, vehicles, and other related activities. Due to geographical proximity and complementarity of resource endowments in the PRD, Hong Kong and Guangzhou share a close partnership both economically and environmentally. The major mineral compositions include kaolinite, vermiculite, micas, gibbsite, quartz, goethite, montmorillonite, and mixed-layer clay minerals (Zhang et al., 2007), similar to those of Guangzhou soils (Guangdong Geological Survey, 2010). The dramatic economic development and rapid urbanization have caused trace metal contamination in both Hong Kong and Guangzhou. Elevated trace metal concentrations, including Cd, Cu, Pb, and Zn have been observed in urban soils in these two regions (Cai et al., 2012; Gu et al., 2016; Lee et al., 2006; Li et al., 2001).

Urban soil records the net effects of human activities over long periods and hence, is a good indicator of the history of urbanization and industrialization of a city (Cannon and Horton, 2009; McIlwaine et al., 2017). However, few studies have been conducted to understand how historical urbanization and industrialization influence trace metal contamination of urban soils, such as those carried out in the US city of Chicago (Cannon and Horton, 2009) and in the UK cities of Belfast and Sheffield (McIlwaine et al., 2017). Moreover, trace metal distribution patterns have been individually studied at a citywide scale (Ha et al., 2014; Imperato, 2003; Lee et al., 2006; Pan et al., 2016), but very few studies have involved interregional comparisons, such as those conducted on soils (McIlwaine et al., 2017) and road dust (Charlesworth et al., 2003). Assuming that soils were undisturbed, surface soil is more susceptible to the on-going or recent anthropogenic sources, while the deeper soil usually indicates the legacy contamination (Luo et al., 2015). The trace metal distribution along soil depth could record the development of a city. However, the anthropogenic influence on the vertical distribution of trace metals in urban soils was seldom studied (Madrid et al., 2006; McIlwaine et al., 2017). Therefore, an interregional comparison of the spatial heterogeneity of soil trace metals is needed to help us better understand the soil geochemical signatures in response to different types of urbanization and industrialization.

Trace metal contamination in different terrestrial compartments (*e.g.*, soils, terrestrial dust, plants) in urban environments received wide attention (Bi et al., 2013a; Christoforidis and Stamatis, 2009; Ji et al., 2018; Sawidis et al., 2011; Shi et al., 2008). Urban soil is a typical fingerprint of urban contamination due to the accumulation and persistence of contaminants in soil. By contrast, terrestrial dust is a short-term receptor of trace metals in urban environments. Different geochemical properties, land use patterns, the intensity of human activities, contamination history, and distance to emission sources may affect trace metal contamination of different compartments to various degrees (Duong and Lee, 2011; Liu et al., 2013; Luo et al., 2012b). Thus, these compartments could be used to monitor the influence of different trace metal sources by deciphering the quantitative contributions. Since terrestrial

compartments coexist in the urban system, trace metals can be transported and interacted among these compartments. Such processes play crucial roles on the transport and fate of trace metals in urban environments. However, many previous studies either focused on the interactions between two compartments (Al-Khashman et al., 2011; Laidlaw et al., 2012), or simply evaluated trace metal contamination in multiple compartments at a relatively small scale (Bi et al., 2013a; Hu et al., 2014; Zhao et al., 2015b), which cannot systematically explore the transport and interactions of trace metals in an entire urban terrestrial environment. Quantitatively identification of metal inputs and exploration of their spatial influence in different environmental compartments may allow a comprehensive knowledge of the environmental processes and fate of trace metals. Hence, the monitoring of multiple compartments with different characteristics could provide an insight into an interactive system of the urban terrestrial environment.

The health risks of trace metals have been characterized predominantly in urban soils in urban terrestrial environments. Bulk soil samples were assumed to be reasonable predictors of human exposures from trace metals (Chen et al., 2005; De Miguel et al., 2007). However, heterogeneous distribution of trace metals in various soil particle size fractions have been reported widely (Luo et al., 2011; Parra et al., 2014). The interactions of trace metals between soils and aerosols were found to be in the forms of fine particulates (Laidlaw et al., 2012; Young et al., 2002). Soil particles involuntarily ingested by children are also usually of smaller diameter than the original soils (Acosta et al., 2009; Choate et al., 2006; Siciliano et al., 2009). Thus, fine particles of soils play a key role in trace metal transport in urban environments. In order to study the trace metal contamination in different particle size fractions of urban soils, soil particles were mainly separated into different size fractions in the laboratory after bulk soil collection (Jayarathne et al., 2017; Juhasz et al., 2011; Luo et al., 2011). However, the particle partitioning of soils by *ex-situ* sieving (dry sieving) was dependent on the original moisture content of the samples. Choate et al. (2006) found that fine soil particles with a certain moisture content could form large aggregates under the influence

of the coagulation effect. Soil dust, as the loose part of surface soil, usually has very low moisture content during sampling, and thus this aggregation may not affect the *in-situ* soil dust. In comparison with urban soils, soil dust may be more likely to be re-suspended in the atmosphere and inhaled/ingested by humans, and accordingly could be a reasonable predictor of human exposures from trace metals. Consequently, exploration of an efficient method for *in-situ* soil dust collection is very important to understand the causes of the heterogeneous trace metal distribution across different size fractions, its interactions with other types of dust, and the potential health risks.

1.2 Objectives

The overall research aims to provide a comprehensive understanding of trace metal distribution and transport in various compartments in urban terrestrial environments. The objectives of the present study are:

1. To explore the vertical and horizontal distribution of soil trace metals in response to urbanization and industrialization, and the interplay of factors that led to the current soil compositions in two typical urban environments;
2. To compare the trace metal distribution in soils, road dust, and foliar dust of an urban environment; and to spatially quantify the natural or anthropogenic contributions of trace metals using the APCS-MLR model, Kriging technique, and Pb isotopes.
3. To elucidate the factors affecting the chemical partitioning of trace metals in various particle size fractions of soil dust; to estimate the interactions between soil dust and other types of dust in urban environments, and to assess the health risks of soil dust in urban environments.

1.3 Scope of work

This thesis focuses on trace metal contamination in urban terrestrial environments of Hong Kong and Guangzhou. Environmental compartments including surface soils (0–3 cm), top soils (0–15 cm), soil dust, road dust, plant leaves, and foliar dust are studied in this thesis. The analytical approaches include analyses of organic matters, mineral compositions, total and bioaccessible trace metals, Pb isotopic compositions, and chemical speciation of trace metals. Geostatistical and statistical methods, and the APCS-MLR model were also used for data interpretation. This thesis provides implications on risk assessment in urban environments as well as contribution to the understanding of trace metal behavior in rapidly changing environments such as those of South China megacities, providing a sound basis for urban environmental management and planning.

1.4 Organization of thesis

This thesis consists of seven chapters (Figure 1.1). Chapter One covers background, research objectives, scope of works, and organization of this thesis. A detailed literature review is given in Chapter Two, which covers the state-of-the-art research outputs in trace metal contamination in urban environmental compartments, with emphasis on urban soils, road dust, plants and foliar dust. Chapter Three focuses on the research methodology and experimental materials for this study. The results and discussion are presented in Chapter Four, Chapter Five, and Chapter Six. Chapter Four discusses the soil geochemical signatures in response to urbanization and industrialization. Chapter Five includes an interactive study of trace metals in different urban terrestrial compartments. Chapter Six summarizes the distribution of trace metals in particle size fractions of urban soil dust and its implication to risk assessment. Finally, an overall conclusion is given in Chapter Seven which reviews the major findings and contributions in this study and gives recommendations for future study areas.

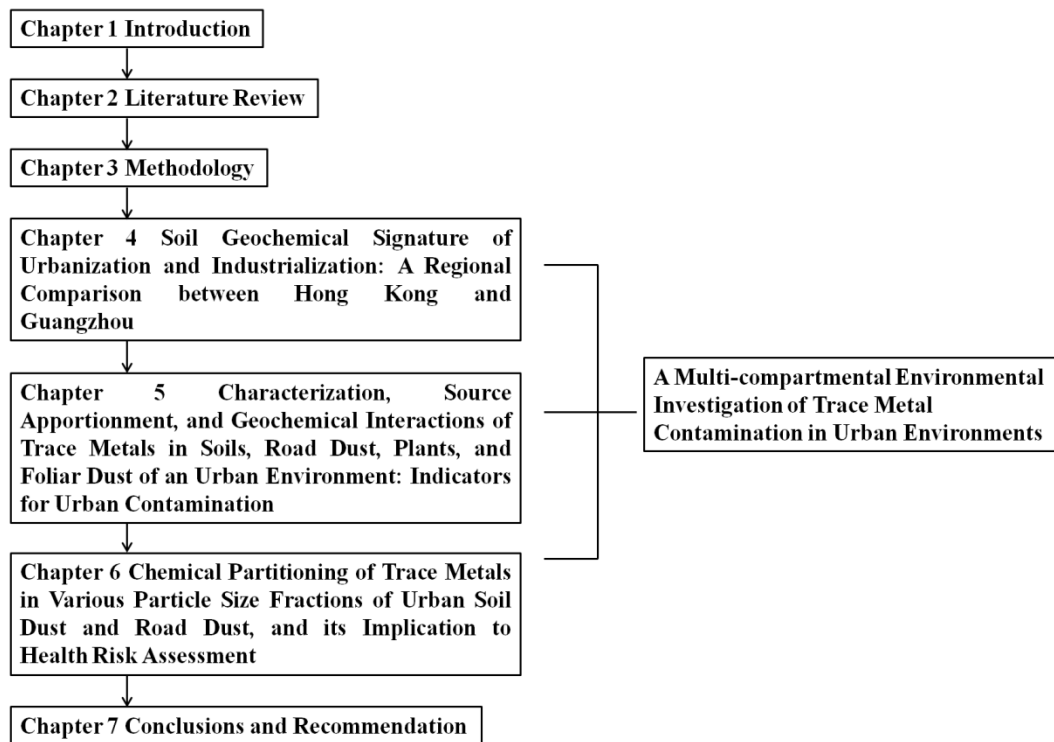


Figure 1.1 Flowchart of the thesis.

Chapter 2 Literature Review

2.1 Urban environment

Towards the end of 2014, 54% of the world's population was living in urban areas, and this figure is predicted to rise to 66% by 2050 (United Nations, 2014). The majority of our daily interactions with nature take place in urban environments, and this has led to a recent upsurge of interest in the dynamics of these relationships. An urban environment is unique in the sense that it is an environment that has been highly modified by humans (Wong et al., 2006). There are many different compartments (*e.g.*, soils, dust, and plants) in urban environments with different responses to environmental contamination. This review provides a comprehensive overview of trace metal contamination in various urban environmental compartments including urban soils, road dust, foliar dust, and plants, and scientific research emphasis.

2.2 Trace metals

Trace metals refer to metals that are normally present at relatively low concentrations in natural and perturbed systems (*e.g.*, soils, plants, or waters), that may or may not be essential for the growth and development of living organisms, and that are toxic to living organisms when present in sufficient concentrations (Adriano, 2001). With such a broad definition, trace metals include a large number of elements with widely ranging chemical characteristics. An element can be dispersed from the time its ore is being mined to the time it becomes a finished product or ingredient of a product, and eventually, is released into the environment. Trace metals included in the present work are cobalt (Co), chromium (Cr), copper (Cu), nickel (Ni), lead (Pb), and zinc (Zn), which are in greatest use commercially and the most emitted with toxicological effects on human in excessive concentration.

2.3 Trace metals in urban soils

2.3.1 Urban soils

Located at the uppermost layer of earth, soils support diverse plant and animal life (Dahiya and Ahlawat, 2010). In natural conditions, soils occur as weathered *in situ* materials derived from bedrock. In urban environments soils vary from the situation in natural condition being slightly disturbed or completely disturbed by human activities. Urban soils are characterized by a strong spatial heterogeneity resulting from the various inputs of exogenous materials and the mixing of original soil material (Ajmone-Marsan and Biasioli, 2010; Guan and Peart, 2006; McIlwaine et al., 2017).

As the ultimate interface, soils act as both a geochemical sink and natural buffer controlling the transport of chemical elements and substances between the geosphere, the atmosphere, the hydrosphere and the biosphere (Kabata-Pendias, 2000). Urban soils are receptors of plenty of contamination, including atmospheric depositions, sewage irrigations, traffic emissions, industrial wastes, fuel combustions, domestic waste, and other human activities (Alloway, 2013; Christoforidis and Stamatis, 2009; McIlwaine et al., 2017). The persistence of contaminants is much longer in soils than in other compartments, but the contaminants still can lead to groundwater contamination and atmospheric contamination through runoff, leaching, weathering, and re-suspension (Shi et al., 2008). In addition, soils establish distinctive relationships with human beings. Soils fulfill basic functions for the human society, not only concretely by providing goods and materials, but also abstractly by stimulating intellectual activity and spiritual wellbeing (Johnson et al., 2011). Urban soils provide esthetical and recreational functions in parks, gardens and green areas, which are frequently used as recreational areas, particularly by children. Due to rapid urbanization and scarcity of land, most of the parks and recreational areas in cities are often located close to major roads or industrial areas where soils are subject to many potential sources of contamination (Li et al.,

2001; Ordóñez et al., 2015).

In urban environments, surface soils (usually shallower than 5 cm) represent the current soil contamination and affect oral ingestion and inhalation, but may be easily transferred or disturbed (Acosta et al., 2009; Madrid et al., 2007). Top soils (usually shallower than 25 cm) that contain originally much deeper soil represent the mixed soils better (Luo et al., 2012a) but may not affect human health under common conditions. Assuming that soils were undisturbed, surface soil, as the uppermost layer of top soil, is more susceptible to the on-going or recent anthropogenic sources, while the deeper soil usually indicates the legacy contamination (Luo et al., 2015).

2.3.2 Trace metals in urban soils

Trace metals from anthropogenic sources can be described as either contaminants or pollutants, but the convention is to use contaminants (and contamination) in the context of soil and land (Alloway, 2013). Soil contamination occurs when the soil chemical state deviates from the normal composition but does not have a detrimental effect on organisms. Soil pollution occurs when an element or a substance is present in greater than natural (background) concentrations as a result of human activity and has a net detrimental effect on the environment and its components (Kabata-Pendias, 2000). Trace metal contamination of urban soils can be categorized as atmospheric or non-point contamination (*i.e.*, broad general disturbance) or point contamination, (*i.e.*, spatially limited disturbance) (Hazelton and Murphy, 2011).

2.3.3 Behavior of trace metals in soils

Anthropogenic trace metals enter soils by a variety of pathways. Trace metals in the form of particulates are transported from contaminant sources (*e.g.*, industry) to soils via dry and wet deposition (Cannon and Horton, 2009; Wong et al., 2006; Wong et al., 2003). Trace metals

deposited on the road surface as a result of wear and tear of vehicle components can be transported to roadside soils by aerial transport and runoff of precipitation (Al-Chalabi and Hawker, 2000). Generally, trace metal concentrations are elevated in the soils adjacent to roads and decrease with increasing distance and soil depth (Werkenthin et al., 2014; Wiseman et al., 2015). Trace metals can also enter soils through direct application of fertilizers, pesticides, sewage sludge and various wastes containing trace metals.

Upon entering the soils, trace metals are bound to soils by initial fast reactions (minutes, hours), followed by slow reactions (days, years) and are redistributed into different chemical forms through various soil processes, including adsorption, organic chelation and complexation, migration, precipitation, dissolution, occlusion, diffusion, microbial fixation, volatilization, etc (Kabata-Pendias, 2000). Trace metals can geochemically exist in various forms, principally adsorbed on the surface of colloidal particles in soils, dissolved in soil solution, and incorporated into biological material, and have varying bioavailability, mobility, and toxicity (Wuana and Okieimen, 2011). Trace metals are adsorbed onto the surface of colloidal particles in soils, principally humus, hydrous oxides of Fe, Mn and Al, alumino-silicate clays and some sparingly soluble salts such as calcium carbonate. Humus is the organic product of ongoing plant and animal decay in a soil environment. Metals can be bound to a range of sites on humus composed of a mix of oxygen, nitrogen and sulfur donor atoms. Both Fe and Mn hydrous oxides have a high adsorption affinity for trace metals and are bound as inner-sphere mono- and bi-dentate surface complexes. The relative affinity of a metal for specific oxides is likely to be determined by oxide charge relations and the morphology and pore sizes within the oxide surface. The sorption capacities of clay minerals to trace metals play an important role to the sorption of trace metals, although clay minerals may contain negligible amounts of trace metals as structural components. The affinity of trace ions for the clay surface is closely related to the specific surface area and cation exchange capacity (CEC) of the minerals. Trace metals also can coprecipitate with carbonates by being incorporated in their structure or be sorbed by oxides (mainly Fe and Mn) that are precipitated

onto the carbonates or other soil particles. Of all these components, clay minerals, hydrated metal oxides, and organic matter are considered to be the most important groups in contributing to the sorption of trace metals (Sparks, 2003).

Trace metals distribute heterogeneously across various particle size fractions in soils, with preferential accumulation in fine particles (Acosta et al., 2009; Ajmone-Marsan et al., 2008; Li et al., 2017; Luo et al., 2011). Trace metal distribution over different particle size fractions is primarily a function of soil characteristics including the presence of sorption sites and mineral composition of soil parent material (Acosta et al., 2011). The affinity of trace metals for soil constituents is strongly influenced by their electrochemical properties and is closely related to the specific surface area and CEC of the minerals. Fine soil particles are dominated by secondary minerals, such as kaolinite and montmorillonite, which have higher specific surface area and CEC and, accordingly, reveal higher sorption capacities compared to primary minerals (*e.g.*, quartz and feldspars) (Kabata-Pendias and Mukherjee, 2007). Furthermore, anthropogenically emitted particles in soils are usually small in size, which may enhance the accumulation of trace metals in fine fractions of soils (Adachi and Tainosho, 2004; Goodarzi, 2006b; Iijima et al., 2007).

Sequential extractions employ a series of successively aggressive reagents to attack specific fractions of the samples, releasing metals associated with these fractions into solution and providing information on operationally defined metal partitioning (Mossop and Davidson, 2003). The metals released in defined fractions depend on the intensity and selectivity of the chemical reagents used (*e.g.*, ion strength of the chemical used in each extraction process), and the strength of the treatment, such as pH of reagents, temperature of extraction, and time of digestion. The modified version of the three-step procedure proposed and validated by the Community Bureau of Reference (BCR) (Ure et al., 1993) is a good option for the analysis of contaminated soils, as it is extensively used in exercises to predict metal mobility in soils, road dust, and sediments (Huang et al., 2014b; Li et al., 2010; Pueyo et al., 2008; Sutherland

et al., 2012). In the BCR extraction, metals released from acid extractable fraction include weakly adsorbed metals retained on the soil surface by relatively weak electrostatic interaction, and those that can be released by ion-exchange processes or precipitated with carbonates; metals released from reducible fraction are mainly bound to hydrous oxides of Mn and Fe; metals released from oxidizable fraction are principally associated with organic matter through complexation or bioaccumulation processes; and metals extracted from residual fraction are strongly bound to crystalline structures of minerals (Ure et al., 1993). Thus, metals extracted in the later fractions are more tightly retained, less labile and bioavailable than those in the earlier fractions.

2.3.4 Trace metal sources in urban soils

Trace metal contents in urban soils are the sum of the metal concentrations from a wide spectrum of sources, which can be from lithogenic and anthropogenic origins. Table 2.1 summarizes the trace metal concentrations in soils throughout the world and in the Earth's crust. Trace metals are naturally released into soils through weathering processes of geological materials and other natural occurrences, which mainly depend on regional characteristics of geological formation (Kim and Thornton, 1993). The high natural variability of trace metal concentrations in soils makes it difficult to set an international standard for soil evaluation (Table 2.2). Furthermore, numerous anthropogenic sources also contribute significantly to trace metals in urban soils due to the wide application of trace metals, resulting in an elevation of trace metal concentrations in urban soils compared to background soils. Geographical variations in background levels, anthropogenic inputs of trace metals, as well as the regional differences in socioeconomic development and enforcement of environmental regulations may influence the trace metal concentrations in urban soils. Additionally, the sampling schemes and analytical procedures varied widely in urban soils research (Table 2.2). These differences have hindered the meaningful comparisons between studies and thus, harmonization of investigation and extraction methodologies is needed.

Table 2.1 Trace metal concentrations in soils and Earth crust^a.

Metal	Soil (mg kg ⁻¹) ^b		Earth crust (mg kg ⁻¹)
	Median	Range	Mean
Co	8	0.05-65	20
Cr	70	5-1500	100
Cu	30	2-250	50
Ni	50	2-750	80
Pb	35	2-300	14
Zn	90	1-900	75

a: Bowen (1979); Sparks (2003); b: Represents soil analyses throughout the world.

Table 2.2 Trace metal concentrations in soils of various regions (mean, mg kg⁻¹).

City	Location	Samples	Sampling depth	Digestion method	Co	Cr	Cu	Ni	Pb	Zn	Reference
Athens, Greece	Urban soil	N=238	0-10 cm	HCl,HNO ₃ , HF,HClO ₄	16	163	48	111	77	122	Argyraki and Kelepertzis (2014)
Amman, Jordan	Industrial site	N=32	0-10 cm	HNO ₃	-	17.2	3.02	-	60.2	51.4	Al-Khashman and Shawabkeh (2009)
Melbourne, Australia	Urban soil	N=39	0-5 cm	HCl,HNO ₃ ,H ₂ O ₂	-	17	40	15	102	218	Laidlaw et al. (2018)
Beijing, China	Urban soil	N=231	0-20 cm	HCl,HNO ₃ , HF,HClO ₄	-	-	20.8	-	25.4	80.3	Liu et al. (2016)
	Background				-	-	19.7	27.9	25.1	59.6	Chen et al. (2004)
Shanghai, China	Urban soil	N=273	0-10 cm	HNO ₃ , HF and HClO ₄	-	108	59.3	31.1	70.7	301	Shi et al. (2008)
	Background				-	75.0	28.6	31.2	25.5	83.7	Wang and Luo (1992)
Hong Kong, China	Urban soil Country park	N=236 N=31	0-15 cm	HNO ₃ , HClO ₄	3.55 3.04	17.8 21.8	16.2 6.37	4.08 5.30	88.1 39.6	103 46.8	Lee et al. (2006)

2.3.4.1 Lithogenic sources

On a spatial basis, the lithology is the dominant factor determining the total concentration of trace metals in soils at regional scale. Two stages are involved in the formation of soils from parent materials: weathering and pedogenesis. Weathering is the alteration of the primary mineral constituents of the parent rocks by physical and chemical processes. Pedogenesis results in the formation of a soil profile from the weathered rock material, leading to the development of a mature zonal soil as the end of the interacting processes. Weathering and pedogenic processes can take place simultaneously at the same sites and are closely interrelated with each other (Kabata-Pendias, 2000).

2.3.4.2 Anthropogenic sources

Numerous anthropogenic sources of trace metals are presented in urban environments, typically including traffic activities, coal combustion, industrial activities, municipal waste, and domestic activities (Luo et al., 2012b; McIlwaine et al., 2017). In addition, there are many other possible trace metal sources in urban soils, including corrosion of metal structures (*e.g.*, galvanized roofs and fences), technogenic (man-made substrate) materials, contaminants from the former agricultural or horticultural use of the land, fertilizers and composts used on urban gardens, sewage sludge, and the incorporation of solid or liquid wastes into soils (Alloway, 2013).

Of all the anthropogenic sources, traffic and industrial sources are the primary and typical sources of trace metals in urban soils (Ajmone-Marsan and Biasioli, 2010; Carrero et al., 2013; Chen et al., 2010; Christoforidis and Stamatis, 2009; Wiseman et al., 2015). Trace metals introduced into the environment from traffic are mainly ascribed to tire wear, brake linings, wear of individual vehicular components, and exhaust. Tire wear particles are generated during the rolling shear of the tire tread against the road surface (Rogge et al., 1993). It is the major Zn contributor in traffic contamination; notwithstanding, the presence of particulate

ZnO may vary from the manufacturing processes of tire tread (Adachi and Tainosho, 2004). Brake dust is introduced into environments during forced deceleration when motor vehicle brake linings are subject to large frictional heat generation and associated brake lining wear (Rogge et al., 1993). The used alloy in vehicular braking systems contains Cu, Sb, and Ni and can be emitted from abrasion of brake lining, particularly in areas with a high occurrence of braking (Harrison et al., 2012; Iijima et al., 2007; Ji et al., 2017; Li et al., 2004; Miner, 1993). It was calculated that 72 to 91% of Cu in traffic emissions originated from brake wear (Schauer et al., 2006). Tetraethyl lead was added to gasoline as an antiknock agent but was phased out in 2000 all over China (Duzgoren-Aydin et al., 2006). However, Pb contamination may continue to influence local environment for a long time, despite the leaded gasoline being phased out for several years (Cundy and Croudace, 2017). Moreover, Pb continues to be emitted by traffic due to the continued use of leaded wheel weights (Root, 2000) and the use of PbCrO₄ in yellow paint for road surface markings (Adachi and Tainosho, 2004; Lee et al., 2016). Other sources, including tailpipe emissions from lubricating oil additives, engine wear debris accumulated in oil, and abrasion of the mechanical components of automobiles may also release a large amount of trace metals into urban environments (Schauer et al., 2006).

Trace metals dispersed into urban environments from industries are usually industry-specific. With respect to the studied trace metals, copper-based alloys are widely used in mechanical manufacturing due to their corrosive resistance, high thermal conductivity, and other desirable qualities (Alloway, 2013; Li et al., 2004). Metallurgy related industries, such as galvanizing iron, and steel products produce a large amounts of Cr, Ni, and Zn (Ajmone-Marsan and Biasioli, 2010; Calvo et al., 2013; Luo et al., 2014; Miner, 1993; Nriagu and Pacyna, 1988; Ordóñez et al., 2015). Anthropogenic Pb and Ni are predominantly released into urban environments via combustion of coal and the burning of oil (Adriano, 2001; Zurbrick et al., 2017). Additionally, electronic equipment and products have become another source for trace metals in recent years (Lincoln et al., 2007).

2.3.4.3 Source identification

Generally, the natural and anthropogenic sources of trace metals in urban soils were identified through enrichment factors (EFs) (Manta et al., 2002; Reimann and Caritat, 2000), multivariate analyses (principal component analysis, PCA; cluster analysis, CA) (Chen et al., 2005; Li et al., 2004), geochemical mapping (Imperato, 2003; Li et al., 2004), and a geostatistical multivariate method which joins spatial correlations and multivariate relationships (Ha et al., 2014; Rodríguez Martín et al., 2006). Trace metals in urban soils were generally from multiple sources, mainly including traffic emissions, coal combustion, and industrial activities (Alloway, 2013; Imperato, 2003; Liu et al., 2016). Thus, it is necessary to quantitatively identify the metal inputs and separate the effect of a specific source to make related regulations and perform specific land remediation. The Absolute Principal Component Scores-Multiple Linear Regression (APCS-MLR) receptor model is an useful tool to evaluate the source contribution of trace metals in environmental compartments (Luo et al., 2015; Thurston et al., 2011; Wang et al., 2016a; Yang et al., 2017). The APCS-MLR model enables the source apportionment at each sampling location and the quantitative contributions of contaminant to each source group (Thurston and Spengler, 1985). Furthermore, the pollution sources of trace metals often were spatially dependent (Ha et al., 2014; Liang et al., 2017; McIlwaine et al., 2017). The contribution of a specific source to trace metal concentrations in an environmental compartment, therefore, should be characterized spatially. However, the spatial pattern of anthropogenic contributions to trace metals in various environmental compartments remains unclear.

Lead contamination in urban soils is a serious concern related to human health (Bradham et al., 2017; Farmer et al., 2011), and accordingly, it is important to determine the Pb sources in soils. Pb isotopic fingerprinting is a powerful tool in the investigation of lead contamination (Bi et al., 2017; Komárek et al., 2008). Pb has four naturally occurring isotopes: ^{204}Pb , ^{206}Pb , ^{207}Pb , and ^{208}Pb . ^{204}Pb is the only primordial stable isotope with a constant abundance on the

Earth, while ^{206}Pb , ^{207}Pb , and ^{208}Pb are products of the radioactive decay of ^{238}U , ^{235}U , and ^{232}Th , respectively (Faure, 1977) (Table 2.3). Natural and anthropogenic sources of Pb usually have distinct isotope ratios or signatures that do not change during industrial and environmental processes. Thus, the study of Pb isotopic compositions becomes a convenient approach for tracing the sources of Pb in various environmental compartments. Previous studies demonstrated that the decrease in the Pb isotopic compositions ($^{206}\text{Pb}/^{207}\text{Pb}$ and $^{208}\text{Pb}/^{207}\text{Pb}$) in soils and dust in Hong Kong and Guangzhou were associated with the enrichment of anthropogenic Pb from sources such as vehicular and industrial emissions (Duzgoren-Aydin, 2007; Lee et al., 2007; Wong et al., 2003). However, the contribution of specific sources could be overestimated or underestimated only based on isotopic ratio analyses, due to the similar Pb isotopic signature of some natural and anthropogenic sources (Duzgoren-Aydin and Weiss, 2008). Therefore, the source differentiation of trace metal contamination in the terrestrial environment should couple isotopic ratio data with other technology such as GIS and APCS-MLR receptor model.

Table 2.3 Decay process of ^{238}U , ^{235}U , and ^{232}Th and their half-lives (Faure, 1977).

Reaction	Decay Half-life (years)	Decay constant (year^{-1})
$^{238}_{92}\text{U} \rightarrow ^{206}_{82}\text{Pb} + 8^4_2\text{He} + 6\beta^-$	4.468×10^9	1.55125×10^{-10}
$^{235}_{92}\text{U} \rightarrow ^{207}_{82}\text{Pb} + 7^4_2\text{He} + 4\beta^-$	7.038×10^8	9.8485×10^{-10}
$^{232}_{90}\text{Th} \rightarrow ^{208}_{82}\text{Pb} + 6^4_2\text{He} + 4\beta^-$	1.4008×10^{10}	4.9475×10^{-11}

2.4 Trace metals in road dust

Solid particles accumulated on road surface are collectively referred to "road dust". It is a term used in general to describe materials including particles larger than 400 μm , which are not referred to "dust" (Charlesworth et al., 2011). The obvious sources of road dust include traffic derived depositions, plant fragments from nearby vegetation, and soil originated depositions (Rogge et al., 1993). Traffic sources mainly include tire wear debris, deposited

vehicle exhaust particles, brake dust, lubricating oil residues, and weathered road surface particles, which are mainly responsible for elevated trace metal inputs. Roadside soils are easily subjected to turbulence as vehicles pass by. The re-suspended soil particles can deposit on road surfaces, turning into a portion of road dust (Chen et al., 2014). In some areas, more than 50% of road dust was attributed to soil materials (Hopke et al., 1980; Hunt et al., 1993).

Trace metals from traffic can be transferred into the surrounding environment via aerial transport or the infiltration of road runoff water. Roadside soils are one of the main targets for trace metals emitted from roads. Spray and road runoff water can be transported into the soils of the adjacent roadside area (Werkenthin et al., 2014). As sweeping efficiency is quite low for finer road dust particles, most of the pollutants associated with the fine fraction of solids remain on the road surfaces, and can adversely affect storm water quality (Jayarathne et al., 2017). Fine road dust can be injected into the atmosphere through wind re-suspension and vehicle-induced turbulences (Amato et al., 2014; Amato et al., 2009; Martuzevicius et al., 2011), thus affecting the particulate matter in the air and the surrounding soils. The road dust re-suspension is related to vehicle speeds, traffic volumes, fractions of heavy trucks, and weather conditions (Amato et al., 2016; Amato et al., 2013; Laidlaw and Filippelli, 2008). Given that road dust is easily re-suspended into the atmosphere, or washed out by regular road surface cleaning and precipitation, road dust does not remain deposited for a long period; hence, it can only reflect recent traffic activities (Amato et al., 2011; Men et al., 2018; Vermette et al., 1991). Table 2.4 illustrates how trace metal concentrations in road dust exhibited high variability in different cities, depending on various local conditions, including traffic volumes, vehicle types, road surface materials, local climate, etc.

Table 2.4 Trace metal concentrations in road dust from various regions (mg kg⁻¹).

City	Cr	Cu	Ni	Pb	Zn	Reference
Shanghai	159	197	84.0	295	734	Shi et al. (2008)
Beijing	92.1	83.1	32.5	60.9	280.7	Men et al. (2018)
Guangzhou	78.8	176	23	240	586	Duzgoren-Aydin et al. (2006)
Xi'an	145	54.7	30.8	125	269	Pan et al. (2016)
Urumqi	54	94.5	43.3	54	294	Wei et al. (2009)
Hong Kong	-	173	-	181	1450	Li et al. (2001)
Massachusetts, US	95	105	-	73	240	Apeagyei et al. (2011)
Birmingham, UK	-	467	-	48	534	Charlesworth et al. (2003)
Madrid, Spain	110	166	18.5	429	271	Johnson et al. (2011)
Tokyo, Japan	52.3	-	29.6	245	1888	Wijaya et al. (2012)
Seoul, Korea	151	396	-	144	795	Kim et al. (2007)
Islamabad, Pakistan	-	52	23	104	116	Faiz et al. (2009)
Karak, Jordan	-	11.3	4.2	11.2	13.1	Al-Khashman (2004)

2.5 Trace metals in plant and foliar dust

Plants reveal various tendencies in the uptake of trace metals that are applied to assess soil and air contamination in urban areas. The response of plants to the chemistry of the surrounding environment is controlled by several external and biochemical factors (Ji et al., 2018; Kabata-Pendias, 2004). The main sources of trace metals in plants are the growth media (*e.g.*, soils and water), whilst trace metals from aerial sources can be absorbed by leaves through cuticular penetration, particularly elements such as Cd, Co, Cu, Fe, Mn, Pb, and Zn (Kabata-Pendias, 2000). Thus, plants are useful biological indicators of the contamination of soils and aerosols in urban environments.

The soil–plant transfer of trace metals is a part of the natural chemical element cycling controlled by geochemical, climatic, biological, and anthropogenic factors. In general, the uptake of trace metals by plants is affected by plant-specific ability and soil properties, and

the most significant factors are pH, Eh, water regime, clay content, organic matter content, CEC, nutrient balance, and concentration of trace elements (Kabata-Pendias, 2000).

Plants also respond directly to the state of the atmosphere. The atmospheric deposition occurs on the surfaces of leaves either under gravity or via impaction due to wind (Ram et al., 2015). In urban environments, plant leaves were considered as accumulators of the atmospheric depositions (Kardel et al., 2010; Sawidis et al., 2011) and traffic contamination along the roadsides (Hassan and Basahi, 2013; Ram et al., 2014). Foliar dust was extensively employed as an indicator of atmospheric depositions (Hassan and Basahi, 2013; Liu et al., 2012; Lu et al., 2008; Shahid et al., 2017; Tomašević et al., 2005). Foliar dust on tree leaves was present in a wide range of diameters, the majority of which was smaller than 2 to 5 μ m, mainly derived from coal combustion, industry activities, traffic emissions, and re-suspended particulate matter such as soil particles and construction dust (Lu et al., 2008; Sgrigna et al., 2015; Song et al., 2015; Tomašević et al., 2005). Trace metal concentrations in foliar dust could be varied depending on the amount of particulate deposition, uptake ability of the plants for different metals, and morphological and anatomical parameters of the leaves, including roughness of the leaf surface, epidermal characteristics, leaf structures, the trichome density, stomata size and density, etc. (Kardel et al., 2010; Shahid et al., 2017; Simon et al., 2014; Song et al., 2015; Tomašević et al., 2005). Once foliar dust is deposited on leaf surface, penetration through the cuticle and stomata openings might represent major pathways for metal entry (Schreck et al., 2012; Shahid et al., 2017).

2.6 Potential health risks of trace metals in urban environments

Most trace metals in excessive concentrations have a deleterious influence on human health, particularly for children (Abrahams, 2002; Magge et al., 2013; Pan et al., 2017). Exposure to As, Pb, Hg, and Cd in children poses an important health threat as it leads to potential predisposition to multisystem ailments, low intelligence quotient (IQ) and dysfunctional

behavior over their lifetime (Levin et al., 2008; Pan et al., 2017; Rodriguez-Barranco et al., 2013). Human exposure to high concentrations of Cd may also cause kidney damage (Buchet et al., 1990; Järup et al., 2000). Copper, Sn, and Se, which are involved in many metabolic processes, can cause health problems both in deficiencies and excesses (Chan et al., 1998). Therefore, trace metal contamination in urban environments is attracting increasing attention from the research community (Bradham et al., 2017; Gualtieri et al., 2008; Li et al., 2018).

In urban soils, trace metals can be directly transported into human body through ingestion, dermal contact, and inhalation (Ljung et al., 2006; Poggio et al., 2008; Yamamoto et al., 2006). Fine particles in surface soils are more likely to be re-suspended and ingested/inhaled by humans; thus, the accumulation of trace metals in urban soil dust is a potential exposure pathway for city residents. Smaller particles (<10 μm) are able to enter into the pulmonary tract, while larger inhaled particles (>10 μm) are intercepted and/or deposited in the upper respiratory tract and swallowed (Gomez et al., 2002). For children, however, the ingestion of urban soils may be the major exposure pathway behavior (Ljung et al., 2006; Mielke et al., 2017; Ruby and Lowney, 2012; Yamamoto et al., 2006), because the soils adhering to the skin of hands, particularly fingers, can be inadvertently ingested by children through so-called “hand to mouth” contact during outdoor activities (Ljung et al., 2006). The USEPA (2000) defined 250 μm as a “reasonable upper-bound” for those particles commonly ingested and/or adhered to skin and associated with dermal exposure. In some dermal contact studies (Kissel et al., 1996; Kissel et al., 1998), soil particles smaller than 65 μm exhibited greater adherence to hands under dry conditions, while larger soil particles (*i.e.*, 135 to 250 μm) appeared to be prone to hand adherence with higher moisture contents (*i.e.*, 10% to 20%). Soil particles involuntarily ingested by children are usually of smaller diameter than the original soils, and hence, trace metals distributed in fine soil particles (*e.g.*, <75 μm (Acosta et al., 2009); <63 μm (Choate et al., 2006); <45 μm (Siciliano et al., 2009)) were suggested to be important for risk assessment. In terms of road dust, metal-enriched dust deposited on the road surface often remains relatively mobile and tends to disperse due to the lack of a means of physical

entrapment and adhesion to substrates (Wong et al., 2006). Tire wear particles finer than 5 μm could enter into the pulmonary tract (Thompson et al., 1966) resulting in reactive oxygen species (ROS) formation and an inflammatory reaction in human alveolar cells (Gualtieri et al., 2008). Iijima et al. (2007) stated that approximately 90% of brake dust are finer than 2.5 μm , and can subsequently enter lungs during respiration and have an adverse effect on human health (Calcabrini et al., 2004). Thus, the health risk of trace metals in urban terrestrial compartments is mainly associated with the ingestion and inhalation of fine particles (Censi et al., 2011; Ljung et al., 2006; Yamamoto et al., 2006).

The total concentration of trace metals in soils is a poor predictor of the potential bioaccessibility of these metals, and is thus a poor proxy parameter for assessing toxicity (Fujimori et al., 2018; Karna et al., 2017; Luo et al., 2012c; Mendoza et al., 2017; Qin et al., 2016). Distribution, mobility, bioavailability and toxicity of metals depend not only on metal concentration but also on the form in which the metals exist. The speciation of trace metals in soils is considered to be more important than the total metal concentration. Generally, trace metals in the exchangeable fraction are considered the most bioavailable; carbonate-bound, easily reducible metal oxide-bound, and organic-matter-bound fractions are potentially bioavailable; while the amorphous, crystalline and residual fractions are mainly not bioavailable (Jayarathne et al., 2017; Kim et al., 2014; Smith et al., 2011). The absorption of trace metals through soil ingestion is greatly dependent on the bioaccessibility of trace metals in the gastrointestinal system. Several *in vitro* methods have been widely used to simulate the trace metal release processes in the gastrointestinal system (Wragg and Cave, 2003). The physiologically based extraction test (PBET) and the simple bioaccessibility extraction test (SBET) are common *in vitro* bioaccessibility assays that have been widely used to assess trace metal bioaccessibility in soils (Fujimori et al., 2018; Gu et al., 2016; Mendoza et al., 2017) and dust (Bi et al., 2015; Hu et al., 2011a; Turner and Ip, 2007). However, few attempts have been made to study the trace metal bioaccessibility as a function of particle size (Juhasz et al., 2011; Karna et al., 2017; Qin et al., 2016).

2.7 Research emphasis on trace metal contamination in urban environments

In this section, research statuses and research gaps of trace metal distribution in urban soils at a city scale, trace metals in multiple compartments in an urban environment, and trace metals in soils as a function of particle size are summarized.

2.7.1 Trace metal contamination in urban soils at a city scale

Trace metal contamination is one of the key urban environmental problems originated from various anthropogenic activities (Alloway, 2013; Li et al., 2004; Yang et al., 2017). Soils in China have been widely contaminated due to rapid industrialization and urbanization over the last several decades (Luo et al., 2012b; Wei and Yang, 2010; Zhao et al., 2015a). However, trace metal levels in urban soils in China varied across different cities, due to geographical variations in background levels, regional history of urbanization and industrialization, and the differences in socioeconomic development and enforcement of environmental regulations (Luo et al., 2012b; Wei and Yang, 2010). For example, the average concentrations of Cu, Pb, and Zn were 20.8 mg kg⁻¹, 25.4 mg kg⁻¹ and 80.3 mg kg⁻¹ in Beijing (Liu et al., 2016), 59.3 mg kg⁻¹, 70.7 mg kg⁻¹, and 301 mg kg⁻¹ in Shanghai (Shi et al., 2008), 35.8 mg kg⁻¹, 87.6 mg kg⁻¹, and 107 mg kg⁻¹ in Guangzhou (Lu et al., 2010), and 16.2 mg kg⁻¹, 88.1 mg kg⁻¹, and 103 mg kg⁻¹ in Hong Kong (Lee et al., 2006), respectively, with the hot spots mainly in areas with higher degree of urbanization and surrounded by intense traffic (Lee et al., 2006; Liu et al., 2016; Shi et al., 2008), and/or in industrial regions (Lu et al., 2010; Shi et al., 2008).

Due to geographical proximity and complementarity of resource endowments in the PRD, Hong Kong and Guangzhou share a close partnership both economically and environmentally. The dramatic economic development and rapid urbanization have caused the trace metal contamination in both Hong Kong and Guangzhou. Based on Kriging interpolation of spatial

data, hot spots of metal contamination were mainly concentrated in the western and southern parts of Guangzhou, and closely related to industrial and long-term domestic activities (Lu et al., 2010). In Hong Kong, the distribution patterns of trace metals in urban soils of the Kowloon Peninsula and Hong Kong Island were investigated with geochemical mapping technology, illustrating the important influence of traffic emissions for trace metal contamination in urban soils (Lee et al., 2006; Li et al., 2004). Urban soils are subject to continuous accumulation of contaminants from either localized or diffuse sources and other physical disturbances, and hence each city would have its own characteristic soil geochemical signature determined by that history (Cannon and Horton, 2009; McIlwaine et al., 2017). Thus, the major sources of trace metal contamination in urban soils varied between Guangzhou and Hong Kong, due to the different historical developments. However, few studies focused on interregional comparison of trace metal distribution in urban soils (McIlwaine et al., 2017). Generally, the sampling schemes and analytical procedures varied widely in urban soils research. These differences have hindered the meaningful comparisons between studies and thus, harmonization of investigation and extraction methodologies is needed. Assuming that soils were undisturbed, surface soil, as the uppermost layer of top soil, is more susceptible to the on-going or recent anthropogenic sources, while the deeper soil usually indicates the legacy contamination (Luo et al., 2015). However, the anthropogenic influence on the vertical distribution of trace metals in urban soils was seldom studied at city scales (Madrid et al., 2006; McIlwaine et al., 2017). Hence, an interregional comparison of the spatial heterogeneity of soil trace metals involving both the horizontal and vertical distribution is needed, to help us better understand the soil geochemical signatures in response to different types of urbanization and industrialization.

2.7.2 Trace metal contamination in multiple environmental compartments

The excessive release of trace metals has posed environmental contamination to various urban compartments including urban soils (Li et al., 2004; Yang et al., 2017; Yu et al., 2016), road

dust (Duzgoren-Aydin et al., 2006; Men et al., 2018; Shi et al., 2008), plants (Hassan and Basahi, 2013; Hofman et al., 2013; Ji et al., 2018; Sawidis et al., 2011), and foliar dust (Burkhardt et al., 2012; Deljanin et al., 2016; Qiu et al., 2009; Sgrigna et al., 2015).

In urban environments, a constant exchange of contaminants exist among the different environmental compartments (Nadal et al., 2009). Regarding aspects of trace metal associations in different urban compartments, Tanushree et al. (2011) found that trace metal concentrations in street dust were associated with the corresponding metal in foliar dust, and Bhattacharya et al. (2013) stated that Cr and Zn concentrations showed similar trends in street dust, foliar dust and suspended particulate matter. Using Pb isotopic signatures, Hu et al. (2014) found that the deposition of airborne Pb was an important Pb source for urban surface soil, whilst road dust and atmospheric dust received Pb from similar sources, including coal emissions and smelting in the studied area. The composition and relationships between trace metal concentrations in PM₁₀ and in plant leaves were studied by Espinosa and Oliva (2006), and the authors illustrated that *N. oleander* can be used in atmospheric biomonitoring of trace metals, such as Cu and Fe. In another study, Oliva and Espinosa (2007) suggested that the *N. oleander* leaf was a good biomonitor of soil contamination by Cu; while Keane et al. (2001) found that Cr, Mn, Pb, and Zn concentrations in *dandelion* leaves increased with soil metal increases, but found no correlation between leaf metal concentrations and PM₁₀. These multi-compartmental studies obtained different results with different studied environmental compartments and locations. Thus, multi-compartmental studies should be conducted by region and the foliage selection should be varied based on the local environment. Furthermore, differences between the compartments were also shown in these studies, while few attempts were found to compare these compartments as indicators of specific sources for trace metal contamination in urban environments.

The various sources in urban area contribute to the complexity of contamination conditions. Urban soils are characterized by significant spatial heterogeneity resulting from the inputs of

exogenous materials (Ajmone-Marsan and Biasioli, 2010; Guan and Peart, 2006). Trace metals in road dust mainly come from road materials, traffic sources, and nearby industrial emissions (Duong and Lee, 2011). As another environment compartment, foliar dust bares the falling particles from typical urban aerosols and other dust re-suspension (Sgrigna et al., 2015; Tomašević et al., 2005). Those urban compartments represent different sources for contaminants. Elucidating the specific source for trace metal contamination from a city scale is critical for urban environmental management. However, elucidating such spatial pattern of anthropogenic contributions to trace metals in various environmental compartments, particularly in a megacity, remains unclear. Furthermore, whether there is any difference or acceptable suitability using different environmental compartments on explaining the trace metal contamination status in urban area still needs more evaluation.

2.7.3 Trace metal distribution in urban soils as a function of particle size

As the uppermost layer of soil, surface soils are an important intervenient medium located between the soil and other compartments. Particulates loaded with trace metals can accumulate in surface soils from atmospheric deposition by sedimentation and by interception (Li et al., 2001). Fine particles of surface soils can be easily re-suspended in the air by wind erosion or human activities, and the finest particles may remain airborne for a long time and then deposit on the surfaces of other media (Luo et al., 2011). In order to study the trace metal contamination in different particle size fractions of urban soils, soil particles were mainly separated into different size fractions in the laboratory after bulk soil collection (Jayarathne et al., 2017; Juhasz et al., 2011; Luo et al., 2011). However, the particle partitioning of soils by *ex-situ* sieving (dry sieving) was dependent on the original moisture content of the samples. Choate et al. (2006) found that fine soil particles with a certain moisture content could form large aggregates under the influence of the coagulation effect. Soil dust, as the loose part of surface soil, usually has very low moisture content during sampling, and thus this aggregation may not affect the *in-situ* soil dust. As the interface between air and soil, soil dust acts as a

link between the atmosphere and soil. In atmospheric deposition, trace metals settle down first as surface dust before they can be fully incorporated into the soil matrix. Therefore, the status of atmospheric contamination may be better revealed by soil dust than by bulk soils. In addition, soil dust may be more likely than bulk soils to be re-suspended in the atmosphere or to adhere to human skin (Laidlaw et al., 2012). Thus, soil dust plays an important role in trace metal contamination, transport and the concomitant health risks in urban environments, which should pay much attention in the environment studies, and the *in situ* sampling method for soil dust should be explored to reveal the situation with respect to particle size fractions.

In urban soils, both inorganic and organic contaminants exhibit a non-uniform distribution across soil particle sizes (Acosta et al., 2009; Bright et al., 2006; Choate et al., 2006; Siciliano et al., 2009). The loadings and availabilities of trace metals in urban soils were generally higher in fine size particles (Li et al., 2017; Luo et al., 2011). Trace metal distribution over different soil particle fractions is primarily a function of soil properties. The finer particles have a higher surface area, dominate secondary minerals (clay minerals, Fe, Mn, and Al oxides and hydroxides, and carbonates) and organic matters (Hardy and Cornu, 2006; Qin et al., 2016). Thus chemical forms of trace metals facilitate the understanding of their distribution in different particle size fraction of soil dust. The absorption of trace metals through soil ingestion is greatly dependent on their bioaccessibility in the gastrointestinal system. Chemical forms and bioaccessibility of trace metals were quite different in soil samples (Luo et al., 2011; Mendoza et al., 2017; Qin et al., 2016), whereas the influence of metals speciation on their bioaccessibility was seldom studied (Fujimori et al., 2018; Mendoza et al., 2017). For example, Mendoza et al. (2017) found a high bioaccessibility for the soluble/exchangeable and reducible metal fractions, while Fujimori et al. (2018) stated a low bioaccessibility for metallic Pb and Pb phosphates and high bioaccessibility for organic Pb species. Due to the higher possibility of soil dust to be re-suspended in the atmosphere or to adhere to human skin compared to urban soils (Laidlaw et al., 2012), more studies are

needed to characterize the metal concentrations, chemical forms and bioaccessibility of soil dust, in order to better understand the health risks of soil dust in urban environments.

2.8 Summary and outlook

Trace metal contamination in urban environments of China is a major environmental problem over the past decades, and it will continue to be one of the key concerns for environment and human health. The contamination levels, distribution patterns, chemical compositions, and sources in various environmental compartments, such as soils, road dust, and plants, have been widely studied. However, research gaps await further study.

Trace metal distribution patterns in urban soils in China varied across different cities (Luo et al., 2012b; Wei and Yang, 2010), while most studies focused on the horizontal distribution of trace metals in urban soils at a city scale. Due to geographical variations in background levels, regional history of urbanization and industrialization, and the differences in socioeconomic development and enforcement of environmental regulations, each city would have its own characteristic soil geochemical signature. In addition, surface soil is generally more susceptible to the on-going or recent anthropogenic sources, while the deeper soil usually indicates the legacy contamination (Luo et al., 2015). However, few attempts have been found to investigate soil contamination regarding both vertical and horizontal distribution of trace metals. Hence, an interregional comparison of the spatial heterogeneity of soil trace metals is needed to better understand the soil geochemical signatures in response to different types of urbanization and industrialization.

Trace metal contamination prevails in not only soils, but also other environmental compartments, such as road dust, foliar dust, and plants (Li et al., 2004; Men et al., 2018; Sawidis et al., 2011; Sgrigna et al., 2015). Most previous studies mainly focused on trace metal contamination in individual compartment. However, the sources of trace metals often

were spatially dependent and compartment-specific, and thus whether there is any difference or acceptable suitability using different environmental compartments on explaining the trace metal contamination status in urban area still needs more evaluation. As the terrestrial compartments coexist in urban system, trace metals can be transported and interacted among these compartments. Hence, the use of multiple compartments with different characteristics and metal sources, in contrast to monitoring single compartment, allows a comprehensive knowledge of the environmental contamination and processes affecting the environment.

As the interface between air and soil, soil dust acts as a link between the atmosphere and soil and is more likely than bulk soils to be re-suspended in the atmosphere or to adhere to human skin. It has been found that trace metals distribute heterogeneously across various particle size fractions of soils, with preferential accumulation in fine particles (Acosta et al., 2009; Ajmone-Marsan et al., 2008; Li et al., 2017; Luo et al., 2011). However, little information is available about soil dust. Consequently, there is a strong need to study the sources, chemical composition, and bioaccessibility of trace metals in different particle size fractions of soil dust in order to understand the reasons for the distribution process, the associations of trace metals between soil dust and other types of dust, and their potential toxicity. It may provide insightful information for health risk and control of trace metal contamination.

Chapter 3 Methodology

3.1 Study region and sample collection

A description of geographical location and characteristics of Hong Kong and Guangzhou (Figure 3.1), and a description of the sampling methodology are given in this section.

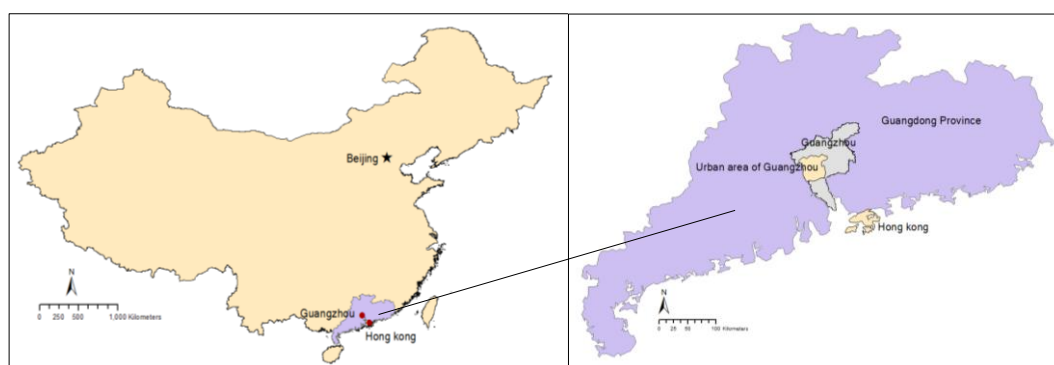


Figure 3.1 Geographical locations of Hong Kong and Guangzhou.

3.1.1 Hong Kong

At the south-eastern tip of China, Hong Kong covers the Hong Kong Island, the Kowloon Peninsula, the New Territories, Lantau Island, and 261 outlying islands ($\geq 500 \text{ m}^2$) (Figure 3.1). The land area of Hong Kong is 1111 km^2 , of which about 267 km^2 is urban area (including residential, commercial, industrial, institution, transportation, open space, vacant land, other urban or built-up land) (Census and Statistics Department, 2016). Hong Kong has a sub-tropical climate with an annual average temperature of $23.3 \text{ }^\circ\text{C}$ and an annual average rainfall of 2399 mm (Hong Kong Observatory). Hong Kong Island and the Kowloon Peninsula are old urban areas of Hong Kong with a long history. The New Territories commenced to be developed in the 1970s to relieve the overgrowth in the two urban districts. Hong Kong's population was approximately 7.35 million in 2016. Due to the scarcity of land,

many residential and commercial areas are built near the high density traffic regions. The centralization of population leads the soil and air quality to become more susceptible to anthropogenic influence.

The industrial revolution in Hong Kong started in 1945–1955. In 1965, about 56% of the net domestic product was contributed by exports of locally manufactured products (Wong, 1975). Secondary production (including manufacturing, construction, and supply of electricity, gas and water) had a significant value-added contribution to the economy before and in the early 1980s. In the 1980s and early 1990s, Hong Kong's industry underwent a major restructuring. Most of the labor-intensive manufacturing industries have been moved to the Chinese mainland. Hong Kong has since been refocusing on knowledge-intensive, service-oriented functions. The value-added contribution to gross domestic product from manufacturing decreased from 13 % in 1992 to less than 2 % in 2012 (Census and Statistics Department, 2013).

3.1.2 Guangzhou

Guangzhou, the capital city of Guangdong province, is located in the southeast of China (22°26'–23°56'N, 112°57'–114°03'E) (Figure 3.1). Guangzhou has a typical subtropical humid monsoon climate with an annual average temperature of 21.2-23.1 °C and an annual precipitation of 1800 mm. At the end of 2012, the population was 6.78 million in the urban districts of Guangzhou, which covered 3843 km² (Guangzhou Bureau of Statistics, 2013). The urban area (~210 km²) was defined as the area encircled by city ring expressways in urban districts (Guangzhou Transport Planning Research Institute, 2012).

The rapid economic growth of Guangzhou started in 1978. The contribution of the primary, secondary, and tertiary production to GDP were 11.67%, 58.59%, and 29.74% in 1978, which shifted to 1.75 %, 37.24%, and 61.01% in 2010 (Nie, 2012). From 1983 to 2012, the gross industrial output increased 144 times (Guangzhou Bureau of Statistics, 1984; 2013).

Furthermore, the total vehicles increased 43 times from 1983 to 2012 in Guangzhou (Guangzhou Bureau of Statistics, 1984; 2013).

3.2 Sample collection

3.2.1 Urban soil collection

Sampling of soils was conducted in two typical urban environments, including the urban area of Hong Kong (Figure 3.2) and the urban area of Guangzhou (Figure 3.3). Our first sampling occupies approximately 200 km² and consists of typical industrial, commercial and residential districts in Guangzhou. The whole area was divided into 200 cells of 1 km × 1 km in size, within which surface soils (0–3 cm, n=180) and top soils (0–15 cm, n=180) were collected.

In Hong Kong, most of the urban areas are discretely located in the northern part of the Hong Kong Island, the Kowloon Peninsular and some new towns in the New Territories. Soil samples of Hong Kong were collected from 44 playgrounds/urban parks (including 131 sampling sites) in the Kowloon Peninsula, 9 playgrounds/parks in Hong Kong Island (including 27 sites), and 7 playgrounds/parks in the New Territories (18 sites). In each playground/urban park, around 3 sites were selected to collect surface soils (0–3cm) and top soils (0–15 cm). A higher sampling density was conducted in Kowloon area (Figure 3.2 b) for an interregional comparison of trace metal distribution between Hong Kong and Guangzhou.

Soils were collected using a stainless-steel trowel. Each of the soil samples consisted of 9 sub-samples obtained in a 2 m×2 m grid. All of the samples were placed in polyethylene bags for transport and storage. The sampling information was listed in Appendix.

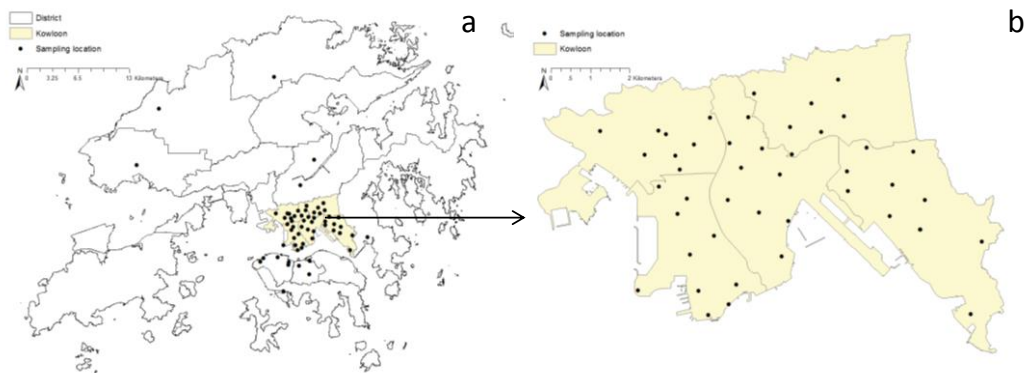


Figure 3.2 Sampling locations of urban soils in Hong Kong.

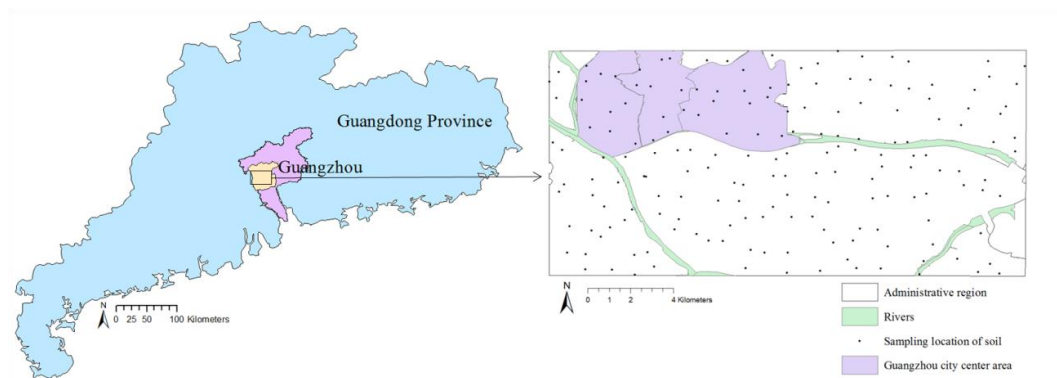


Figure 3.3 Sampling locations of urban soils in Guangzhou. Samples collected from Guangzhou city center area were used for comparison with Hong Kong.

3.2.2 Soil dust collection

Soil dust, the loose part of surface soils, was collected by a vacuum cleaner (Panasonic MC-CG 381) equipped with a specially designed particle separator (Figure 3.4). The particle separator, which was 26 cm long and 7 cm in diameter, contained several filters with specific pore sizes and a quartz microfibre filter (Whatman, England). Field and laboratory blank filters were collected and weighed before and after the collection of the samples. The dust samples were divided into four size fractions *in situ*: <50 μm , 50–99 μm , 100–249 μm , and 250–1000 μm during the sampling in Guangzhou, while the samples were divided into five

size fractions *in situ*: <10 μm , 10–49 μm , 50–99 μm , 100–249 μm , and 250–1000 μm during the sampling in Hong Kong. Surface and top soil samples (0–3 cm and 0–15 cm) were collected within the same sampling area of soil dust using a stainless steel hand auger and road dust samples were obtained at the roadside near the soil dust sampling sites using the soil dust sampling method for comparison.

Thirty sampling sites were selected in Hong Kong urban area, including thirteen non-roadside sites where only soil dust samples were collected, and sixteen roadside sites where both soil dust and road dust were collected (Figure 3.5). Seven sampling sites were selected in Guangzhou urban area, including three urban park sites (UP-UP3) and four street sites (S1-S4) with different traffic flows (Figure 3.6). Both soil dust and road dust were collected at the 7 sampling sites.

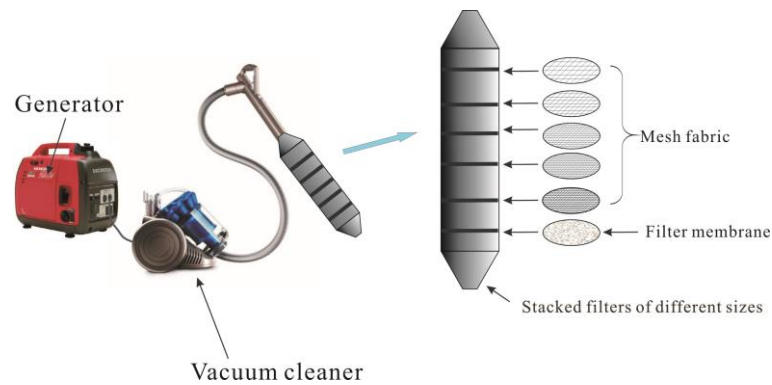


Figure 3.4 Soil and road dust sampling device.

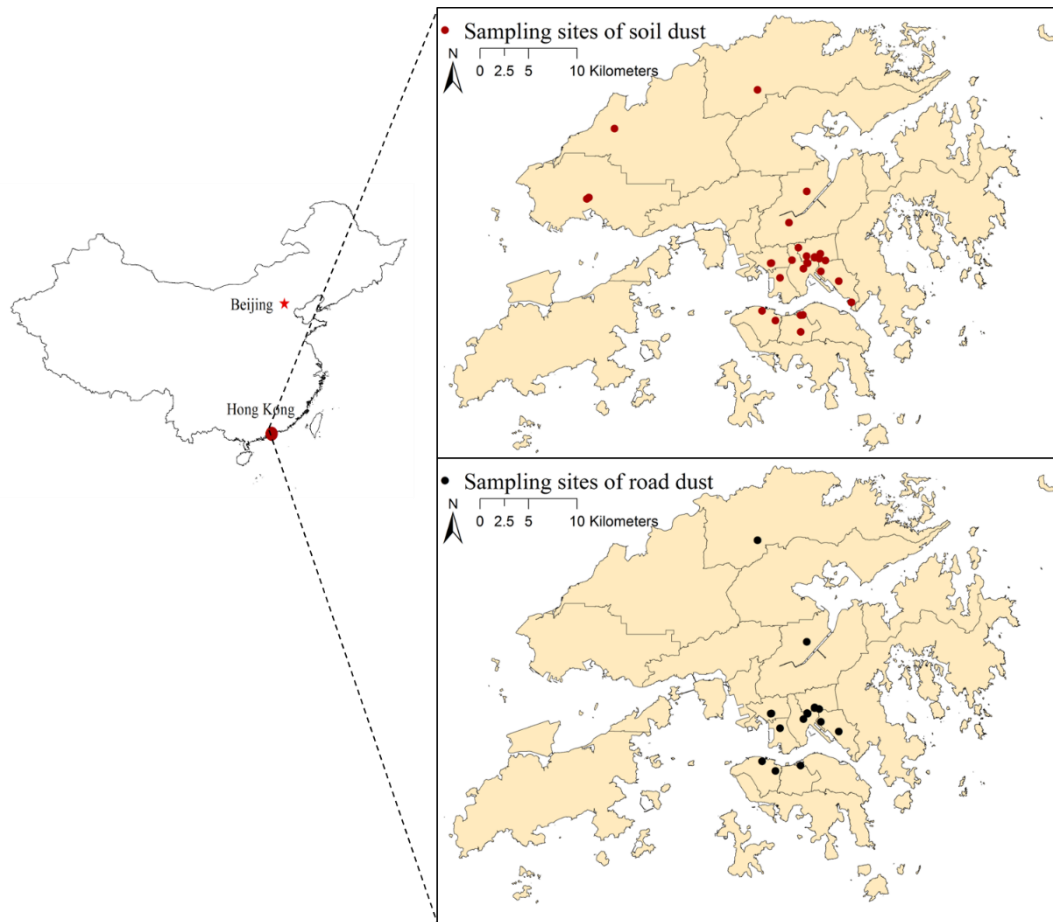


Figure 3.5 Sampling locations of soil dust (n=30, including 14 non-roadside sites and 16 roadside sites) and road dust (n=16, corresponding to the roadside sites of soil dust) in Hong Kong. Detail information is listed in the Appendix.

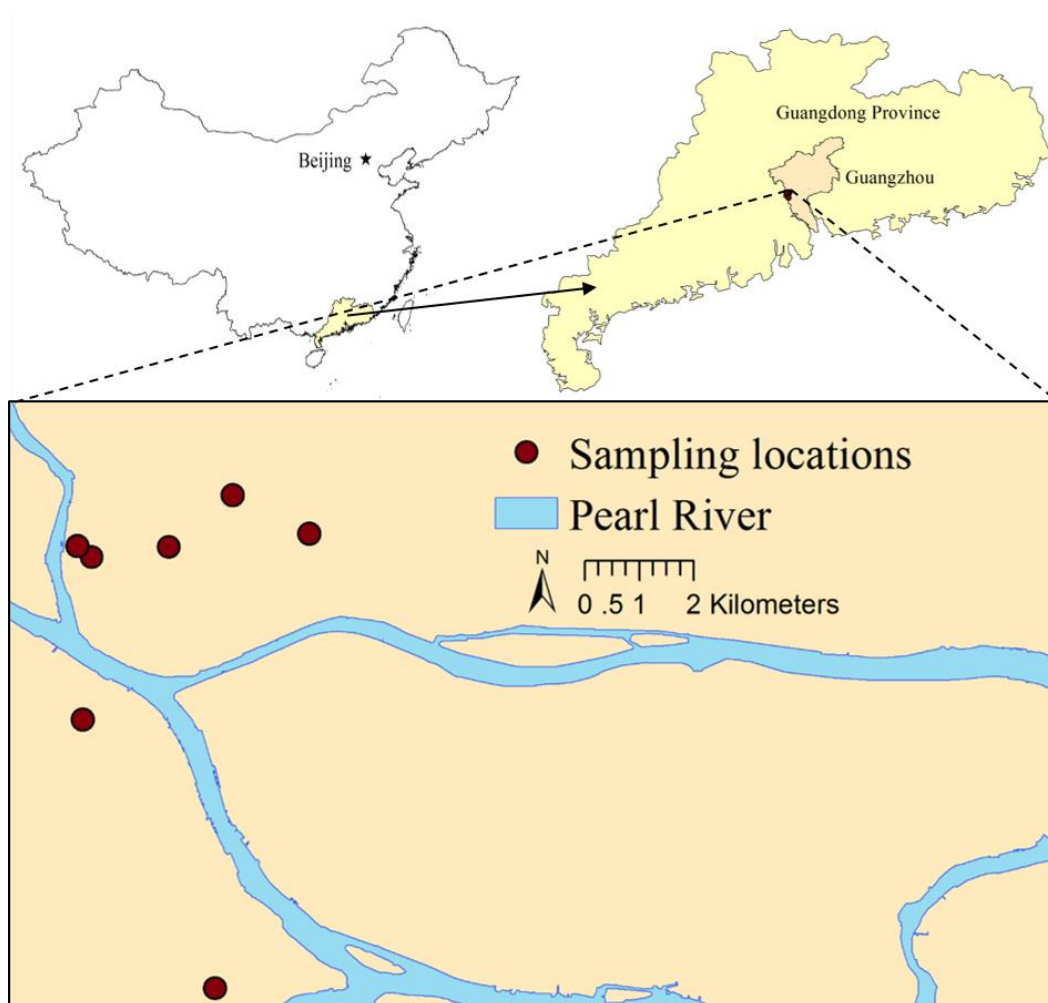


Figure 3.6 Sampling locations of soil dust (n=7) and road dust (n=7) in Guangzhou. Detail information is listed in the Appendix.

3.2.3 Multi-compartments collection

During the soil sampling in Guangzhou urban area, road dust (n=178), tree leaves (n=160), and grass (n=87) samples were also collected to study their differences and interactions as indicators for trace metal contamination in urban environment (Figure 3.7). Road dust samples were obtained at the roadsides near the soil sampling sites by using a brush and dustpan to reveal the impact of traffic related emissions. Tree leaves were collected from banyan trees (*Ficus microcarpa*), which can be found throughout Guangzhou. To keep the tree leaves consistency, the heights of sampled tree leaves ranged from 1.5 to 2 m. Because

the banyan trees (*Ficus microcarpa*) can not be found throughout all the sampling sites, the numbers of plant samples were lower than those of soil samples. All of the samples were placed in polyethylene bags for transport and storage.

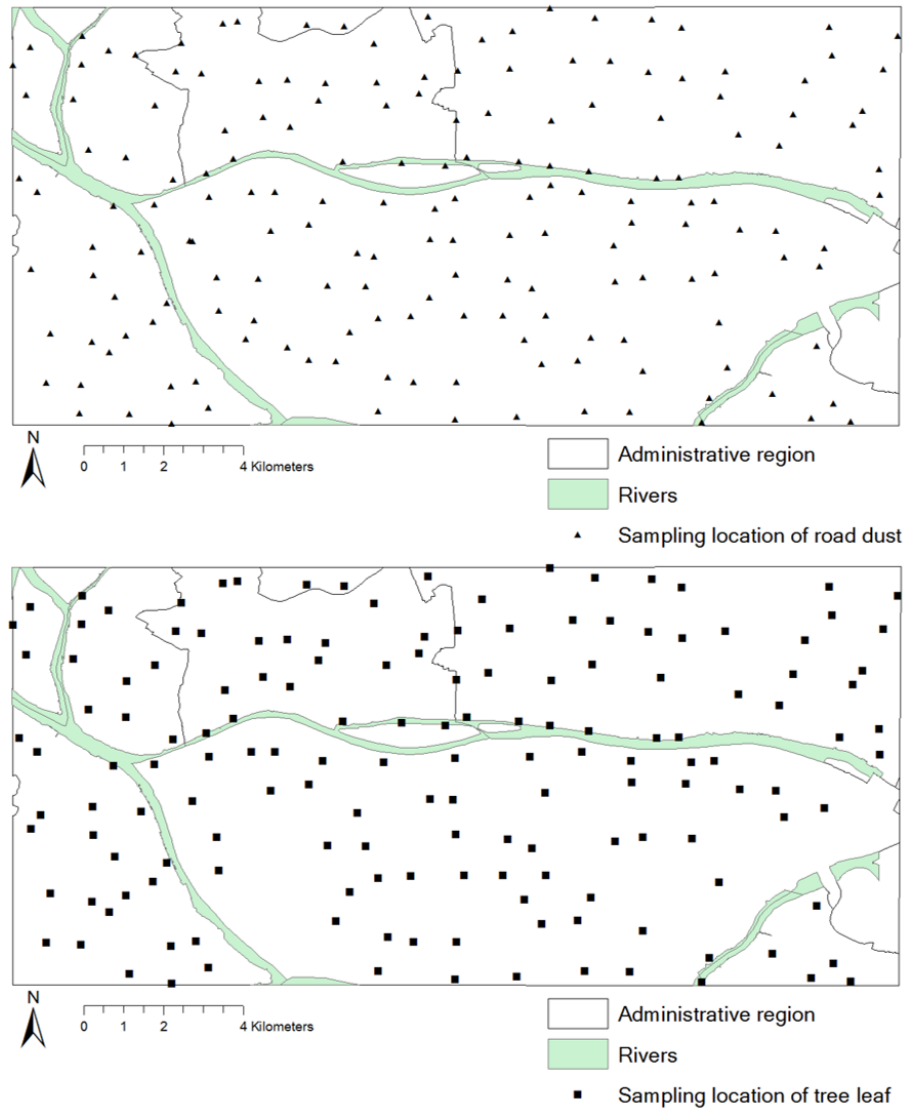


Figure 3.7 Sampling locations of road dust (n=178) and tree leaf (n=160) in Guangzhou.

Detail information is listed in the Appendix.

3.3 Sample preparation

The soil and dust samples were dried in an oven at 60 °C for 3 days. After that, they were crashed and sieved through a 2 mm polyethylene sieve to remove stones, coarse materials, and other debris. The soils, bulk dust samples, and the vacuum cleaner collected dust samples that were larger than 100 µm, were ground into powder with a agate mortar for total digestion. The filters used to collect dust were pre-baked for 8 h at 450 °C to remove any contamination caused by carbonaceous material. Before and after the sampling, the filters were weighed using a balance (Sartorius, Analytic) with an accuracy of 0.1 mg. Each of the plant samples was divided into two batches: washed by deionized water to eliminate the main part of foliar dust and unwashed. Both the washed and unwashed plant samples were dried in an oven at 60 °C for 3 days, and then ground into powder with a stainless steel coffee grinder.

3.4 Analytical methods

3.4.1 Total digestion

To determine the metal concentrations of the samples, the prepared samples (0.20 g ground soils, 0.10 g ground road dust, and 1.0 g plant samples) were treated using a strong acid digestion method (Li et al., 2004). Briefly, the samples are digested with concentrated HNO₃ and HClO₄ (4:1 (v/v) for soils and dust; 8:1 (v/v) for plants) in an aluminum heating block until dry, and then leached with 10 ml of 5% (v/v) HNO₃ at 70 °C for 1 h. Finally, the total concentrations of some trace metals (Co, Cr, Cu, Ni, Pb, and Zn) and major elements (Al, Ca, Fe, Mg, Mn) are determined by inductively coupled plasma-atomic emission spectrometry (ICP-AES, Perkin Elmer Optima 3300DV). Quality assurance and quality control (QA/QC) were confirmed using standard reference materials including NIST SRM 2709a and ERM-CC141 (matrix for soil and road dust) and NIST SRM 1515 and 1573a (matrix for tree leaves and grass), reagent blanks, and 10% replicates of the total samples. The recovery rates

of the majority elements for NIST SRM 2709a were approximately 80–100% except for Pb, which showed a recovery rate of 50–60% probably because of its low concentration. The recovery rates of all the elements were approximately 75–105% for ERM-CC141 and 70–110% for NIST SRM 1515 and 1573a. The duplicate samples showed the analytical precision was less than 5%.

3.4.2 Sequential extraction

Selected soil dust samples were analyzed with the modified BCR sequential extraction procedure (Ure et al., 1993). Briefly, it can be described as follows: First step (exchangeable and weak acid soluble fraction): 0.500 g soil dust sample was extracted with 20.0 mL of 0.11 mol L⁻¹ acetic acid solution by shaking on a mechanical shaker at room temperature for 16 hours. The extract was separated by centrifugation at 4000 rpm for 20 minutes, decanted in polyethylene tubes and stored at 4 °C until analysis. The residue was washed by vortexing for 2 minutes with 20.0 mL of deionised water and then centrifuged, discarding the supernatant. Second step (reducible fraction): 20.0 mL of 0.5 mol L⁻¹ hydroxylammonium chloride solution was added to the residue from the first step, and the mixture was shaken at room temperature for 16 hours. The extract was separated, and the residue was washed as in the first step. Third step (oxidisable fraction): 5.0 mL of 8.8 mol L⁻¹ hydrogen peroxide solution was carefully added to the residue from the second step. The mixture was digested for 1 hour at room temperature and for 1 hour at 85 °C until the volume was reduced to less than 3 mL. A further 5.0 mL of hydrogen peroxide was added, the mixture was digested for 1 hour at 85 °C until the volume was reduced to approximately 1 mL. The residue was extracted with 25.0 mL of 1 mol L⁻¹ ammonium acetate solution with pH approximated to 2.0, at room temperature for 16 hours. The extract was separated, and the residue was washed as in previous steps. Residue from the third step (residual fraction): the residue from step 3 was digested with HClO₄/HNO₃(1:4 (v:v)) until dry. The residue was leached with 10 mL 5% (v/v) HNO₃ at 70 °C for 1 hour, and then decanted in polyethylene tubes and stored at 4 °C until

analysis. Mean recoveries with respect to pseudototal values were in the range of 109-122%, which is acceptable given the intrinsic heterogeneity of urban soils (Mossop and Davidson, 2003; Poggio et al., 2009).

3.4.3 Bioaccessibility

The *in vitro* simple bioaccessibility extraction test (SBET) was used to assess trace metal bioaccessibility in soil dust samples. The SBET test is a static gastric model by which bioaccessible metals are extracted under acid conditions simulating those in the human stomach. Briefly, the gastric solution was simulated by extracting 0.200 g of sample with 20 mL glycine (0.4 mol L⁻¹; pH = 1.5 adjusted with concentrated HCl) at 37 °C at 30 rpm for 1 hour, the pH variation of which was within 0.5 pH units. The mixture was centrifuged at 4000 rpm for 10 minutes and 10 mL supernatant was collected for metal concentration analysis by ICP-AES. Variation coefficients of duplicates were within 10%.

3.4.4 Lead isotopic composition analysis

The Pb isotopic compositions of selected samples were measured by Inductively Coupled Plasma Mass Spectrometry (ICP-MS, Agilent Technologies 7700 series). An international standard reference material (NIST SRM 981, common lead) was used for sample calibration and analytical control. The relative standard deviation (RSD) of the 100 replicates was generally below 0.6%. The measured ²⁰⁴Pb/²⁰⁷Pb, ²⁰⁶Pb/²⁰⁷Pb and ²⁰⁸Pb/²⁰⁷Pb ratios of NIST SRM 981 were 0.0646±0.0001, 1.0933±0.0017 and 2.3720±0.0018), which were in close agreement with the standard reference values of 0.0645, 1.0933, 2.3704, respectively.

3.4.5 Total carbon and total organic carbon in solids

The analysis of solid sample can be conducted by combining the SSM-5000A (solid sample combustion unit, SHIMADZU) with a TOC-L analyzer. SSM-5000A consists of two parts,

the TC-port and the IC-port. To test the total organic carbon (TOC), samples were extracted with HCl to remove inorganic carbon. Briefly, around 1.0 g sample was mixed with 20 mL HCl (1 mol/L) in a weighed 50 mL centrifuge tube, and then was shaken by using a reciprocating mechanical shaker for 12 hours. Then the solid residue was separated from the extract by centrifugation at 4000g for 10 min and decanting the supernatant. Thereafter, the residue was washed with 20 mL deionized water and then separated from the supernatant. The centrifuge tube and washed residue were dried in an oven at 60 °C and weighed. This enables real TOC analysis via the TC measurement by TOC-L analyzer. For TC measurement, the HCl extracted sample (around 0.1 g) was weighed onto a ceramic boat and was pushed into the combustion tube via the TC-port, where a catalyst guarantees the complete conversion to CO₂. The combustion process takes place normally at 900 °C. The result of TC measurement was the TOC content of the sample.

3.4.6 X-ray powder diffraction

Samples were ground in an agate mortar and randomly mounted on petrographic slide prior to X-ray powder diffraction (XRD) analysis. The diffractograms of samples were recorded on a Rigaku SmartLab X-Ray diffractometer at 40 kV, 100 mA using a Cu target tube and a graphite monochromator. Scans were made in the 2θ range of 5° to 90° with a step size of 0.02° and a count time of 2 s per step. The analysis of the XRD was performed using MDI Jade 6 with the PDF-2 reference database from the International Center for Diffraction Data database.

3.4.7 Scanning electron microscopy-energy dispersive X-ray spectroscopy

The surface morphology and chemical composition of selected samples were observed and estimated by using a JEOL Model JSM-6490 scanning electron microscope (SEM) with an Oxford energy dispersive X-ray (EDX) analyzer. Samples for SEM analysis were mounted on an aluminum stub and coated with gold for 90 s using a Denton™ vacuum system prior to

microscopic observations.

3.5 Statistical analysis

3.5.1 Calculation of trace metal concentrations in foliar dust

Trace metal concentrations in foliar dust can be estimated by the following equations:

$$C_{dust} \cdot (\rho_{dust} \cdot S_{leaf}) + C_{leaf} \cdot (\rho_{leaf} \cdot S_{leaf}) = C_{total} \cdot Mass_{total} \dots\dots(1)$$

$$Mass_{total} = \rho_{dust} \cdot S_{leaf} + \rho_{leaf} \cdot S_{leaf} \dots\dots(2)$$

Where C_{dust} , C_{total} , C_{leaf} are metal concentration in foliar dust, unwashed tree leaves, and washed tree leaves, respectively; $Mass_{total}$ is the mass of unwashed tree leaves; S_{leaf} is the area of leaf surface; ρ_{leaf} is leaf mass per unit area of leaf surface and was measured in the lab which approximated to $60.00 \text{ g}\cdot\text{m}^{-2}$; ρ_{dust} is foliar dust mass per unit area of leaf surface. ρ_{dust} is approximated to $1.16 \text{ g}\cdot\text{m}^{-2}$, the average maximum dust-retention amount ($\text{g}\cdot\text{m}^{-2}$) on the same type of tree leaves (*Ficus microcarpa*) in commercial/traffic areas in Guangzhou (Liu et al., 2013). Only one data was assigned to ρ_{dust} regardless the land use types, because almost all the samples were collected at roadsides, and variation from the land use types could be reduced during storage and transportation. It is important to note that the mass density of foliar dust under real-world conditions could be varied depending on the land use types. The calculated concentrations of Co, Cr, Cu, Ni, Pb, and Zn were 72%, 109%, 111%, 99%, 93%, and 73% of the corresponding metal concentrations of foliar dust measured by Zheng et al. (Zheng et al., 2013) in Guangzhou.

3.5.2 Enrichment factor

Enrichment factor (EF), defined as the ratio of trace metal concentration in samples to the corresponding background concentration in Guangzhou (Guangdong Geological Survey, 2010), was used to estimate the anthropogenic influence on trace metal contamination in soil and road dust (Manta et al., 2002). An EF value below 1 indicates that the source of trace metal is mainly crustal origin or natural weathering, while trace metals may come from anthropogenic sources if the EF is greater than 1.

3.5.3 Multivariate statistical analysis

Statistical analysis was conducted with PASW Statistic Version 18.0. A one-way ANOVA test ($p < 0.05$) was used to analyze the variance in metal concentrations among different sampling sites. Paired-sample *t*-tests were used to examine the differences of metal concentrations between surface and top soils, and between washed and unwashed tree leaves. The Pearson correlation was conducted to analyze correlations. The level of significance was set at $p < 0.05$ and $p < 0.01$ (two-tailed). Data were standardized to the Z score (with a mean of 0 and a standard variation of 1) or logarithm transformed prior to statistical analysis to reduce the influence of high data values and to reduce the variations among the major and trace metal concentrations.

Principal component analysis (PCA) was conducted for source identification using factor extraction with eigenvalues > 1 after varimax rotation. The data set of surface soil, road dust, and foliar dust was suitable for PCA with Bartlett test ($p < 0.01$) and Kaiser-Meyer-Olkin (KMO) data ranging from 0.749 to 0.882, showing the data is suitable for Factor Analysis (Zhang, 2002). PCA is an advanced method to cluster metals that behaved similarly to identify potential sources. Factor loadings describe the association between variables and factors, while factor scores characterize the relation between observations and factors. Each factor scores is standardized to a mean of zero so that if a respondent has a value greater than

zero for a certain factor, it exhibits the characteristic described by the factor above the average (Mooi and Sarstedt, 2011).

The APCS-MLR receptor model, was developed by Thurston and Spengler (1985) to identify the sources of airborne metals and estimate the source contributions of each metal. It has been widely used in aerosol studies (Guo et al., 2004; Harrison et al., 1996; Luo et al., 2014; Thurston et al., 2011) and was conducted in the urban soil study by Luo et al. (2015) recently. APCS-MLR was used to estimate the contributions (%) of various anthropogenic sources to each metal in urban soils, road dust, and foliar dust. The APCS-MLR method enabled major contaminant sources to be identified at each sampling location along with the quantitative contributions of contaminant species to each source group (Harrison et al., 1996; Thurston and Spengler, 1985). Briefly, the raw data were standardized to the Z score. Then a true zero for each factor score was calculated by introducing an artificial sample with concentrations equal to zero for all variables, as the factor scores obtained from PCA are normalized with mean zero and standard deviation equal to unity. The factor scores of variables were obtained from PCA by analysis of standardized metal concentrations. The absolute principal component scores (APCS) for each component were then estimated by subtracting the factor scores for the artificial sample from the factor scores of each one of the true samples. Stepwise MLR was then applied using metal concentrations (mg kg^{-1}) as dependent variables and absolute factor scores (obtained from PCA) as independent variables. If a negative value was obtained for the constant included in MLR (which represents non-specified sources), the regression was re-run without the inclusion of any constant. The resultant regression coefficients were then employed to convert the absolute factor scores to produce estimates of each PC source contribution. In our results, the contributions of non-specified sources were negligible for most of the modeling results because the estimated values of constant were usually very small (Guo et al., 2004). The correlation of predicted and measured concentration of each metal was listed as R^2 values (Table 5.8). Most metals had R^2 greater

than 0.80, indicating a good fit between observed and calculated concentrations (Guo et al., 2004).

3.5.4 Geostatistical analysis

Geostatistical analysis was conducted for trace metal concentrations, factor scores from PCA, and source contributions obtained using APCS-MLR. The Kriging interpolation is the principal technique to predict attribute values at un-sampled locations using information related to one or several attributes through capitalizing on the spatial correlation between observations (Wackernagel, 2003).

The experimental variogram was calculated based on a rough "rule of thumb" that the product of the lag size and the number of lags should be about half of the largest distance among all sampling points. It was then generally fitted with a theoretical model, such as a spherical or exponential model. The optimal models provide information about the structure (*e.g.*, model selection) of the spatial variation and the input parameters (*i.e.*, nugget, sill, range, lag size, and lag number) for spatial prediction by kriging interpolation. These parameters also provide insights into the trace metal distribution patterns.

Cross-validation was applied to select the best-fit variogram model. In the process of leave-one-out cross-validation, data points are deleted one by one and predicted by kriging using the remaining data. In general, the absolute values of mean errors and mean standard errors should be near zero (*i.e.*, the minimum errors); the root-mean-squared standardized errors should be closest to 1 and the root-mean-square should be close to the average standard errors (Crosier, 2004). The selection of experimental variogram model, Kriging interpolation and mapping were conducted using ArcGIS 10.2 (ESRI Inc., USA). All the modelling results and cross-validation results were listed in the Appendix.

Chapter 4 Soil Geochemical Signature of Urbanization and Industrialization: A Regional Comparison between Hong Kong and Guangzhou

Based on a large-scale sampling of surface soils (0 to 3 cm) and top soils (0 to 15 cm) in urban environments of Hong Kong and Guangzhou, this chapter aims to understand how historical development of a city influence trace metals in urban soils and whether soil metals can be used as a tracer for urbanization by: investigating trace metal concentrations of urban soils in the two cities; identifying the major sources of trace metals in the two cities; and exploring the vertical and horizontal distribution of soil trace metals in the two cities.

4.1 General soil properties

The TOC contents and pH values of soil samples collected from urban areas of Hong Kong and Guangzhou are listed in Table 4.1. In Hong Kong soil pH ranged from 4.60 to 8.46 with a median pH of 6.06, while in Guangzhou soil pH ranged from 3.75 to 8.17 with a median pH of 7.45. Median TOC of Hong Kong soils (12.4 mg/g) was remarkably lower than that of Guangzhou soils (24.8 mg/g). Base on X-ray diffraction (XRD) analysis (Figure 4.1), quartz, feldspars (K-feldspars and plagioclase), kaolinite, illite, and chlorites were identified in urban soils of Hong Kong. Similarly, mineral compositions of urban soils of Guangzhou mainly included quartz, feldspars (K-feldspars and plagioclase), kaolinite, muscovite, chlorite, and calcite (Figure 4.1).

Table 4.1 Physicochemical properties of soil samples from Hong Kong and Guangzhou.

		TOC (g kg ⁻¹ , n=40)	pH (n=172)
Hong Kong	Mean±SD	13.7±4.79	6.15±0.78
	Median	12.4	6.06
	Range	6.78-25.4	4.6-8.46
Guangzhou	Mean±SD	29.1±18.8	6.99±1.03
	Median	24.8	7.45
	Range	3.54-70.6	3.75-8.17

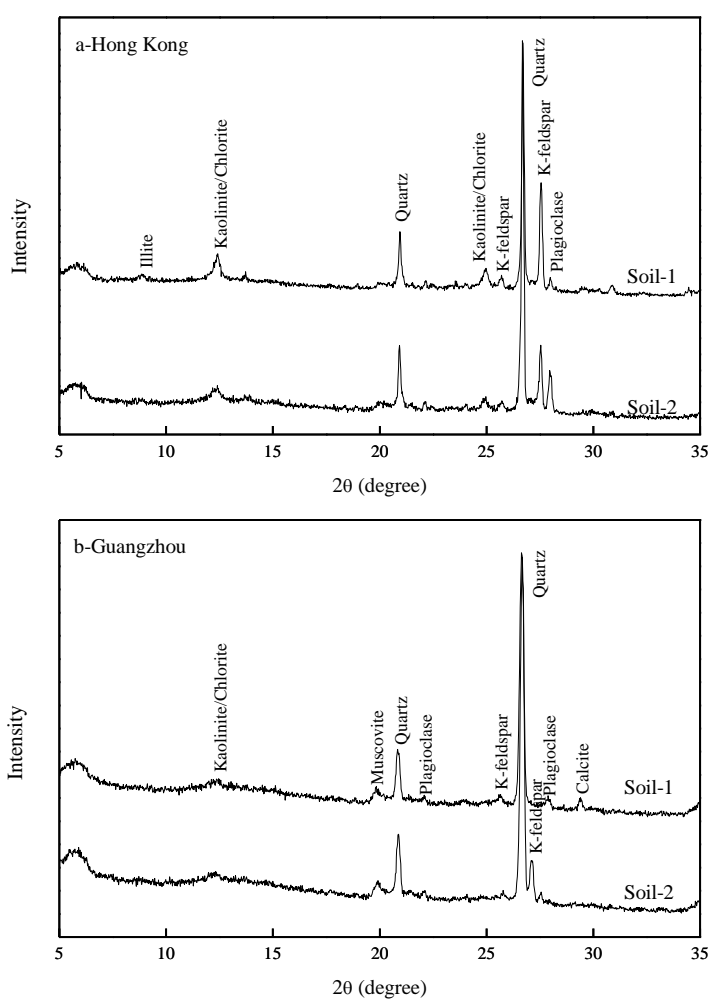


Figure 4.1 The XRD pattern of selected soil samples of two cities. (a:Hong Kong; b: Guangzhou)

4.2 Trace metal concentrations in urban soils

Trace metal concentrations of surface soils (0 to 3 cm) and top soils (0 to 15 cm) from Hong Kong and Guangzhou are tabulated in Table 4.2 and Table 4.3. In general, a wide range of trace metal concentrations was observed in the two studied regions, consistent with the extreme variability of urban soil properties (Ajmone-Marsan et al., 2008; Biasioli et al., 2006; Li et al., 2004; Madrid et al., 2006). Due to the wide range of trace metal concentrations, the median concentration was used for comparison in this section.

In Hong Kong, the median concentrations of Co, Cr, Cu, Ni, Pb, and Zn were 2.63, 12.5, 15.4, 6.68, 49.9, 80.8 mg/kg with a range of 0.25–54.0, 0.58–62.31, 2.62–155, 0.50–47.0, 6.93–214, 25.5–733 mg/kg, respectively, in surface soils (0 to 3 cm), and were 2.84, 14.6, 15.1, 7.41, 57.1, 82.4 mg/kg, with a range of 0.40–15.0, 0.80–65.3, 2.26–227, 1.37–60.3, 5.69–263, 16.7–1025 mg/kg, respectively, in top soils (0-15cm). Compared to background levels (Zhang et al., 2007) (Table 4.4), the median concentrations of Cu, Ni, Pb, and Zn in surface and top soils were enriched by 1.7, 1.4–1.5, 1.2–1.4, and 1.6 folds, respectively, indicating a soil contamination by these metals. Compared with historical dataset, trace metals including Cu, Pb, and Zn in urban soils decreased, respectively, from 28.4, 195, and 237 mg/kg (Wong and Mak, 1997), to 22.3, 89.7, and 146 mg/kg (Li et al., 2001), and to 15.1, 57.1 and 82.4 mg/kg in the present study (Table 4.5 and Figure 4.2). This comparison result reflected a decline of trace metal inputs in Hong Kong soils over the last twenty years. In comparison with top soils, surface soils had significantly lower concentrations of Cu, Pb ($p < 0.01$), and Ni ($p < 0.05$), corroborating the decrease of trace metal inputs.

In Guangzhou, the median concentrations of Co, Cr, Cu, Ni, Pb, and Zn were 7.81, 47.9, 34.3, 20.0, 48.6, 125 mg/kg with a range of 2.75–18.2, 17.0–283, 4.90–155, 7.86–201, 14.5–212, 31.9–671, respectively, in surface soils, and were 44.0, 30.1, 17.2, 45.4, 105 mg/kg, with a

range of 2.50–32.0, 20.2–152, 4.48–261, 5.53–478, 8.35–371, 23.2–693 mg/kg, respectively, in top soils. All the median concentrations of these metals were enriched 1.2–3.1 folds in Guangzhou urban soils compared to the corresponding background concentrations (Guangdong Geological Survey, 2010). The enrichment of Cu (2.9–3.3) and Zn (1.8–2.2) were much higher than those of other trace metals (1.1–1.6). A temporal comparison with previous studies (Guan et al., 2001; Lu et al., 2010) showed that trace metals displayed a generally increasing pattern over the last twenty years with an exception of Pb in urban soils (Table 4.5 and Figure 4.2). The increased trace metals can be attributed to the vast industrial developments and the increasing number of vehicles in Guangzhou (Liu and Diamond, 2005), whereas the Pb concentrations dropped greatly because of environmental improvements after the prohibition of leaded gasoline. Trace metal concentrations (except for Co) in surface soils were significantly higher than those in top soils ($p < 0.01$ for Cu, Zn, and Ni; $p < 0.05$ for Cr and Pb), probably caused by the preferentially metal retention on surface soil from the surface contamination and the widespread atmospheric deposition (Werkenthin et al., 2014).

In comparison with international guidelines (Table 4.4), trace metal concentrations in surface and top soils in Hong Kong and Guangzhou were below Chinese and Canadian soil quality standards (CCME, 2007; CEPA, 1995). Against the Netherlands Soil Contamination Guidelines (VROM, 2000) benchmark, mean trace metal concentrations in surface and top soils of Hong Kong were within the target values, while mean concentrations of Cu and Zn in surface soils and Cu in top soils of Guangzhou exceeded the target values. Compared with other cities in China (Table 4.6), the metal concentrations in urban soil in both Hong Kong and Guangzhou were generally lower than those in Shanghai (Shi et al., 2008), but relatively higher than those in Beijing (Liu et al., 2016). Compared with foreign countries, the concentration levels in Hong Kong and Guangzhou were relatively lower than those in Athens (Greece) (Kelepertzis and Argyraki, 2015) and Melbourne (Australia), but relatively higher than those in Amman (Jordan) (Al-Khashman and Shawabkeh, 2009).

Between the two studied cities, the concentrations of Co, Cr, Cu, Ni and Zn were significantly lower in Hong Kong soils than those in Guangzhou soils ($p < 0.01$). Considering the local background, the significantly lower concentrations of Co, Cr, and Ni in Hong Kong soils might result from the lower geogenic background concentrations. The higher concentration of Cu and Zn in Guangzhou soils was probably caused by anthropogenic activities, as Cu and Zn share similar background values in the two regions. Atmospheric deposition of trace metals is known to significantly alter the composition of urban soils (Cannon and Horton, 2009; Carter et al., 2015; Yu et al., 2016). Severe atmospheric pollution and heavier dry and wet depositions were found in Guangzhou compared to Hong Kong (Deng et al., 2007; Lee et al., 2007; Lee, 2007). Such results infer that atmospheric depositions are important sources of trace metals in urban soils (Cannon and Horton, 2009). Different from other metals, Pb concentration was higher in Hong Kong soils compared to Guangzhou soils, which might be related to the use of leaded gasoline (Wong and Li, 2004). In Hong Kong, a stepwise reduction of tetraethyl lead in leaded gasoline was initiated by the Hong Kong Government in 1992 (Wong and Li, 2004). The sale of leaded gasoline was officially banned in October 1997 in Guangzhou (Duzgoren-Aydin, 2007) and then in April 1999 in Hong Kong (EPD, 2000), respectively. According to government reports (Census and Statistics Department, 2000; Guangzhou Bureau of Statistics, 2000), the vehicle density of the Guangzhou urban area was 290 vehicles/km², much lower than that of Hong Kong (456 vehicles/km²) in 1999, before the phase-out of leaded gasoline in the two cities. Given that the aging Pb emitted from the combustion of leaded gasoline was a major Pb source in urban soils, the higher Pb concentrations in Hong Kong soils suggested a heavier historical soil contamination in Hong Kong compared to Guangzhou. The comparison result is in agreement with the historical urbanization of Hong Kong and Guangzhou, thus implying that urban soils are good indicators of the history of urbanization and industrialization of a city.

Table 4.2 Metal concentrations (mg kg⁻¹) of urban soils in Hong Kong.

Sample (n)		Al	Ca	Co	Cr	Cu	Fe	Mg	Mn	Ni	Pb	Zn
Surface soil (172)	Mean±SD	30000±8250	1990±2220	3.31±4.46	16.3±13.6	21.1±22.3	12200±2950	742±396	314±140	8.29±5.79	57.1±31.4	104±88.4
	Median	29200	1460	2.63	12.5	15.4	11700	672	312	6.68	49.9	80.8
	Range	5810-60700	245-20170	0.25-54.1	0.58-62.3	2.62-155	3990-23300	28.9-2812	39.9-778	0.50-47.0	6.93-214	25.5-733
Top soil (172)	Mean±SD	34400±8810	2100±2920	3.08±1.67	16.3±12.9	23.5±29.1	13000±2810	792±406	356±161	9.43±7.62	65.1±38.4	106±102
	Median	32600	1380	2.84	14.6	15.1	12600	725	339	7.41	57.1	82.4
	Range	5150-60000	155-27100	0.40-15.0	0.80-65.3	2.26-227	4120-23600	4.68-3108	24.5-941	1.37-60.3	5.69-263	16.7-1025

Table 4.3 Metal concentrations (mg kg⁻¹) of urban soils in Guangzhou.

Sample (n)		Al	Ca	Co	Cr	Cu	Fe	Mg	Mn	Ni	Pb	Zn
Surface soil (172)	Mean±SD	38345±14489	7256±6839	8.3±3.06	53.±27.5	40.2±25.8	22300±5910	2476±992	344±311	23.3±17.	55.5±29.3	148±97.0
	Median	37600	4940	7.81	47.9	34.3	21800	2433	293	20.0	48.6	125
	Range	5710-85900	439-42100	2.75-18.2	17.0-283	4.9-155	6920-42100	396-6227	43.9-3405	7.86-201	14.5-212	31.9-671
Top soil (172)	Mean±SD	47300±15200	6060±6160	8.45±3.69	48.2±19.3	37.6±29.1	23100±6150	2473±1079	332±268	21.0±35.8	53.3±36.2	130±98.7
	Median	47100	4280	7.87	44.0	30.1	22500	2421	287	17.2	45.4	105
	Range	7200-94400	289-41300	2.50-32.0	20.2-152	4.48-261	9830-42600	194-5900	9.10-2720	5.53-478	8.35-371	23.2-693

Table 4.4 Trace metal concentrations (mg kg⁻¹) in backgrounds and guidelines.

	Co	Cr	Cu	Ni	Pb	Zn
Backgrounds of Hong Kong ^a	3.88	15.7	10.2	4.86	26.7	63.4
Backgrounds of Guangzhou ^b	6.3	39	10.4	12.3	41	58
Chinese soil quality standard II ^c	-	200	100	50	300	250
Dutch ^d	9	100	36	35	85	140
Canadian(residential/parkland) ^e	-	64	63	50	140	200
Canadian(commercial) ^e	-	87	91	50	260	360
Canadian(industrial) ^e	-	87	91	50	600	360
Canadian(agricultural) ^e	-	64	60	50	70	200

a: Zhang et al. (2007); b: Guangdong Geological Survey (2010); c: CEPA (1995); d: VROM (2000); e: CCME (2007).

Table 4.5 Temporal variations of trace metal concentrations (mean, mg kg⁻¹) in urban soils of Hong Kong and Guangzhou.

Location	Sampling depth (n)	Co	Cr	Cu	Ni	Pb	Zn	Reference
Hong Kong	0-5cm (7)	-	-	28.4	-	195	237	Wong and Mak (1997)
	0-10cm (594)	-	-	24.8	-	93.4	168	Li et al. (2001)
	0-3cm (172)	3.31	16.3	21.1	8.29	57.1	104	This study
	0-15cm (172)	3.08	16.3	23.5	9.43	65.1	106	
Guangzhou	0-20cm (17) [*]	-	86.9	23.7	16.9	63.1	121	Guan et al. (2001)
	0-10 cm (426)	-	-	35.8	18.7	87.6	107	Lu et al. (2010)
	0-3cm (172)	8.3	53	40.2	23.3	55.5	148	This study
	0-15cm (172)	8.45	48.2	37.6	21	53.3	130	

*: Samples including 9 roadside soils and 8 park soils.

Table 4.6 Regional comparison of trace metal concentrations (mg kg⁻¹) in urban soils.

City	Location	Samples	Sampling depth	Digestion method	Co	Cr	Cu	Ni	Pb	Zn	Reference
Hong Kong	Urban area	172	0-15cm	HNO ₃ , HClO ₄	3.08	16.3	23.5	9.43	65.1	106	This study
	background				3.88	15.7	10.2	4.86	26.7	63.4	Zhang et al. (2007)
Guangzhou	Urban area	172	0-15 cm	HNO ₃ , HClO ₄	8.45	48.2	37.6	21	53.3	130	This study
	background										58
Athens, Greece	Urban soil	N=238	0-10 cm	HCl, HNO ₃ , HF, HClO ₄	16	163	48	111	77	122	Argyrazi and Kelepertzis (2014)
Amman, Jordan	Industrial site	N=32	0-10 cm	HNO ₃	-	17.2	3.02	-	60.2	51.4	Al-Khashman and Shawabkeh (2009)
Melbourne, Australia	Urban soil	N=39	0-5 cm	HCl, HNO ₃ , H ₂ O ₂	-	17	40	15	102	218	Laidlaw et al. (2018)
Beijing, China	Urban soil	N=231	0-20 cm	HCl, HNO ₃ , HF, HClO ₄	-	-	20.8	-	25.4	80.3	Liu et al. (2016)
	Background				-	-	19.7	27.9	25.1	59.6	Chen et al. (2004)
Shanghai, China	Urban soil	N=273	0-10 cm	HNO ₃ , HF and HClO ₄	-	108	59.3	31.1	70.7	301	Shi et al. (2008)
	Background				-	75.0	28.6	31.2	25.5	83.7	Wang and Luo (1992)

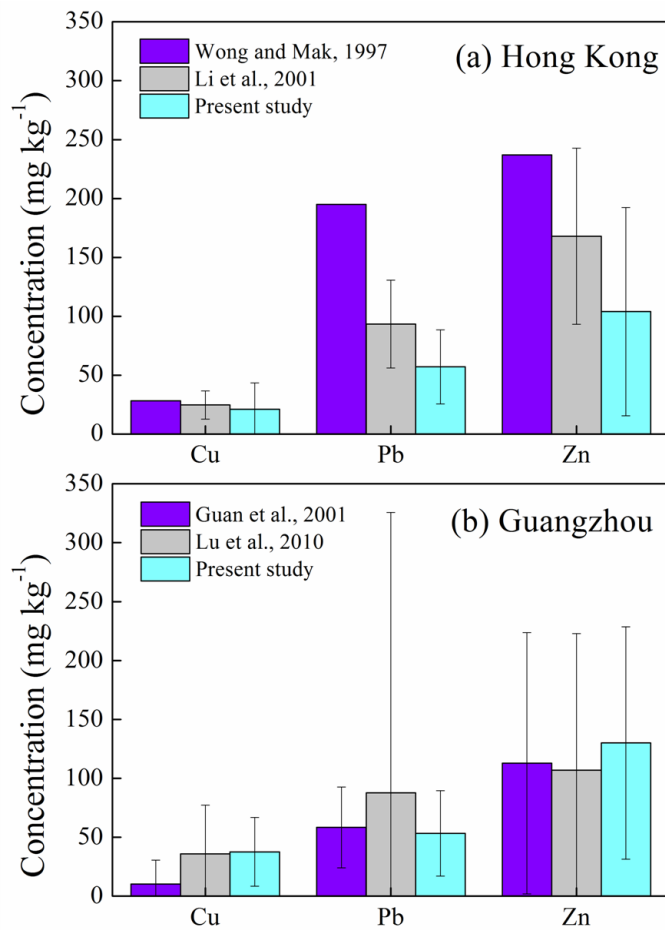


Figure 4.2 Temporal variation of trace metal concentrations in urban soils of Hong Kong (a) and Guangzhou (b).

4.3 Lead isotopic compositions

To elucidate the sources of Pb in urban soils, the Pb isotopic compositions of selected surface and top soils collected from Hong Kong and Guangzhou were compared with known natural and anthropogenic sources in the PRD (Table 4.7 and Table 4.8). Lead isotopic compositions of urban soils in Hong Kong ranged from 1.1371 to 1.2073 ($^{206}\text{Pb}/^{207}\text{Pb}$) and from 2.4253 to 2.5181 ($^{208}\text{Pb}/^{207}\text{Pb}$). Significant linear correlation ($R^2=0.96$) between $^{206}\text{Pb}/^{207}\text{Pb}$ and $^{208}\text{Pb}/^{207}\text{Pb}$ was observed within urban soils, backgrounds (Wong and Li, 2004) and Australian Pb ore (Bollhöfer and Rosman, 2001) (Figure 4.3 a), suggesting a binary mixing of

Pb sources in Hong Kong. Specifically, a decreasing pattern of Pb isotopic compositions ($^{206}\text{Pb}/^{207}\text{Pb}$ and $^{208}\text{Pb}/^{207}\text{Pb}$) was found from roadsides to non-roadsides soils, the range of which was within the Pb isotopic compositions of natural backgrounds and Australian Pb ore, indicating that the soil contamination resulted from traffic exhausts.

The Pb isotopic compositions ($^{206}\text{Pb}/^{207}\text{Pb}$: 1.1699 to 1.2039, and $^{208}\text{Pb}/^{207}\text{Pb}$: 2.4506 to 2.4934) of urban soils in Guangzhou fell within the range of local traffic/industrial/coal sources and background values (Table 4.7, Table 4.8, and Figure 4.3 b). The data indicated the mixed sources of Pb in urban soils. Specifically, the industrial sites contributed to the nearby surface soils, with a decreasing pattern of Pb isotopic ratios ($^{206}\text{Pb}/^{207}\text{Pb}$ and $^{208}\text{Pb}/^{207}\text{Pb}$) in some samples from industrial regions. Lead isotopic ratios ($^{206}\text{Pb}/^{207}\text{Pb}$ and $^{208}\text{Pb}/^{207}\text{Pb}$) of some surface soils decreased with increasing traffic volume, pointing to the vehicle exhausts including historical leaded gasoline and unleaded gasoline exhausts.

Table 4.7 The Pb isotopic compositions and Pb concentrations of urban soils in Hong Kong and Guangzhou.

Sampling area	Sample	Soil type	$^{206}\text{Pb}/^{207}\text{Pb}$	$^{208}\text{Pb}/^{207}\text{Pb}$	Pb (mg kg ⁻¹)	
Hong Kong						
Industrial/roadsides	#KTE-2	Surface	1.1477	2.4367	146.8	
		Top	1.1371	2.4253	203.5	
Roadsides	#SKLR-2	Surface	1.1788	2.4699	46.18	
		Top	1.1721	2.4626	71.64	
	#LWSP2-3	Surface	1.1955	2.4905	72.83	
		Top	1.1903	2.4851	93.69	
Non-roadsides	#PSP-3	Surface	1.1998	2.4968	33.2	
		Top	1.1985	2.496	33.2	
	#LRP-1	Surface	1.2073	2.5181	61.15	
		Top	1.2054	2.5167	61.98	
Guangzhou						
Industrial area	#120	Surface	1.1751	2.4506	184.2	
		Top	1.1784	2.456	73.02	
	#3	Surface	1.1732	2.4597	109.9	
		Top	1.1802	2.456	78.85	
	#44	Surface	1.1699	2.4572	119.5	
		Top	1.1721	2.4627	101.8	
	Roadsides with high traffic flow	#139	Surface	1.1824	2.4645	57.7
			Top	1.184	2.4767	40.74
#154		Surface	1.1814	2.4675	70.61	
		Top	1.1968	2.4928	70.38	
#93		Surface	1.1841	2.481	24.25	
		Top	1.1851	2.4847	22.8	
Roadsides with low traffic flow	#136	Surface	1.1961	2.4897	22.05	
		Top	1.1965	2.4909	22.96	
	#152	Surface	1.1831	2.4669	23.79	
		Top	1.1958	2.4915	23.42	
	#123	Surface	1.2016	2.4804	72.66	
		Top	1.2039	2.4934	66.97	

Table 4.8 The Pb isotopic compositions of natural and anthropogenic sources of Hong Kong and Guangzhou.

Sample	$^{206}\text{Pb}/^{207}\text{Pb}$	$^{208}\text{Pb}/^{207}\text{Pb}$	Reference
Road dust in Hong Kong	1.1575±0.0024	2.4447±0.0049	Present study
Road dust in Guangzhou	1.1668±0.0080	2.4520±0.0089	
Natural backgrounds of the PRD			Zhu et al. (2001)
Uncontaminated soil	1.1952	2.4815	Zhu et al. (2001)
Volcanic rock	1.1993	2.4965	Zhu et al. (2001)
Granite	1.1842	2.4824	Zhu et al. (2001)
Power station in Guangzhou	1.1732	2.4676	Zhu et al. (2001)
Leaded vehicle in the PRD			Zhu et al. (2001)
Automobile exhaust	1.1619	2.4182	Zhu et al. (2001)
Automobile exhaust	1.1562	2.4243	Zhu et al. (2001)
Automobile exhaust	1.1632	2.426	Zhu et al. (2001)
Dockyard in Guangzhou	1.176	2.461	Bi et al. (2013b)
Ironwork in Guangzhou	1.178	2.468	Bi et al. (2013b)
Urban PM _{2.5} in Guangzhou	1.1675 ± 0.0040	2.4491 ± 0.0066	Ming (2016)
PM _{2.5} in the rural PRD	1.1655 ± 0.0046	2.4447 ± 0.0054	Ming (2016)
Unleaded gasoline in Chengdu			Gao et al. (2004)
Automobile exhaust	1.170	2.461	Gao et al. (2004)
Unleaded gasoline in Shanghai			Zheng et al. (2004)
Automobile exhaust	1.143	2.457	Zheng et al. (2004)
Automobile exhaust	1.135	2.428	Zheng et al. (2004)
Automobile exhaust	1.13	2.417	Zheng et al. (2004)
Automobile exhaust	1.125	2.417	Zheng et al. (2004)
Automobile exhaust	1.117	2.403	Zheng et al. (2004)
Unleaded gasoline in Hangzhou			Li and Lu (2008)
Automobile exhaust	1.09	2.36	Li and Lu (2008)
Automobile exhaust	1.089	2.365	Li and Lu (2008)
Automobile exhaust	1.114	2.383	Li and Lu (2008)
Automobile exhaust	1.113	2.383	Li and Lu (2008)
Automobile exhaust	1.164	2.448	Li and Lu (2008)
Unleaded gasoline in Guiyang			Zhao et al. (2015b)
Automobile exhaust	1.1503	2.4327	Zhao et al. (2015b)
Automobile exhaust	1.1536	2.4366	Zhao et al. (2015b)

Table 4.8 Continued.

	$^{206}\text{Pb}/^{207}\text{Pb}$	$^{208}\text{Pb}/^{207}\text{Pb}$	Reference
Automobile exhaust	1.1621	2.4537	Zhao et al. (2015b)
Automobile exhaust	1.1595	2.4418	Zhao et al. (2015b)
Coals used in Guangzhou			Bi (personal communication)
Coal	1.207	2.511	Bi (personal communication)
Coal	1.184	2.458	Bi (personal communication)
Coal	1.214	2.507	Bi (personal communication)
Coal	1.194	2.479	Bi (personal communication)
Coal	1.202	2.492	Bi (personal communication)
Coal	1.190	2.479	Bi (personal communication)
Coal	1.198	2.489	Bi (personal communication)
Coal	1.209	2.495	Bi (personal communication)
Coal	1.287	2.479	Bi (personal communication)

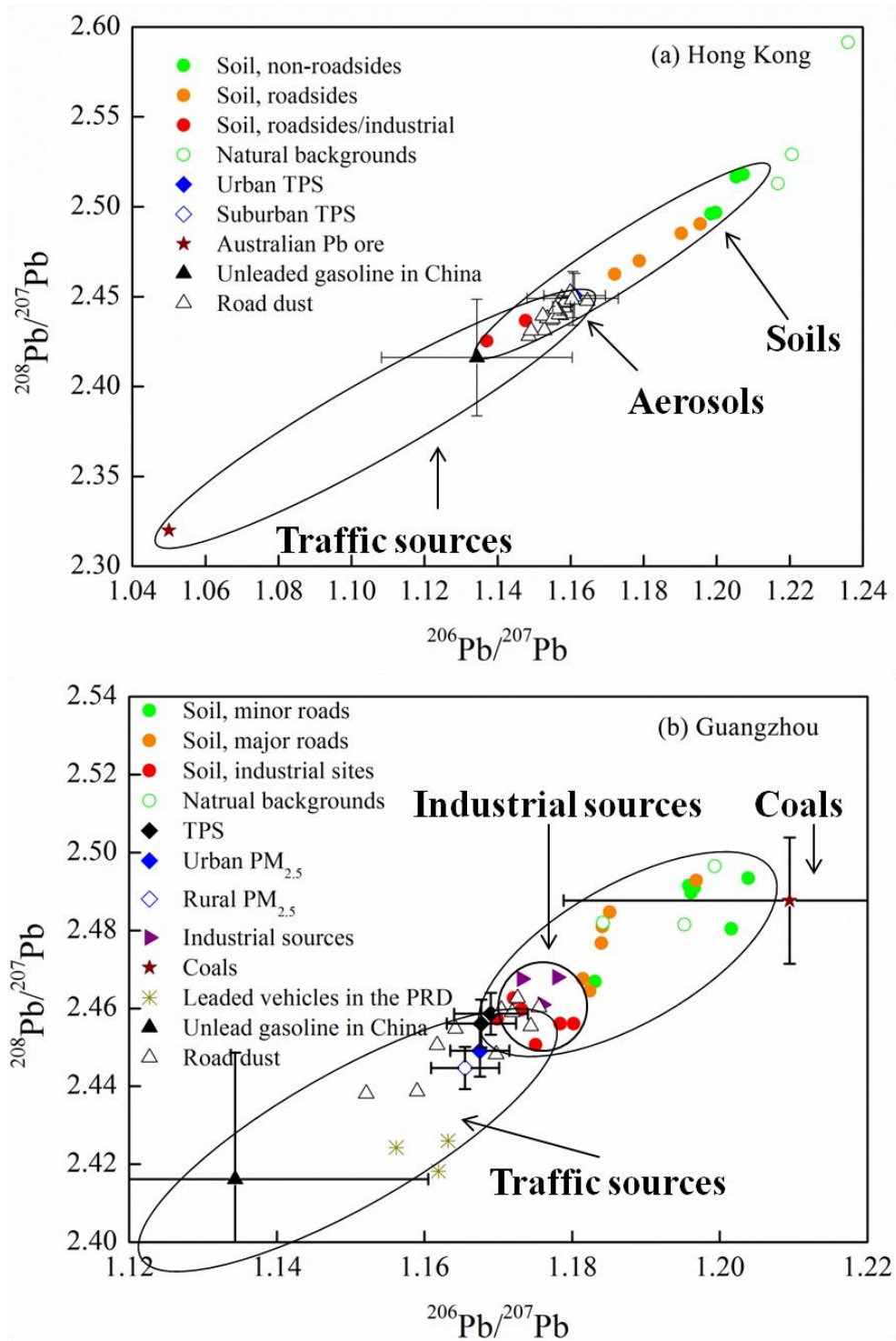


Figure 4.3 Lead isotopic compositions ($^{206}\text{Pb}/^{207}\text{Pb}$ vs $^{208}\text{Pb}/^{207}\text{Pb}$) of urban soils in Hong Kong (a) and Guangzhou (b) and other environmental samples. Detail information is listed in Table 4.7 and Table 4.8.

4.4 Vertical distribution of trace metals

To compare the difference of metal concentrations between surface and top soils, we calculated the surface accumulation factor (SAF, Table 4.9), which is defined as follows:

$$\text{SAF} = \frac{M_s - M_t}{M_t} \times 100\% ,$$

where, M_s is the metal concentration in surface soils (0 to 3 cm), and M_t is the corresponding metal concentration in top soils (0 to 15 cm). SAFs decreased in order of Ni (-3.1) > Zn (-4.9) > Cr (-5.6) > Co (-6.9) > Cu (-8.5) > Pb (-11) in urban soils of Hong Kong, while it decreased as Ni (23) > Cr (9.0) > Zn (7.8) > Cu (6.4) > Pb (4.8) > Co (0.7) in urban soils of Guangzhou (Figure 4.4). Assuming that the studied soils were undisturbed, surface soil, as the uppermost layer of top soil, is more susceptible to the on-going or recent anthropogenic sources, while the deeper soil usually indicates the legacy contamination (Luo et al., 2015). In both cities, SAFs of Pb showed the lowest or lower values, implying the low Pb inputs through atmospheric depositions. It was in line with the decreasing concentrations of Pb in urban soils after the phase-out of leaded gasoline (Figure 4.2).

51-76% of Guangzhou soils showed positive SAFs, whereas 51-76% of Hong Kong soils showed negative SAFs (Figure 4.4). The positive SAFs of Guangzhou soils indicated a continuous input of trace metals in urban soils of Guangzhou, which could be ascribed to the fast urbanization and industrial development. Table 4.10 summarized the historical developments of the two cities. The rapid economic growth of Guangzhou began in 1978. From 1982 to 2012, the gross industrial output, total number of vehicles, total consumption of energy, population density, domestic solid waste, and industrial solid waste, increased 159, 56, 6.5, 2.6, 7.5, and 3.7 folds, respectively, in Guangzhou (Guangzhou Bureau of Statistics, 1984; 2013). Thus, the rapid developments enhanced the surface accumulation of trace metals in Guangzhou urban soils. Conversely, the negative SAFs of Hong Kong soils could be caused by a decrease of trace metal inputs (Werkenthin et al., 2014). In Hong Kong, the industrial revolution started between 1945 and 1955. Secondary production (including manufacturing,

construction, and supply of electricity, gas and water) had a significant value-added contribution to the economy before the early 1980s. However, after a major restructuring of industry in the 1980s and early 1990s, the value-added contribution to gross domestic product (GDP) from manufacturing decreased 32% from 1982 to 2012 in Hong Kong (Census and Statistics Department, 2013). It can be further supported by the Pb isotopic compositions (Figure 4.5). The lower Pb isotopic compositions ($^{206}\text{Pb}/^{207}\text{Pb}$) of surface soils compared to top soils in Guangzhou illustrated the continuous anthropogenic inputs of Pb in Guangzhou urban soils through atmospheric deposition. In contrast, the higher Pb isotopic compositions ($^{206}\text{Pb}/^{207}\text{Pb}$) of surface soils than those of top soils in Hong Kong implied the decline of Pb inputs. Apparently, the historical urbanization and industrialization of a city can result in a somewhat-unique characteristic soil geochemical signature.

Once trace metals from anthropogenic sources enter the soil, their distribution and transport are primarily a function of soil properties, such as TOC, pH, mineral composition, and others (Davis et al., 2009; Li et al., 2015; Walraven et al., 2014). The average TOC of Hong Kong soils was 13.7 g kg^{-1} , much lower than that of Guangzhou soils (29.1 g kg^{-1}). The higher TOC of urban soils in Guangzhou could enhance the binding with trace metals, and hence improve metal retention (Turer et al., 2001; Walraven et al., 2014). In addition, the higher contents of clay minerals in Guangzhou soils (14.4%, (Lu et al., 2007)) provide more adsorption sites for trace metals, resulting in the stronger binding capacity of Guangzhou soils compared to Hong Kong soils (7%, (Luo et al., 2012a)). The median pH of Hong Kong soils was 6.06 with a range of 4.6 to 8.5, whereas the median pH of Guangzhou soils was 7.4 with a range from 3.8 to 8.2. The neutral or even above neutral pH of Guangzhou soils can reduce metal mobility as compared to Hong Kong soils (Kocher et al., 2005). Furthermore, the higher annual precipitation of Hong Kong (2399 mm, 1981 to 2010, Hong Kong Observatory) than Guangzhou (around 1800 mm, Guangzhou Meteorological Bureau) may also facilitate trace metal transport from surface to deeper soils (Werkenthin et al., 2014). These different geochemical and climatic conditions could reinforce the different SAFs in the two cities.

Table 4.9 Surface accumulation factors (SAFs, %) of urban soils in Hong Kong and Guangzhou.

		Al	Ca	Co	Cr	Cu	Fe	Mg	Mn	Ni	Pb	Zn
Hong Kong	Mean±SD	-12±14	12±45	0.4±51	9.4±76	-2.4±30	-6.2±12	-5.0±25	-7.2±30.5	4.3±59	-9.0±23	3.1±29
	Median	-13	3.1	-6.9	-5.6	-8.5	-6.4	-8.2	-12	-3.1	-11	-4.9
	Range	-47–73	-78–240	-65–359	-79–610	-57–222	-46–51	-85–99	-78–134	-97–411	-70–90	-45–110
Guangzhou	Mean±SD	-17±24	66±187	2.3±26	15±451	32±124	-1.2±21	10±48	38±221	30±51	17±56	30±95
	Median	-20	7.5	0.7	9.0	6.4	-2.3	2.4	1.6	23	4.8	7.8
	Range	-80–83	-69–1488	-64–86	-75–191	-83–1331	-67–106	-68–358	-100–1957	-62–297	-76–345	-84–982

Table 4.10 Historical development of Guangzhou and Hong Kong.

Guangzhou	Hong Kong				
	1982	2012		1982	2012
Population density (person/km ²)	4.79E+02	1.73E+03	Population density (person/km ²)	4.93E+03	6.48E+03
Vehicle number	4.31E+04	2.44E+06	Vehicle number	3.40E+05	7.18E+05
Gross output value of industry (Yuan)	1.07E+10	1.71E+12	Gross output value of manufacturing (HKD)	4.52E+10	3.06E+10
Total consumption of energy (standard coal, tonne)	6.91E+06	5.16E+07	Primary energy requirements (terajoule)	2.47E+05	5.78E+05
Industrial solid waste produced (tonne)	1.31E+06	6.14E+06	Industrial solid waste produced (tonne)	3.45E+05	2.67E+05
Domestic solid waste(tonne)	4.87E+05	4.13E+06	Domestic solid waste(tonne)	1.37E+06	2.30E+06

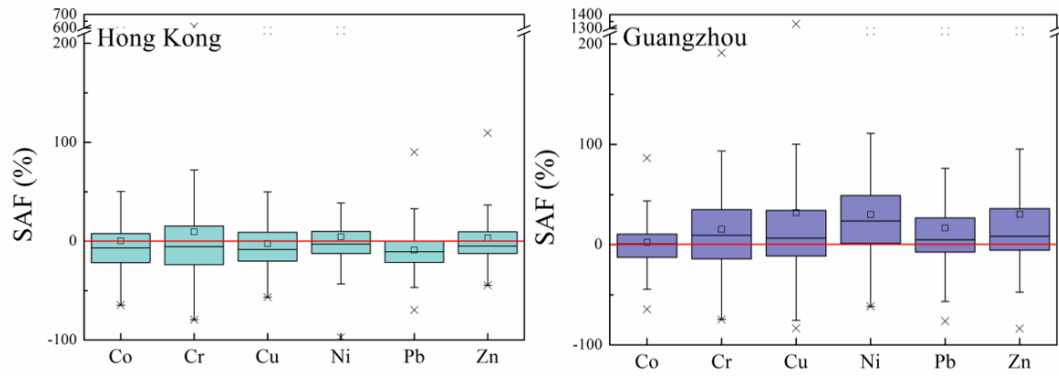


Figure 4.4 Surface accumulation factor (SAF,%) of urban soils in Hong Kong and Guangzhou.

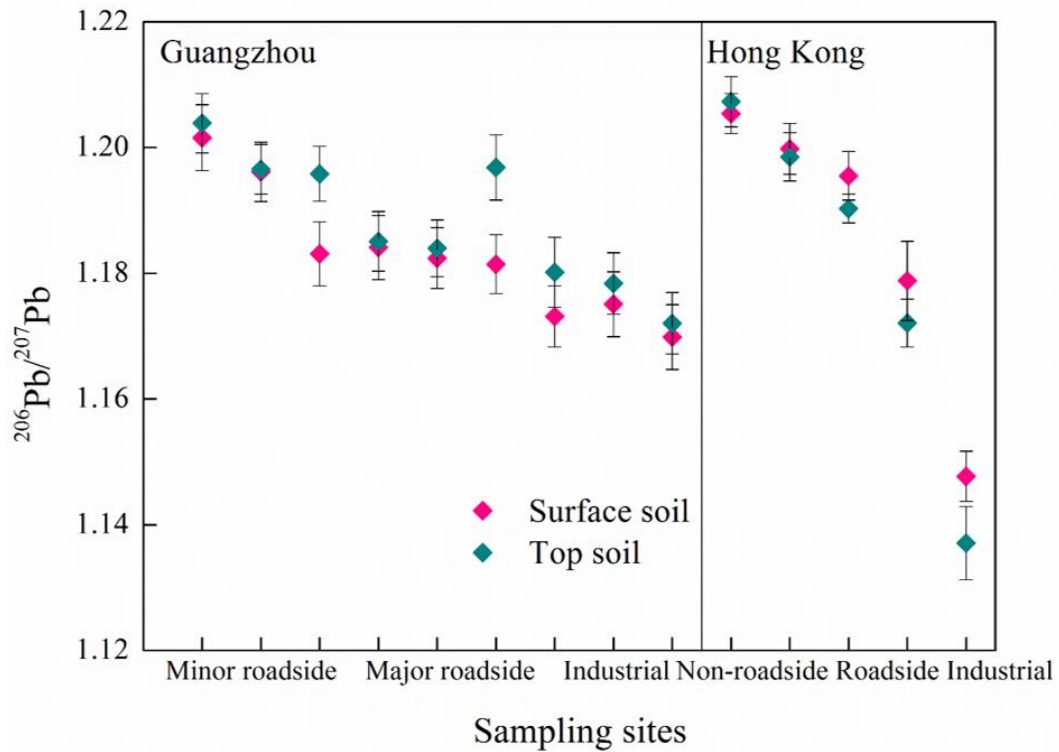


Figure 4.5 Comparison of Pb isotopic compositions ($^{206}\text{Pb}/^{207}\text{Pb}$) of surface and top soils in Hong Kong and Guangzhou. The error bars denote 1 SD.

4.5 Horizontal distribution of trace metals

In urban soils, metal enrichment results from different input sources, particularly anthropogenic activities. In order to investigate the metal distribution patterns and sources in

urban soils, geographical information system (GIS) mapping techniques were employed to produce spatial distribution maps for the trace metals in soils of Hong Kong and Guangzhou. The best-fit variogram model was selected according to cross-validation and the detail information was listed in the Appendix.

4.5.1 Trace metal distribution in urban soils of Hong Kong

To compare trace metal distribution patterns in the two urban regions, a higher density of sampling was conducted in the Kowloon area, which is highly urbanized with an extensive network of roads and high-rise buildings. A comparison of Figure 4.6 and Figure 4.7 shows that trace metals were distributed similarly in surface soils and top soils, reflecting the homogeneous sources of trace metals within the top 15 cm soil layer. With respect to different trace metals, similar spatial distribution patterns of Cu, Ni, Zn, and Pb were found in the geochemical maps, consistent with the statistical analysis in which strong associations were found among these metals (Table 4.11). Each of these four metals showed elevated concentrations in soils collected in the close vicinity of industrial buildings (the hot spots in Figure 4.6), indicating the past industrial contributions to trace metal accumulations in urban soils. Hot spot 1 was also found to be a major junction of roads that have a large amount of traffic, and at hot spot 2 frequent vehicle braking and stop-start maneuvers were observed (Figure 4.6 e). Therefore, traffic emissions seemed to be another important factor for trace metal contamination. The hot spots identified in the present study were also revealed in the study conducted by Li et al. (2004) based on similar distribution maps and comparable sampling area; however, no new hot spots was observed in the present study. Taking hot spot 1 as an example, Pb in top soils decreased from 131 to 118 mg/kg over the past ten years. Together with the negative SAF of Pb (-11%) at this location, it indicated a decrease of some anthropogenic sources (*e.g.*, leaded gasoline and industrial exhausts). This is in line with the development of Hong Kong that most of the labor-intensive industries moved to the China mainland in the 1980s and early 1990s, and a large number of the industrial buildings were

reformed to warehouses. In contrast, Cu and Zn in top soils slightly increased from 103 to 123 mg/kg, and from 477 to 489 mg/kg, respectively, over the past ten years, which can be attributed to the continuous production of traffic exhaust. The increases of Cu and Zn over the last decade only accounted for 16% of the Cu and 2% of the Zn in urban soils of this site, whereas the concentrations of Cu and Zn in soils of this site were enriched by 12 and 7.7 fold as compared to background. It infers that the past pollutant emissions were predominantly responsible for the metal contamination in these soils and that it may continue to influence local soils for a long time.

4.5.2 Trace metal distribution in urban soils of Guangzhou

The trace metal distribution in urban soils of the whole studied area of Guangzhou (about 200 km²) is discussed in Chapter Five. In this section, a comparable area including two districts (Liwan district and Yuexiu district) of Guangzhou was selected to compare trace metal distribution patterns with those in Hong Kong. The spatial distribution maps of trace metals in surface soils and top soils are shown in Figure 4.8 and Figure 4.9, respectively. Similar spatial distribution patterns of Cr, Cu, Pb, and Zn were found in the geochemical maps, consistent with their strong correlations in statistical analysis (Table 4.12). Different distribution patterns of each trace metal were found between surface soils and top soils in Guangzhou. In surface soils, Cr, Cu, Pb, and Zn concentrated in Liwan district where emissions from power plant and heavy traffic were found, reflecting the industrial and traffic influence on trace metal contamination (Duzgoren-Aydin et al., 2006; Luo et al., 2012b). Considering the processes involved in industrial and traffic activities, their influence on soil metals was mainly through atmospheric deposition. Compared with the surface soil layer Cu, Cr, Ni, and Zn concentrations, top soil layer contained lower metal concentrations. In top soils, all the trace metals displayed high concentrations in Yuexiu district, which has the longest development history and the highest population density. Municipal waste and domestic activities could contribute significantly to the trace metal contamination in this district. Therefore, the surface

soils in Guangzhou presented the impact through particle deposition while top soils recorded trace metal contamination resulting from urban development history.

4.5.3 Comparison between Hong Kong and Guangzhou

Trace metal concentrations presented uneven distribution patterns across the studied region from the two cities. In semi-variogram analysis, the ratio of nugget to sill (sum of partial sill and nugget) is commonly used to express the spatial autocorrelation of regional variables (Robertson et al., 1997; Shi et al., 2008). Generally, the variable has strong spatial autocorrelation, moderate spatial autocorrelation, and weak spatial autocorrelation when the ratio is less than 25%, 25 to 75%, and greater than 75%, respectively (Robertson et al., 1997; Rodríguez Martín et al., 2006). A weak spatial autocorrelation indicates that the variable is dominated by a short-range structure and greatly associated with human activities. The spatial autocorrelations of trace metals in urban soils at the two regional sites are listed in Table 4.13. In urban soils of Hong Kong, Cr, Cu, Ni, Pb, and Zn showed moderate spatial autocorrelations, indicating that these metals were affected by both anthropogenic and natural factors, while Co showed strong spatial autocorrelations, indicating its natural origin. In urban soils of Guangzhou, Cu, Pb, and Zn showed weak spatial autocorrelations, which implied that these metals were predominated by anthropogenic sources, while Co, Cr, and Cu showed moderate spatial autocorrelations, indicating their mixed sources from both anthropogenic and natural processes. Compared to trace metals in Hong Kong soils, the metals of Guangzhou soils presented weaker spatial autocorrelations, illustrating the stronger anthropogenic impacts on urban soils of Guangzhou. This result is in accordance with the higher contamination levels of urban soils in Guangzhou.

In terms of the spatial distribution patterns, remarkable hot spots of trace metals were in close vicinity of industrial buildings and heavy traffic areas with a long development history in both surface and top soils in Hong Kong. In these areas, trace metal concentrations were higher in top soils than those in surface soils, indicating the past industrial and traffic contributions to

trace metal accumulations in urban soils. Although trace metal concentrations declined in Hong Kong soils over the last twenty years, metal contamination was still existed in the past industrial areas and might continue to influence local soils for a long time. In Guangzhou, different distribution patterns of each trace metal were found between surface and top soils. The hot spots of trace metals resulting from industrial emissions were found in surface soils, implying the continuous industrial inputs through atmospheric deposition, while hot spot in top soils was in a district with the longest development history. Both located in the PRD region, Hong Kong soils recorded soil contamination mainly caused by historical development, whereas Guangzhou soil reflected soil contamination resulting from the on-going urbanization and industrialization. The different developing processes, and the concomitant soil contamination patterns in Hong Kong and Guangzhou highlighted the consistence of soil contamination. Hence, it is important to balance the urbanization and industrialization processes with environmental quality. As urban areas continue to grow, previous land uses and trace metal concentrations in soils should be paid more attention for an appropriate development and sustainable management of a city.

Table 4.11 Correlation matrix for trace metals in urban soils of Hong Kong.

	Surface soil					Top soil				
	Co	Cr	Cu	Ni	Pb	Co	Cr	Cu	Ni	Pb
Cr	0.216**					0.248**				
Cu	0.310**	0.448**				0.210**	0.433**			
Ni	0.180*	0.469**	0.635**			0.112	0.245**	0.319**		
Pb	0.053	0.244**	0.563**	0.383**		0.093	0.326**	0.561**	0.315**	
Zn	0.129	0.417**	0.877**	0.626**	0.539**	0.230**	0.372**	0.896**	0.365**	0.546**

** : $p < 0.01$; * : $p < 0.05$.

Table 4.12 Correlation matrix for trace metals in urban soils of Guangzhou.

	Surface soil					Top soil				
	Co	Cr	Cu	Ni	Pb	Co	Cr	Cu	Ni	Pb
Cr	0.354**					0.498**				
Cu	0.372**	0.653**				0.289**	0.704**			
Ni	0.309**	0.808**	0.578**			0.107	0.519**	0.672**		
Pb	0.325**	0.410**	0.662**	0.322**		0.351**	0.578**	0.595**	0.232**	
Zn	0.252**	0.401**	0.775**	0.348**	0.727**	0.246**	0.557**	0.694**	0.434**	0.691**

** : $p < 0.01$.

Table 4.13 Theoretical semivariogram models of predication.

		Surface soil		Top soil	
	Metal	Semivariogram model	Nugget/sill	Semivariogram model	Nugget/sill
Hong Kong	Co	Exponential	0.21	Exponential	0.21
	Cr	Exponential	0.34	Spherical	0.33
	Cu	Exponential	0.37	Spherical	0.34
	Ni	Exponential	0.36	Exponential	0.31
	Pb	Exponential	0.48	Exponential	0.46
	Zn	Spherical	0.38	Spherical	0.34
Guangzhou	Co	Exponential	0.29	Exponential	0.28
	Cr	Exponential	0.61	Spherical	0.59
	Cu	Exponential	0.93	Exponential	0.92
	Ni	Exponential	0.43	Spherical	0.38
	Pb	Exponential	0.78	Exponential	0.78
	Zn	Exponential	0.91	Exponential	0.88

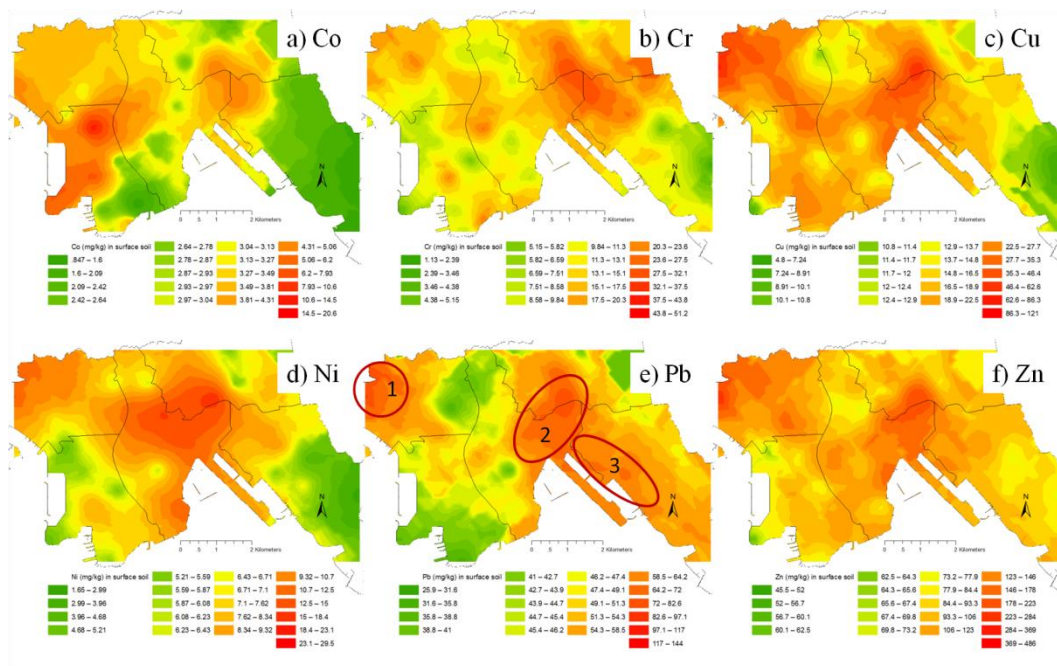


Figure 4.6 Trace metal distribution in surface soils of Hong Kong. The hot spots were circled with red in (e).

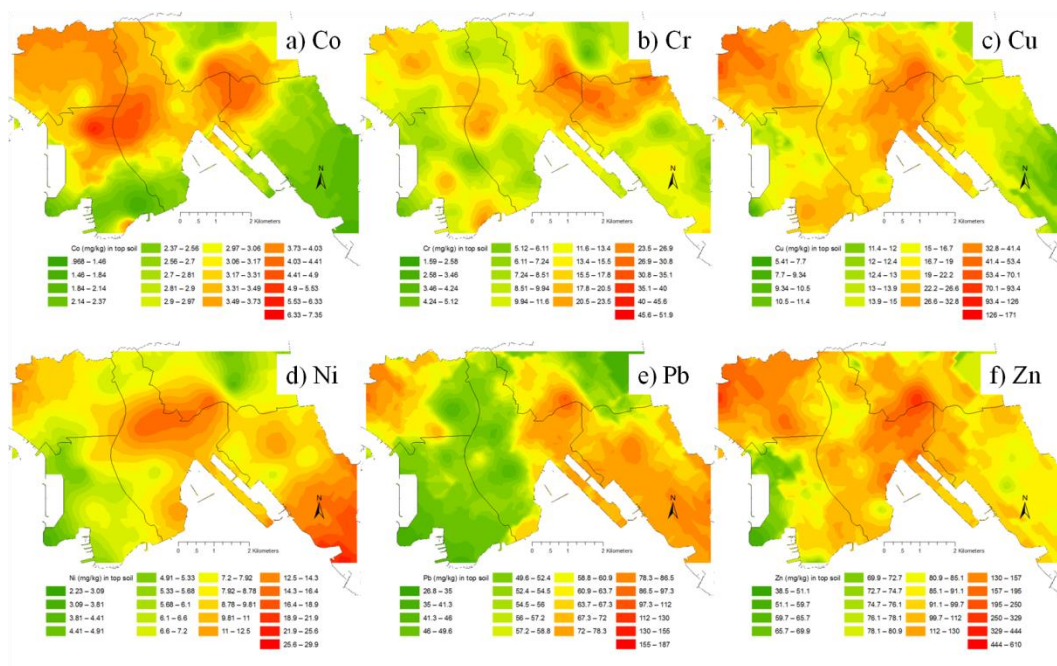


Figure 4.7 Trace metal distribution in top soils of Hong Kong.

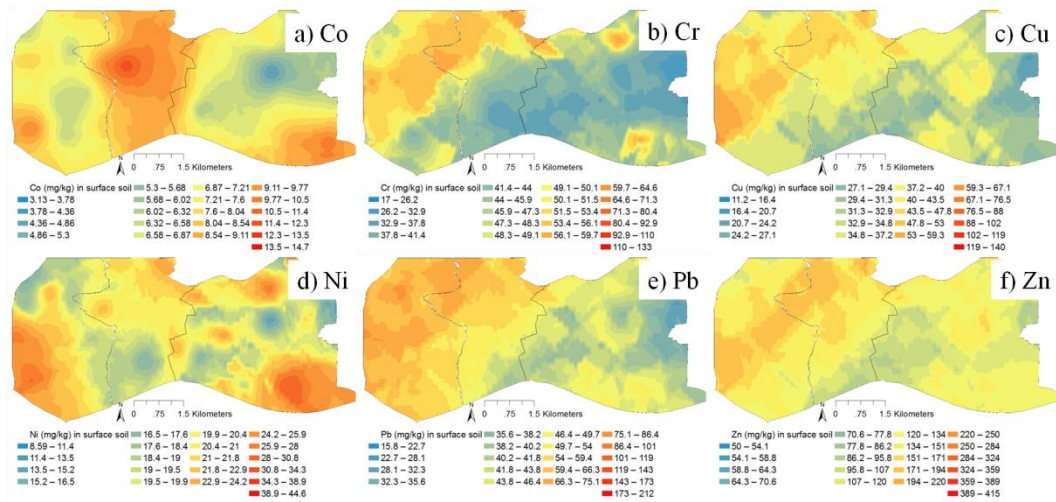


Figure 4.8 Trace metal distribution in surface soils of Guangzhou.

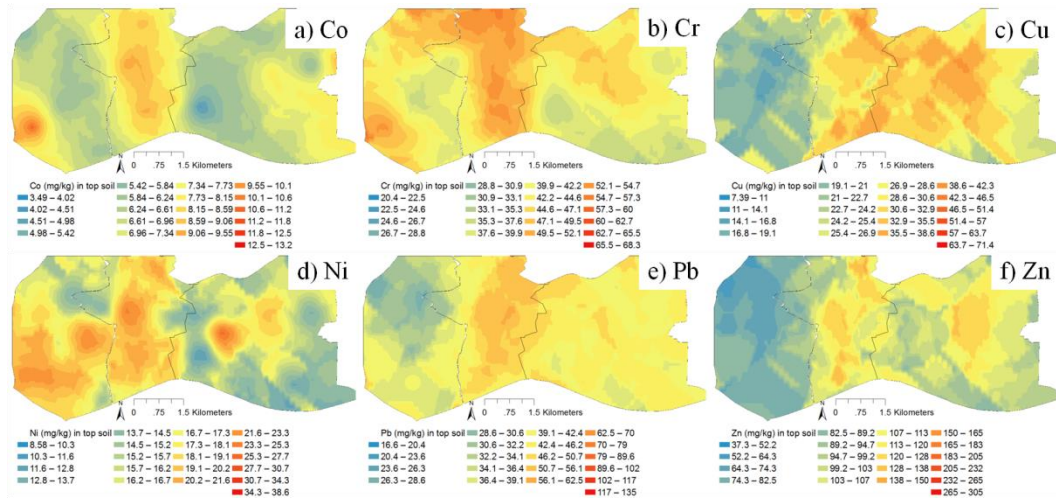


Figure 4.9 Trace metal distribution in top soils of Guangzhou.

4.6 Summary

This study made an interregional comparison on trace metal distribution in urban soils at a city scale. The major results are listed below:

1. Trace metals including Cu, Ni, Pb, and Zn in urban soils of Hong Kong and Co, Cr, Cu, Ni, Pb, and Zn in urban soils of Guangzhou exceed their background values, indicating a soil

contamination by these metals. Compared with historical dataset, Cu, Pb, and Zn in urban soils of Hong Kong decreased, while Co, Cr, Cu, Ni, and Zn in urban soils of Guangzhou increased over the last twenty years.

2. In Hong Kong, significant linear correlation between $^{206}\text{Pb}/^{207}\text{Pb}$ and $^{208}\text{Pb}/^{207}\text{Pb}$ was observed within urban soils, backgrounds and Australian Pb ore, suggesting a binary mixing of lead sources. The Pb isotopic compositions of urban soils in Guangzhou fell within the range of traffic/industrial/coal combustion sources and background, indicating the influence of Pb from mixing sources in urban soils of Guangzhou.

3. The median values of surface accumulation factors (SAFs) of Hong Kong soils were negative (-10.7 to -3.1), as a result of the decreasing anthropogenic inputs. In contrast, the SAFs of Guangzhou soils were positive (0.7 to 23.4), indicating the continuous influence of trace metals from the developments of industries and transportation in Guangzhou. The vertical distribution of trace metals in top soil layers (0–15cm), therefore, can be used to reflect the temporal changes of trace metal contamination caused by specific urbanization and industrialization of a city.

4. In Hong Kong, the remarkable hotspots of trace metals in both surface and top soils were in close vicinity of industrial buildings and heavy traffic areas. A temporal comparison of a heavily polluted hot spot showed that Cu and Zn slightly elevated while Pb declined over the last twenty years. In surface soils of Guangzhou, hot spots were attributed to industry and heavy traffic, while in top soils, hot spot was in a district with the longest development history.

In summary, this interregional comparison showed a wide trace metal contamination in the two cities and that urban soils are good indicators of the history of urbanization and industrialization of a city. Industrial and traffic sources primarily contributed to the trace metal contamination in the two cities. Deciphering the contributions of contamination sources

to the urban environment matrix is critical for their corresponding regulation and remediation; however, the specific industrial and traffic contributions to soil contamination were not deciphered from each other in this study. As the trace metal contamination was heavier in Guangzhou soils than that in Hong Kong soils, more urban environmental compartments (*e.g.*, road dust, foliar dust, and plants) will be introduced in Guangzhou urban environment, to address their suitability for describing urban contamination conditions in a typical megacity in Chapter Five.

Chapter 5 Characterization, Source Apportionment, and Geochemical Interactions of Trace Metals in Soils, Road Dust, Plants, and Foliar Dust of an Urban Environment: Indicators for Urban Contamination

In this chapter, a multi-compartmental investigation was conducted in the urban environment of Guangzhou, which aims to understand whether there is any difference using different environmental compartments to monitor the trace metal contamination status in urban area and the transport of pollutants among environmental media, and the investigation was fulfilled by (1) investigating the spatial distribution of trace metal contamination in different environmental compartments, including surface soils, road dust, foliar dust and plants; (2) spatially quantifying the natural or anthropogenic contributions of trace metals using the APCS-MLR model, Kriging technique, and Pb isotopes; and (3) elucidating the transport of trace metals in the urban environment of Guangzhou.

5.1 Trace metal concentrations in different urban compartments

5.1.1 Urban soil

The concentrations of trace metals (Co, Cr, Cu, Ni, Pb, and Zn) in surface soils (0 to 3 cm) and top soils (0 to 15 cm) of Guangzhou urban area are summarized in Table 5.1. As compared to the background levels, 73–76% of the Co, 68–74% of the Cr, 93–97% of the Cu, 78–93% of the Ni, 59–69% of the Pb and 87–93% of the Zn in surface and top soils exceeded the corresponding concentration (Guangdong Geological Survey, 2010) (Table 5.2), indicating a wide range of soil contamination in Guangzhou. For surface soil, trace metals generally exhibited a significant correlation to that of top soil (0–15 cm) ($p < 0.01$, Table 5.3), showing their similar roles on identification for urban soil contamination. Because surface soil is more easily suspended to the air than top soil for human inhalation (Acosta et al., 2009;

Miguel et al., 1998), only surface soil would be discussed in the following sections.

The concentrations of Co, Cr, Cu, Ni, Pb, and Zn in different land use areas in Guangzhou are shown in Figure 5.1. Approximately 70–100% of the suburban samples, 73–97% of the institution/park samples, 67–96% of the residential samples, 54–96% of the commercial samples, 85–100% of the industrial samples, and 100% of the orchard samples exceeded the background value of Guangzhou. Specifically, trace metal concentrations from industrial and orchard areas were significantly ($p < 0.05$) higher than those from other land use areas, showing severe trace metal contamination from those anthropogenic activities in urban environment, which needs remediation before further land reuse. Compared to the standards (Table 5.2), the average concentrations of Pb (106 mg kg^{-1}) and Zn (328 mg kg^{-1}) in industrial soils exceeded the soil quality guideline of the Netherlands (Pb, 85 mg kg^{-1} ; Zn, 140 mg kg^{-1}) (VROM, 2000), and the average concentrations of Cu (102 mg kg^{-1}), Pb (94.5 mg kg^{-1}) and Zn (250 mg kg^{-1}) in orchard soils exceeded the soil quality guidelines of the Netherlands (VROM, 2000) and agricultural soil guidelines of Canada (Cu, 60 mg kg^{-1} ; Pb, 70 mg kg^{-1} ; Zn, 200 mg kg^{-1}) (CCME, 2007).

5.1.2 Road dust

Greater variability in metal concentrations of road dust was observed for Cr, Cu, Ni, Pb, and Zn with ranges of 15.1 to 498 mg Cr/kg, 20.5 to 438 mg Cu/kg, 9.2 to 88.8 mg Ni/kg, 25.6 to 280 mg Pb/kg, and 87.9 to 992 mg Zn/kg (Table 5.1), corresponding to anthropogenic origins (Ordóñez et al., 2015). Comparing to the nearby corresponding soil samples, most of the road dust showed higher concentrations of trace metals, particularly for Cu, Zn and Pb, consistent with previous publication (Shi et al., 2008). In comparison with the background values (Table 5.2), the median concentrations of Cu and Zn in road dust were enriched by 7.7 and 6.3 folds, respectively, suggesting their specific traffic origins, probably from brake abrasion and tire wear (Li et al., 2018; Li et al., 2001; Rogge et al., 1993). The road dust samples generally showed black color, suggesting brake abrasion and tire debris products. Various traffic

conditions including traffic volume and speed considerably affect trace metal concentrations if considering the traffic source as the primary contribution source (Duong and Lee, 2011). By grouping the samples based on traffic volume and speed, it was found that the concentrations of Cu, Zn, and Co in road dust slightly increased with the increasing traffic volume (Figure 5.2). Some studies have reported that high occurrence of braking on road, particularly during heavily congested traffic periods, produces more Cu/Zn/Pb contamination in road dust (Harrison et al., 2012; Sahu and Elumalai, 2017). The effect of traffic speeds on trace metal variation was not quite discernible (Figure 5.3). Interestingly for Pb concentrations in road dust, no significant effect was observed by traffic volume and speed possibly because of the use of lead-free petrol in Guangzhou since 1997. In addition, a great decline of Pb concentrations in the road dust was found, from 199 mg/kg in 2003 (Duzgoren-Aydin et al., 2007) (Table 5.2) to 76.2 mg/kg in 2012 as a result of the phase-out of leaded gasoline in Guangzhou, while the concentrations of Cu and Zn in 2003 (Duzgoren-Aydin et al., 2007) and in 2012 (present study) did not vary much over time. Therefore, considering the relation of Cu/Zn to traffic conditions (Figure 5.2), Cu/Zn levels may be considered as an environmental marker for traffic sources in recent years rather than Pb.

In addition to traffic factors, we observed increasing concentrations of trace metals including Cr, Cu, Pb, and Zn in road dust in the industrial area, suggesting considerable influence of industrial sources on road dust (Figure 5.1). Other factors such as urban waste during transportation; city construction and building restorations; the use of pesticides, fertilizers, and medical devices; plant fragments from nearby vegetation; and soil originated deposits may also result in contamination to road dust, making the contamination sources more complex (Charlesworth et al., 2011; Men et al., 2018; Rogge et al., 1993).

5.1.3 Plants and foliar dust

Trace metal concentrations in plants decreased remarkably and the ranges of trace metal concentrations narrowed greatly compared to trace metals in soils and road dust (Table 5.1). Median trace metal concentrations of the washed grass (0.25 mg Co/kg, 6.79 mg Cr/kg, 11.9 mg Cu/kg, 5.19 mg Ni/kg, 2.96 mg Pb/kg, and 46.0 mg Zn/kg) were significantly higher than those of the washed tree leaves (0.16 mg Co/kg, 0.967 mg Cr/kg, 6.68 mg Cu/kg, 0.645 mg Ni/kg, 1.67 mg Pb/kg, and 19.8 mg Zn/kg), which could be ascribed to the different abilities of plants to absorb trace metals. In both washed tree leaves and washed grass, trace metal concentrations were within the limit of excessive or toxic levels of plant (Kabata-Pendias, 2000) (Table 5.2), indicating that trace metals in the Guangzhou urban environment pose little threat to plant growth.

The washing process removed 12 to 79%, 13 to 92%, 13 to 71%, 4 to 87%, 14 to 98%, and 5 to 76% of Co, Cr, Cu, Ni, Pb, and Zn on tree leaves, respectively, which was similar to some recent studies (Al-Khashman et al., 2011; Bi et al., 2012; Serbula et al., 2012). The efficiency of the washing process decreased as: Cr > Pb > Ni > Co > Cu \approx Zn (Table 5.4), probably due to the foliar uptake abilities for different metals. Similarly, Kabata-Pendias (2000) found that only a small portion of Cu and Zn could be washed off from plants due to the greater foliar uptake of these trace metals by plants compared to other trace metals, such as Pb. Trace metal concentrations of the washed samples showed significant differences ($p < 0.05$) in comparison to those of the unwashed samples, suggesting deposited trace metals on leaf surface from suspended soil particles and atmospheric particular matter (Deljanin et al., 2016). Foliar dust in industrial region showed relatively higher concentrations of trace metals than those from the other land use areas (Figure 5.1) with significance for Pb ($p < 0.05$), showing deposition of atmospheric particles from industrial sources. Correspondingly, trace metal in foliar dust decreased with increasing distance from the emission source (*e.g.*, a power plant and steel factory), as identified by Pb and Zn with significant difference ($p < 0.05$, Figure 5.4).

Table 5.1 Trace metal concentrations (mg kg⁻¹) in different compartments.

Sample (n)		Co	Cr	Cu	Ni	Pb	Zn
Surface soils (180)	Mean±SD	8.60±3.34	54.8±29.5	44.1±32.9	24.2±17.4	57.4±30.4	153±99.4
	Median	7.94	48.7	35.2	20.2	49.4	126
	Range	2.75-18.2	17.0-283	4.90-209	7.86-201	14.5-212	31.9-671
Top soils (180)	Mean±SD	8.77±3.97	50.2±21.4	43.1±45.2	21.7±35.2	56.9±46.8	136±101
	Median	7.95	45.8	32.5	17.6	47.0	108
	Range	2.50-32.0	14.4-109	4.48-441	5.53-478	8.35-451	23.2-693
Road dust (178)	Mean±SD	6.90±1.76	64.3±49.9	102±78.6	23.6±11.2	84.1±41.2	384±164
	Median	6.67	55.4	80.1	20.8	76.2	361
	Range	3.77-14.0	15.1-498	20.5-438	9.20-88.8	25.6-280	87.9-992
Foliar dust (160)	Mean±SD	8.09±3.97	129±77.1	225±126	40.8±25.4	216±277	744±731
	Median	7.51	115	201	34.8	165	563
	Range	1.21-21.7	7.66-541	47.2-895	3.73-192	33.6-3024	72-7533
Washed leaves (160)	Mean±SD	0.16±0.032	1.03±0.473	6.90±1.71	0.70±0.264	2.30±2.71	20.6±5.63
	Median	0.16	0.967	6.68	0.65	1.67	19.8
	Range	0.09-0.28	nd* -3.10	3.83-13.3	0.26-2.24	0.24-26.7	11.3-45.9

*: nd, non-detectable.

Table 5.2 Trace metal concentrations (mg kg⁻¹) in standards, backgrounds, and some environmental samples.

Sample	Co	Cr	Cu	Ni	Pb	Zn	Reference
Chinese soil quality standard II	-	200	100	50	300	250	CEPA (1995)
Dutch	9	100	36	35	85	140	VROM (2000)
Canadian(residential/parkland)		64	63	50	140	200	CCME (2007)
Canadian(commercial)	-	87	91	50	260	360	CCME (2007)
Canadian(industrial)	-	87	91	50	600	360	CCME (2007)
Canadian(agricultural)	-	64	60	50	70	200	CCME (2007)
Guangzhou background soil	6.3	39	10.4	12.3	41	58	Guangdong Geological Survey (2010)
Road dust (n=13)	-	-	93	-	199	360	Duzgoren-Aydin et al. (2007)
Excessive/toxic level of plants	5-30	20-100	10-100	30-300	-	100-400	Kabata-Pendias (2000)

Table 5.3 Correlation matrix for trace metals in each compartment.

		Surface soil	Top soil	Road dust	Washed leaf
Co	Top soil	0.803**			
	Road dust	0.098	0.136		
	Washed leaf	-0.046	0.041	0.096	
	Foliar dust	-0.040	0.102	0.072	0.045
Cr	Top soil	0.568**			
	Road dust	0.269**	0.120		
	Washed leaf	-0.061	0.002	0.111	
	Foliar dust	-0.090	-0.014	0.038	0.188*
Cu	Top soil	0.728**			
	Road dust	0.111	0.014		
	Washed leaf	0.102	0.001	0.159*	
	Foliar dust	0.077	0.019	-0.004	0.286**
Ni	Top soil	0.705**			
	Road dust	0.183*	0.188*		
	Washed leaf	0.119	0.017	-0.020	
	Foliar dust	0.015	0.078	-0.071	0.059
Pb	Top soil	0.689**			
	Road dust	0.180*	0.132		
	Washed leaf	0.139	0.131	0.208**	
	Foliar dust	0.170*	0.128	0.210**	0.530**
Zn	Top soil	0.737**			
	Road dust	0.289**	0.234**		
	Washed leaf	0.236**	0.178*	0.225**	
	Foliar dust	0.199*	0.099	0.170*	0.380**

*: significant at the 0.05 level (2-tailed); **: significant at the 0.01 level (2-tailed).

Table 5.4 Washing efficiency (%) of tree leaves.

	Co	Cr	Cu	Ni	Pb	Zn
Mean	46.2	66.8	35.6	49.6	63.7	35.6
Range	11.9-78.8	12.9-92.3	12.7-70.5	4.24-86.5	14.1-97.9	5.09-76.3

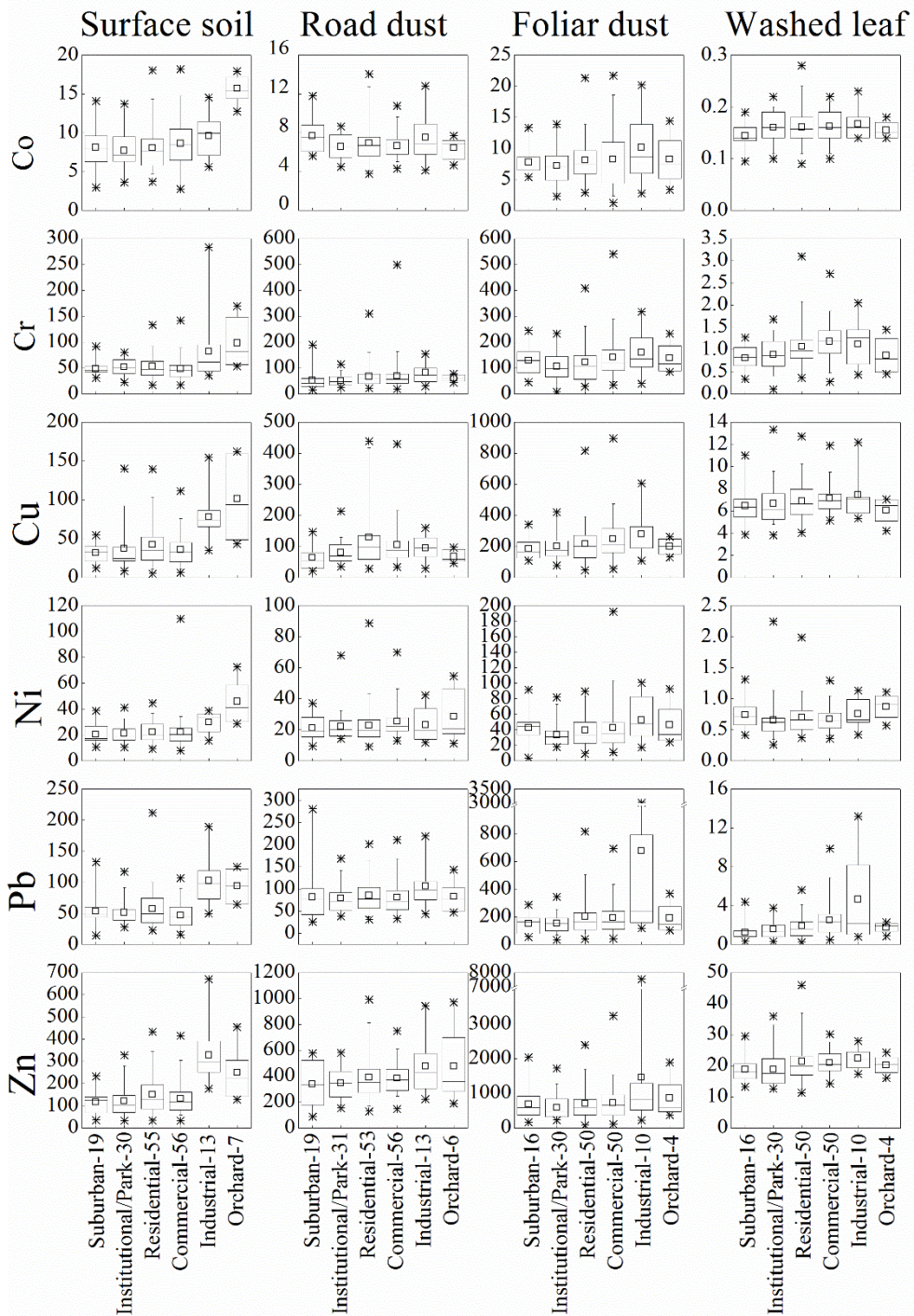


Figure 5.1 Distribution of trace metal concentrations (mg kg^{-1}) of environmental compartments in different urban land use areas with the sample numbers listed below the x-axis. The box represents the data between the 25th and 75th percentiles. The horizontal line inside the box indicates the median data. The small square indicates the mean data. The whiskers (error bars) above and below the box indicate the 95th and 5th percentiles. The asterisks indicate the 1st and 99th percentile.

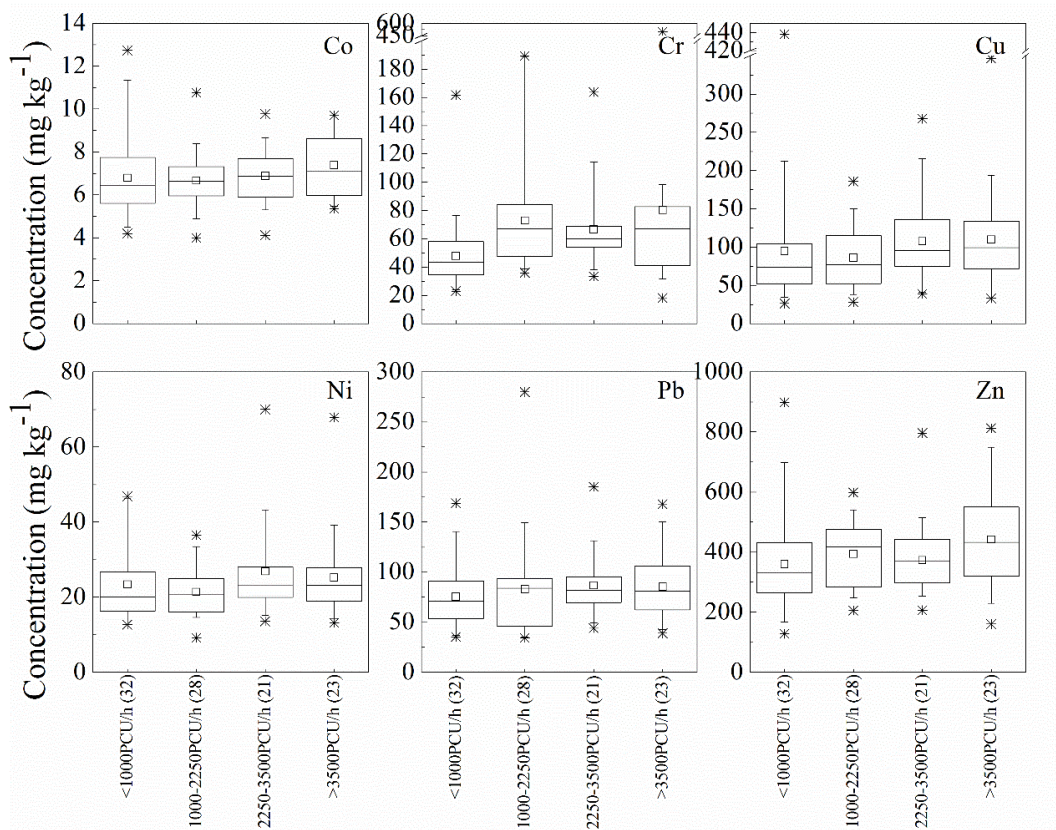


Figure 5.2 Impact of traffic volume on trace metal distribution in road dust with the sample numbers listed below the x -axis. Traffic flow of 104 roadside sampling sites (excluded industrial sites) were identified based on the traffic volume plotted by Guangzhou Transport Planning Research Institute (2012). The bars were defined (from the bottom) as the 1st percentile, 5th percentile, 25th percentile, median, mean (the square), 75th percentile, 95th percentile and 99th percentile.

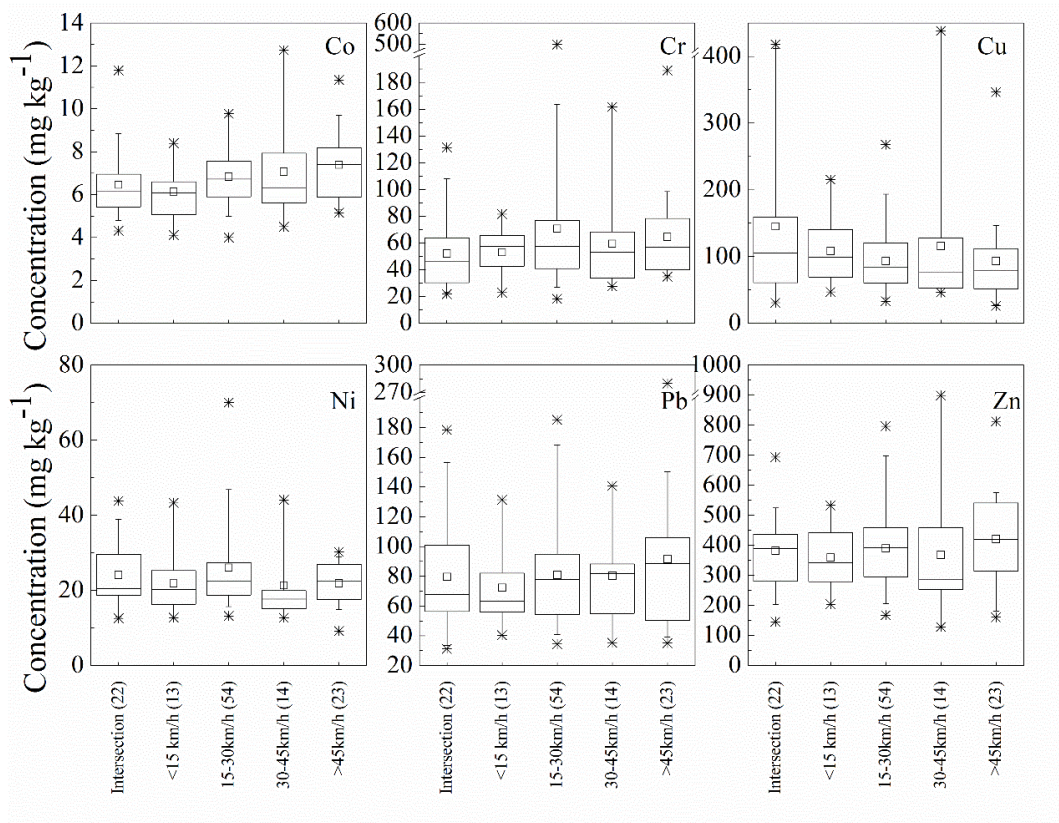


Figure 5.3 Impact of traffic speed on trace metal distribution in road dust with the sample numbers listed below the x -axis. Traffic flow of 104 roadside sampling sites (excluded industrial sites) were identified based on the vehicle speed plotted by Guangzhou Transport Planning Research Institute (2012). 22 samples collected near intersections were used for comparison. The bars were defined (from the bottom) as the 1st percentile, 5th, percentile, 25th percentile, median, mean (the square), 75th percentile, 95th percentile and 99th percentile.

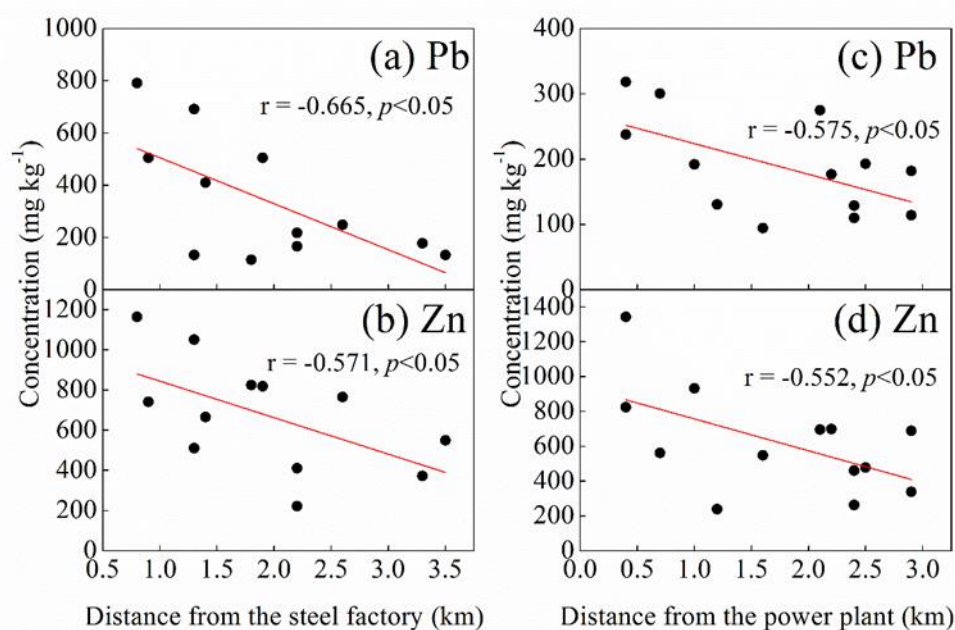


Figure 5.4 Impact of the steel factory (a-b) and power plant (c-d) on the Pb and Zn concentrations in the foliar dust. The x -axis indicates increasing distance from the industrial source. Pearson's r and p values were listed in the figure.

5.2 Spatial distribution of trace metals in surface soil, road dust, foliar dust, and tree leaves

A distribution map was developed for each element in each environmental compartment (Figure 5.5–Figure 5.8). In surface soils, high concentrations of trace metals were observed near a steel factory (southwest Guangzhou, Figure 5.5) and around the orchards (south Guangzhou, Figure 5.5). Trace metal contamination at similar sites has been reported in previous studies (Bi et al., 2013a; Li et al., 2006). Another hot spot was in a well-established commercial/industrial district with a dense population (Figure 5.5), which were possibly caused by coal combustion, and typical urban emissions from vehicles and commerce (Li et al., 2018; Luo et al., 2012b).

In road dust, the trace metal distribution patterns are shown in Figure 5.6, with clear spatial heterogeneity. High concentrations of Cu, Zn, Ni, and Pb were found in the area with high density of major roads and heavily congested traffic (shown with high volumes of traffic (Figure 5.9) and low vehicle speed (Figure 5.10)). Hot spots of Pb, Zn, Cr, and Co were also found in the areas near the industrial sites, such as the steel factory at southwest, brickyard, and some chemical industries in northeast, suggesting the industrial influence on road dust. In addition, the intensive traffic volume for industrial transport and frequent brake abrasion and stop-start maneuvers during loading/unloading often produce high amount of trace metals in industrial regions (Duong and Lee, 2011; Duzgoren-Aydin et al., 2006). It was demonstrated that driving conditions such as heavy load applied on the tire surface and harsh braking could increase the emission of tire wear particles which contained a large amount of trace metals, particularly Zn (Kim and Lee, 2018).

Tree leaves and foliar dust generally showed similar distribution patterns of trace metals to those of surface soil (Figure 5.5, Figure 5.7, and Figure 5.8), with hot spots around the power plant and the southwest and northeast areas where industrial activities prevail. Consistently, Liu et al. (2012) found the highest dust accumulation on leaves collected in the industrial areas of Guangzhou and significant accumulation of dust depositions on leaves was also found in industrial regions of a city in Italy (Sgrigna et al., 2015). It has been reported that gravity or wind impacts contribute to atmospheric dust deposits on leaves (Sgrigna et al., 2015; Song et al., 2015); therefore, foliar dust can reflect nearby contamination sources. Trace metal concentrations (mg kg^{-1}) in foliar dust varied with a decreasing order of Zn (744) > Cu (223) > Pb (216) > Cr (129) > Ni (40.8) > Co (8.09). This decreasing trend among metals of foliar dust was similar to that of the Guangzhou atmospheric dry depositional fluxes ($\text{mg/m}^2/\text{yr}$, Zn (54.1) > Cu (9.77) > Cr (6.53) > Ni (3.01) > Co (0.48)) (Huang et al., 2014a), indicating that trace metal concentrations in foliar dust were close associated with atmospheric dry deposition.

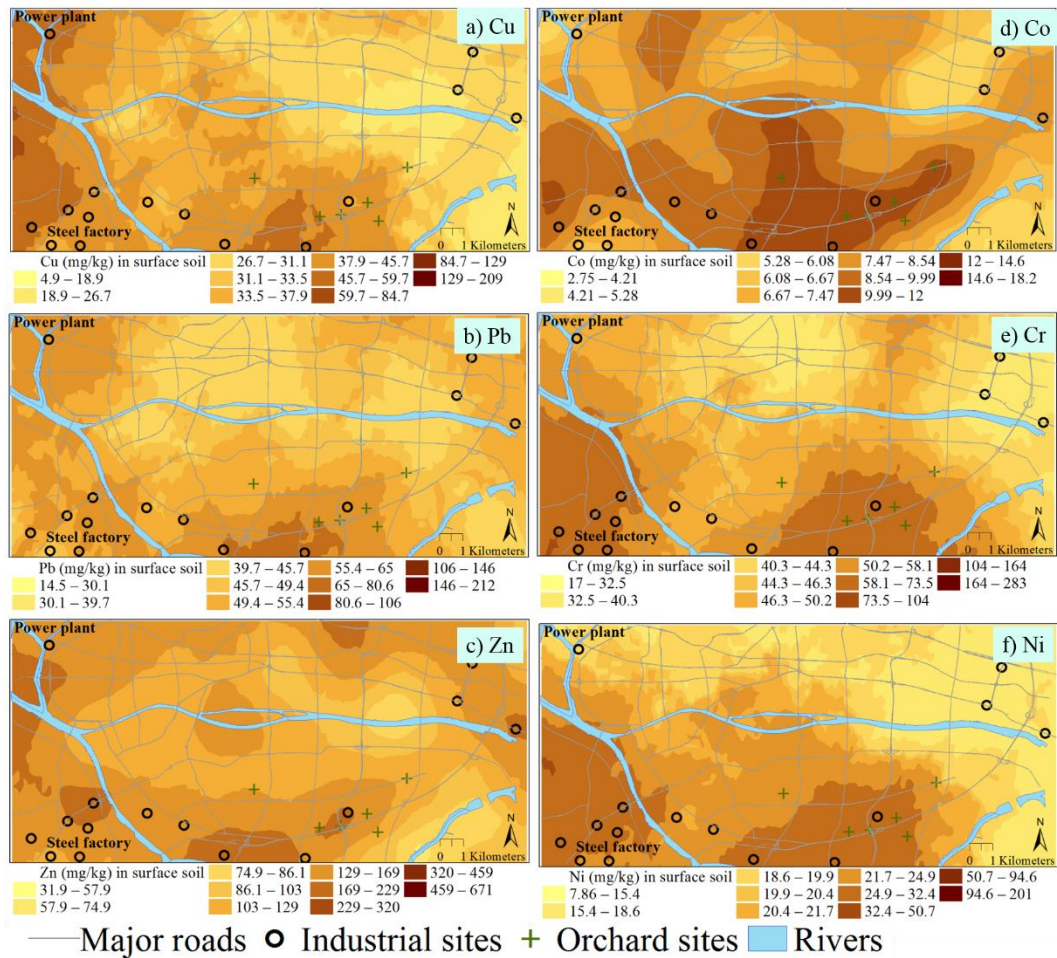


Figure 5.5 Distribution of trace metals (mg kg⁻¹) in surface soil.

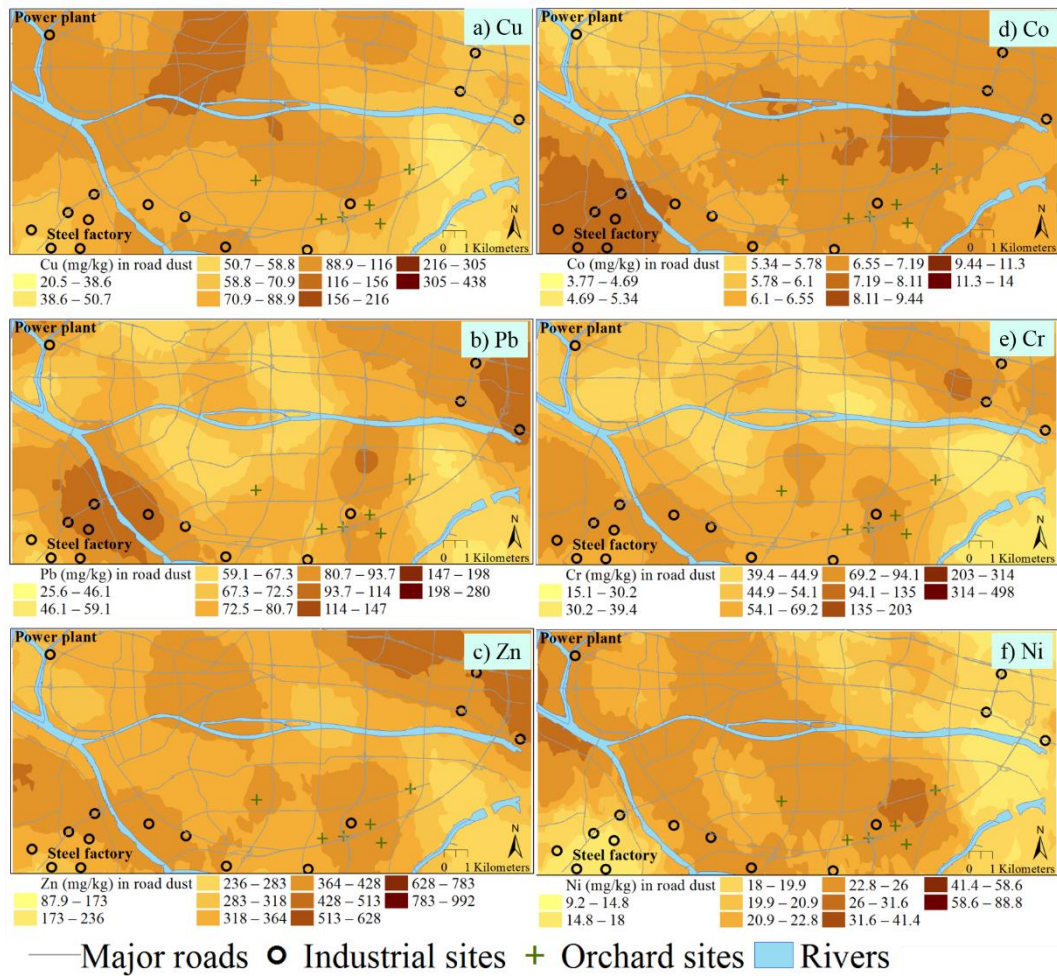


Figure 5.6 Distribution of trace metals (mg kg⁻¹) in road dust.

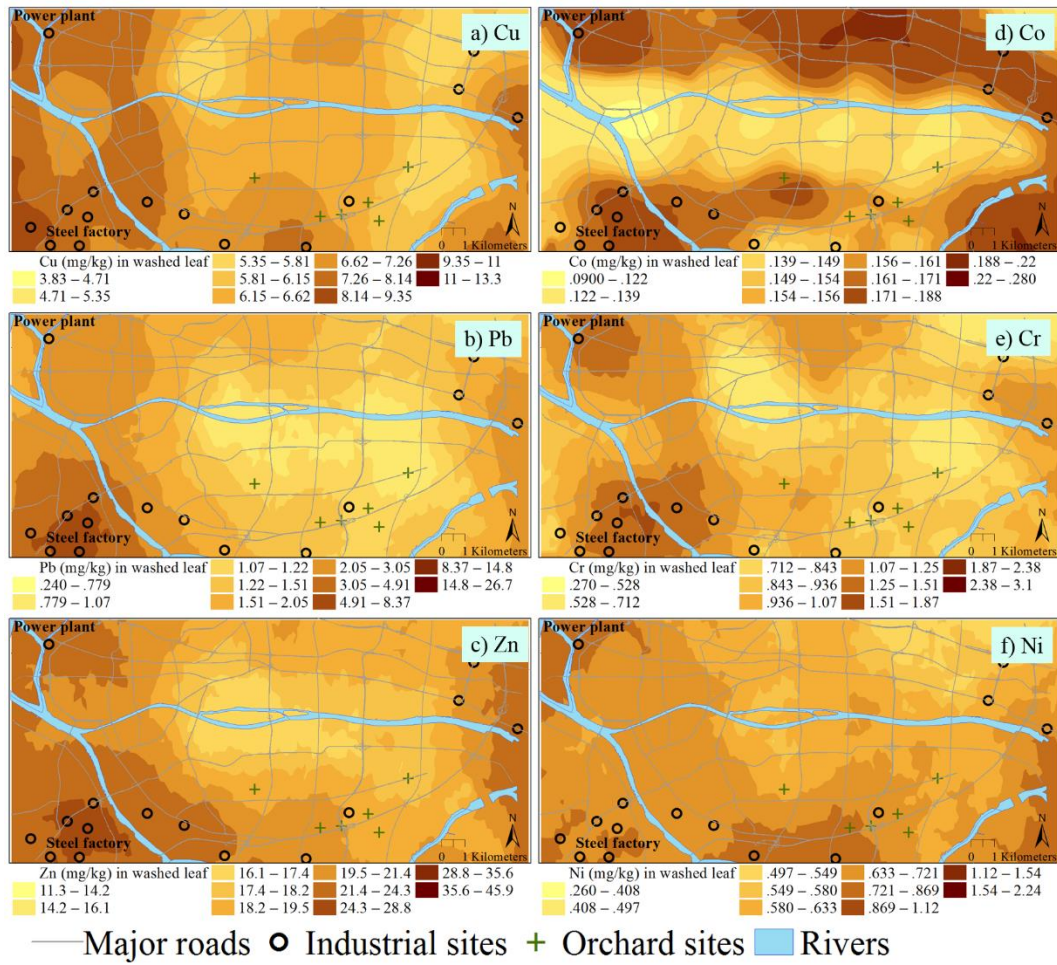


Figure 5.7 Distribution of trace metals (mg kg^{-1}) in washed tree leaves.

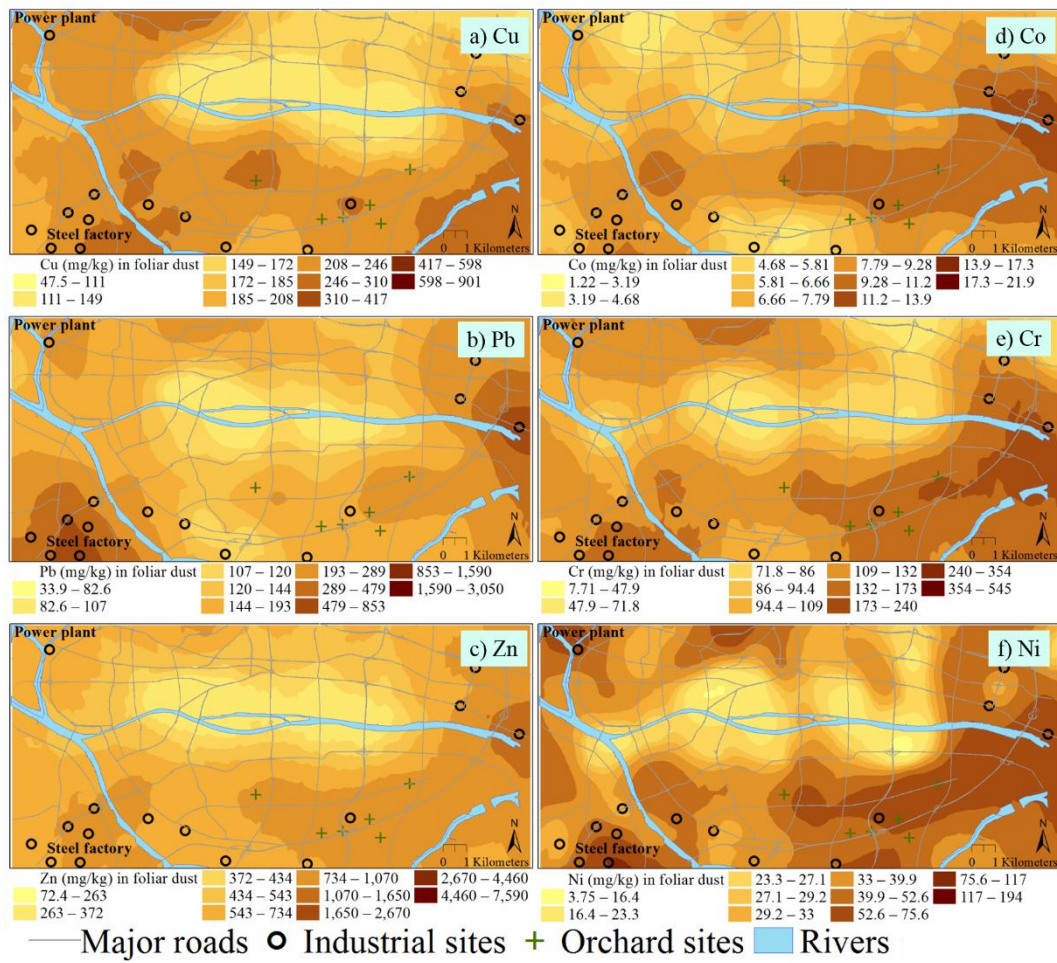


Figure 5.8 Distribution of trace metals (mg kg^{-1}) in foliar dust.



Figure 5.9 Distribution of major traffic network with traffic volume in Guangzhou urban area in 2012 (Guangzhou Transport Planning Research Institute, 2012). Traffic volume indicated from yellow to red lines approximated to <1000 , $1000-2250$, $2250-3500$, $3500-4750$, and >4750 PCU h^{-1} . The sampling area of the present study was within the black rectangle.

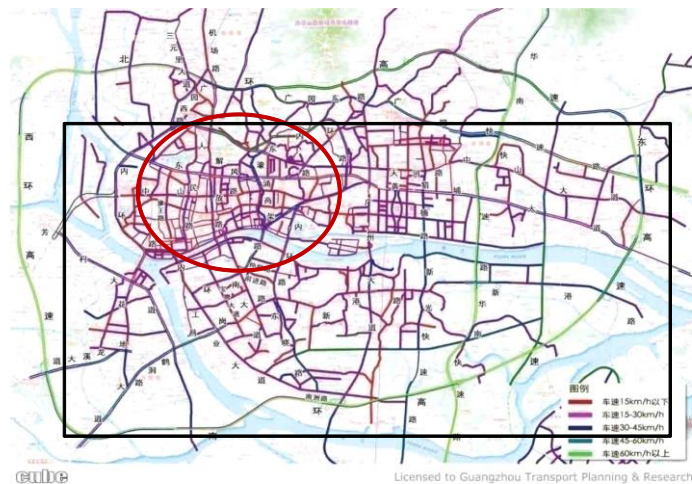


图4.17核心区道路车速分布图

Figure 5.10 Distribution of major traffic network with traffic speed in Guangzhou urban area in 2012 (Guangzhou Transport Planning Research Institute, 2012). Traffic speed indicated by red, purple, blue, dark green, and light green lines approximated to ≤ 15 , $15-30$, $30-45$, $45-60$, and ≥ 60 $km\ h^{-1}$. The sampling area of the present study was within the black rectangle. Roads with lowest traffic speed ($\leq 15\ km\ h^{-1}$) were concentrated in the area circled with red.

5.3 Source identification by Pb isotopic compositions

Lead isotopes were analyzed to identify the potential sources of trace metals, particularly Pb, in surface soil, road dust, tree leaves and foliar dust (Table 5.5). Generally, surface soil showed much higher $^{206}\text{Pb}/^{207}\text{Pb}$ and $^{208}\text{Pb}/^{207}\text{Pb}$ ratios compared to those in road dust, foliar dust, and $\text{PM}_{2.5}$. Similar scopes of Pb isotopic compositions were found in road dust, foliar dust, tree leaves, and $\text{PM}_{2.5}$, showing similar Pb sources and the possible transports between each other.

Lead isotopic compositions in surface soils were 1.1699–1.2039 for $^{206}\text{Pb}/^{207}\text{Pb}$ and 2.4506–2.4934 for $^{208}\text{Pb}/^{207}\text{Pb}$ (Table 5.5). The Pb isotopic compositions fell within a range of local traffic/industrial/coal sources and background values in Guangzhou (Figure 5.11), showing mixing sources contributed to the Pb contamination in urban soils. The higher Pb concentrations in soil were linked to the lower $^{206}\text{Pb}/^{207}\text{Pb}$ and $^{208}\text{Pb}/^{207}\text{Pb}$ ratios (Figure 5.12 a), and thus Pb isotopic compositions ($^{206}\text{Pb}/^{207}\text{Pb}$ and $^{208}\text{Pb}/^{207}\text{Pb}$) in the heavier contaminated soils were found to be closer to the vehicular and industrial emission sources, which was consistent with the results discussed in section 4.3.

For road dust, the Pb isotopic compositions ($^{206}\text{Pb}/^{207}\text{Pb}$ and $^{208}\text{Pb}/^{207}\text{Pb}$) were in the region between the unleaded gasoline, leaded gasoline, industrial sources, and urban soils (Figure 5.11). Historical used gasoline with Pb additives significantly contributed to Pb in the Guangzhou road dust before the prohibition of leaded gasoline and even several years thereafter (Duzgoren-Aydin, 2007). Nevertheless, in the present study, a significant linear correlation between $^{206}\text{Pb}/^{207}\text{Pb}$ and $^{208}\text{Pb}/^{207}\text{Pb}$ ($R^2=0.96$) was found in road dust samples and unleaded gasoline used in Chinese cities (Figure 5.11). Additionally, an overlap of Pb isotopic compositions ($^{206}\text{Pb}/^{207}\text{Pb}$ and $^{208}\text{Pb}/^{207}\text{Pb}$) was observed between road dust samples and unleaded gasoline samples (Figure 5.11). As shown in Figure 5.11, the Pb isotopic ratios ($^{206}\text{Pb}/^{207}\text{Pb}$ and $^{208}\text{Pb}/^{207}\text{Pb}$) of road dust were higher than those of soils with significant

difference ($p < 0.05$ for $^{206}\text{Pb}/^{207}\text{Pb}$; $p < 0.01$ for $^{208}\text{Pb}/^{207}\text{Pb}$), demonstrating the different sources of Pb between road dust and urban soils. Furthermore, the level of Pb contamination of road dust was negatively linked to the Pb isotopic ratios ($^{206}\text{Pb}/^{207}\text{Pb}$ and $^{208}\text{Pb}/^{207}\text{Pb}$) (Figure 5.12 b). Because a small amount of Pb (60–280 $\mu\text{g}/\text{L}$) remains in unleaded gasoline in China (Bi et al., 2017), this negative correlation highlighted the significance of unleaded gasoline (with lower Pb isotopic ratios) on Pb contamination in road dust. Similarly, vehicle exhaust from unleaded gasoline and diesel fuels has been reported as the major sources in Chinese road dust after the prohibition of leaded gasoline in Beijing (Yu et al., 2016) and Nanjing (Hu et al., 2014). The combined results indicated that the major Pb sources of road dust were from unleaded gasoline. In the industrial regions with heavier Pb contamination of road dust, the Pb isotopic compositions of road dust differed from those of the industrial sources but were near those of unleaded gasoline. Intensive vehicular traffic for industrial transport could cause an increase in the Pb concentration in industrial road dust (Duong and Lee, 2011; Duzgoren-Aydin et al., 2006). Our results indicated that heavy-duty vehicles for industrial transport instead of direct industrial emissions could largely contribute to the Pb contamination of road dust in industrial regions.

For tree leaves (Figure 5.11 and Table 5.5), the unwashed leaves showed values of 1.1677–1.1738 for $^{206}\text{Pb}/^{207}\text{Pb}$ and 2.4416–2.4633 for $^{208}\text{Pb}/^{207}\text{Pb}$; the corresponding washed leaves showed values of 1.1670–1.1762 for $^{206}\text{Pb}/^{207}\text{Pb}$ and 2.4357–2.4645 for $^{208}\text{Pb}/^{207}\text{Pb}$. The Pb isotopic compositions of the washed leaves generally fell within the range between unwashed leaves/ $\text{PM}_{2.5}$ and soils, but were much closer to unwashed leaves/ $\text{PM}_{2.5}$, in line with studies conducted in Shanghai (Bi et al., 2018), Nanjing (Hu et al., 2011b), the North Pennines of the United Kingdom (Chenery et al., 2012), and Biesbosch National Park in the Netherlands (Notten et al., 2008). The discrepancy of Pb isotopic ratios ($^{206}\text{Pb}/^{207}\text{Pb}$ and $^{208}\text{Pb}/^{207}\text{Pb}$) between leaves and soils, is probably due to 1) the mobile/bioavailable/bioaccessible fractions of soil had Pb isotopic ratios ($^{206}\text{Pb}/^{207}\text{Pb}$ and $^{208}\text{Pb}/^{207}\text{Pb}$) closer to anthropogenic sources (Farmer et al., 2011; Luo et al., 2012a; Wong and

Li, 2004) and thus plants preferentially took up more labile anthropogenic forms of Pb (Shetaya et al., 2018); 2) Pb in the plant leaves was primarily a function of foliar uptake from atmospheric deposition (Bi et al., 2018; Chenery et al., 2012) as supported by the similarity of the Pb isotopic compositions in the unwashed leaves/PM_{2.5} and leaves. Based on the calculation process of trace metal concentration (section 3.2), it was estimated that the Pb isotopic compositions (²⁰⁶Pb/²⁰⁷Pb and ²⁰⁸Pb/²⁰⁷Pb) in the unwashed leaves were the mixed results from those in the corresponding foliar dust and washed leaves. By comparing the Pb isotopic compositions (²⁰⁶Pb/²⁰⁷Pb and ²⁰⁸Pb/²⁰⁷Pb) between the washed and the corresponding unwashed leaf samples in Table 5.5, the possible Pb isotopic compositions (²⁰⁶Pb/²⁰⁷Pb and ²⁰⁸Pb/²⁰⁷Pb) of foliar dust were estimated and circled in red in Figure 5.11, which were similar to those of the Guangzhou PM_{2.5} particles, and within the range of the industrial sources and traffic exhaust. The comparison results indicated air particle deposition on tree leaves from nearby contamination sources. Furthermore, the unwashed leaf samples from the industrial contaminated regions exhibited a Pb isotopic composition encircling the industrial sources, suggesting the industrial influence on nearby foliar dust. It should be noted that the Pb isotopic compositions of an unwashed leaf sample from a construction site showed different Pb isotopic compositions. Thus, the construction activities may also alter the Pb isotopic signatures of foliar dust. It should be noted that the contribution of specific sources could be overestimated or underestimated only based on Pb isotopic ratio analyses, due to the similar Pb isotopic signature of some natural and anthropogenic sources (Duzgoren-Aydin and Weiss, 2008). Therefore, the source differentiation of trace metal contamination in the terrestrial environment should couple isotopic ratio data with other source identification methods such as GIS and APCS-MLR receptor model which would be discussed in the next section.

Table 5.5 Summary of Pb isotopic compositions and corresponding Pb concentrations.

Location	Sample ID	Sample type	$^{206}\text{Pb}/^{207}\text{Pb}$	$^{208}\text{Pb}/^{207}\text{Pb}$	Pb concentration (mg kg ⁻¹)	
Industrial area	#3	Surface soil	1.1732	2.4597	110	
		Road dust	1.1617	2.4506	165	
		Unwashed leaf	1.1726	2.4633	26	
		Washed leaf	1.1759	2.4645	10.9	
	#44	Surface soil	1.1699	2.4572	119	
		Road dust	1.1642	2.4548	91.4	
		Unwashed leaf	1.1738	2.459	6.88	
		Washed leaf	1.1762	2.4615	4.99	
	#120	Surface soil	1.1751	2.4506	184	
		Road dust	1.1697	2.4482	171	
		Unwashed leaf	1.1689	2.4422	52.3	
		Washed leaf	1.1678	2.4357	9.77	
	Roadside	#93	Surface soil	1.1841	2.481	24.2
			Road dust	1.1726	2.4627	50.1
			Unwashed leaf	1.1732	2.4458	2.7
			Washed leaf	1.1733	2.4387	1.15
#123		Surface soil	1.2016	2.4804	72.7	
		Road dust	1.1521	2.4381	55.4	
		Unwashed leaf	1.1689	2.4446	2.9	
		Washed leaf	1.1693	2.4422	1.41	
#136		Surface soil	1.1961	2.4897	22.1	
		Road dust	1.1744	2.4554	44.3	
		Unwashed leaf	1.1726	2.4416	2.39	
		Washed leaf	1.1733	2.4357	1.04	
#139		Surface soil	1.1824	2.4645	57.7	
		Road dust	1.159	2.4387	594	
		Unwashed leaf	1.168	2.4428	13.8	
		Washed leaf	1.1686	2.4387	3.18	
#142	Surface soil	1.1678	2.4578	95		
	Road dust	1.1704	2.4597	33.4		
	Unwashed leaf	1.1689	2.453	3.85		
	Washed leaf	1.1692	2.4494	2.04		

Table 5.5 Continued.

Location	Sample ID	Sample type	$^{206}\text{Pb}/^{207}\text{Pb}$	$^{208}\text{Pb}/^{207}\text{Pb}$	Pb concentration (mg kg ⁻¹)
	#154	Surface soil	1.1814	2.4675	70.6
		Road dust	1.1755	2.4603	58.3
		Unwashed leaf	1.1695	2.4446	4.87
		Washed leaf	1.1693	2.4452	1.07
Construction site	#152	Surface soil	1.1831	2.4669	23.8
		Road dust	1.1719	2.459	48.3
		Unwashed leaf	1.1677	2.4554	1.89
		Washed leaf	1.167	2.45	1.76

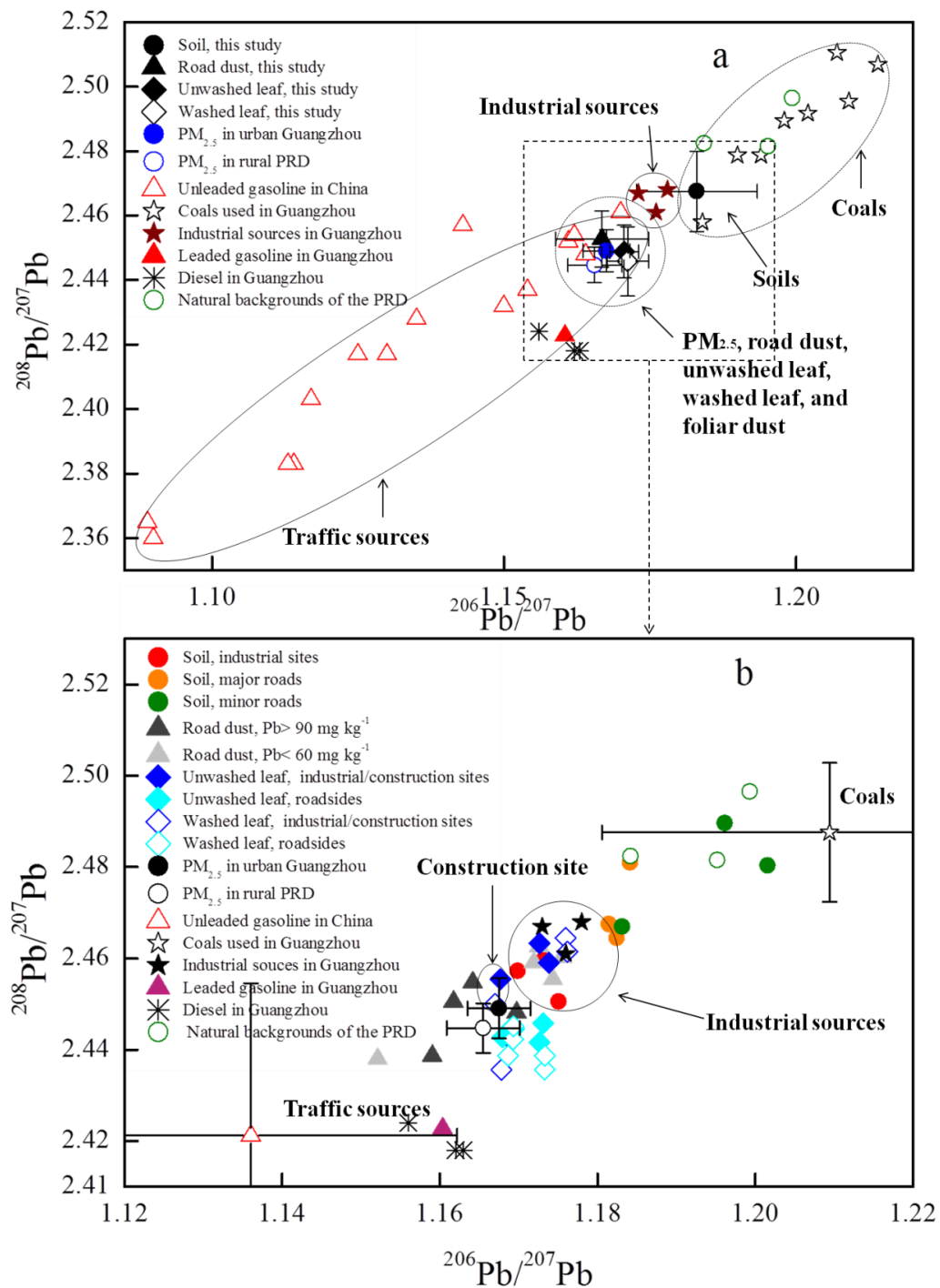


Figure 5.11 Lead isotopic compositions ($^{206}\text{Pb}/^{207}\text{Pb}$ vs. $^{208}\text{Pb}/^{207}\text{Pb}$) of different urban compartments. Data of Pb sources were all included in (a) for comparison. All data in the dashed rectangle of (a) are enlarged to (b). Detail information is listed in Table 5.5 and Table 4.8.

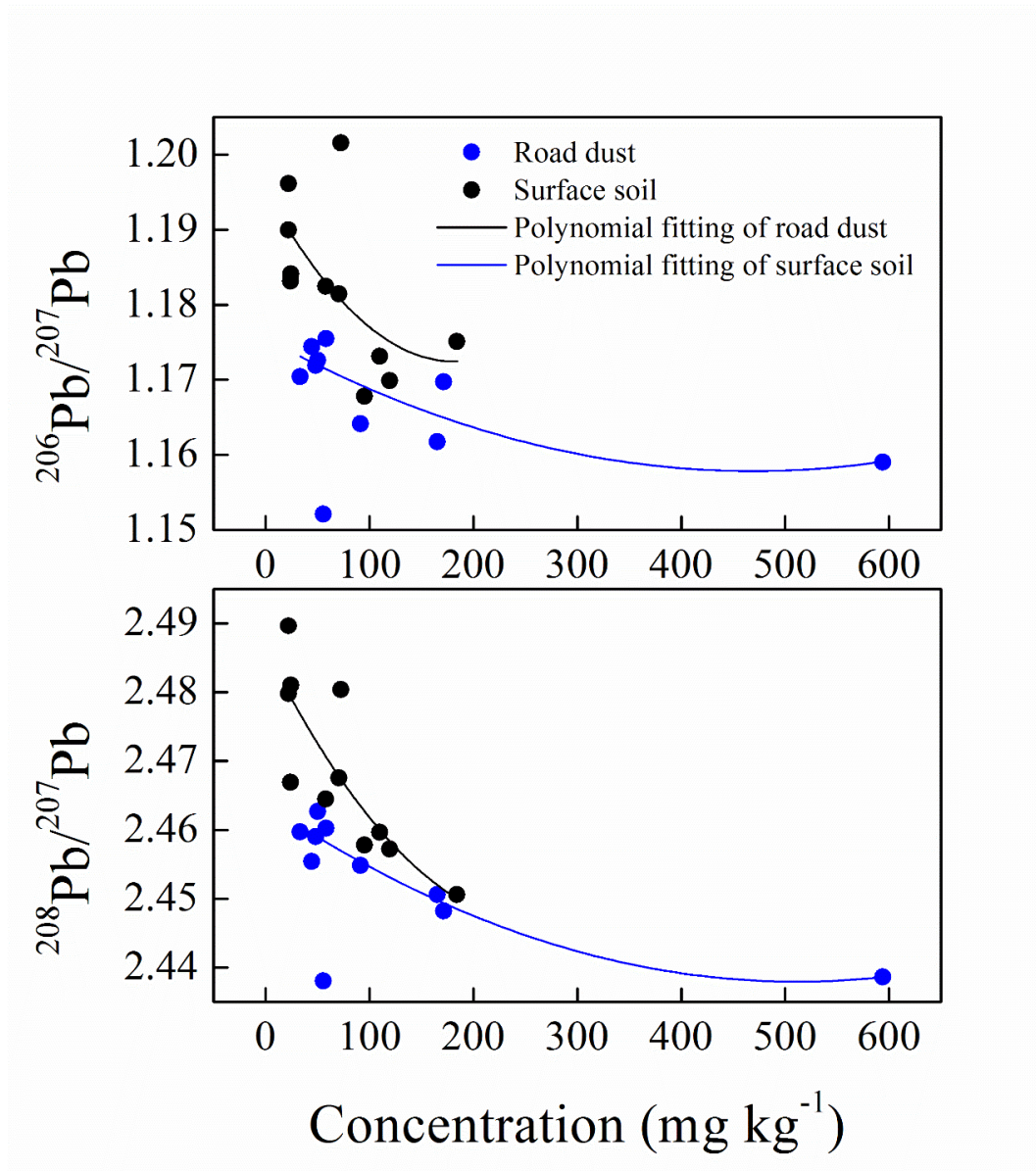


Figure 5.12 $^{208}\text{Pb}/^{207}\text{Pb}$ and $^{206}\text{Pb}/^{207}\text{Pb}$ ratios vs. Pb concentration in surface soil and road dust. The curve lines are the Polynomial fitting results ($R_{adj.}^2$ of $^{206}\text{Pb}/^{207}\text{Pb}$ and $^{208}\text{Pb}/^{207}\text{Pb}$ in surface soil equal to 0.63 and 0.66, respectively; $R_{adj.}^2$ of $^{206}\text{Pb}/^{207}\text{Pb}$ and $^{208}\text{Pb}/^{207}\text{Pb}$ in road dust equal to 0.58, and 0.87, respectively).

5.4 Source apportionment using APCS-MLR and its spatial variations

The aforementioned analysis indicated that there are primarily two sources contributing to the urban contamination: industry and traffic. Nevertheless, the exact contribution extent of

various contamination sources to these trace metals in each urban compartment is not clear, which is critical for further environmental assessment and remediation. Therefore, statistical PCA and APCS-MLR were employed to identify the source contribution to the urban environmental matrix (Table 5.6, Table 5.7, Table 5.8, and Figure 5.13–Figure 5.16). Because trace metals in leaves were resulted from a complex process governed by both source and uptake pathway, trace metals in unwashed and washed leaves were not discussed here. Compared to geogenic influences, the anthropogenic contributions accounted for much higher percentage of trace metals, particularly for Cu, Pb, and Zn in all the compartments (Table 5.8), and thus only the sources of Cu, Pb, and Zn were deciphered.

PCA analysis indicated three components, accounting for 69–89% of the total variance of the data (Table 5.6). The factor scores of each component were interpolated for source identification according to previous studies (Ha et al., 2014; Rodríguez Martín et al., 2006) as shown in Figure 5.13. In surface soil, the first component (PC1) was composed of Cr, Mn, Ni and the second component (PC2) comprised Cu, Pb, Zn. Approximately 65–97% of those elements in these PCs (PC1 and PC2) showed EF values higher than 1. PC1 exhibited two hot spots around a steel factory and orchards, and high loadings of PC2 were mainly located in the industrial areas, around the power plant, and at roadsides with high traffic volumes (Figure 5.13 a–b), indicating their anthropogenic industrial, traffic, and agricultural sources. Quantitative analysis using APCS-MLR indicated that anthropogenic sources (PC1 and PC2) accounted for 80% of the Cu, 58% of the Pb, and 78% of the Zn concentrations in surface soils. The average anthropogenic contribution (PC1 and PC2) of Cu, Pb, and Zn in the urban soils decreased in the order of industrial sites (70–85%) >high traffic sites (61–81%) >low traffic sites (57–79%) (Table 5.10), generally in line with the Pb isotopic results. In particular, the anthropogenic contribution to Cu, Pb and Zn in urban soils of industrial sites showed significant difference ($p < 0.05$) with those of the other sites. The results were generally in line with the Pb isotopic analysis, indicating that the Cu, Pb, and Zn contamination in the Guangzhou urban environment is mainly caused by anthropogenic influence and urban soil

was a good indicator of the development a city. In addition, anthropogenic materials such as coal ash, construction materials, paper, glass, garbage and other wastes are also possible to be incorporated into urban soils (Guan and Peart, 2006). For example, the anthropogenic sources (PC2) accounted for 87% of the Cu, 84% of the Pb and 90% of the Zn in surface soils of an urban park (site 142), resulting in extremely high metal concentrations (140 mg Cu/kg, 117 mg Pb/kg, 251 mg Zn/kg) (Figure 5.14 e). Such soil contamination in urban parks of Guangzhou was also observed by Bi et al. (2013a) and Lu et al. (2007). Considering the previous capacity of the park as a dump, it also revealed the influence of the reallocation of lands on trace metal contamination in urban areas (Ajmone-Marsan and Biasioli, 2010). The third component (PC3) was associated with Co, Al, Fe with low EFs (0.2–1.4), and should be classified as background lithogenic sources (Ha et al., 2014).

Once deposited into soils, trace metals from these sources are hardly removed, whereby the contamination of urban soils could be a mixed result of these anthropogenic trace metals. As shown in the model of multiple linear regressions (Table 5.11), the variations of trace metal concentrations were explained (0.326–0.654 of R^2_{adj}) by the TOC content, the concentration of Fe and/or Mn, indicating that the distribution of trace metals was under the influence of the geochemical interactions between trace metals and soil constituents (Davis et al., 2009; Li et al., 2015). Thus, urban contamination sources cannot be deciphered by urban soils, because trace metals in soils are an integration of many processes (Cannon and Horton, 2009).

In road dust, PC1 was composed of Co, Cr, Fe, Mn, Pb, and Zn with EF values of 1.1–6.9, showing hot spots in industrial areas and some major roads with high traffic volumes, which contributed as the major sources in road dust. The APCS-MLR model indicated that $71 \pm 12\%$ of the Pb and $48 \pm 14\%$ of the Zn was derived from industrial activities and heavy traffic (PC1) all over the urban area (Table 5.8). PC2 included Cu and Ni, with extremely high Cu (10.3) and Ni (2.0) EF values. The major hot spot (Figure 5.13 d) was coincided with high traffic volumes (Figure 5.9), major road systems, and heavily congested traffic as indicated by the

low vehicle speed (Figure 5.10). Other high factor loadings of PC2 were also overlapped with high traffic volumes shown in Figure 5.9. These results indicated the major contribution of traffic emissions to PC2, which is consistent with that Cu and Ni mainly originate from exhaust emissions and brake abrasion (Duong and Lee, 2011; Li et al., 2004; Miner, 1993). The direct traffic sources (PC2) contributed to 100% of the Cu, 40–50% of the Pb, and 50–60% of the Zn in road dust in the area with highest population density (Guangzhou Transport Planning Research Institute, 2012) and dense traffic network (Figure 5.10). This is in line with the concentration levels that trace metals, particularly for Cu, increased due to the heavily congested traffic. Similarly, the emission rates (g mile^{-1}) of total particulate matters, elemental and organic carbon from vehicles were also found to be highest during the creep phase (slow driving in heavily congested traffic) as compared to arterial road driving and highway driving (Shah et al., 2004). Thus, the spatial distribution of traffic impacts was clearly represented by PC2 in the road dust and Cu was a possible indicator of road dust contamination. PC3 in road dust included Al with a low EF value (0.1–0.7), suggesting a source of soil matrix to road dust.

In foliar dust, Al, Fe, and Pb together constituted PC1 and were attributed to local coal combustion and other industrial emissions (Calvo et al., 2013), as supported by the overlap between the hot spots and known industrial activities (Figure 5.13 g). The contribution of industrial sources (PC1) to trace metals in foliar dust increased in the hot spots around the power plant and industrial regions (Figure 5.16 a–c). As shown by the Pb and Zn concentrations in Figure 5.4, the significant influence from such emissions was highest near the emission source and gradually decreased as the plume dispersed (Brock, 2003) ($p < 0.05$). Thus, the spatial industrial influence was clearly exhibited by the distribution of PC1 in the foliar dust. PC2 was composed of Cu, Zn and Cr, with hot spots located at roadsides under overpasses (Figure 5.13 h), indicating the traffic contribution of PC2. The gravity and wind impacts could contribute to traffic dust from overpasses deposited on plant leaves. Traffic contributions (PC2) contributed to more than 40% of the Cu and Zn, and 16–56% of the Pb in

foliar dust next to overpasses (Figure 5.16 e–f). Cobalt and Ni comprised PC3, and were attributed to soil re-suspension, according to the similar concentrations of Co between surface soils and foliar dust (Table 5.1). Chromium and Ni revealed similar moderate loadings on different PCs (Table 5.7), indicating the multiple source influence on their distribution.

Table 5.6 Cumulative variance of PCA results.

Cumulative %	Surface soil	Road dust	Foliar dust
PC1	52.936	41.664	72.380
PC2	70.315	57.575	80.719
PC3	82.506	69.004	87.724

Table 5.7 Rotated component matrix of PCA analysis.

	Surface soil			Road dust			Foliar dust		
	PC1	PC2	PC3	PC1	PC2	PC3	PC1	PC2	PC3
Al	-0.015	-0.047	0.937	0.029	-0.023	0.948	0.829	0.143	0.363
Co	0.242	0.280	0.760	0.625	0.288	0.533	0.285	0.314	0.866
Cr	0.822	0.346	0.245	0.667	0.316	-0.225	0.514	0.559	0.520
Cu	0.410	0.750	0.177	0.085	0.861	-0.059	0.210	0.908	0.249
Fe	0.452	0.224	0.782	0.793	0.094	0.124	0.808	0.487	0.221
Mn ^a	0.878	0.180	0.093	0.736	-0.159	0.214	-	-	-
Ni	0.876	0.234	0.186	0.191	0.822	0.106	0.562	0.491	0.581
Pb	0.164	0.874	0.166	0.662	0.396	-0.044	0.872	0.289	0.225
Zn	0.211	0.902	0.036	0.646	0.443	0.058	0.440	0.699	0.415

a: Data of Mn was not available for foliar dust.

Table 5.8 Contribution (%) of each source for trace metals in urban soils, road dust, and foliar dust.

	Component PCA	of Source	Co	Cr	Cu	Ni	Pb	Zn
Surface soil	PC1	Industrial and agricultural	6±7	29±16	22±15	40±22	7±7	12±10
	PC2	Traffic and industrial	13±10	23±16	58±20	22±18	51±19	66±18
	PC3	Geogenic	81±11	43±14	20±12	39±16	30±14	9±6
		Constant		5±2			11±5	13±8
		R ^{2a}	0.961	0.853	0.910	0.951	0.815	0.858
Road dust ^b	PC1	Industrial and traffic	23±10	58±14		7±5	71±12	48±14
	PC2	Traffic	24±9	42±14		75±11	28±12	42±13
	PC3	Soil re-suspension	38±10			18±9	1±1	4±2
		Constant	15±3					6±2
		R ²	0.780	0.800		0.949	0.932	0.630
Foliar dust	PC1	Industrial/Coal combustion	11±12	20±19	10±16	22±20	35±32	19±19
	PC2	Traffic	18±16	34±24	46±35	30±22	26±21	43±28
	PC3	Soil re-suspension	58±23	46±26	25±20	48±26	31±24	38±27
		Constant	13±6		19±10		8±5	
		R ²	0.929	0.958	0.929	0.967	0.893	0.946

a: R² is the square of the coefficient of multiple correlation; b: In the modeling for Cu in road dust, only PC2 was selected as a independent by the MLR calculation, so the contribution was not calculated here.

Table 5.9 Trace metal enrichment factors (EFs) of urban soils and road dust.

Sample (n)		Co	Cr	Cu	Ni	Pb	Zn
Surface soil (180)	Mean	1.4	1.4	4.2	2	1.4	2.6
	Median	1.3	1.2	3.4	1.6	1.2	2.2
Top soil (180)	Mean	1.4	1.3	4.1	1.8	1.4	2.3
	Median	1.3	1.2	3.1	1.4	1.1	1.9
Road dust (178)	Mean	1.1	1.7	10.3	2	2.2	6.9
	Median	1.1	1.4	7.7	1.7	1.9	6.3

Table 5.10 Anthropogenic contribution (PC1+PC2, mean) to Cu, Pb and Zn concentrations in urban soils obtained using APCS-MLR modeling.

Sampling site	Anthropogenic contribution (%)		
	Cu	Pb	Zn
Low traffic sites (traffic lanes <8, n=132)	79	57	77
High traffic sites (traffic lanes >8, n=35)	81	61	80
Industrial sites (n=13)	85	70	82

Table 5.11 The stepwise linear regression models of log(metal concentration) against log(TOC), log(Mn concentration), log(Fe concentration), and soil pH.

		R^2_{adj}
Co	$-1.992+0.212\log\text{Mn}+0.544\log\text{Fe}$	0.438
Cr	$-4.075+1.276\log\text{Fe}+0.154\log\text{TOC}$	0.654
Cu	$-4.489+1.255\log\text{Fe}+0.453\log\text{TOC}$	0.392
Ni	$-2.62+0.900\log\text{Fe}$	0.440
Pb	$0.325+0.434\log\text{Mn}+0.260\log\text{TOC}$	0.326
Zn	$-2.842+0.272\log\text{Mn}+0.321\log\text{TOC}+0.897\log\text{Fe}$	0.409

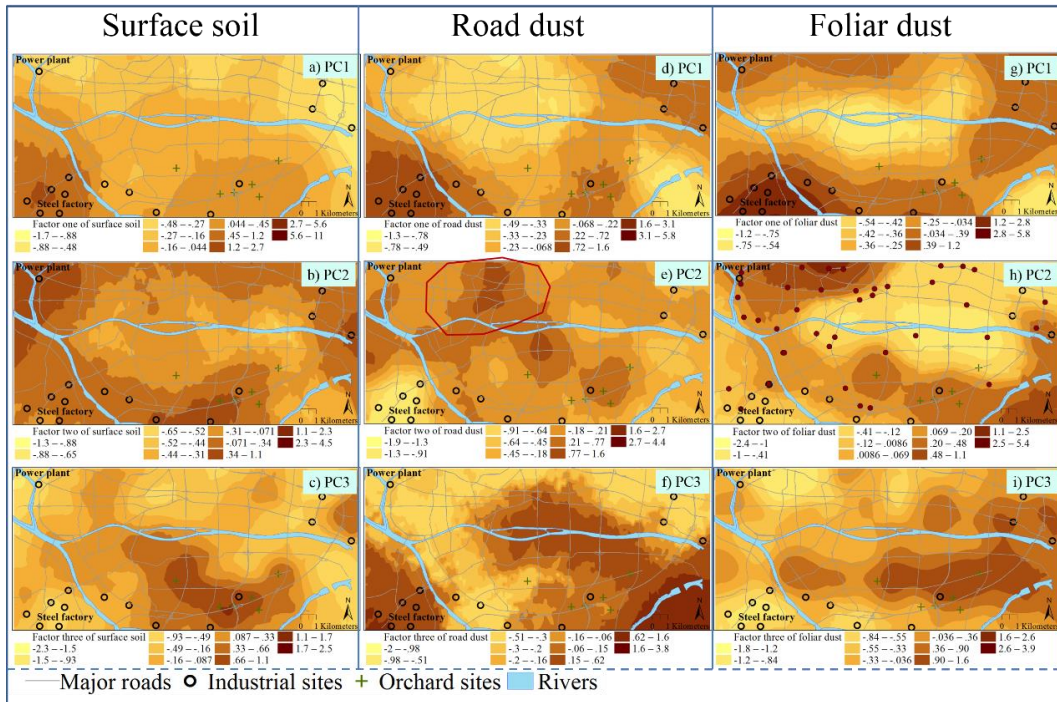


Figure 5.13 The spatial distribution maps of robust factor scores interpolated by ordinary kriging. (a) factor 1 of surface soils primarily representing Cr, Ni, and Mn; (b) factor 2 of surface soils primarily representing Cu, Pb and Zn; (c) factor 3 of surface soils primarily representing Co, Al, and Fe; (d) factor 1 of road dust primarily representing Co, Cr, Pb, Zn, Fe, and Mn; (e) factor 2 of road dust primarily representing Cu and Ni; and (f) factor 3 of road dust primarily representing Al; (g) factor 1 of foliar dust primarily representing Al, Fe, and Pb; (h) factor 2 of foliar dust primarily representing Cu, Zn and Cr; and (i) factor 3 of foliar dust primarily representing Co and Ni. The area with highest population density (Guangzhou Transport Planning Research Institute, 2012) and dense traffic network (Figure 5.10) was circled in red in (e) and sampling sites next to overpasses were marked with red dots in (h).

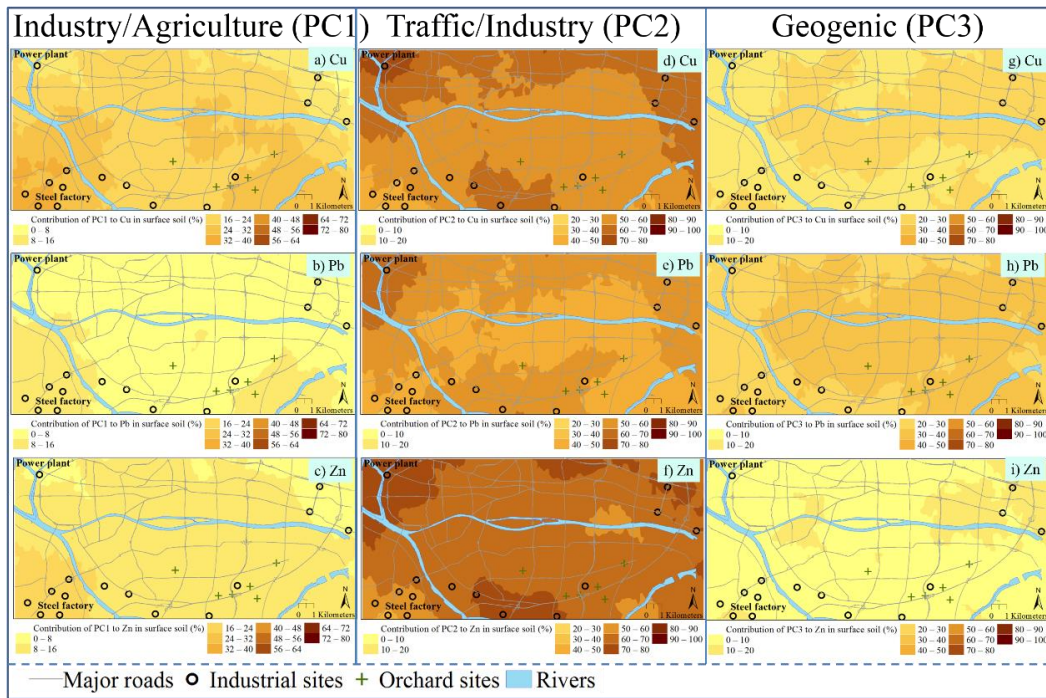


Figure 5.14 Spatial variation of contributions from industrial and agricultural sources (PC1) to Cu (a), Pb (b), and Zn (c); traffic and industrial sources (PC2) to Cu (d), Pb (e), and Zn (f); and geogenic sources (PC3) to Cu (g), Pb (h), and Zn (i) in surface soils.

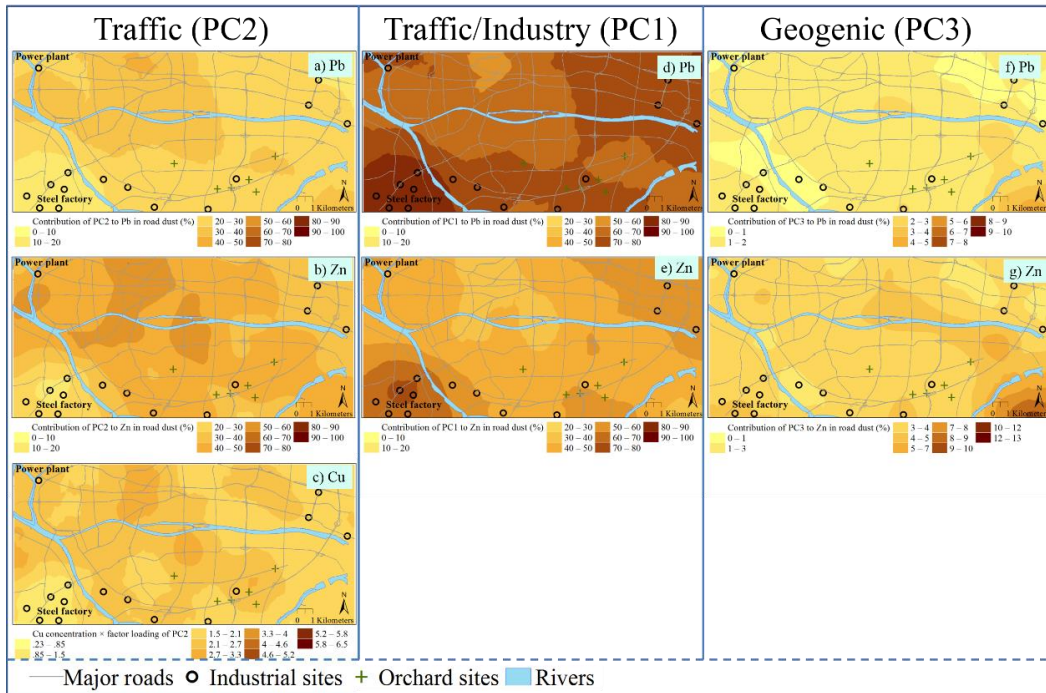


Figure 5.15 Spatial variation of the contribution from traffic sources (PC2) to Pb (a) and Zn (b), industrial/traffic sources (PC1) to Pb (d) and Zn (e), and geogenic sources (PC3) to Pb (f) and Zn (g) in road dust. PC1 and PC3 were not independent variable for Cu concentration in the APCS-MLR modeling of road dust. c (Cu) is the product of the Cu concentration and the corresponding absolute factor score of PC2.

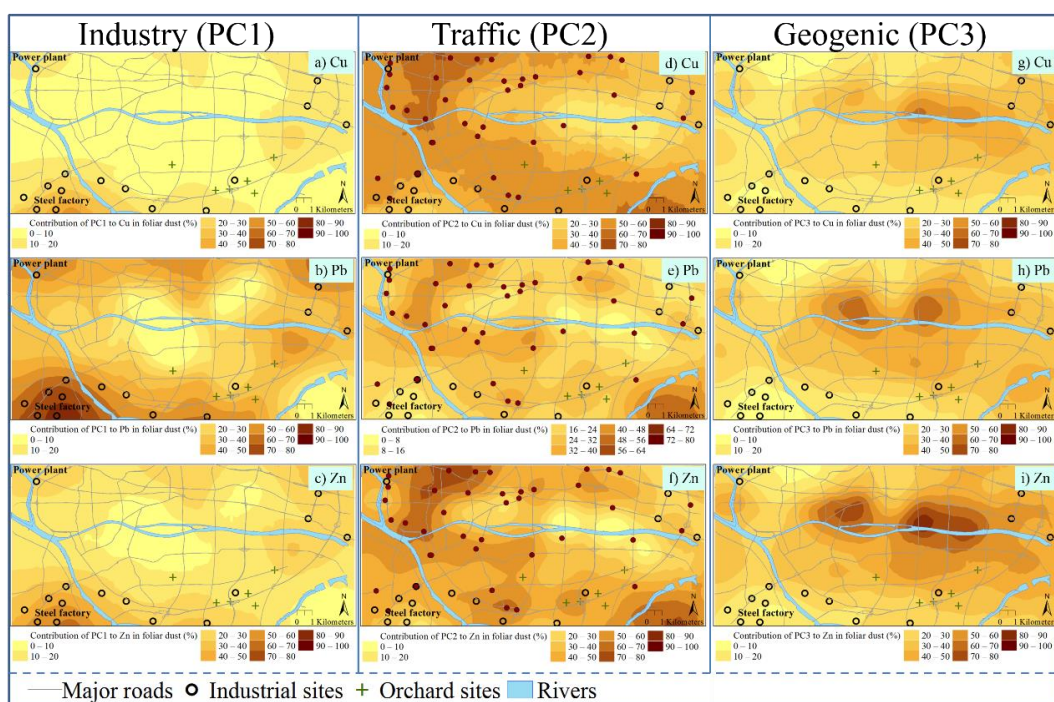


Figure 5.16 Spatial variation of contributions from industrial sources (PC1) to Cu (a), Pb (b), and Zn (c); traffic sources (PC2) to Cu (d), Pb (e), and Zn (f); and geogenic sources (PC3) to Cu (g), Pb (h), and Zn (i) in foliar dust. Sampling sites next to overpasses were marked with red dots in (d-f).

5.5 Geochemical cycling of trace metals in soil, road dust, and foliar dust in urban environment

Trace metals in a megacity spread from various anthropogenic sources to environmental compartments, and there is exchange between them (see Figure 5.17). Pairwise correlations among surface soil, road dust, and foliar dust were found for Pb and Zn (Table 5.3), reflecting the similar responses among these environmental compartments to Pb and Zn sources. As previously suggested, the most important entrance pathways of Pb and Zn for these compartments are atmospheric deposition from industrial and traffic emissions. The accumulation of trace metals in surface soil layers as compared to top soils (Table 5.1) further proved the atmospheric deposition on terrestrial compartments. At a citywide scale (Figure

5.16 g–i) and zooming in on industrial regions (Figure 5.4) our study showed the spatial industrial influence on foliar dust with an affecting distance of approximately 3 to 4 km, similar to studies conducted in soils (Aelion et al., 2009; Bermudez et al., 2010; Martley et al., 2004). However, soil metals were not negatively correlated with the distance from the sources in our study probably because of more varied sources in urban soils (Aelion et al., 2009). As another important source of trace metals, the traffic influence on road dust decreased along with the distance from the city center at a city scale (Figure 5.15 a–c). When zooming in on specific roads, the traffic influence on soil metals was generally limited from 3 to 250 m (Carrero et al., 2013; Chen et al., 2010; Zhang et al., 2015), although it was not clearly shown in our study using a 1 km × 1 km sampling density. In urban environments, trace metals are transported from these sources to terrestrial compartments via dry and wet deposition, while the re-suspension of terrestrial dust also contribute considerable trace metals to nearby compartments (Charlesworth et al., 2011).

In urban environments, trace metals are transported from these sources to terrestrial compartments via dry and wet deposition, while the resuspension of terrestrial dust also contributes considerable trace metals to nearby compartments (Charlesworth et al., 2011). The similar scopes of Pb isotopic compositions among road dust, foliar dust, and PM_{2.5} (Ming, 2016) shown in Figure 5.11 illustrated similar Pb sources and the possible transport between each other in the form of fine particles. The contribution of road dust to atmospheric particulates through dust re-suspension around the world contribute to 16–56% of the PM₁₀ and 1–19% of the PM_{2.5}, respectively (Amato et al., 2016; Amato et al., 2009; Avino et al., 2014; Bukowiecki et al., 2010; Chen et al., 2012; Cheng et al., 2015; Karanasiou et al., 2011; Kuhns et al., 2001). Although the Pb isotopic compositions of urban soils differed from those of other dust, re-suspended soil contributed 0–38% and 25–58% of the trace metals in the Guangzhou road dust and foliar dust, respectively (Table 5.8). Moreover, Zahran et al. (2013) found that 1% increase in the amount of re-suspended soil resulted in a 0.39% increase in the concentration of Pb in the atmosphere. Thus, re-suspension of soils in the forms of fine

particles also contribute significantly to the metal cycling in urban environments.

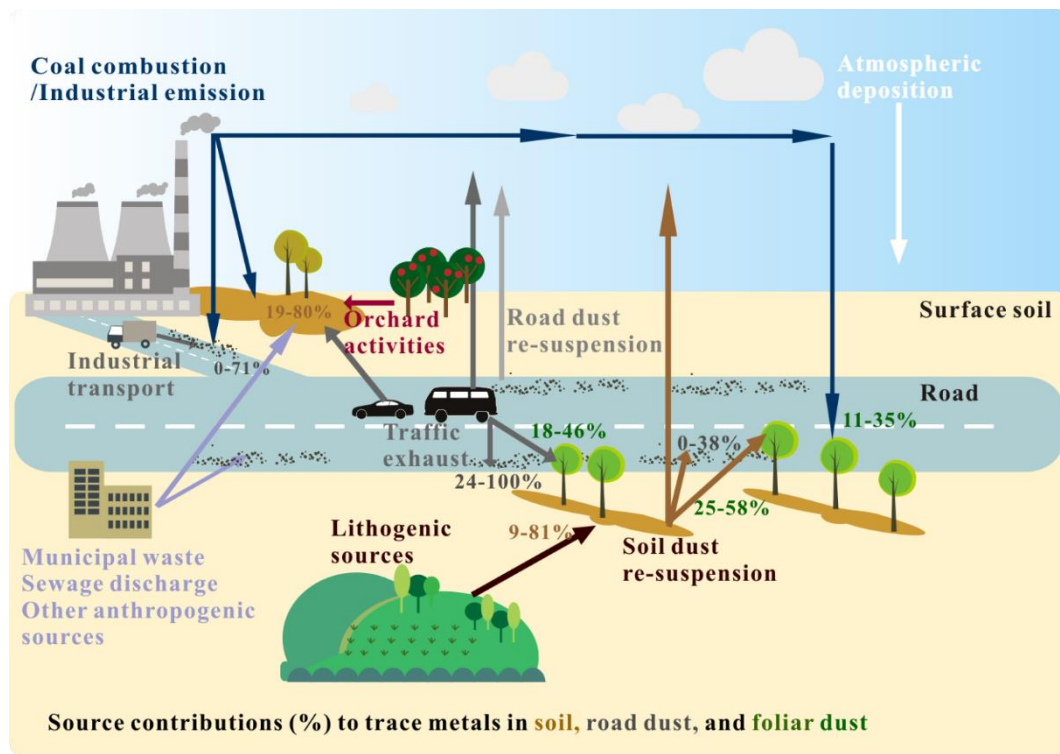


Figure 5.17 Scheme for trace metal sources and cycling in urban compartments including surface soil, road dust, and foliar dust in the megacity Guangzhou. The arrows indicate the transport of trace metals from sources, such as lithogenic sources, industrial emission/coal combustion, traffic exhaust/industrial transport, orchard activity, atmospheric deposition, particle re-suspension from surface soil and road dust, and other anthropogenic sources. The numbers are the ranges of certain sources contributing to the trace metals in each terrestrial urban compartment obtained using APCS-MLR modeling.

5.6 Summary

Trace metal contamination was found in urban soils, road dust, and foliar dust in Guangzhou urban environment. The main results are shown below:

1. The hot spots of trace metals in urban soils were mainly related to industrial, traffic, and orchard activities. The distribution of Cu and Ni in road dust was related to traffic activities, with elevations corresponding to a dense population and concentrated traffic network in the

city center. Hot spots for trace metals in tree leaves and foliar dust in industrial regions, indicated the severe industrial influence.

2. Lead isotopic data and APCS-MLR analysis identified industrial and traffic emissions as the major sources of trace metals in surface soil, road dust, and foliar dust in Guangzhou. Spatial distribution patterns of EFs and source contributions implied that Cu in road dust was a good indicator for traffic contamination, particularly influenced by traffic volume and vehicle speed; Pb and Zn in foliar dust indicated the industrial contamination, which decreased from the emission source (*e.g.*, power plant and steel factory) to the surrounding environment.

3. Pairwise correlations among surface soils, road dust, and foliar dust were found for Pb and Zn, indicating the similar responses among various environmental compartments to the Pb and Zn sources. The plots of $^{206}\text{Pb}/^{207}\text{Pb}$ vs. $^{208}\text{Pb}/^{207}\text{Pb}$ implied the similar Pb sources of road dust, foliar dust, and atmospheric particles ($\text{PM}_{2.5}$), and potential transports of Pb between these compartments in urban environments. Re-suspended soil contributed to 0–38% and 25–58% of the trace metals in the road dust and foliar dust, respectively, indicating the transport of the different terrestrial dust.

In conclusion, Chapter Four and Chapter Five provided a comprehensive knowledge of the exact spatial contamination source contributed to urban environments, and the suitability of soil, road dust, and foliar dust as indicators for describing urban contamination conditions in a typical megacity. Moreover, the results indicated that the cycling of trace metals in urban environment was primarily in the form of fine dust. Thus, more studies are needed to characterize the metal distribution, chemical forms and bioaccessibility in different particle size fractions of soil dust, in order to comprehensively investigate the environmental associations of trace metals and evaluate the concomitant health risks in urban environments. .

Chapter 6 Chemical Partitioning of Trace Metals in Various Particle Size

Fractions of Urban Soil Dust and Road Dust, and its Implication to Health

Risk Assessment

In this chapter, we collected soil dust samples from the loose part of surface soils in urban environments of Hong Kong and Guangzhou. And the partitioning of soil particles and trace metals in bulk soils and soil dust samples were compared. The distribution of trace metals in various particle sizes of soil dust and road dust samples was characterized and factors controlling the distribution process were investigated. Furthermore, the possible associations between trace metals in soil dust and other dust samples (road dust and atmospheric particulate matters) were explored. Finally, health risks resulting from trace metal contamination in soil dust were comprehensively assessed.

Dust samples were divided into four size fractions *in situ* during the sampling in Guangzhou: <50 μm , 50–99 μm , 100–249 μm , and 250–1000 μm . During the sampling in Hong Kong, the samples were divided into five size fractions *in situ*: <10 μm , 10–49 μm , 50–99 μm , 100–249 μm , and 250–1000 μm . Finally, we compared the dust results in Guangzhou and Hong Kong considering the particle size distribution. The mass proportion of the finest particle fraction (0–10 μm) accounted for only 0.004% to 0.15% of the bulk soil dust samples collected from Hong Kong, with an average proportion of 0.02%. Therefore to make comparisons between samples collected from Hong Kong and Guangzhou, the <10 μm fraction was included in the <50 μm fraction of Hong Kong soil dust if no specific description is given.

6.1 General properties of bulk soil, soil dust and road dust

Figure 6.1 depicts the particle size distribution in soil dust and bulk surface soils of Hong Kong and Guangzhou. The variations between different sampling sites were higher in soil dust than those in dry-sieved soils. In soil dust, the particle size distribution varied greatly, from 3 (100–249 μm) to 23 (<50 μm) times and 4 (100–249 μm) to 21 (<50 μm) times among the different sampling sites in Hong Kong and Guangzhou, respectively. As compared to dry-sieved soils, the mass proportions of fine particle size fractions (100–249 μm , 50–99 μm , and <50 μm) were generally higher in soil dust. The particle partitioning of soils by *ex-situ* sieving (dry sieving) was dependent on the original moisture content of the samples. According to Choate et al. (2006), fine soil particles with a certain moisture content could form large aggregates under the influence of the coagulation effect. However, it did not affect *in situ* soil dust, because soil dust usually had very low moisture content during sampling. Thus, the *in situ* sampling method was more recommended than *ex situ* methods at revealing the situation with respect to particle size fractions.

The particle size distribution and TOC contents of soil dust collected from urban sites in Hong Kong and Guangzhou are listed in Table 6.1. On average, the mass proportion of different soil dust particle fractions in Hong Kong decreased with decreasing fraction size: 250–1000 μm (47%), 100–249 μm (32%), 50–99 μm (13%), and <50 μm (8%), which was not observed in samples from Guangzhou. In Guangzhou, the particle size fraction of 100–249 μm was the most abundant (40%), followed by the fractions of 50–99 μm (29%), 250–1000 μm (28%), and <50 μm (3%). This difference could be caused by the different mineral compositions of soil dust samples collected from the two cities. The average TOC contents of soil dust samples (Hong Kong: 28.5 mg/g; Guangzhou: 66.2 mg/g, Table 6.1) were remarkably higher than those of urban soils (Hong Kong: 13.1 mg/g; Guangzhou: 27 mg/g, Table 4.1), probably due to the higher accumulation of plant debris in soil dust at the uppermost soil layer. With respect to regional variability, TOC contents in both soil and soil

dust of Hong Kong were much lower than those of Guangzhou. In Hong Kong soil dust, TOC contents tended to be evenly distributed among the particle size fractions, whereas in Guangzhou soil dust the TOC contents were higher in the fractions of 100–249 μm (77.4 g Kg^{-1}) and 50–99 μm (72.3 g Kg^{-1}) than those of 250–1000 μm (58.9 g Kg^{-1}) and <50 μm (56.3 g Kg^{-1}). The regional variability of TOC could be resulted from the different mineral compositions and plant debris in soil dust of the two cities.

Base on XRD analysis (Figure 6.2), quartz, feldspars (K-feldspars and plagioclase), kaolinite, illite, muscovite, and chlorite were identified in soil dust of Hong Kong. Mineral compositions of soil dust samples from Guangzhou mainly included quartz, feldspars (K-feldspars and plagioclase), kaolinite, muscovite, chlorite, and calcite (Figure 6.2). The characterization based on scanning electron microscopy-energy dispersive X-ray (SEM-EDX) analysis also showed that quartz and aluminosilicates (mainly composed of Si, Al oxides with varying concentrations of K, Ca, Fe, Mg, and Na) dominated in the mineral compositions of soil dust samples from the two cities. As seen in Figure 6.3, a large amount of rough-surfaced tire debris was observed in soil dust of Hong Kong where C, O, Zn, Al, Si, Cl, K, and Ca were recognized by SEM-EDX (Gunawardana et al., 2012). High concentrations of C were also identified in spherical particles and irregular fragments in Guangzhou soil dust (Figure 6.4), and C, O, Al, Si and Ca were detected in these particles, which were likely to be caused by fly ash emission from coal combustion (Bourliva et al., 2016; Goodarzi, 2006a).

In road dust, quartz, feldspars and kaolinite were identified by XRD and SEM-EDX (Figure 6.5–Figure 6.7), indicating that soil particles were present in road dust of the two cities. In addition, calcite was another major component found in road dust, which could be attributed to the debris from abrasion of concrete pavements and other construction materials (Duzgoren-Aydin et al., 2007; Schauer et al., 2006). Tire-abrasion particles with distinct irregular shapes were identified in road dust of the two cities by SEM analysis, similar to the results from other studies (Gunawardana et al., 2012; Kreider et al., 2010). In comparison

with Guangzhou, tire debris dominated the road dust in Hong Kong, suggesting the strong influence of traffic on urban environment of Hong Kong.

Table 6.1 Physicochemical properties and characteristic of soil dust samples from two cities.

Sampling region(number)		Mass proportion (%)				TOC (g Kg ⁻¹)				Average
		1000-250 μm	249-100 μm	99-50 μm	<50 μm	1000-250 μm	249-100 μm	99-50 μm	<50 μm	
Hong Kong (30)	Mean	49	31	12	8	31.6	27.6	28.9	27.1	29.0
	Range	12-79	16-45	2-28	1-23	1.27-137	2.74-103	11.1-88.2	4.26-65.3	1.27-137
Guangzhou (7)	Mean	28	40	29	3	58.9	77.4	72.3	56.3	66.2
	Range	4-60	14-51	8-72	0.5-10	6.84-96.4	11.4-121	41.8-99.2	35.2-84.8	6.84-121

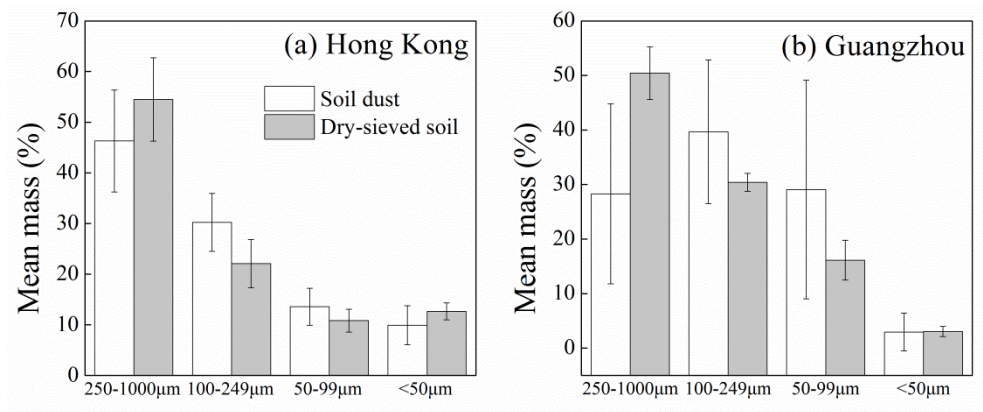


Figure 6.1 Particle size distribution in soil dust and bulk surface soils of Hong Kong (a, n=5) and Guangzhou (b, n=7). The error bars represent 1 SD.

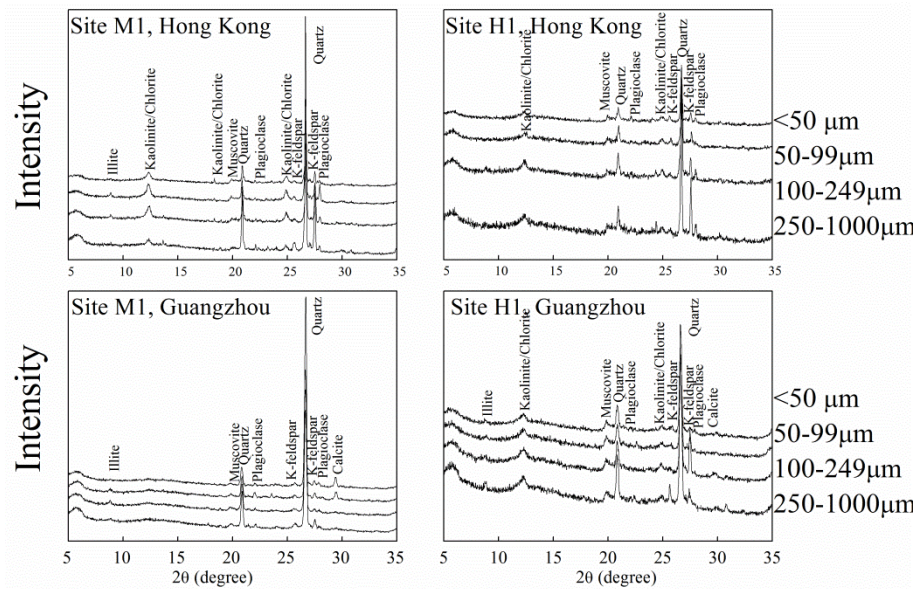


Figure 6.2 The XRD pattern of selected soil dust samples collected from two cities.

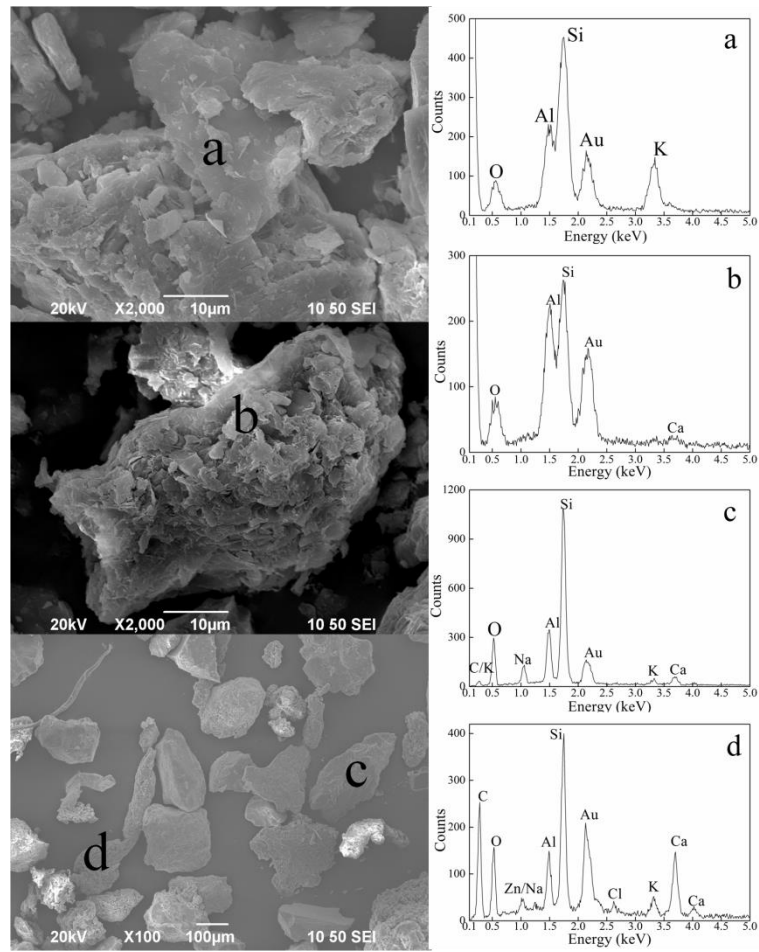


Figure 6.3 SEM photomicrographs and EDX analyses of selected soil dust samples in Hong Kong. a: K-feldspar; b: quartz; c: feldspars; d: tire debris.

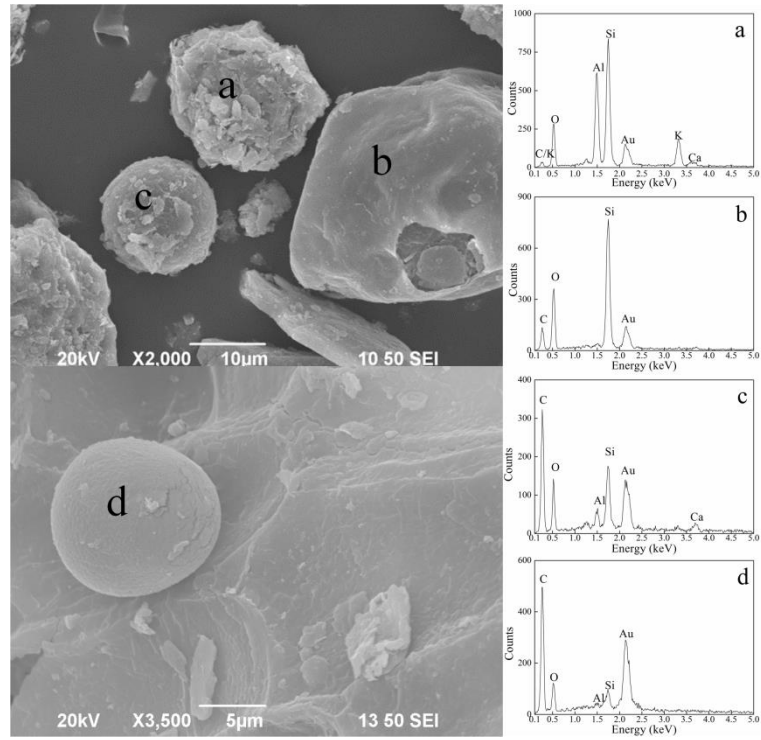


Figure 6.4 SEM photomicrographs and EDX analyses of selected soil dust samples in Guangzhou. a: K-feldspar; b: quartz; c, d: fly ash.

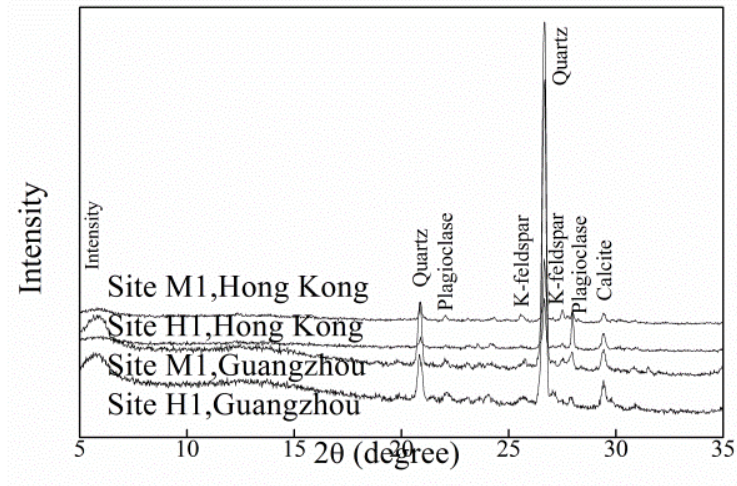


Figure 6.5 The XRD pattern of selected road dust samples (50-99 µm fraction) collected from two cities.

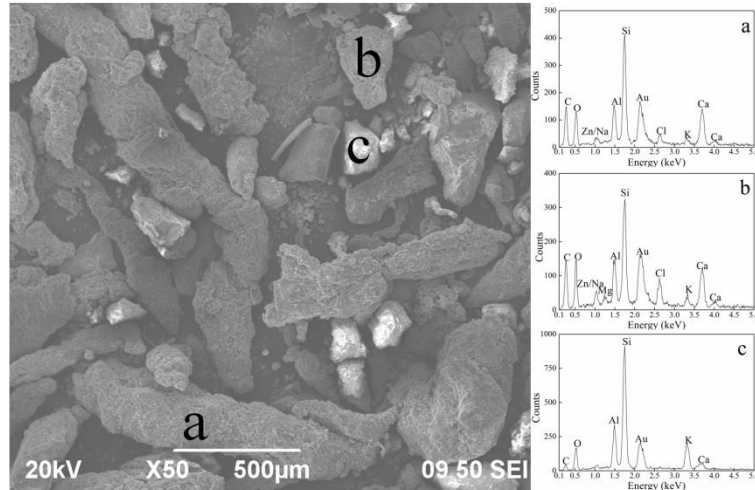


Figure 6.6 SEM photomicrographs and EDX analyses of selected road dust samples in Hong Kong. a and b: tire debris; c: soil particle.

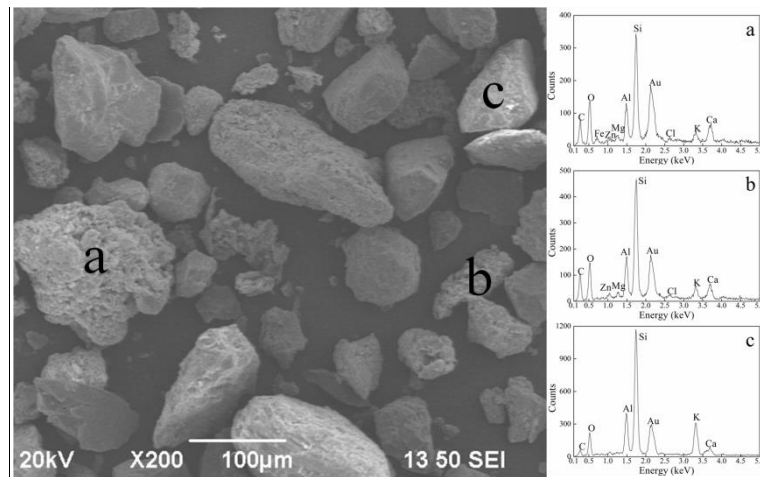


Figure 6.7 SEM photomicrographs and EDX analyses of selected road dust samples in Guangzhou. a and b: tire debris; c: soil particle.

6.2 Metal concentrations in soil dust, bulk soil, and road dust

6.2.1 Trace metal concentrations in bulk soil dust and soil

The average trace metal concentrations in each particle size fraction of soil dust, bulk soil dust, surface soils, top soils, and road dust from Hong Kong and Guangzhou are summarized in Table 6.2 and Table 6.3. Against the background benchmarks (Guangdong Geological Survey,

2010; Zhang et al., 2007), the mean trace metal concentrations in bulk soil dust, surface and top soils of Hong Kong and Guangzhou exceed the background concentrations, except for Co in bulk soil dust of Hong Kong and Guangzhou as well as Co in surface and top soils of Hong Kong. In both cities, the average concentrations of Co, Cr, Cu, Ni, and Pb in soil dust were comparable to those in urban soils, whereas the average concentrations of Zn in soil dust were much higher than those in urban soils (with significant difference in Hong Kong samples, $p < 0.05$) (Figure 6.8). Because soil dust was in the uppermost layer of urban soil, it was more likely to be affected by exogenous inputs than the bulk soil. Traffic emissions from tire wear produce a large amount of Zn into the urban environment (Harrison et al., 2012; Li et al., 2001). As a result, higher Zn concentrations in soil dust (Hong Kong: 129 mg kg^{-1} ; Guangzhou: 256 mg kg^{-1}) than those of bulk soils (Hong Kong: 93.2 mg kg^{-1} ; Guangzhou: 212 mg kg^{-1}) indicated that soil dust is more sensitive to traffic emissions than surface soils.

6.2.2 Trace metal concentrations in different particle size fractions of soil dust

In the soil dust samples collected from both Hong Kong and Guangzhou, trace metal concentrations were significantly different ($p < 0.05$) among the various particle size fractions, except for Co in soil dust from Guangzhou. As shown in Figure 6.9 and Figure 6.10, a negative correlation was found between trace metal concentrations and particle sizes in the two cities, indicating the preferential enrichment of trace metals in fine particles of soil dust. Nonetheless, the enrichments were more distinctive in samples from Guangzhou than those from Hong Kong. Trace metals from atmospheric depositions tend to accumulate in fine particle forms in terrestrial compartments (Ajmone-Marsan et al., 2008; Tomašević et al., 2005; Yu et al., 2016). Much heavier dry and wet depositions were found in Guangzhou urban areas compared to Hong Kong urban areas by Lee (2007), as well as higher total suspended particulates (TSP) (Deng et al., 2007; Lee et al., 2007). In the PRD region, industrial activities, vehicles exhausts and power plants were the major contributors to local fine atmospheric

particles (PM_{2.5}), accounting for 43.1%, 35.5% and 18.7%, respectively, of the total PM_{2.5} emissions in the year of 2006 (Zheng et al., 2009). According to the annual reports from 2012, energy consumption from coal combustion approximated to 1,961,154 terajoules in Guangzhou (Guangzhou Bureau of Statistics, 2013), which was more than six times higher than that in Hong Kong (305,268 terajoules) (Census and Statistics Department, 2013). The total number of vehicles in Guangzhou (2,440,810) was over three times higher than that in Hong Kong (718109). Furthermore, secondary production (including manufacturing, construction, and supply of electricity, gas and water) accounted for 34.84% of GDP of Guangzhou in 2012 (Guangzhou Bureau of Statistics, 2013), whereas most of the labor-intensive manufacturing industries in Hong Kong moved to the Chinese mainland in the 1980s and early 1990s. Consequently, the higher potential emissions from coal combustion, traffic exhausts, and industrial activities are likely to aggravate the accumulation of trace metals in fine dust fractions in Guangzhou.

6.2.3 Trace metal concentrations in different particle size fractions of road dust

Trace metal concentrations in road dust of Hong Kong were much higher than those of Guangzhou (Table 6.2 and Table 6.3) and other cities in China (*e.g.*, Beijing and Shanghai (Tanner et al., 2008)). The higher traffic density and less re-suspended soil depositions on the road surface are likely to result in the elevated trace metal concentrations in road dust of Hong Kong. In road dust of Hong Kong, trace metals were negatively associated with particle size (with significant differences for Co, Cu, and Ni, $p < 0.05$) (Figure 6.11). As shown in Figure 6.6, road dust was dominated by tire tread, which was the major contributor of Zn. Furthermore, the debris of yellow paint lines was found in all the fractions of road dust. The Cr and Pb concentrations in measured yellow line samples ranged from 152–306 mg kg⁻¹ and 2020–3170 mg kg⁻¹, much higher than Cr and Pb concentrations in road dust (102 mg kg⁻¹ and 148 mg kg⁻¹). Therefore, the distribution of traffic contaminants (*i.e.*, yellow line and tire

debris) could be the major factors controlling Cr, Pb and Zn concentrations in the various particle size fractions of road dust in Hong Kong.

In road dust of Guangzhou, trace metals were also negatively correlated with particle size ($p < 0.05$) (Figure 6.12), and this trend was more distinctive in road dust of Guangzhou when compared to Hong Kong. According to the higher anthropogenic inputs and more serious atmospheric depositions in Guangzhou compared to Hong Kong, the metal preferential partitioning in the fine particle size fractions of road dust in Guangzhou could be ascribed to the anthropogenically emitted metal-embedded particles from coal combustion, traffic exhausts, and industrial activities.

Table 6.2 Summary of trace metal concentrations (mg kg⁻¹) in soil dust, urban soils, road dust, and backgrounds (mean ± standard deviation) in Hong Kong.

		Co	Cr	Cu	Ni	Pb	Zn
Soil dust(n=30)	1000-250µm	2.4±1.53	19.3±13.9	27.7±59.6	6.85±5.71	59.8±39.5	135±205
	249-100µm	3.25±1.36	26.6±18.2	32.7±48.5	9.45±7.51	72.8±43.3	181±207
	99-50µm	4.03±1.60	27.8±13.9	41.6±53.0	12.6±9.50	85.0±45.4	224±224
	<50µm	4.28±1.65	32.6±17.1	48.2±52.0	14.2±8.69	91.5±45.6	247±227
	Bulk	2.97±1.51	23.5±15.9	31.6±51.6	9.02±7.62	69.0±41.8	168±214
Surface soil(n=30)		3.17±1.61	24.9±12.1	24.3±26.7	10.1±4.74	62.4±29.2	107±82.5
Top soil(n=30)		3.24±1.23	24.2±14.0	29.3±39.6	9.67±4.66	72.5±35.9	114±93.4
Road dust(n=16)	1000-250µm	4.33±1.25	77.8±47.7	174±83.0	23.6±9.43	145±57.1	1707±709
	249-100µm	5.39±1.10	121±98.0	258±125	38.6±22.3	153±40.0	1849±523
	99-50µm	5.40±1.56	130±91.8	342±170	46.9±28.5	157±50.4	1728±619
	<50µm	6.51±1.90	119±61.0	438±250	62.0±38.9	165±48.3	1524±525
	Bulk	4.95±1.05	102±69.6	235±91.5	34.2±15.6	148±42.2	1730±535
Backgrounds of Hong Kong ^a		3.88	15.7	10.2	4.86	26.7	63.4

a: Zhang et al. (2007).

Table 6.3 Summary of trace metal concentrations (mg kg⁻¹) in soil dust, urban soils, road dust, and backgrounds (mean ± standard deviation) in Guangzhou.

		Co	Cr	Cu	Ni	Pb	Zn
Soil dust(n=7)	1000-250µm	4.43±3.51	44.7±24.4	46.3±28.6	15.9±8.13	49.7±28.2	164±93.2
	249-100µm	4.78±2.63	57.1±26.3	58.4±32.2	17.3±6.71	76.1±36.2	230±121
	99-50µm	5.61±1.80	78.8±13.4	99.4±34.1	21.8±4.38	98.6±26.1	344±69.3
	<50µm	4.27±1.85	77.2±14.4	163±45.7	22.4±3.55	114±33.6	366±69.8
	Bulk	4.82±2.51	61.9±23.2	69.9±30.7	18.2±6.20	77.9±30.3	256±113
Surface soil(n=7)		6.88±1.50	50.3±16.6	67.2±59.3	20.4±3.62	78.8±53	212±127
Top soil (n=7)		6.63±1.60	42.5±18.5	70.4±82.9	21.3±4.07	78.6±72.9	173±112
Road dust (n=7)	1000-250µm	1.60±2.29	25.6±12.3	68.6±71.6	6.94±3.04	35.8±26.7	147±69.5
	249-100µm	2.31±0.713	66.4±29.0	169±173	18.3±10.8	70.5±38.7	313±150
	99-50µm	4.77±1.42	112±26.3	211±97.6	28.5±9.22	125±55.2	602±244
	<50µm	4.45±1.87	142±54.5	362±123	36.3±11.6	200±60.6	805±256
	Bulk	3.28±2.10	86.5±55.3	203±157	22.5±14.2	108±77.2	467±318
Backgrounds of Guangzhou ^a		6.3	39	10.4	12.3	41	58

a: Guangdong Geological Survey (2010).

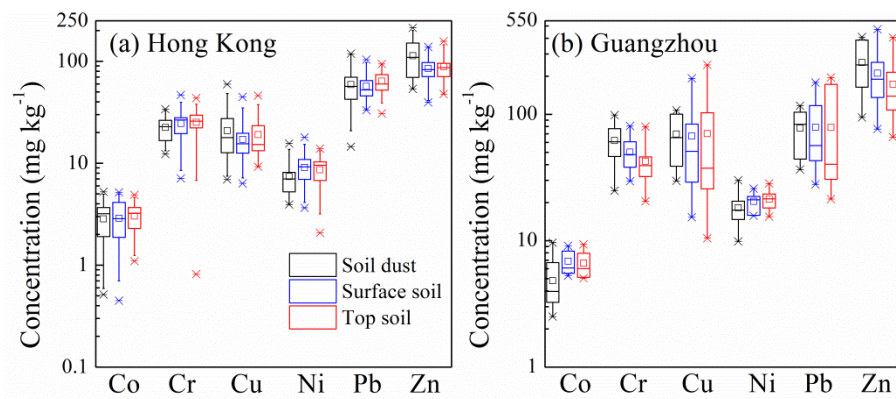


Figure 6.8 Trace metal concentrations in bulk soil dust, surface soils and top soils of Hong Kong (a, n=30) and Guangzhou (b, n=7). The bars were defined (from the bottom) as the 1st percentile, 5th, percentile, 25th percentile, median, mean (the square), 75th percentile, 95th percentile and 99th percentile.

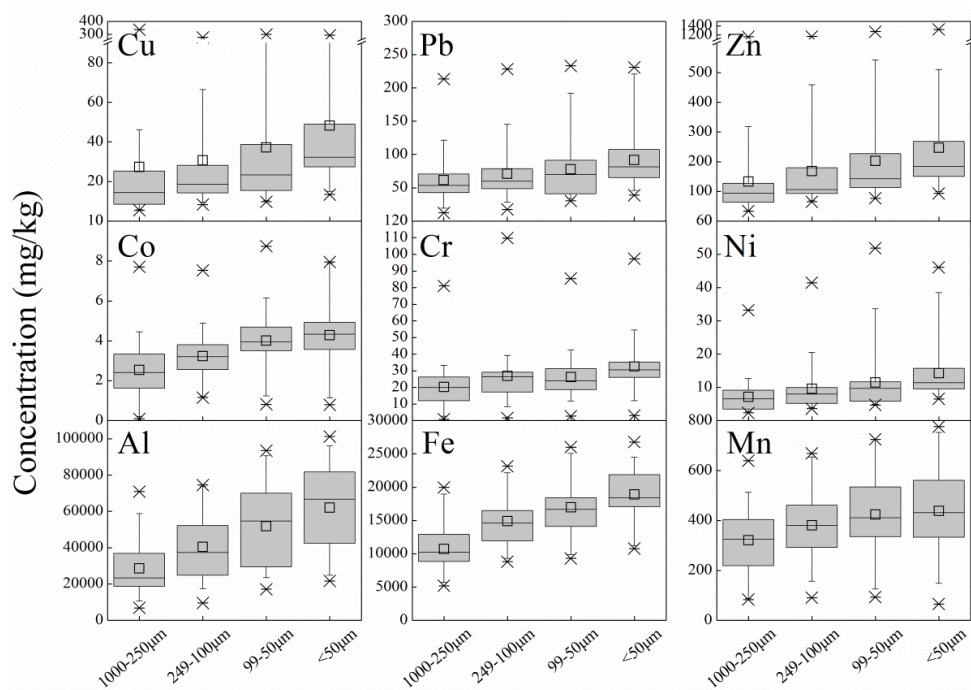


Figure 6.9 Metal distribution in different particle size fractions of soil dust in Hong Kong. n=30; The bars were defined (from the bottom) as the 1st percentile, 5th, percentile, 25th percentile, median, mean (the square), 75th percentile, 95th percentile and 99th percentile.

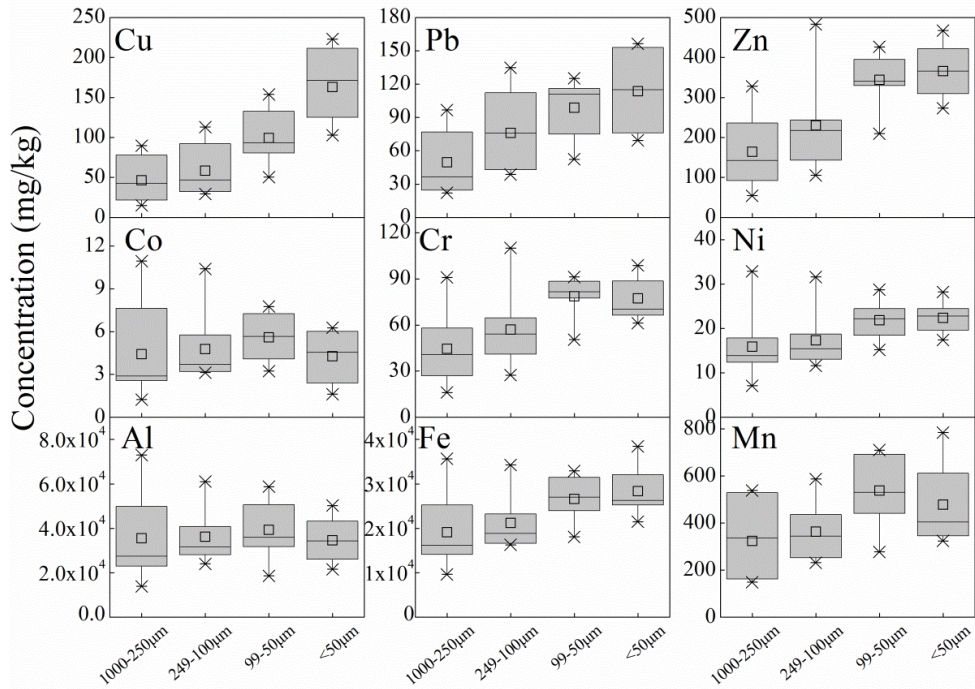


Figure 6.10 Metal distribution in different particle size fractions of soil dust in Guangzhou. $n=7$; The bars were defined (from the bottom) as the 1st percentile, 5th percentile, 25th percentile, median, mean (the square), 75th percentile, 95th percentile and 99th percentile.

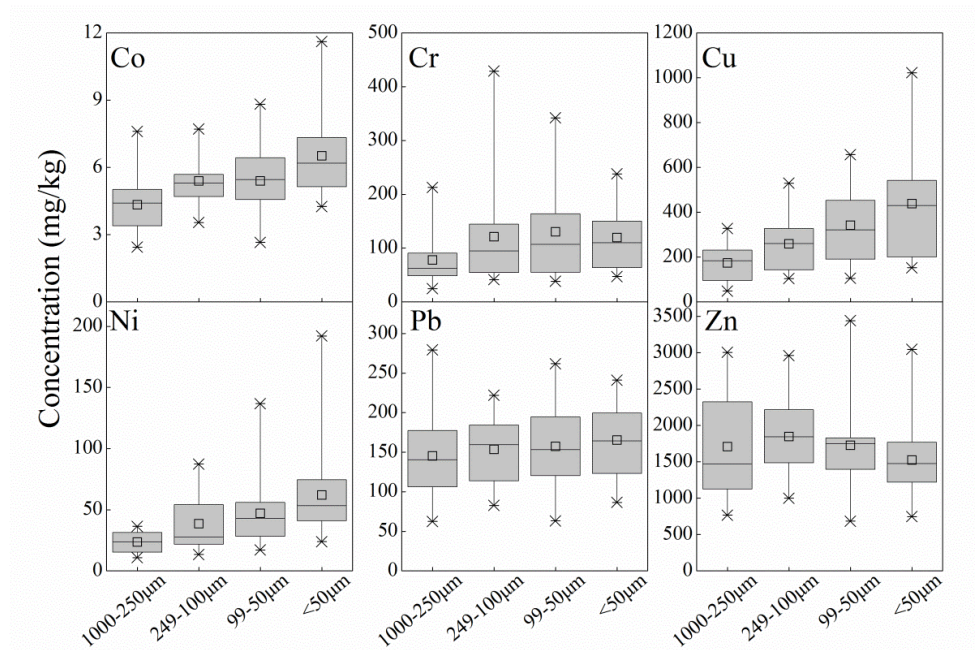


Figure 6.11 Trace metal distribution in different particle size fractions of road dust in Hong Kong. $n=16$; The bars were defined (from the bottom) as the 1st percentile, 5th percentile, 25th percentile, median, mean (the square), 75th percentile, 95th percentile and 99th percentile.

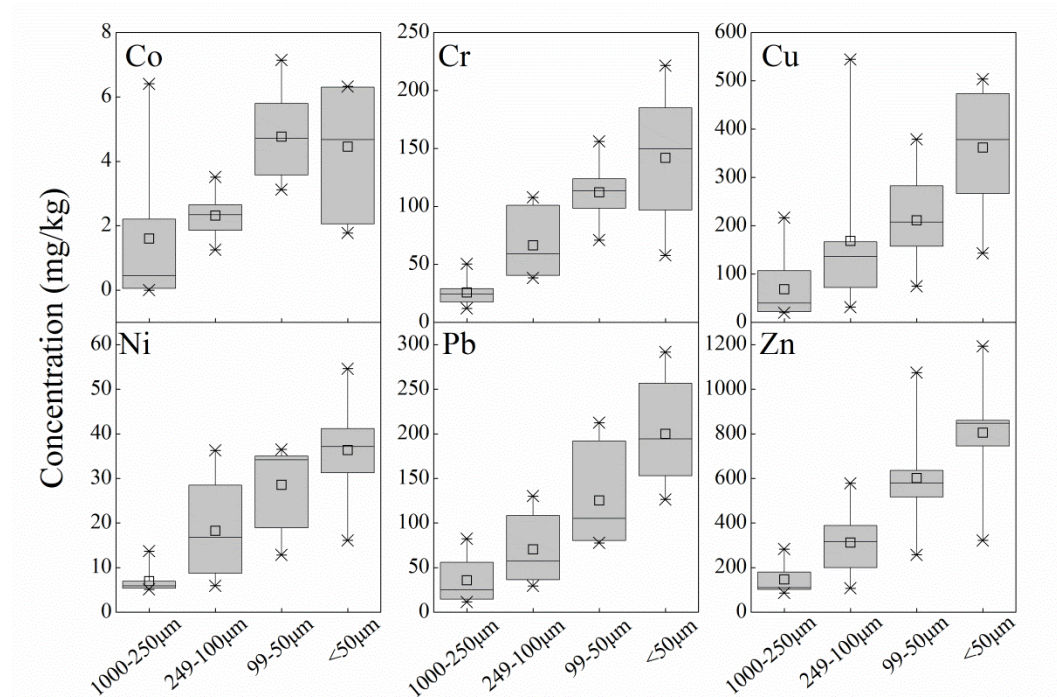


Figure 6.12 Trace metal distribution in different particle size fractions of road dust in Guangzhou. $n=7$; The bars were defined (from the bottom) as the 1st percentile, 5th, percentile, 25th percentile, median, mean (the square), 75th percentile, 95th percentile and 99th percentile.

6.3 Lead isotopic compositions in soil dust and road dust

Lead isotopic compositions in soil dust and road dust in Hong Kong (Table 6.4 and Table 6.5) and Guangzhou (Table 6.6) are tabulated. The plots of $^{206}\text{Pb}/^{207}\text{Pb}$ versus $^{208}\text{Pb}/^{207}\text{Pb}$ are depicted in Figure 6.13 to explore the possible Pb sources in soil dust. The ranges of Pb isotopic compositions ($^{206}\text{Pb}/^{207}\text{Pb}$ and $^{208}\text{Pb}/^{207}\text{Pb}$) of soil dust were similar to those of urban soils. Significant linear correlation was found between $^{206}\text{Pb}/^{207}\text{Pb}$ and $^{208}\text{Pb}/^{207}\text{Pb}$ within soil dust, backgrounds and Australian Pb ore ($R^2=0.95$) in Hong Kong, suggesting a binary mixing of lead sources from traffic and geogenic origins. Specifically, Pb isotopic compositions ($^{206}\text{Pb}/^{207}\text{Pb}$ and $^{208}\text{Pb}/^{207}\text{Pb}$) were negatively correlated with Pb concentrations and traffic volumes, respectively. In highly contaminated sites, Pb isotopic compositions ($^{206}\text{Pb}/^{207}\text{Pb}$ and $^{208}\text{Pb}/^{207}\text{Pb}$) of soil dust and soils were lower than the current traffic sources (road dust), indicating the historical contamination from leaded gasoline. As shown in Figure 6.13 b, the

anthropogenic Pb in soil dust of Guangzhou was a mixed result of coal combustion, industrial emissions, and traffic emissions, similar to it in urban soils.

The relationships between Pb compositions and particle sizes were illustrated in Figure 6.14 and Figure 6.15. In general, the Pb isotopic compositions ($^{206}\text{Pb}/^{207}\text{Pb}$) decreased with particle sizes among soil dust fractions, which was consistent with the occurrence of the small sizes of the anthropogenic metal embedded particles (Adachi and Tainosho, 2004; Goodarzi, 2006b; Iijima et al., 2007; Li et al., 2017). The decreasing tendency of Pb isotopic compositions ($^{206}\text{Pb}/^{207}\text{Pb}$) with particle size were more distinctive in soil dust from Guangzhou, as compared to soil dust of Hong Kong. This result was in line with the stronger preferential enrichment of trace metals to fine particles of Guangzhou soil dust, confirming the great influence of anthropogenic sources on trace metal accumulation in finer soil dust fractions.

As shown in Figure 6.16 and Figure 6.17, the Pb isotopic compositions ($^{206}\text{Pb}/^{207}\text{Pb}$) of road dust presented an inverse relationship with particle size, in contrary to the distribution of Pb isotopic compositions ($^{206}\text{Pb}/^{207}\text{Pb}$) of soil dust. Thus, the difference of the Pb isotopic compositions ($^{206}\text{Pb}/^{207}\text{Pb}$) between soil dust and road dust declined with particle sizes, indicating the overlapped sources of Pb and the interactive transport of Pb resulting from the re-suspension of finer particles of soil dust and road dust.

Table 6.4 The Pb isotopic compositions and Pb concentrations of soil dust in Hong Kong.

Sample NO	Sample ID	Particle size	Pb ²⁰⁴ /Pb ²⁰⁷	Pb ²⁰⁶ /Pb ²⁰⁷	Pb ²⁰⁸ /Pb ²⁰⁷	Pb (mg kg ⁻¹)
L1	YMSR	1000-250µm	0.0635	1.2172	2.5056	45.17
		249-100µm	0.0635	1.2146	2.5008	72.64
		99-50µm	0.0635	1.2129	2.4970	76.25
		<50 µm	0.0635	1.2123	2.4942	82.32
L2	LRP	1000-250µm	0.0637	1.2087	2.5108	30.82
		249-100µm	0.0636	1.2078	2.5086	34.44
		99-50µm	0.0634	1.2025	2.5032	42.66
		<50 µm	0.0635	1.2063	2.5067	46.85
M1	RJ	1000-250µm	0.0634	1.1934	2.4755	58.74
		249-100µm	0.0634	1.1865	2.4730	87.08
		99-50µm	0.0632	1.1849	2.4682	106.7
		<50 µm	0.0633	1.1863	2.4712	98.25
M2	LWSP2	1000-250µm	0.0637	1.1955	2.4908	85.90
		249-100µm	0.0637	1.1915	2.4894	78.73
		99-50µm	0.0635	1.1944	2.4927	75.50
		<50 µm	0.0635	1.1920	2.4845	82.49
H1	KTE	1000-250µm	0.0641	1.1513	2.4381	213.5
		249-100µm	0.0639	1.1513	2.4353	228.2
		99-50µm	0.064	1.1532	2.4398	233.2
		<50 µm	0.0638	1.1478	2.4304	230.9
H2	SKLR	1000-250µm	0.064	1.1539	2.4380	78.45
		249-100µm	0.064	1.1424	2.4193	130.9
		99-50µm	0.0641	1.1434	2.4271	192.0
		<50 µm	0.0641	1.1416	2.4262	220.8

Table 6.5 The Pb isotopic compositions and Pb concentrations of road dust in Hong Kong.

Sample NO	Sample ID	Particle size (μm)	$\text{Pb}^{204}/\text{Pb}^{207}$	$\text{Pb}^{206}/\text{Pb}^{207}$	$\text{Pb}^{208}/\text{Pb}^{207}$	Pb (mg kg^{-1})
L1	YMSR	1000-250 μm	0.0638	1.1546	2.4369	193.2
		249-100 μm	0.0639	1.1528	2.4314	222.0
		99-50 μm	0.0640	1.1486	2.4281	261.9
		<50 μm	0.0639	1.1492	2.4312	237.2
M1	RJ	1000-250 μm	0.0635	1.1536	2.4381	154.0
		249-100 μm	0.0635	1.1564	2.4428	110.7
		99-50 μm	0.0635	1.1585	2.4440	108.2
		<50 μm	0.0634	1.1646	2.4476	115.7
M2	LWSP2	1000-250 μm	0.0640	1.1585	2.4466	161.6
		249-100 μm	0.0640	1.1576	2.4493	177.6
		99-50 μm	0.0639	1.1583	2.4471	202.3
		<50 μm	0.0640	1.1599	2.4525	207.7
H1	KTE	1000-250 μm	0.0639	1.1524	2.4395	279.3
		249-100 μm	0.0639	1.1570	2.4414	199.9
		99-50 μm	0.0640	1.1574	2.4398	186.7
		<50 μm	0.0640	1.1551	2.4378	191.1
H2	SKLR	1000-250 μm	0.0641	1.1610	2.4502	151.8
		249-100 μm	0.0641	1.1604	2.4483	154.6
		99-50 μm	0.0642	1.1569	2.4401	125.4
		<50 μm	0.0641	1.1559	2.4433	128.5

Table 6.6 The Pb isotopic compositions and Pb concentrations of soil dust and road dust in Guangzhou.

Sample NO	Sample ID	Particle size (μm)	$\text{Pb}^{204}/\text{Pb}^{207}$	$\text{Pb}^{206}/\text{Pb}^{207}$	$\text{Pb}^{208}/\text{Pb}^{207}$	Pb (mg kg^{-1})
Soil dust						
L1	LHH	250-1000	0.0638	1.1876	2.4709	36.35
		100-249	0.0638	1.1671	2.4564	76.63
		50-99	0.0634	1.1810	2.4670	74.88
		<50	0.0636	1.1797	2.4632	69.35
M1	ZJD	250-1000	0.0637	1.1879	2.4794	24.58
		100-249	0.0638	1.1806	2.4807	51.71
		50-99	0.0640	1.1783	2.4682	97.84
		<50	0.0638	1.1792	2.4750	156.3
M2	GZDS	250-1000	0.0637	1.1829	2.4746	35.20
		100-249	0.0638	1.1804	2.4726	38.70
		50-99	0.0639	1.1778	2.4713	52.32
		<50	0.0638	1.1782	2.4656	115.7
H1	LXG	250-1000	0.0635	1.1835	2.4657	76.71
		100-249	0.0635	1.1830	2.4639	75.70
		50-99	0.0632	1.1813	2.4584	113.3
		<50	0.0636	1.1789	2.4657	152.8
Road dust						
L1	LHH	250-1000	0.0636	1.1733	2.4779	55.88
		100-249	0.0639	1.1680	2.4591	108.5
		50-99	0.0638	1.1680	2.4603	212.5
		<50	0.0634	1.1740	2.4836	256.7
M1	ZJD	250-1000	0.0637	1.1812	2.4682	14.66
		100-249	0.0636	1.1770	2.4804	29.50
		50-99	0.0634	1.1864	2.4754	77.74
		<50	0.0635	1.1917	2.4862	126.5
M2	GZDS	250-1000	0.0639	1.1704	2.4684	82.45
		100-249	0.0636	1.1627	2.4582	130.3
		50-99	0.0638	1.1829	2.4702	192.1
		<50	0.0636	1.1751	2.4843	223.8

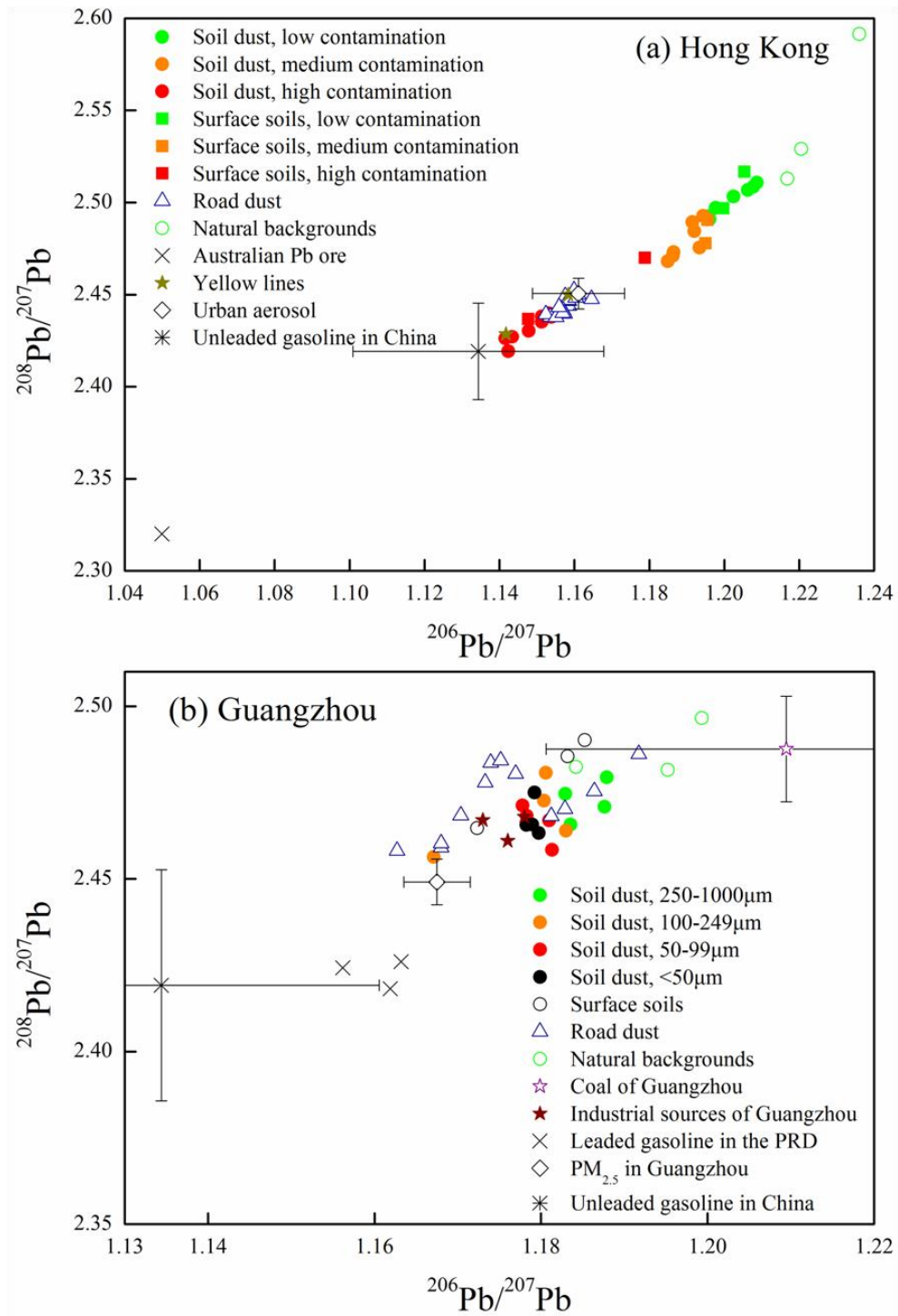


Figure 6.13 Lead isotopic compositions ($^{206}\text{Pb}/^{207}\text{Pb}$ vs $^{208}\text{Pb}/^{207}\text{Pb}$) in soil dust, soils, road dust and some Pb sources. The references of Pb sources were listed in Table 4.8 of Chapter Four.

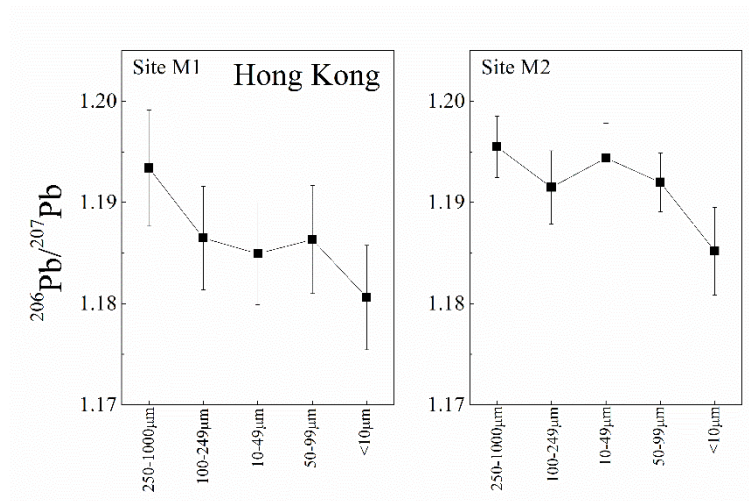


Figure 6.14 Distribution of Pb isotopic compositions ($^{206}\text{Pb}/^{207}\text{Pb}$) in different particle size fractions of soil dust from selected sampling sites in Hong Kong. The error bars represent 1 SD.

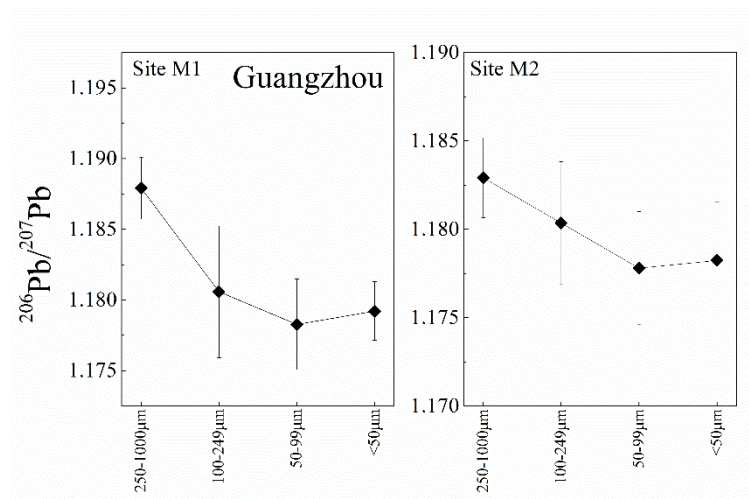


Figure 6.15 Distribution of Pb isotopic compositions ($^{206}\text{Pb}/^{207}\text{Pb}$) in different particle size fractions of soil dust from selected sampling sites in Guangzhou. The error bars represent 1 SD.

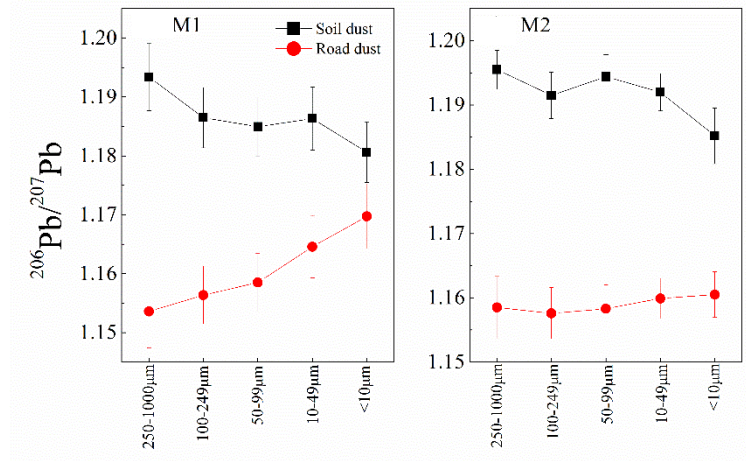


Figure 6.16 Distribution of Pb isotopic compositions ($^{206}\text{Pb}/^{207}\text{Pb}$) in different particle size fractions of soil dust and road dust incorporating the fraction of <10 μm in Hong Kong. The error bars represent 1 SD.

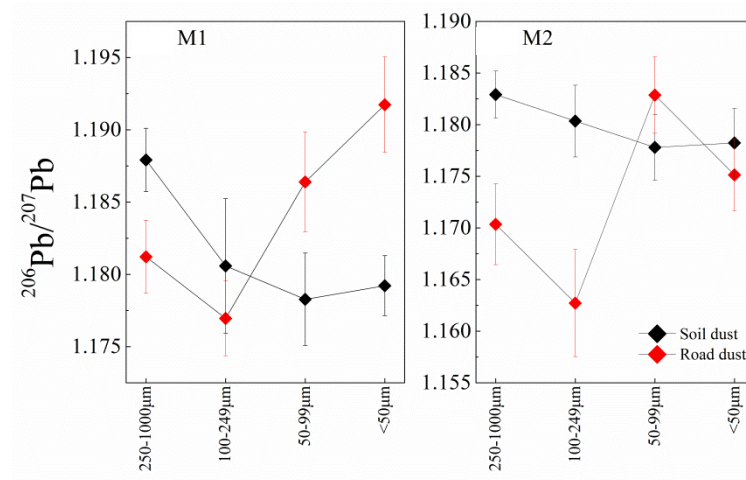


Figure 6.17 Distribution of Pb isotopic compositions ($^{206}\text{Pb}/^{207}\text{Pb}$) in different particle size fractions of soil dust and road dust in Guangzhou. The error bars represent 1 SD.

6.4 Trace metal speciation in soil dust

6.4.1 Sequential extraction of trace metals in soil dust

Behaviors of trace metals identified through BCR sequential extraction are provided in Figure 6.18. Mean recoveries with respect to pseudototal values of Cu, Pb, and Zn were in the range of 109 to 122%, which is acceptable given the intrinsic heterogeneity of urban soils (Mossop and Davidson, 2003; Poggio et al., 2009). The percentage of trace metals released from sequential extraction was quite similar between soil dust samples of the two cities, which decreased with the pattern of reducible (step 2) \geq oxidisable (step 3) $>$ exchangeable (step 1) $>$ residual (step 4) (Cu), reducible $>$ oxidisable $>$ residual $>$ exchangeable (Pb), and exchangeable $>$ reducible \approx oxidisable $>$ residual (Zn). 77 % to 84 % of the Cu and 92 % to 94 % of the Pb in Hong Kong soil dust, and 68% to 84 % of the Cu and 80% to 90% of the Pb in Guangzhou dust, were released in the reducible fraction and oxidizable fraction. Moreover, Cu and Pb in these two fractions showed the highest correlations with total concentrations (Table 6.7), and increased with decreasing particle sizes (Figure 6.19). Generally, metals released from reducible fraction are mainly bound to hydrous oxides of Mn and Fe and metals released from oxidizable fraction are principally associated with organic matter through complexation or bioaccumulation processes (Ure et al., 1993). Therefore, the adsorption of Mn/Fe oxides and organic complexes seemed to be an important transfer mechanism of Cu and Pb from their sources to the soil environment (Acosta et al., 2014). The release of Zn were comparable in the four fractions, with the highest proportion in the acid extractable fraction. Acid extractable Zn, reducible Zn, and oxidisable Zn were significantly correlated with the total concentration of Zn ($p < 0.01$ in Hong Kong samples and $p < 0.05$ in Guangzhou samples, Table 6.7). In addition, inverse relationships were found between particle size and Zn released from these fractions (Figure 6.19), implying that the Zn enrichments in fine particles were mainly linked to ion-exchange processes/carbonates, oxides, and organic

complexes (Hardy and Cornu, 2006; Qin et al., 2016). Furthermore, the affinity of Cu, Pb and Zn for exchangeable, reducible and oxidisable fractions indicated their high mobility in soil dust (Jayarathne et al., 2017).

6.4.2 Lead isotopic compositions of extracted Pb in soil dust

Lead isotopic compositions of different chemical fractions varied among different sampling sites, with highest Pb isotopic compositions in residual fractions (Hong Kong: $^{206}\text{Pb}/^{207}\text{Pb}$: 1.1727–1.2587; $^{208}\text{Pb}/^{207}\text{Pb}$: 2.4645–2.5028; Guangzhou: $^{206}\text{Pb}/^{207}\text{Pb}$: 1.1716–1.2323; $^{208}\text{Pb}/^{207}\text{Pb}$: 2.4482–2.5078) and lower Pb isotopic compositions in the other three fractions (Hong Kong: $^{206}\text{Pb}/^{207}\text{Pb}$: 1.1444–1.1920; $^{208}\text{Pb}/^{207}\text{Pb}$: 2.4274–2.4749; Guangzhou: $^{206}\text{Pb}/^{207}\text{Pb}$: 1.1721–1.1824; $^{208}\text{Pb}/^{207}\text{Pb}$: 2.4476–2.4639). The Pb isotopic compositions ($^{206}\text{Pb}/^{207}\text{Pb}$) of residual fractions were similar to those from local backgrounds, indicating that Pb in this fraction mainly originated from natural geological materials (Wong and Li, 2004). Lower Pb isotopic compositions ($^{206}\text{Pb}/^{207}\text{Pb}$) of the other three fractions indicated an anthropogenic Pb source in these fractions. The Pb isotopic compositions ($^{206}\text{Pb}/^{207}\text{Pb}$) increased in the order of: exchangeable fraction < oxidizable fraction < reducible fraction < residual fraction at Site M1 of Hong Kong and Site M1 of Guangzhou; reducible fraction \leq exchangeable fraction < oxidizable fraction < residual fraction at Site H1 of Hong Kong and Site H1 of Guangzhou (Figure 6.20). The lowest Pb isotopic compositions ($^{206}\text{Pb}/^{207}\text{Pb}$) of reducible fraction in the highly contaminated soils (Sites H1) suggested that anthropogenically introduced Pb was mainly bound to Fe/Mn oxides (Acosta et al., 2014). Generally, trace metals from anthropogenic sources were commonly precipitated on hydrous oxides or adsorbed in the interior of the oxides (Alloway, 2013). Moreover, the Pb isotopic compositions ($^{206}\text{Pb}/^{207}\text{Pb}$) in the reducible fractions presented a weak trend toward lower isotopic ratios as particle size decreased (Figure 6.20), suggesting the important role of anthropogenic Pb in the form of Fe/Mn oxides on the preferential enrichment of Pb in fine particles of soil dust.

Table 6.7 Pearson correlation coefficients of total metal concentrations (mg kg^{-1}) in different particle size fractions as related to the sequentially extracted fractions (mg kg^{-1}) in soil dust samples collected from Hong Kong ($n=24$) and Guangzhou ($n=8$).

	Hong Kong			Guangzhou		
	Cu	Pb	Zn	Cu	Pb	Zn
Metal released from step1	.940**	.502*	.992**	-0.120	-0.330	0.877*
Metal released from step2	.998**	.992**	.994**	0.937**	0.785*	0.831*
Metal released from step3	.990**	.906**	.992**	0.523	0.981**	0.763*
Metal released from step4	.944**	.483*	.850**	0.621	0.738*	0.681

** $p < 0.01$; * $p < 0.05$.

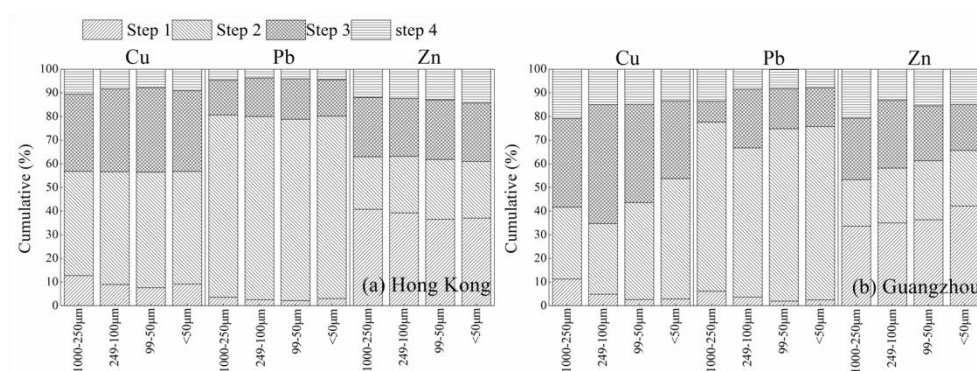


Figure 6.18 Trace metal proportion (%) of different soil dust particle size fractions extracted from BCR analysis in Hong Kong (a, $n=24$) and Guangzhou (b, $n=8$).

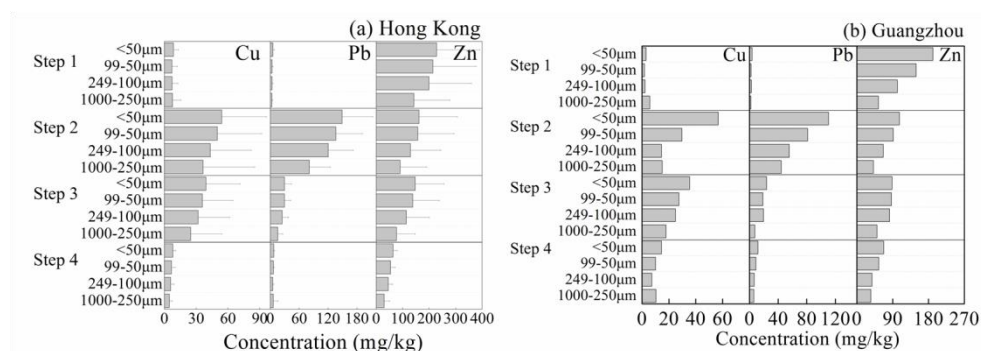


Figure 6.19 Trace metal concentrations of different soil dust particle size fractions in Hong Kong (a, $n=24$) and Guangzhou (b, $n=8$, Because only two groups of soil dust in Guangzhou were selected for the BCR extraction, no error bar was available) extracted from BCR analysis.

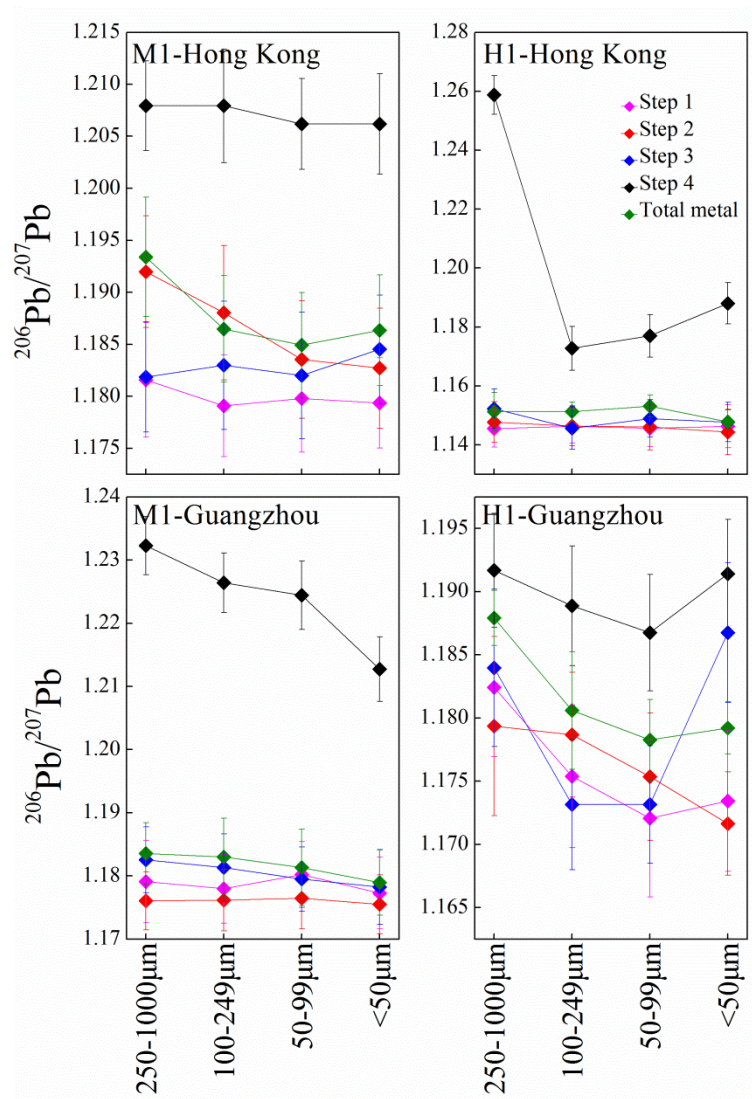


Figure 6.20 Distribution of BCR extracted Pb isotopic compositions ($^{206}\text{Pb}/^{207}\text{Pb}$) in different particle size fractions of soil dust. The error bars represent the standard deviation.

6.5 Association of trace metals between soil dust and atmospheric particulate matters

Once trace metals are emitted from their sources to the atmosphere, transport from atmosphere to soils by dry and wet deposition is likely to happen (Cannon and Horton, 2009; Wong et al., 2006; Wong et al., 2003). Atmospheric deposition of trace metals significantly alters the trace metal distribution of urban soils, particularly for trace metal accumulation in

finer soil particles (Ajmone-Marsan et al., 2008; Tomašević et al., 2005; Yu et al., 2016). Fine soil dust particles can be easily re-suspended by air turbulence generated by wind or mechanical activity (Charlesworth et al., 2011; Laidlaw and Filippelli, 2008), which may significantly contribute to the load of atmospheric particulate matters, such as PM₁₀ (Laidlaw et al., 2012; Luo et al., 2011; Young et al., 2002). Therefore, the transport of trace metals between soils and atmospheric particulate matters is predominantly in the forms of fine particulates. In order to investigate the environmental associations of trace metals, the relationships of trace metals among soil dust and PM₁₀ were studied in the Hong Kong urban area.

6.5.1 Trace metal accumulation in the finest soil dust particles (<10 µm) and comparison with PM₁₀

Soil dust samples finer than 10 µm were collected in Hong Kong. As shown in Figure 6.21, the mean concentrations of Cu (55.7 mg kg⁻¹), Pb (129 mg kg⁻¹) and Zn (438 mg kg⁻¹) in soil dust finer than 10 µm were dramatically higher than the corresponding concentrations in other fractions ($p < 0.05$). Table 6.8 summarized the trace metal concentrations in soil particles finer than 10 µm and PM₁₀ in Hong Kong. From 2000 to 2012, the concentrations of Cu, Pb, and Zn in PM₁₀ decreased 0.61, 0.66, 0.73 folds, respectively (Ho et al., 2003b; Jiang et al., 2015). During the similar time period (2001 to 2013), the concentrations of Cu, Pb, and Zn in fine soil particles (<10 µm) in the present study decreased 0.65, 0.79, 0.73 folds respectively, compared to a study conducted by Ho et al. (2003a). However, the temporal variations of trace metal concentrations in urban soils were much weaker than those of the finest soil particle fraction (<10 µm). Copper, Pb, and Zn in urban soils decreased 0.23, 0.32, and 0.47 folds (from 24.8 mg kg⁻¹, 93.4 mg kg⁻¹, and 168 mg kg⁻¹ (Li et al., 2001) to 19.1 mg kg⁻¹, 63.8 mg kg⁻¹, and 88.6 mg kg⁻¹), respectively. These results demonstrated that the decline of trace metal concentrations in the finest soil particle fraction (<10µm) is strongly related to the trace metal variations of aerosols, and hence trace metal concentrations in PM₁₀ is a crucial factor

influencing the enrichment of trace metals in fine soil particles, particularly for the <10 μ m particle fraction.

6.5.2 Re-suspension of fine particles of soil dust

Fine soil dust particles can be easily re-suspended by air turbulence generated by wind or mechanical activity (Charlesworth et al., 2011; Laidlaw and Filippelli, 2008). Suspended soil particles finer than 10 μ m in the atmosphere are possible trace metal sources in PM₁₀ (Hsu et al., 2016; Laidlaw and Filippelli, 2008; Young et al., 2002). The soil particles (<10 μ m) yielded from soil dust (0 to 1000 μ m) ranged from 0.04 to 1.51 g kg⁻¹, with an average of 0.27 g kg⁻¹, comparable to the study by Young et al. (2002), and in that study, 0.169 to 0.869 g kg⁻¹ of soil particles (<10 μ m) were found to re-suspend from dry soils in a chamber. Soil loss during wind events was simulated by Fryrear et al. (1991), and the authors measured a maximum soil mass transportable by wind over the field surface with 374 kg m⁻¹. As the soil moved over the field surface, the soil particles smaller than 10 μ m could be re-suspended. Based on the transportable soil mass provided by Fryrear et al. (1991), in a 12 hour duration with a 11 km/hour wind (the average wind velocity of Hong Kong) and a 6 m mixing height (a conservative mixing level near the emission sources suggested by Young et al. (2002)), the soil derived Cu, Pb, and Zn in PM₁₀ in Hong Kong were 1.26 to 34.6 ng m⁻³, 2.6 to 77.5 ng m⁻³, and 10.7 to 246 ng m⁻³, respectively (see Table 6.9). As compared to trace metal concentrations in PM₁₀ (Cu = 19 ng m⁻³, Pb = 34 ng m⁻³, Zn = 110 ng m⁻³) (Jiang et al., 2015), the average contribution of the soil-derived trace metals to Cu, Pb, and Zn in PM₁₀ approximated 34%, 46%, and 47%, respectively. Similarly in central Taiwan, soil dust and crustal source contributed to 41.1–50.3% of trace metals in PM₁₀ (Hsu et al., 2016), and Artíñano et al. (2003) found that natural sources from soil re-suspension accounted, on the average, for 40% of PM₁₀ in Madrid. However, the actual emission rates from soil dust should be lower in view of the field surface roughness, soil moisture, and the vegetative cover; whereas, higher emission rates could result from strong windstorms or mechanical

disturbance of the soils (Luo et al., 2011; Young et al., 2002). Additionally, the changes of wind direction could also impact the soil re-suspension which was not considered in the simulation.

Table 6.8 Trace metal concentrations in soil particles finer than 10 µm and PM₁₀ in Urban Hong Kong.

Sample (unit, collecting year)	Cu	Pb	Zn	reference
PM _{2.5} (ng m ⁻³ , winter/2012)	23.6	47.4	146	Jiang et al. (2015)
PM _{2.5-10} (ng m ⁻³ , winter/2012)	9.4	2.9	24.9	
PM ₁₀ (ng m ⁻³ , winter/2012) ^a	19.34	34.05	109.67	
PM ₁₀ (ng m ⁻³ , winter/2000)	49.5	99.6	400	Ho et al. (2003b)
Metal concentration in soil particles <10 µm (mg kg ⁻¹ , 2012-2013)	55.7	129	438	This study
Metal concentration in soil particles <10 µm (mg kg ⁻¹ , 2001)	161	619	1651	Ho et al. (2003a)

a: Data of PM₁₀ were calculated from PM_{2.5} and PM_{2.5-10}, with an assumption that PM_{2.5} accounts for 70% (the average proportion in urban PM₁₀ obtained from Ho et al. (2003b)) of PM₁₀.

Table 6.9 Information of soil dust particles finer than 10 µm.

Particles <10 µm in bulk soil dust (g kg ⁻¹)		< 10µm metal yield from bulk soil dust (mg kg ⁻¹)			Soil-derived metal in PM ₁₀ (ng m ⁻³)		
		Cu	Pb	Zn	Cu	Pb	Zn
Average	0.27	0.03	0.03	0.11	6.41	15.6	51.1
Range	0.04-1.51	0.003-0.07	0.006-0.16	0.02-0.52	1.26-34.6	2.6-77.5	10.7-246

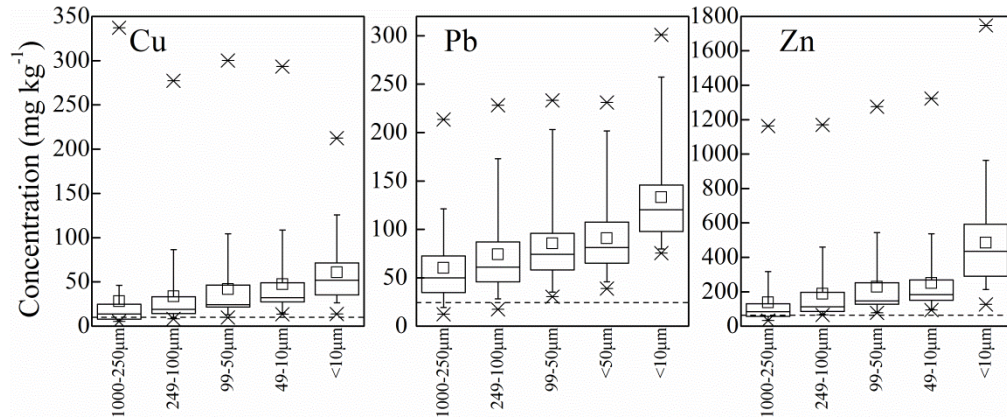


Figure 6.21 Trace metal distribution among different particle size fractions of soil dust incorporating with the fractions of <10 μm in Hong Kong. The dash lines indicated the background concentrations of Hong Kong soil (Zhang et al., 2007).

6.6 Trace metal bioaccessibility and human health risks

6.6.1 Trace metal bioaccessibility

In Hong Kong, the average bioaccessible concentrations of Co, Cr, Cu, Ni, Pb, and Zn were 0.57 mg kg^{-1} , 0.73 mg kg^{-1} , 23.8 mg kg^{-1} , 1.00 mg kg^{-1} , 56.3 mg kg^{-1} , and 107 mg kg^{-1} , accounting for 14%, 6%, 59%, 8%, 62%, and 44% of the total concentrations, respectively. In Guangzhou, the average bioaccessible concentrations of Co, Cr, Cu, Ni, Pb, and Zn were 0.75 mg kg^{-1} , 2.52 mg kg^{-1} , 28.7 mg kg^{-1} , 3.15 mg kg^{-1} , 44.7 mg kg^{-1} , and 193 mg kg^{-1} , accounting for 11%, 4%, 32%, 16%, 50%, and 62% of the total concentrations, respectively. As shown in Figure 6.22, the bioaccessible proportions of Co and Cr were comparable in soil dust of the two cities, the bioaccessible proportions of Cu and Pb in Hong Kong soil dust were higher than those in Guangzhou soil dust, contrary to that of Ni and Zn. Soil properties, such as pH, organic matter, clay particles, and mineral composition, can influence the bioaccessibility of trace metals in soils, due to the interactions of trace metals with soil constituents (Pelfrène et al., 2013; Ruby et al., 1999). The influence of soil properties on the bioaccessibility of trace metals were investigated by multiple linear models, and in these models bioaccessible metal

concentration was selected as dependent variable, and corresponding total metal concentration, their forms determined by the BCR sequential extraction, soil pH, TOC, and particle size fraction were selected as independent variables (Table 6.10). Relationships were established between bioaccessible metal concentrations and variables related to the chemical form of the metal estimated by the BCR method, such as metals bound to the reducible fraction (for Cu and Pb), or exchangeable metals (for Zn), similar to the result of Mendoza et al. (2017). The influence of particle size and residual metal concentration was also found for Pb, with a negative effect on the Pb bioaccessibility. In soil dust, the bioaccessible concentrations and bioaccessibility of trace metals generally increased with decreasing particle size (Figure 6.22). It could be ascribed to the enrichments of hydrous oxides and organic matter in fine soil particles, because metals adsorbed to organic phase or Fe/Mn oxides usually had high bioaccessibility (Fujimori et al., 2018; Rasmussen et al., 2011). Furthermore, given that anthropogenic trace metals were distributed predominantly in the earlier chemical fractions (see section 6.4.2), anthropogenic trace metals appeared to have higher bioaccessibility compared to those of geological origin (Luo et al., 2012a). Hence, the accumulation of the anthropogenic trace metals in the fine soil particle fractions also aggravated the bioaccessibility of fine soil dust.

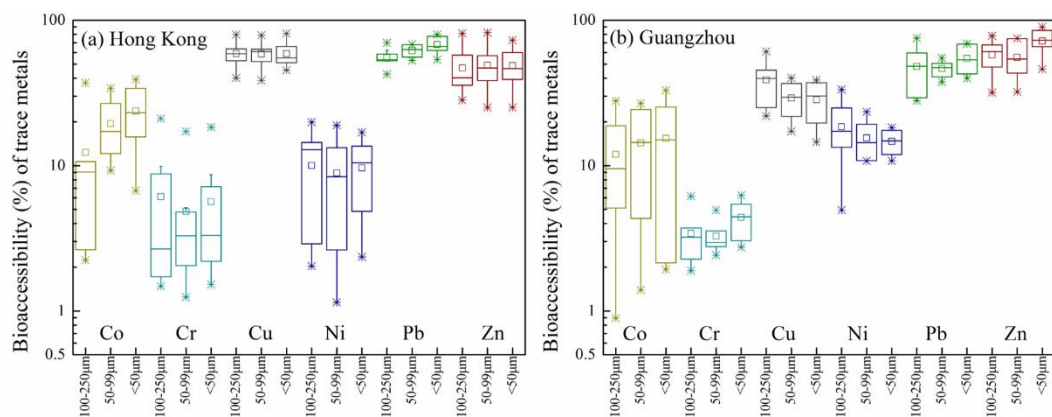


Figure 6.22 Bioaccessibility of trace metals among different particle size fractions in Hong Kong (n=7) and Guangzhou (n=6). The bars were defined (from the bottom) as minimum, 25th percentile, median, mean (the square), 75th percentile, and maximum.

Table 6.10 The stepwise linear regression models to estimate the bioaccessible metals (n=18).

Model*	R^2
$Co_{SBRC} = 0.49Co_{Total} - 0.295Co_{BCR4} - 0.522$	0.972
$Cr_{SBRC} = 0.09Cr_{BCR3} + 0.028Cr_{BCR4} - 0.107$	0.980
$Cu_{SBRC} = 1.548Cu_{BCR2} - 0.137Cu_{Total} + 2.345$	0.989
$Ni_{SBRC} = 0.151Ni_{Total} - 0.151Ni_{BCR4} + 0.02TOC - 0.579pH + 4.176$	0.985
$Pb_{SBRC} = 1.172Pb_{BCR2} - 0.098Pb_{Total} - 0.079Pb_{Size} - 3.583Pb_{BCR4} + 13.073$	0.992
$Zn_{SBRC} = 1.954Zn_{BCR1} - 12.216$	0.999

*: The data of particle size of samples with particle size of 100-250 μm , 50-99 μm , and <50 μm , were assigned with 250, 100, and 50, respectively. Variables include total metal concentration ($Metal_{total}$), exchangeable metal concentration ($Metal_{BCR1}$), reducible metal concentration ($Metal_{BCR2}$), oxidisable metal concentration ($Metal_{BCR3}$), residual metal concentration ($Metal_{BCR4}$), soil pH, TOC, and particle size ($Metal_{size}$). Variables with a significance level of $p < 0.05$ were entered into the predictive models.

6.6.2 Human health risk assessment

6.6.2.1 Human health risk assessment of trace metals in soil dust incorporating bioaccessibility

The exposure of trace metals for children through dust ingestion was used to evaluate the total trace metal risks from soils to children, because it is the most important exposure pathway among ingestion, inhalation and dermal contact (Ljung et al., 2007). The average daily intake (ADI) of trace metals through unintentional dust ingestion was calculated as follows (USEPA, 1989; 1996):

$$ADI_{ing-nc} = \frac{C \times IngR \times EF \times ED}{BW \times AT_{nc}} \times 10^{-6}$$

where C is the total concentration or bioaccessible concentration of trace metals in each particle size fraction; IngR is the ingestion rate of soil dust, which is assumed to be 200 mg day⁻¹ (USDOE, 2011); EF is the exposure frequency, which is assumed to be 350 days year⁻¹ (USDOE, 2011); ED is the exposure duration, namely six years; BW is the average body

weight, set at 18 kg for pre-school children (MOHC, 2011); and AT is the averaging time, equivalent to $ED \times 365$ days.

The hazard quotient (HQ) was subsequently calculated as follows:

$$HQ = \frac{ADI}{RfD}$$

where RfD is a reference dose for Co, Cr, Cu, Ni, Pb, and Zn (USDOE, 2011) (Table 6.11). The HQ assumes that there is a level of exposure (RfD), below which it is unlikely for sensitive populations to experience adverse health effects. If the exposure level exceeds this threshold ($HQ > 1$), it suggests the probability of adverse health effects.

The mean HQ for children by total concentration were Pb (2.66E-01) >Co (1.28E-01) >Cr (7.84E-02) >Cu (1.01E-02) >Zn (7.69E-03) >Ni (5.75E-03) in Hong Kong, which were similar to those in Guangzhou Pb (2.83E-01) >Cr (2.46E-01) >Co (1.79E-01) >Cu (2.63E-02) >Zn (1.1E-02) >Ni (1.07E-02). All the HQ levels were lower than 1, showing negligible adverse health effects of soil dust posed by trace metals in both cities. In comparison with other cities, the HQ levels for children in Hong Kong and Guangzhou were higher than those in Nanjing (Wang et al., 2016b), Xiamen (HQ for multi-pathway exposure (Luo et al., 2012c), and Madrid (Izquierdo et al., 2015).

The mean HQ for children incorporating bioaccessible Co, Cr, Cu, Ni, Pb, and Zn was 2.02E-02, 2.58E-03, 6.34E-03, 5.94E-04, 1.71E-01, and 3.80E-03 in Hong Kong, and 2.86E-02, 8.94E-03, 7.65E-03, 1.68E-03, 1.36E-01, and 6.84E-03 in Guangzhou, respectively (Figure 6.23). The HQ values calculated from total concentrations were obviously higher than those from bioaccessible concentrations. Compared with the total concentration, the bioaccessible concentrations can produce more rational results in the exposure assessments (Fendorf et al., 1997; Luo et al., 2012c; Ma et al., 2006). It was found that the bioaccessible Pb from the gastric simulation had a higher correlation with the *in vivo* Pb relative

bioavailability (Li et al., 2014; Ruby et al., 1996; Smith et al., 2011). The HQ levels were comparable between the two cities. According to HQ levels of both total and bioaccessible metal concentrations, Pb in soil dust of the present study and in soils of some other studies (Izquierdo et al., 2015; Luo et al., 2012c; Wang et al., 2016b) had the highest health risk for children compared to other trace metals. It was also reported that blood Pb concentrations were correlated significantly with concentrations of Pb in soils/ re-suspended soils (Bradham et al., 2017; Zahran et al., 2013). Furthermore, Pb in excessive concentrations deteriorates human memory abilities, prolongs reaction time and reduces the understanding abilities (Levin et al., 2008). Thus, attention should be focused on the health risk of Pb through oral ingestion for children.

HQ levels of trace metals estimated by the two methods elevated as soil particle size decreased (Figure 6.23), indicating higher health risks from fine soil dust particles. Moreover, soil particles involuntarily ingested by children are usually of smaller diameter than the original soils (Acosta et al., 2009; Choate et al., 2006; Ljung et al., 2006; Siciliano et al., 2009). Thus, health risks would be underestimated based on metal concentration in bulk soils. The increased HQ level is also relevant in assessing children health risks from exposure to contaminated soils in areas with frequent strong wind. Contaminated soil dust re-suspension can be brought to the downwind areas through northerly winds during the winter monsoon periods or oceanic winds from the south in Hong Kong and Guangzhou. Fine soil particles with high Pb concentration can be entrained into the atmosphere by air turbulence generated by wind or mechanical actions (Charlesworth et al., 2011; Laidlaw and Filippelli, 2008). Zahran et al. (2013) found that 1% increase in the amount of re-suspended soil resulted in a 0.39% increase in the concentration of Pb in the atmosphere. Re-suspended soil particles are closely related to elevated local blood Pb levels (Laidlaw and Filippelli, 2008). Due to the greater relevance of fine particles for both inhalation and ingestion pathways, as well as the enhanced HQ level, fine fractions of soil dust should be considered as an appropriate proxy during the assessment of health risks.

6.6.2.2 Human health risk assessment of trace metals in soil dust <10µm in Hong Kong

The aforementioned analysis has indicated a greater relevance of fine particles for both inhalation and ingestion pathways and higher health risks posed by trace metals. Therefore, in this section, carcinogenic and non-carcinogenic risks posed by trace metals in the finest soil dust fraction (< 10µm) in Hong Kong via ingestion, inhalation and dermal contact to humans were calculated according to the following equations (USDOE, 2011; USEPA, 1989; 1996). Specifically, the noncarcinogenic risk from trace metal exposure to children and carcinogenic risk for the lifetime exposure (adult) were calculated. The parameters used in the equations were listed in Table 6.11.

Non-carcinogenic hazard (child):

$$ADI_{ing-nc} = \frac{C \times IngR \times EF \times ED}{BW \times AT_{nc}} \times 10^{-6}$$

$$ADI_{inh-nc} = \frac{C \times ET \times EF \times ED}{PEF \times 24 \times AT_{nc}}$$

$$ADI_{dermal-nc} = \frac{C \times SA \times AF \times ABS_d \times EF \times ED}{BW \times AT_{nc}} \times 10^{-6}$$

where C is the total concentration of trace metals in soil dust < 10µm; IngR is the ingestion rate of soil dust, which is assumed to be 200 mg day⁻¹ (USDOE, 2011); EF is the exposure frequency, which is assumed to be 350 days year⁻¹ (USDOE, 2011); ED is the exposure duration, namely six years for children and 30 years for adult; BW is the average body weight, set at 18 kg for pre-school children and 61.8 kg for adult (MOHC, 2011); and AT is the averaging time, equivalent to ED × 365 days; ET is the exposure time, which is assumed to be 24 hours day⁻¹ in residential area (USDOE, 2011); PEF is soil to air particulate emission factor, assumed to 1.36×10⁹ m³ kg⁻¹ (USDOE, 2011); SA is skin surface area available for exposure, assumed to 2800 cm² event⁻¹ for child and 5700 cm² event⁻¹ for adult (USDOE,

2011); AF is soil to skin adherence factor, assumed to 0.2 mg cm⁻² for child and 0.07 mg cm⁻² for adult (USDOE, 2011); ABS_d is dermal absorption factor, assumed to 0.001 for these trace metals (USEPA, 2011).

The hazard quotient (HQ) was subsequently calculated as follows:

$$HQ = \frac{ADI}{RfD}$$

where RfD is a reference dose for trace metals. And $RfD_{dermal} = RfD_{ing} \times ABS_{GI}$, where ABS_{GI} is gastrointestinal absorption factor.

Carcinogenic risk (adult):

$$ADI_{ing-ca} = \frac{C \times IngR_{adj} \times EF}{AT_{ca}} \times 10^{-6}$$

$$IngR_{adj} = \frac{ED_{child} \times IngR_{child}}{BW_{child}} + \frac{(ED_{resident} - ED_{child}) \times IngR_{adult}}{BW_{adult}}$$

$$ADI_{inh-ca} = \frac{C \times ET \times EF \times ED}{PEF \times 24 \times AT_{ca}} \times 10^3$$

$$ADI_{dermal-ca} = \frac{C \times ABS_d \times EF \times DFS_{adj}}{AT_{ca}} \times 10^{-6}$$

$$DFS_{adj} = \frac{ED_{child} \times SA_{child} \times AF_{child}}{BW_{child}} + \frac{(ED_{resident} - ED_{child}) \times SA_{adult} \times AF_{adult}}{BW_{adult}}$$

For carcinogens, the dose (Co, Cr, Ni, and Pb) was multiplied by the corresponding slope factor to produce a level of excess lifetime cancer Risk as follows:

$$Risk = ADI_{ca} \times CSF$$

where CSF is chronic oral/dermal slope factor for trace metals. IUR (CSF for inhalation) is the chronic inhalation unit risk.

And $CSF_{dermal} = CSF_{ing} \times ABS_{GI}$, where ABS_{GI} is gastrointestinal absorption factor.

It can be assumed that all the metal risks are additive, although interactions between some metals might result in their synergistic manner (Xu et al., 2011). Thus, it is possible to calculate the cumulative non-carcinogenic hazard using Hazard Index (HI) and carcinogenic risk expressed as the total cancer RISK, which were calculated as:

$$HI = \sum HQ = HQ_{ing} + HQ_{inh} + HQ_{dermal}$$

$$RISK = \sum Risk = Risk_{ing} + Risk_{inh} + Risk_{dermal}$$

For noncarcinogenic risk, $HQ > 1$ suggests the probability of adverse health effects. Generally, carcinogenic risks lower than 1×10^{-6} can be negligible, and risks lower than 1×10^{-4} are considered to be acceptable (USEPA, 1989; 2011).

The non-carcinogenic hazards characterized for children were shown in Figure 6.24. Among the different exposure pathways, HQ for combined metals decreased in the order of HQ_{ing} (0.95) \gg HQ_{dermal} (0.072) $>$ HQ_{inh} (0.0016). 37% of the samples exhibited HQ_{ing} level higher than 1, indicating the probability of adverse health effects through ingestion. Among the different trace metals, HQ of each metal for multi-pathways for all samples was lower than 1, and Pb showed the highest values with an average of 0.41. Cumulatively, the range of HI was 0.46–1.78 with an average of 1.02. 53% of samples showed HI level higher than 1, indicating the probability of noncarcinogenic hazards posed by trace metals in soil dust $< 10\mu\text{m}$.

The carcinogenic risks to adults were shown in Figure 6.25. the risks posed by Cr through ingestion and dermal contact, and Pb through dermal contact for all the samples were higher than 1×10^{-6} , showing nonnegligible carcinogenic risks. Cumulatively, the range of RISK was $1.52\text{E-}5$ – $1.58\text{E-}4$ with an average of $7.3\text{E-}5$, showing the nonnegligible carcinogenic risks. Particularly, the RISK pose by soil dust $< 10\mu\text{m}$ at an extremely contaminated site was higher than 1×10^{-4} , which should be paid attention due to its unacceptable carcinogenic risk. However, it should be noted that both the noncarcinogenic risk and carcinogenic risk posed by

the trace metals in soil dust < 10µm were calculated by total concentration. Because the total metal concentrations were not absolutely bioaccessible, the risk assessment based on total concentrations would result in an overestimate of health risks.

Table 6.11 Parameters for risk assessment calculation (USDOE, 2011; USEPA, 2011).

Factor	RfD _{ing} (mg kg ⁻¹ d ⁻¹)	ABS _{GI}	RfC _{inh} (mg m ⁻³)	CSF _{ing} (mg kg ⁻¹ d ⁻¹) ⁻¹	IUR (µg m ⁻³) ⁻¹
Co	3.00E-04	1	6.00E-06		9.00E-03
Cr	3.00E-03	0.013			1.20E-02
Cr (III)	1.50E+00	0.013			
Cr (VI)	3.00E-03	0.025	1.00E-04	5.00E-01	
Cu	4.00E-02	1			
Ni	2.00E-02	0.04	9.00E-05		2.60E-04
Pb	3.50E-03	1		8.50E-03	1.20E-05
Zn	3.00E-01	1			

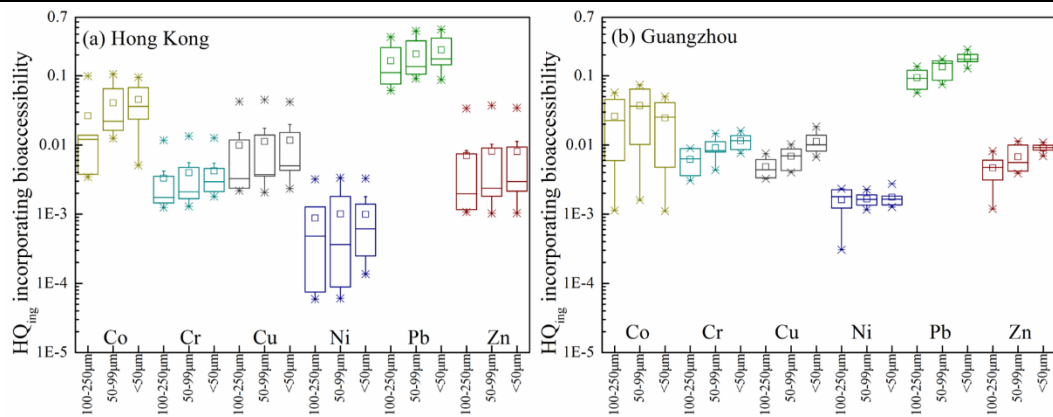


Figure 6.23 Hazard Quotient (HQ) of metals incorporating bioaccessibility in Hong Kong (a, n=7) and Guangzhou (b, n=6). The bars were defined (from the bottom) as minimum, 25th percentile, median, mean (the square), 75th percentile, and maximum.

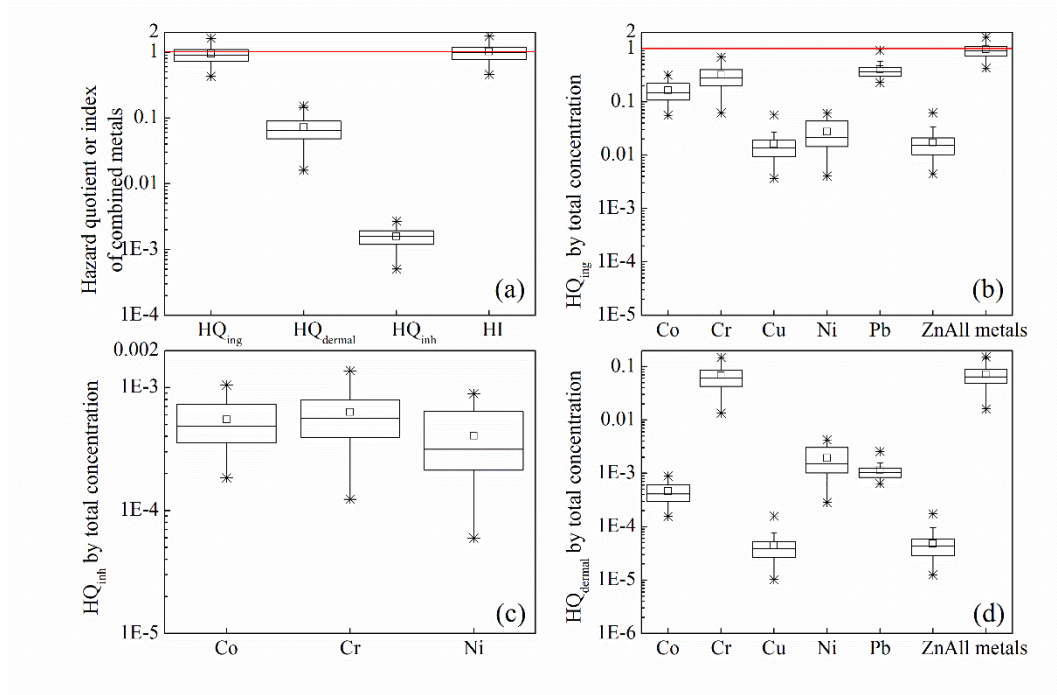


Figure 6.24 Hazard Quotient (HQ) and Hazard Index (HI) of trace metals in soil dust < 10µm in Hong Kong through various exposure pathways (ingestion, inhalation, dermal) for children. (a) HQ of combined metals through the three pathways and the overall HI; (b) HQ of each metal through ingestion; (c) HQ of each metal through inhalation; (d) HQ of each metal through dermal contact. Data above the red line indicates the probability of adverse health effects. The bars were defined (from the bottom) as minimum, 25th percentile, median, mean (the square), 75th percentile, and maximum.

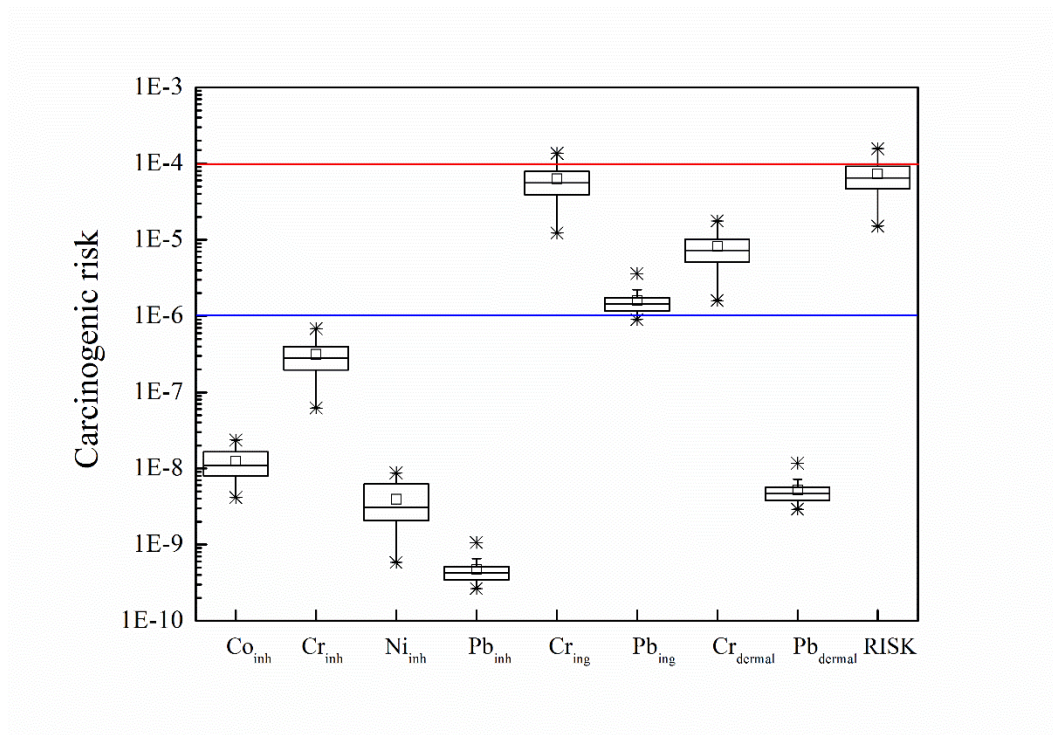


Figure 6.25 Carcinogenic risks of trace metals in soil dust < 10µm in Hong Kong through various exposure pathways (ingestion, inhalation, dermal) and the overall risks (RISK) for adult. Data above the red line indicates unacceptable carcinogenic risk; data within the red line and blue line indicates nonnegligible but acceptable carcinogenic risk; and data below the blue line indicates negligible carcinogenic risk. The bars were defined (from the bottom) as minimum, 25th percentile, median, mean (the square), 75th percentile, and maximum.

6.7 Summary

In this chapter, trace metal distribution, chemical speciation, and health effects of soil dust were investigated in Guangzhou and Hong Kong. Detailed results are listed below:

1. Similar distribution patterns of trace metals in urban soil dust were found in the two cities, with more trace metals associated with smaller particle sizes. However, the metal preferential partitioning in fine particles of soil dust was more distinctive in Guangzhou. The interregional comparison of Pb isotopic compositions ($^{206}\text{Pb}/^{207}\text{Pb}$), atmospheric deposition, and the emission inventories revealed the importance of anthropogenic metal-embedded particle from

atmospheric deposition on metal accumulation in fine particles of soil dust. The results of BCR extraction showed that the adsorption of Mn/Fe oxides and organic complexes was crucial for the metal enrichments in the fine particle size fractions.

2. Temporal declines of trace metals were observed in finest soil particles (<10 µm), atmospheric particulate matters (PM₁₀), and bulk soils in Hong Kong. The comparison of the three media showed that trace metal concentrations in the finest soil particle fraction (<10 µm) were strongly related to the trace metal variations of aerosols. In turn, the average contribution of the soil-derived trace metals to Cu, Pb, and Zn in PM₁₀ approximated to 34%, 46%, and 47%, respectively in Hong Kong.

3. The bioaccessibility of trace metals generally increased with decreasing particle sizes, due to the high mobility of metal species held by the fine particles. Based on the HQ levels, Pb in soil dust had the highest health risk for children. The HQ levels of trace metals estimated by both bioaccessibility and total concentrations elevated with decreasing soil particle sizes, indicating higher health risks from fine soil dust particles. In the soil dust <10 µm in Hong Kong, 53% of the samples showed HI levels higher than 1 and all the samples exhibited RISK levels higher than 1×10^{-6} , indicating the probability of noncarcinogenic hazards and the nonnegligible carcinogenic risks posed by trace metals in soil dust < 10µm.

Conclusively, Chapter Four, Chapter Five, together with Chapter Six, provided a comprehensive knowledge of the trace metal contamination and processes affecting the urban environments, which facilitates our understanding of the suitability using environmental compartments on explaining the trace metal contamination status, the trace metal transports, and the possible health risks in urban environments.

Chapter 7 Conclusions and Recommendation

7.1 Summary of major scientific findings

A multi-compartmental environmental surveillance of trace metal contamination was conducted in urban environments of Hong Kong and Guangzhou. The major findings are as follows:

1. Vertical distribution of trace metals in top soil layers (0–15cm) can be used to reflect the temporal changes of trace metal contamination caused by specific urbanization and industrialization of a city. For Hong Kong, a temporally decrease of trace metal concentrations including Cu, Pb, and Zn was found in urban soils, indicating a decline of trace metal inputs over the last twenty years. The decreasing anthropogenic inputs and possible vertical transport of metals resulted in negative surface accumulation factors (SAFs, -10.7 to -3.1). For Guangzhou urban soils, trace metals displayed a generally increasing pattern over the last twenty years with an exception of Pb due to the vast industrial developments and the increasing number of vehicles, resulting in positive SAFs of Guangzhou soils (0.7 to 23.4).

2. The distribution patterns and links between historical development and trace metal concentrations in Hong Kong and Guangzhou indicated that urban soil was a useful tool to record development history of a city. The remarkable hotspots of trace metals in both surface and top soils in Hong Kong were in close vicinity of past industrial buildings with heavy traffic, indicating the predominant response of past pollutant emissions for the metal contamination in such soils and that it may continue to influence local soils for a long time. In surface soils of Guangzhou, hot spots were attributed to industry and heavy traffic, while hot spot in top soils was in a district with the longest development history..

3. A multi-compartmental investigation was then conducted in the urban environment of Guangzhou to address the suitability of urban soil, road dust, and foliar dust as indicators for describing urban contamination conditions. Lead isotopic data and APCS-MLR analysis identified industrial and traffic emissions as the major sources of trace metals in surface soils, road dust, and foliar dust in Guangzhou. Spatial distribution patterns of EFs and source contributions implied that Cu in road dust was a good indicator for traffic contamination, particularly influenced by traffic volume and vehicle speed; Pb and Zn in foliar dust indicated the industrial contamination, which decreased from the emission source (*e.g.*, power plant and steel factory) to the surrounding environment.

4. Soil dust was collected and divided into different size fractions *in situ*, to study the environmental associations of trace metals in urban environments. Similar distribution patterns of trace metals in urban soil dust were found in the two cities, with more trace metals associated with finer particle sizes. The interregional comparison of Pb isotopic compositions ($^{206}\text{Pb}/^{207}\text{Pb}$), atmospheric deposition, and the emission inventories, revealed the importance of anthropogenic metal-embedded particles from atmospheric deposition on metal accumulation in fine particles of soil dust. The results of chemical speciation of trace metals showed that the adsorption of Mn/Fe oxides and organic complexes were crucial for the metal enrichments in the fine particle size fractions.

5. The transport of trace metals between soil dust and road dust was found in the form of fine particulates, as indicated by the distribution of Pb isotopic compositions ($^{206}\text{Pb}/^{207}\text{Pb}$). Temporal decrease of trace metals in the finest soil particle fraction ($<10\mu\text{m}$) was strongly related to aerosols in Hong Kong, indicating that PM_{10} was a crucial factor of the enrichment of trace metals in fine soil particles. In turn, the average contribution of the soil-derived trace metals to Cu, Pb, and Zn in PM_{10} approximated to 34%, 46%, and 47%, respectively.

6. The bioaccessibility of trace metals generally increased with decreasing particle sizes, probably due to the high mobility of metal species held by the fine particles. Based on the HQ

levels, Pb in soil dust had the highest health risk for children. HQ levels of trace metals elevated with decreasing particle sizes, indicating higher health risks from fine soil dust particles. In the soil dust <10 µm in Hong Kong, 53% of the samples showed HI levels higher than 1 and all the samples exhibited RISK levels higher than 1×10^{-6} , indicating the probability of noncarcinogenic hazards and the nonnegligible carcinogenic risks posed by trace metals in soil dust < 10µm. Thus, the re-suspension of soil dust should be paid more attention to control health risks caused by trace metal contamination in urban environments.

7.2 Limitations and future research

The Pb isotope technique was used to assess the sources and transport of Pb in urban environments. However, sometimes the Pb signatures of the known sources are too close to distinguish. More precise analytical instruments, such as MC-ICP-MS, are required to increase the accuracy of Pb isotopic signature in environmental materials. Moreover, the Pb isotopic signatures of Pb source are insufficient. The major Pb sources, such as coal combustion and vehicle exhaust, are spatially dependent. Thus, more Pb isotopic composition of Pb sources, particularly local sources, should be determined to identify the exact major sources and their contribution to Pb in urban environments. Furthermore, other isotopic fingerprints, such as Cu and Zn, should be explored, as they presented higher contamination levels in urban soils conducted by this study.

Fine soil dust particles, particularly for particles smaller than 10 µm or 2.5µm, are crucial for trace metal transport in terrestrial environments, and influence human health. The metal speciation and bioaccessibility in fine soil dust are related to subsequent health effects and hence, are needed further investigation. In order to provide sufficient material to be used for speciation and bioaccessibility analysis, extraction of a sufficient quantity of *in situ* fine soil dust particles is urgently required. In addition to the traditional chemical methods, metal speciation can be achieved by spectroscopic techniques such as X-ray absorption

spectroscopy (XAS) and X-ray fluorescence microscopy. Spectroscopic techniques are able to examine specific metal speciation and association in complex environmental media due to their high resolution and their selectivity in terms of studied element. Hence, the application of spectroscopic techniques are required to better investigate the metal sources, speciation, and behavior in soil dust in future work. Furthermore, bioaccessibility of trace metals in not only gastrointestinal system but also respiratory system should be examined, because fine soil particles can enter into the respiratory tissue or even lung tissues causing toxic effect.

Exchanges of contaminants take place among different environmental compartments, and thus, monitoring of multi-contaminants in related sources and receptors (environmental compartments in the forms of fine particulates) should be carried out. It is crucial to understand the exchanges, partition, and transport pathways of contaminants in urban environments. The application and development of transport models for trace metals are needed to be further explored, for prediction and management of trace metal contamination in urban environments.

References

- Abrahams, P.W., 2002. Soils: their implications to human health. *Sci. Total Environ.* 291 (1-3), 1-32.
- Acosta, J.A., Martínez-Martínez, S., Faz, A., Arocena, J., 2011. Accumulations of major and trace elements in particle size fractions of soils on eight different parent materials. *Geoderma* 161 (1-2), 30-42.
- Acosta, J.A., Cano, A.F., Arocena, J.M., Debela, F., Martínez-Martínez, S., 2009. Distribution of metals in soil particle size fractions and its implication to risk assessment of playgrounds in Murcia City (Spain). *Geoderma* 149 (1-2), 101-109.
- Acosta, J.A., Faz, A., Kalbitz, K., Jansen, B., Martínez-Martínez, S., 2014. Partitioning of heavy metals over different chemical fraction in street dust of Murcia (Spain) as a basis for risk assessment. *J. Geochem. Explor.* 144, 298-305.
- Adachi, K., Tainosho, Y., 2004. Characterization of heavy metal particles embedded in tire dust. *Environ. Int.* 30 (8), 1009-1017.
- Adriano, D.C., 2001. Trace elements in terrestrial environments: Biogeochemistry, bioavailability, and risks of metals (2nd ed.), Springer, New York.
- Aelion, C.M., Davis, H.T., McDermott, S., Lawson, A.B., 2009. Soil metal concentrations and toxicity: Associations with distances to industrial facilities and implications for human health. *Sci. Total Environ.* 407 (7), 2216-2223.
- Ajmone-Marsan, F., Biasioli, M., 2010. Trace elements in soils of urban areas. *Water Air Soil Poll.* 213 (1-4), 121-143.
- Ajmone-Marsan, F., Biasioli, M., Kralj, T., Grčman, H., Davidson, C.M., Hursthouse, A.S., Madrid, L., Rodrigues, S., 2008. Metals in particle-size fractions of the soils of five European cities. *Environ. Pollut.* 152 (1), 73-81.
- Al-Chalabi, A.S., Hawker, D., 2000. Distribution of vehicular lead in roadside soils of major roads of Brisbane, Australia. *Water Air Soil Poll.* 118 (3-4), 299-310.
- Al-Khashman, O.A., 2004. Heavy metal distribution in dust, street dust and soils from the work place in Karak industrial estate, Jordan. *Atmos. Environ.* 38 (39), 6803-6812.
- Al-Khashman, O.A., Shawabkeh, R.A., 2009. Metal distribution in urban soil around steel industry beside Queen Alia Airport, Jordan. *Environ. Geochem. Health* 31 (6), 717-726.

- Al-Khashman, O.A., Al-Muhtaseb, A.a.H., Ibrahim, K.A., 2011. Date palm (*Phoenix dactylifera* L.) leaves as biomonitors of atmospheric metal pollution in arid and semi-arid environments. *Environ. Pollut.* 159 (6), 1635-1640.
- Alloway, B.J., 2013. Heavy metals in soils, Springer Netherlands.
- Amato, F., Pandolfi, M., Alastuey, A., Lozano, A., Contreras González, J., Querol, X., 2013. Impact of traffic intensity and pavement aggregate size on road dust particles loading. *Atmos. Environ.* 77, 711-717.
- Amato, F., Pandolfi, M., Escrig, A., Querol, X., Alastuey, A., Pey, J., Perez, N., Hopke, P.K., 2009. Quantifying road dust resuspension in urban environment by Multilinear Engine: A comparison with PMF2. *Atmos. Environ.* 43 (17), 2770-2780.
- Amato, F., Karanasiou, A., Cordoba, P., Alastuey, A., Moreno, T., Lucarelli, F., Nava, S., Calzolari, G., Querol, X., 2014. Effects of road dust suppressants on PM levels in a mediterranean urban area. *Environ. Sci. Technol.* 48 (14), 8069-8077.
- Amato, F., Pandolfi, M., Moreno, T., Furger, M., Pey, J., Alastuey, A., Bukowiecki, N., Prevot, A.S.H., Baltensperger, U., Querol, X., 2011. Sources and variability of inhalable road dust particles in three European cities. *Atmos. Environ.* 45 (37), 6777-6787.
- Amato, F., Favez, O., Pandolfi, M., Alastuey, A., Querol, X., Moukhtar, S., Bruge, B., Verlhac, S., Orza, J.A.G., Bonnaire, N., Le Priol, T., Petit, J.F., Sciare, J., 2016. Traffic induced particle resuspension in Paris: Emission factors and source contributions. *Atmos. Environ.* 129, 114-124.
- Apeageyi, E., Bank, M.S., Spengler, J.D., 2011. Distribution of heavy metals in road dust along an urban-rural gradient in Massachusetts. *Atmos. Environ.* 45 (13), 2310-2323.
- Argyaki, A., Kelepertzis, E., 2014. Urban soil geochemistry in Athens, Greece: The importance of local geology in controlling the distribution of potentially harmful trace elements. *Sci. Total Environ.* 482-483, 366-377.
- Artiñano, B., Salvador, P., Alonso, D.G., Querol, X., Alastuey, A., 2003. Anthropogenic and natural influence on the PM₁₀ and PM_{2.5} aerosol in Madrid (Spain). Analysis of high concentration episodes. *Environ. Pollut.* 125 (3), 453-465.
- Avino, P., Capannesi, G., Rosada, A., 2014. Source identification of inorganic airborne particle fraction (PM₁₀) at ultratrace levels by means of INAA short irradiation. *Environ. Sci. Pollut. R.* 21 (6), 4527-4538.

- Bermudez, G.M., Moreno, M., Invernizzi, R., Pla, R., Pignata, M.L., 2010. Heavy metal pollution in topsoils near a cement plant: the role of organic matter and distance to the source to predict total and hcl-extracted heavy metal concentrations. *Chemosphere* 78 (4), 375-381.
- Bhattacharya, T., Chakraborty, S., Tuteja, D., Patel, M., 2013. Zinc and chromium load in road dust, suspended particulate matter and foliar dust deposits of Anand city, Gujarat. *O. J. Metal* 03 (02), 42-50.
- Bi, C.J., Zhou, Y., Chen, Z.L., Jia, J.P., Bao, X.Y., 2018. Heavy metals and lead isotopes in soils, road dust and leafy vegetables and health risks via vegetable consumption in the industrial areas of Shanghai, China. *Sci. Total Environ.* 619-620, 1349-1357.
- Bi, X.Y., personal communication.
- Bi, X.Y., Liang, S.Y., Li, X.D., 2013a. Trace metals in soil, dust, and tree leaves of the urban environment, Guangzhou, China. *Chin. Sci. Bull.* 58 (2), 222-230.
- Bi, X.Y., Liang, S.Y., Li, X.D., 2013b. A novel *in situ* method for sampling urban soil dust: Particle size distribution, trace metal concentrations, and stable lead isotopes. *Environ. Pollut.* 177, 48-57.
- Bi, X.Y., Li, Z.G., Sun, G.Y., Liu, J.L., Han, Z.X., 2015. In vitro bioaccessibility of lead in surface dust and implications for human exposure: A comparative study between industrial area and urban district. *J. Hazard. Mater.* 297, 191-197.
- Bi, X.Y., Li, Z.G., Wang, S.X., Zhang, L., Xu, R., Liu, J.L., Yang, H.M., Guo, M.Z., 2017. Lead isotopic compositions of selected coals, Pb/Zn ores and fuels in China and the application for source tracing. *Environ. Sci. Technol.* 51 (22), 13502-13508.
- Biasioli, M., Barberis, R., Ajmonemarsan, F., 2006. The influence of a large city on some soil properties and metals content. *Sci. Total Environ.* 356, 154-164.
- Bollhöfer, A., Rosman, K., 2001. Isotopic source signatures for atmospheric lead: the Northern Hemisphere. *Geochim. Cosmochim. Ac.* 65 (11), 1727-1740.
- Bourliva, A., Papadopoulou, L., Aidona, E., 2016. Study of road dust magnetic phases as the main carrier of potentially harmful trace elements. *Sci. Total Environ.* 553, 380-391.
- Bowen, H.J.M., 1979. *Environmental chemistry of the elements*, Academic Press.
- Bradham, K.D., Nelson, C.M., Kelly, J., Pomales, A., Scruton, K., Dignam, T., Misenheimer, J.C., Li, K., Obenour, D.R., Thomas, D.J., 2017. Relationship between total and bioaccessible lead on children's blood lead levels in urban residential Philadelphia soils. *Environ. Sci. Technol.* 51 (17), 10005-10011.

- Bright, D.A., Richardson, G.M., Dodd, M., 2006. Do current standards of practice in Canada measure what is relevant to human exposure at contaminated sites? I: a discussion of soil particle size and contaminant partitioning in soil. *Hum. Ecol. Risk Assess.* 12 (3), 591-605.
- Brock, C.A., 2003. Particle growth in urban and industrial plumes in Texas. *J. Geophys. Res.* 108 (D3).
- Buchet, J.P., Lauwerys, R., Roels, H., Bernard, A., Bruaux, P., Claeys, F., Ducoffre, G., Plaen, P.d., Staessen, J., Amery, A., Lijnen, P., Thijs, L., Rondia, D., Sartor, F., Remy, A.S., Nick, L., 1990. Renal effects of cadmium body burden of the general population. *Lancet* 336 (8717), 699-702.
- Bukowiecki, N., Lienemann, P., Hill, M., Furger, M., Richard, A., Amato, F., Prévôt, A.S.H., Baltensperger, U., Buchmann, B., Gehrig, R., 2010. PM₁₀ emission factors for non-exhaust particles generated by road traffic in an urban street canyon and along a freeway in Switzerland. *Atmos. Environ.* 44 (19), 2330-2340.
- Burkhardt, J., Basi, S., Pariyar, S., Hunsche, M., 2012. Stomatal penetration by aqueous solutions - an update involving leaf surface particles. *New Phytol.* 196 (3), 774-787.
- Cabral, P., Augusto, G., Tewolde, M., Araya, Y., 2013. Entropy in urban systems. *Entropy* 15 (12), 5223-5236.
- Cai, Q.Y., Mo, C.H., Li, H.Q., Lü, H.X., Zeng, Q.Y., Li, Y.W., Wu, X.L., 2012. Heavy metal contamination of urban soils and dusts in Guangzhou, South China. *Environ. Monit. Assess.* 185 (2), 1095-1106.
- Calcabrini, A., Meschini, S., Marra, M., Falzano, L., Colone, M., Berardis, B.D., Paoletti, L., Arancia, G., Fiorentini, C., 2004. Fine environmental particulate engenders alterations in human lung epithelial A549 cells. *Environ. Res.* 95 (1), 82-91.
- Calvo, A.I., Alves, C., Castro, A., Pont, V., Vicente, A.M., Fraile, R., 2013. Research on aerosol sources and chemical composition: Past, current and emerging issues. *Atmos. Res.* 120, 1-28.
- Cannon, W.F., Horton, J.D., 2009. Soil geochemical signature of urbanization and industrialization – Chicago, Illinois, USA. *Appl. Geochem.* 24 (8), 1590-1601.
- Carrero, J.A., Arrizabalaga, I., Bustamante, J., Goienaga, N., Arana, G., Madariaga, J.M., 2013. Diagnosing the traffic impact on roadside soils through a multianalytical data analysis of the concentration profiles of traffic-related elements. *Sci. Total Environ.* 458-460, 427-434.

- Carter, M.R., Gaudet, B.J., Stauffer, D.R., White, T.S., Brantley, S.L., 2015. Using soil records with atmospheric dispersion modeling to investigate the effects of clean air regulations on 60years of manganese deposition in Marietta, Ohio (USA). *Sci. Total Environ.* 515-516, 49-59.
- CCME, 2007. Canadian soil quality guidelines for the protection of environmental and human health, Canadian Council of Ministers of the Environment.
- Censi, P., Zuddas, P., Randazzo, L.A., Tamburo, E., Speziale, S., Cuttitta, A., Punturo, R., Aricò, P., Santagata, R., 2011. Source and nature of inhaled atmospheric dust from trace element analyses of human bronchial fluids. *Environ. Sci. Technol.* 45 (15), 6262-6267.
- Census and Statistics Department, 2000. Annual report of Hong Kong, 1999, The Government of the Hong Kong Special Administrative Region.
- Census and Statistics Department, 2013. Annual report of Hong Kong, 2012, The Government of the Hong Kong Special Administrative Region.
- Census and Statistics Department, 2016. Broad land usage. http://www.pland.gov.hk/pland_en/info_serv/statistic/landu.html, retrieved 2017-11-24.
- CEPA, 1995. Environmental quality standard for soils (GB 15618-1995), Chinese Environmental Protection Administration.
- Chan, S., Gerson, B., Subramaniam, S., 1998. The role of copper, molybdenum, selenium, and zinc in nutrition and health. *Clin. Lab. Med.* 18 (4), 673-685.
- Charlesworth, S., De Miguel, E., Ordóñez, A., 2011. A review of the distribution of particulate trace elements in urban terrestrial environments and its application to considerations of risk. *Environ. Geochem. Health* 33 (2), 103-123.
- Charlesworth, S., Everett, M., McCarthy, R., Ordóñez, A., de Miguel, E., 2003. A comparative study of heavy metal concentration and distribution in deposited street dusts in a large and a small urban area: Birmingham and Coventry, West Midlands, UK. *Environ. Int.* 29 (5), 563-573.
- Chen, H., Lu, X.W., Li, L.Y., Gao, T.N., Chang, Y.Y., 2014. Metal contamination in campus dust of Xi'an, China: A study based on multivariate statistics and spatial distribution. *Sci. Total Environ.* 484, 27-35.
- Chen, J., Wang, W., Liu, H., Ren, L., 2012. Determination of road dust loadings and chemical characteristics using resuspension. *Environ Monit Assess* 184 (3), 1693-1709.

- Chen, T.B., Zheng, Y.M., Chen, H., Zheng, G.D., 2004. Background concentrations of soil heavy metals in Beijing. *Chinese Journal of Environmental Science* 25 (1), 117-122. in Chinese.
- Chen, T.B., Zheng, Y.M., Lei, M., Huang, Z.C., Wu, H.T., Chen, H., Fan, K.K., Yu, K., Wu, X., Tian, Q.Z., 2005. Assessment of heavy metal pollution in surface soils of urban parks in Beijing, China. *Chemosphere* 60 (4), 542-551.
- Chen, X., Xia, X.H., Zhao, Y., Zhang, P., 2010. Heavy metal concentrations in roadside soils and correlation with urban traffic in Beijing, China. *J. Hazard. Mater.* 181 (1-3), 640-646.
- Chenery, S.R., Izquierdo, M., Marzouk, E., Klinck, B., Palumbo-Roe, B., Tye, A.M., 2012. Soil-plant interactions and the uptake of Pb at abandoned mining sites in the Rookhope catchment of the N. Pennines, UK — A Pb isotope study. *Sci. Total Environ.* 433, 547-560.
- Cheng, Y., Lee, S.C., Gu, Z.L., Ho, K.F., Zhang, Y.W., Huang, Y., Chow, J.C., Watson, J.G., Cao, J., Zhang, R., 2015. PM_{2.5} and PM_{10-2.5} chemical composition and source apportionment near a Hong Kong roadway. *Particuology* 18, 96-104.
- Choate, L.M., Ranville, J.F., Bunge, A.L., Macalady, D.L., 2006. Dermally adhered soil: 1. Amount and particle-size distribution. *Integr. Environ. Asses* 2 (4), 375-384.
- Christoforidis, A., Stamatis, N., 2009. Heavy metal contamination in street dust and roadside soil along the major national road in Kavala's region, Greece. *Geoderma* 151 (3-4), 257-263.
- Crosier, S., 2004. *ArcGIS 9: Geocoding in ArcGIS*, ESRI Press.
- Cundy, A.B., Croudace, I.W., 2017. The fate of contaminants and stable Pb isotopes in a changing estuarine environment: 20 years on. *Environ. Sci. Technol.* 51 (17), 9488-9497.
- Dahiya, P., Ahlawat, M., 2010. *Environmental science: A new approach*, Alpha Science.
- Davis, H.T., Marjorie Aelion, C., McDermott, S., Lawson, A.B., 2009. Identifying natural and anthropogenic sources of metals in urban and rural soils using GIS-based data, PCA, and spatial interpolation. *Environ. Pollut.* 157 (8-9), 2378-2385.
- De Miguel, E., Iribarren, I., Chacón, E., Ordoñez, A., Charlesworth, S., 2007. Risk-based evaluation of the exposure of children to trace elements in playgrounds in Madrid (Spain). *Chemosphere* 66 (3), 505-513.
- Deljanin, I., Antanasijević, D., Bjelajac, A., Urošević, M.A., Nikolić, M., Perić-Grujić, A., Ristić, M., 2016. Chemometrics in biomonitoring: Distribution and correlation of trace elements in tree leaves. *Sci. Total Environ.* 545-546, 361-371.

- Deng, W.J., Zheng, J.S., Bi, X.H., Fu, J.M., Wong, M.H., 2007. Distribution of PBDEs in air particles from an electronic waste recycling site compared with Guangzhou and Hong Kong, South China. *Environ. Int.* 33 (8), 1063-1069.
- Duong, T.T.T., Lee, B.K., 2011. Determining contamination level of heavy metals in road dust from busy traffic areas with different characteristics. *J. Environ. Manage.* 92 (3), 554-562.
- Duzgoren-Aydin, N.S., 2007. Sources and characteristics of lead pollution in the urban environment of Guangzhou. *Sci. Total Environ.* 385 (1-3), 182-195.
- Duzgoren-Aydin, N.S., Weiss, A.L., 2008. Use and abuse of Pb-isotope fingerprinting technique and GIS mapping data to assess lead in environmental studies. *Environ. Geochem. Health* 30 (6), 577-588.
- Duzgoren-Aydin, N.S., Wong, C.S.C., Aydin, A., Song, Z., You, M., Li, X.D., 2006. Heavy metal contamination and distribution in the urban environment of Guangzhou, SE China. *Environ. Geochem. Health* 28 (4), 375-391.
- Duzgoren-Aydin, N.S., Wong, C.S.C., Song, Z.G., Aydin, A., Li, X.D., You, M., 2007. Fate of heavy metal contaminants in road dusts and gully sediments in Guangzhou, SE China: A chemical and mineralogical assessment. *Hum. Ecol. Risk Assess.* 12 (2), 374-389.
- EPD, 2000. Hong Kong Environmental Protection Department.
- Espinosa, A.J.F., Oliva, S.R., 2006. The composition and relationships between trace element levels in inhalable atmospheric particles (PM₁₀) and in leaves of *Nerium oleander* L. and *Lantana camara* L. *Chemosphere* 62 (10), 1665-1672.
- Faiz, Y., Tufail, M., Javed, M.T., Chaudhry, M.M., Naila, S., 2009. Road dust pollution of Cd, Cu, Ni, Pb and Zn along Islamabad Expressway, Pakistan. *Microchem. J.* 92 (2), 186-192.
- Farmer, J.G., Broadway, A., Cave, M.R., Wragg, J., Fordyce, F.M., Graham, M.C., Ngwenya, B.T., Bewley, R.J.F., 2011. A lead isotopic study of the human bioaccessibility of lead in urban soils from Glasgow, Scotland. *Sci. Total Environ.* 409 (23), 4958-4965.
- Faure, G., 1977. Principles of isotope geology.
- Fendorf, S., Eick, M.J., Grossl, P., Sparks, D.L., 1997. Arsenate and chromate retention mechanisms on goethite. 1. surface structure. *Environ. Sci. Technol.* 31 (2), 315-320.
- Fryrear, D.W., Stout, J.E., Hagen, L.J., Vories, E.D., 1991. Wind erosion: field measurement and analysis. *Trans. ASAE* 34 (1), 155-160.

- Fujimori, T., Taniguchi, M., Agusa, T., Shiota, K., Takaoka, M., Yoshida, A., Terazono, A., Ballesteros, F.C., Jr., Takigami, H., 2018. Effect of lead speciation on its oral bioaccessibility in surface dust and soil of electronic-wastes recycling sites. *J. Hazard Mater.* 341, 365-372.
- Gao, Z.Y., Yin, G., Ni, S.J., Zhang, C.J., 2004. Geochemical feature of the urban environmental lead isotope in Chengdu city. *Carsologica. Sinica.* 23 (4), 267-272. in Chinese.
- Gomez, B., Palacios, M.A., Gomez, M., Sanchez, J.L., Morrison, G., Rauch, S., McLeod, C., Ma, R., Caroli, S., Alimonti, A., 2002. Levels and risk assessment for humans and ecosystems of platinum-group elements in the airborne particles and road dust of some European cities. *Sci. Total Environ.* 299 (1), 1-19.
- Goodarzi, F., 2006a. Characteristics and composition of fly ash from Canadian coal-fired power plants. *Fuel* 85 (10-11), 1418-1427.
- Goodarzi, F., 2006b. Morphology and chemistry of fine particles emitted from a Canadian coal-fired power plant. *Fuel* 85 (3), 273-280.
- Gu, Y.G., Gao, Y.P., Lin, Q., 2016. Contamination, bioaccessibility and human health risk of heavy metals in exposed-lawn soils from 28 urban parks in southern China's largest city, Guangzhou. *Appl. Geochem.* 67, 52-58.
- Gualtieri, M., Mantecca, P., Cetta, F., Camatini, M., 2008. Organic compounds in tire particle induce reactive oxygen species and heat-shock proteins in the human alveolar cell line A549. *Environ. Int.* 34 (4), 437-442.
- Guan, D.S., Peart, M.R., 2006. Heavy metal concentrations in plants and soils at roadside locations and parks of urban Guangzhou. *J. Environ. Sci.* 18 (3), 495-502.
- Guan, D.S., Chen, Y.J., Yuan, G.B., 2001. Study on heavy metal concentrations and the impact of human activity on them in urban and suburb soils of Guangzhou. *Acta Scientiarum Naturalium Universitatis Sunyatseni* 40, 93-96.
- Guangdong Geological Survey, 2010. Multi-purposes geochemical survey: Pear River Delta, Guangdong province.
- Guangzhou Bureau of Statistics, 1984. Annual report of Guangzhou, 1983.
- Guangzhou Bureau of Statistics, 2000. Annual report of Guangzhou, 1999.
- Guangzhou Bureau of Statistics, 2013. Annual report of Guangzhou, 2012.

- Guangzhou Transport Planning Research Institute, 2012. Guangzhou transport development annual report.
- Gunawardana, C., Goonetilleke, A., Egodawatta, P., Dawes, L., Kokot, S., 2012. Source characterisation of road dust based on chemical and mineralogical composition. *Chemosphere* 87 (2), 163-170.
- Guo, H., Wang, T., Louie, P.K., 2004. Source apportionment of ambient non-methane hydrocarbons in Hong Kong: application of a principal component analysis/absolute principal component scores (PCA/APCS) receptor model. *Environ. Pollut.* 129 (3), 489-498.
- Ha, H., Olson, J.R., Bian, L., Rogerson, P.A., 2014. Analysis of heavy metal sources in soil using Kriging interpolation on principal components. *Environ. Sci. Technol.* 48 (9), 4999-5007.
- Hardy, M., Cornu, S., 2006. Location of natural trace elements in silty soils using particle-size fractionation. *Geoderma* 133 (3-4), 295-308.
- Harrison, R.M., Smith, D.J.T., Luhana, L., 1996. Source apportionment of atmospheric polycyclic aromatic hydrocarbons collected from an urban location in Birmingham, UK. *Environ. Sci. Technol.* 30 (3), 825-832.
- Harrison, R.M., Jones, A.M., Gietl, J., Yin, J., Green, D.C., 2012. Estimation of the contributions of brake dust, tire wear, and resuspension to nonexhaust traffic particles derived from atmospheric measurements. *Environ. Sci. Technol.* 46 (12), 6523-6529.
- Hassan, I.A., Basahi, J.M., 2013. Assessing roadside conditions and vehicular emissions using roadside lettuce plants. *Pol. J. Environ. Stud.* 22 (2), 387-393.
- Hazelton, P., Murphy, B., 2011. *Understanding soils in urban environments*, Csiro publishing.
- Ho, K.F., Lee, S.C., Chow, J.C., Watson, J.G., 2003a. Characterization of PM₁₀ and PM_{2.5} source profiles for fugitive dust in Hong Kong. *Atmos. Environ.* 37 (8), 1023-1032.
- Ho, K.F., Lee, S.C., Chan, C.K., Jimmy, C.Y., Chow, J.C., Yao, X.H., 2003b. Characterization of chemical species in PM_{2.5} and PM₁₀ aerosols in Hong Kong. *Atmos. Environ.* 37 (1), 31-39.
- Hofman, J., Stokkaer, I., Snauwaert, L., Samson, R., 2013. Spatial distribution assessment of particulate matter in an urban street canyon using biomagnetic leaf monitoring of tree crown deposited particles. *Environ. Pollut.* 183, 123-132.
- Hopke, P.K., Lamb, R.E., Natusch, D.F.S., 1980. Multielemental characterization of urban roadway dust. *Environ. Sci. Technol.* 14 (2), 164-172.

- Hsu, C.Y., Chiang, H.C., Lin, S.L., Chen, M.J., Lin, T.Y., Chen, Y.C., 2016. Elemental characterization and source apportionment of PM₁₀ and PM_{2.5} in the western coastal area of central Taiwan. *Sci. Total Environ.* 541, 1139-1150.
- Hu, X., Zhang, Y., Luo, J., Wang, T., Lian, H., Ding, Z., 2011a. Bioaccessibility and health risk of arsenic, mercury and other metals in urban street dusts from a mega-city, Nanjing, China. *Environ. Pollut.* 159 (5), 1215-1221.
- Hu, X., Zhang, Y., Luo, J., Xie, M.J., Wang, T.J., Lian, H.Z., 2011b. Accumulation and quantitative estimates of airborne lead for a wild plant (*Aster subulatus*). *Chemosphere* 82 (10), 1351-1357.
- Hu, X., Sun, Y.Y., Ding, Z.H., Zhang, Y., Wu, J.C., Lian, H.Z., Wang, T.J., 2014. Lead contamination and transfer in urban environmental compartments analyzed by lead levels and isotopic compositions. *Environ. Pollut.* 187, 42-48.
- Huang, W., Duan, D.D., Zhang, Y.L., Cheng, H.F., Ran, Y., 2014a. Heavy metals in particulate and colloidal matter from atmospheric deposition of urban Guangzhou, South China. *Mar. Pollut. Bull.* 85 (2), 720-726.
- Huang, Z.Y., Xie, H., Cao, Y.L., Cai, C., Zhang, Z., 2014b. Assessing of distribution, mobility and bioavailability of exogenous Pb in agricultural soils using isotopic labeling method coupled with BCR approach. *J. Hazard. Mater.* 266, 182-188.
- Hunt, A., Johnson, D.L., Thornton, I., Watt, J.M., 1993. Apportioning the sources of lead in house dusts in the London borough of Richmond, England. *Sci. Total Environ.* 138 (1), 183-206.
- Iijima, A., Sato, K., Yano, K., Tago, H., Kato, M., Kimura, H., Furuta, N., 2007. Particle size and composition distribution analysis of automotive brake abrasion dusts for the evaluation of antimony sources of airborne particulate matter. *Atmos. Environ.* 41 (23), 4908-4919.
- Imperato, M., 2003. Spatial distribution of heavy metals in urban soils of Naples city (Italy). *Environ. Pollut.* 124 (2), 247-256.
- Izquierdo, M., De Miguel, E., Ortega, M.F., Mingot, J., 2015. Bioaccessibility of metals and human health risk assessment in community urban gardens. *Chemosphere* 135, 312-318.
- Järup, L., Hellström, L., Alfvén, T., Carlsson, M.D., Grubb, A., Persson, B., Pettersson, C., Spång, G., Schütz, A., Elinder, C.G., 2000. Low level exposure to cadmium and early kidney damage: the OSCAR study. *Occup. Environ. Med.* 57 (10), 668-672.
- Jayarathne, A., Egodawatta, P., Ayoko, G.A., Goonetilleke, A., 2017. Geochemical phase and particle size relationships of metals in urban road dust. *Environ. Pollut.* 230, 218-226.

- Ji, Y., Sarret, G., Schulin, R., Tandy, S., 2017. Fate and chemical speciation of antimony (Sb) during uptake, translocation and storage by rye grass using XANES spectroscopy. *Environ. Pollut.* 231 (Pt 2), 1322-1329.
- Ji, Y., Wu, P., Zhang, J., Zhang, J., Zhou, Y., Peng, Y., Zhang, S., Cai, G., Gao, G., 2018. Heavy metal accumulation, risk assessment and integrated biomarker responses of local vegetables: A case study along the Le'an river. *Chemosphere* 199, 361-371.
- Jiang, S.Y., Kaul, D.S., Yang, F.H., Sun, L., Ning, Z., 2015. Source apportionment and water solubility of metals in size segregated particles in urban environments. *Sci. Total Environ.* 533, 347-355.
- Johnson, C.C., Demetriades, A., Locutura, J., Ottesen, R.T., 2011. Mapping the chemical environment of urban areas, Wiley Online Library.
- Juhasz, A.L., Weber, J., Smith, E., 2011. Impact of soil particle size and bioaccessibility on children and adult lead exposure in peri-urban contaminated soils. *J. Hazard. Mater.* 186 (2-3), 1870-1879.
- Kabata-Pendias, A., 2000. Trace elements in soils and plants, CRC press.
- Kabata-Pendias, A., 2004. Soil-plant transfer of trace elements—an environmental issue. *Geoderma* 122 (2-4), 143-149.
- Kabata-Pendias, A., Mukherjee, A.B., 2007. Trace elements from soil to human, Springer.
- Karanasiou, A., Moreno, T., Amato, F., Lumbreras, J., Narros, A., Borge, R., Tobías, A., Boldo, E., Linares, C., Pey, J., Reche, C., Alastuey, A., Querol, X., 2011. Road dust contribution to PM levels – Evaluation of the effectiveness of street washing activities by means of Positive Matrix Factorization. *Atmos. Environ.* 45 (13), 2193-2201.
- Kardel, F., Wuyts, K., Babanezhad, M., Vitharana, U.W.A., Wuytack, T., Potters, G., Samson, R., 2010. Assessing urban habitat quality based on specific leaf area and stomatal characteristics of *Plantago lanceolata* L. *Environ. Pollut.* 158 (3), 788-794.
- Karna, R.R., Noerpel, M., Betts, A.R., Scheckel, K.G., 2017. Lead and arsenic bioaccessibility and speciation as a function of soil particle size. *J. Environ. Qual.* 46 (6), 1225-1235.
- Keane, B., Collier, M.H., Shann, J.R., Rogstad, S.H., 2001. Metal content of dandelion (*Taraxacum officinale*) leaves in relation to soil contamination and airborne particulate matter. *Sci. Total Environ.* 281 (1), 63-78.

- Kelepertzis, E., Argyraki, A., 2015. Geochemical associations for evaluating the availability of potentially harmful elements in urban soils: Lessons learnt from Athens, Greece. *Appl. Geochem.* 59, 63-73.
- Kim, E.J., Yoo, J.C., Baek, K., 2014. Arsenic speciation and bioaccessibility in arsenic-contaminated soils: Sequential extraction and mineralogical investigation. *Environ. Pollut.* 186, 29-35.
- Kim, G., Lee, S., 2018. Characteristics of tire wear particles generated by a tire simulator under various driving conditions. *Environ. Sci. Technol.*
- Kim, K.W., Thornton, I., 1993. Influence of uraniferous black shales on cadmium, molybdenum and selenium in soils and crop plants in the Deog-Pyoun-g area of Korea. *Environ. Geochem. Health* 15 (2-3), 119-133.
- Kim, W., Doh, S.J., Park, Y.H., Yun, S.T., 2007. Two-year magnetic monitoring in conjunction with geochemical and electron microscopic data of roadside dust in Seoul, Korea. *Atmos. Environ.* 41 (35), 7627-7641.
- Kissel, J.C., Richter, K.Y., Fenske, R.A., 1996. Factors affecting soil adherence to skin in hand-press trials. *B. Environ. Contam. Tox.* 56 (5), 722-728.
- Kissel, J.C., Shirai, J.H., Richter, K.Y., Fenske, R.A., 1998. Investigation of dermal contact with soil in controlled trials. *J. Soil Contam.* 7 (6), 737-752.
- Kocher, B., Wessolek, G., Stoffregen, H., 2005. Water and heavy metal transport in roadside soils. *Pedosphere* 15 (6), 746-753.
- Komárek, M., Ettler, V., Chrastný, V., Mihaljevič, M., 2008. Lead isotopes in environmental sciences: A review. *Environ. Int.* 34 (4), 562-577.
- Kreider, M.L., Panko, J.M., McAtee, B.L., Sweet, L.I., Finley, B.L., 2010. Physical and chemical characterization of tire-related particles: Comparison of particles generated using different methodologies. *Sci. Total Environ.* 408 (3), 652-659.
- Kuhns, H., Etyemezian, V., Landwehr, D., MacDougall, C., Pitchford, M., Green, M., 2001. Testing re-entrained aerosol kinetic emissions from roads : a new approach to infer silt loading on roadways. *Atmos. Environ.* 35 (16), 2815-2825.
- Laidlaw, M.A.S., Filippelli, G.M., 2008. Resuspension of urban soils as a persistent source of lead poisoning in children: A review and new directions. *Appl. Geochem.* 23 (8), 2021-2039.

- Laidlaw, M.A.S., Zahran, S., Mielke, H.W., Taylor, M.P., Filippelli, G.M., 2012. Re-suspension of lead contaminated urban soil as a dominant source of atmospheric lead in Birmingham, Chicago, Detroit and Pittsburgh, USA. *Atmos. Environ.* 49, 302-310.
- Laidlaw, M.A.S., Alankarage, D.H., Reichman, S.M., Taylor, M.P., Ball, A.S., 2018. Assessment of soil metal concentrations in residential and community vegetable gardens in Melbourne, Australia. *Chemosphere* 199, 303-311.
- Lee, C., Li, X., Shi, W., Cheung, S., Thornton, I., 2006. Metal contamination in urban, suburban, and country park soils of Hong Kong: A study based on GIS and multivariate statistics. *Sci. Total Environ.* 356 (1-3), 45-61.
- Lee, C.S.L., Li, X.D., Zhang, G., Li, J., Ding, A.J., Wang, T., 2007. Heavy metals and Pb isotopic composition of aerosols in urban and suburban areas of Hong Kong and Guangzhou, South China-Evidence of the long-range transport of air contaminants. *Atmos. Environ.* 41 (2), 432-447.
- Lee, P.K., Yu, S., Chang, H.J., Cho, H.Y., Kang, M.J., Chae, B.G., 2016. Lead chromate detected as a source of atmospheric Pb and Cr (VI) pollution. *Sci. Rep.* 6, 36088.
- Lee, S.L., 2007. Study of atmospheric trace metals in particulate matter, dry and wet depositions, and mosses in the Pearl River Delta region, The Hong Kong Polytechnic University.
- Levin, R., Brown, M.J., Kashtock, M.E., Jacobs, D.E., Whelan, E.A., Rodman, J., Schock, M.R., Padilla, A., Sinks, T., 2008. Lead exposures in U.S. children, 2008: Implications for prevention. *Environ. Health Persp.* 116 (10), 1285-1293.
- Li, G., Sun, G.X., Ren, Y., Luo, X.S., Zhu, Y.G., 2018. Urban soil and human health: a review. *Eur. J. Soil Sci.* 69 (1), 196-215.
- Li, H., Ji, H., Shi, C., Gao, Y., Zhang, Y., Xu, X., Ding, H., Tang, L., Xing, Y., 2017. Distribution of heavy metals and metalloids in bulk and particle size fractions of soils from coal-mine brownfield and implications on human health. *Chemosphere* 172, 505-515.
- Li, H.B., Cui, X.Y., Li, K., Li, J., Juhasz, A.L., Ma, L.Q., 2014. Assessment of in vitro Lead bioaccessibility in house dust and its relationship to in vivo Lead relative bioavailability. *Environ. Sci. Technol.* 48 (15), 8548-8555.
- Li, J.H., Lu, Y., Shim, H., Deng, X.L., Lian, J., Jia, Z.L., Li, J.H., 2010. Use of the BCR sequential extraction procedure for the study of metal availability to plants. *J. Environ. Monit.* 12 (2), 466.

- Li, J.T., Qiu, J.W., Wang, X.W., Zhong, Y., Lan, C.Y., Shu, W.S., 2006. Cadmium contamination in orchard soils and fruit trees and its potential health risk in Guangzhou, China. *Environ. Pollut.* 143 (1), 159-165.
- Li, X.D., Poon, C.S., Liu, P.S., 2001. Heavy metal contamination of urban soils and street dusts in Hong Kong. *Appl. Geochem.* 16 (11), 1361-1368.
- Li, X.D., Lee, S.L., Wong, S.C., Shi, W.Z., Thornton, I., 2004. The study of metal contamination in urban soils of Hong Kong using a GIS-based approach. *Environ. Pollut.* 129 (1), 113-124.
- Li, Y., Duan, Z., Liu, G., Kalla, P., Scheidt, D., Cai, Y., 2015. Evaluation of the possible sources and controlling factors of toxic metals/metalloids in the Florida everglades and their potential risk of exposure. *Environ. Sci. Technol.* 49 (16), 9714-9723.
- Li, Y.G., Lu, Y.F., 2008. Lead isotopes as a tracer of tea Pb contamination in the west lake tea plantation. *Geophysical and Geochemical Exploration* 32 (2), 180-185. in Chinese.
- Liang, J., Feng, C., Zeng, G., Gao, X., Zhong, M., Li, X., Li, X., He, X., Fang, Y., 2017. Spatial distribution and source identification of heavy metals in surface soils in a typical coal mine city, Lianyuan, China. *Environ. Pollut.* 225, 681-690.
- Lincoln, J.D., Ogunseitan, O.A., Shapiro, A.A., Saphores, J.D.M., 2007. Leaching assessments of hazardous materials in cellular telephones. *Environ. Sci. Technol.* 41 (7), 2572-2578.
- Liu, J.G., Diamond, J., 2005. China's environment in a globalizing world. *Nature* 435 (7046), 1179.
- Liu, L., Guan, D.S., Peart, M.R., 2012. The morphological structure of leaves and the dust-retaining capability of afforested plants in urban Guangzhou, South China. *Environ. Sci. Pollut. R.* 19 (8), 3440-3449.
- Liu, L., Guan, D.S., Peart, M.R., Wang, G., Zhang, H., Li, Z.W., 2013. The dust retention capacities of urban vegetation—a case study of Guangzhou, South China. *Environ. Sci. Pollut. R.* 20 (9), 6601-6610.
- Liu, R., Wang, M.E., Chen, W.P., Peng, C., 2016. Spatial pattern of heavy metals accumulation risk in urban soils of Beijing and its influencing factors. *Environ. Pollut.* 210, 174-181.
- Ljung, K., Selinus, O., Otabbong, E., Berglund, M., 2006. Metal and arsenic distribution in soil particle sizes relevant to soil ingestion by children. *Appl. Geochem.* 21 (9), 1613-1624.
- Ljung, K., Oomen, A., Duits, M., Selinus, O., Berglund, M., 2007. Bioaccessibility of metals in urban playground soils. *J. Environ. Sci. Health., Part A* 42 (9), 1241-1250.

- Lu, S.G., Zheng, Y.W., Bai, S.Q., 2008. A HRTEM/EDX approach to identification of the source of dust particles on urban tree leaves. *Atmos. Environ.* 42 (26), 6431-6441.
- Lu, Y., Yin, W., Zhu, F., Zhang, G.L., 2010. The spatial distribution and sources of metals in urban soils of Guangzhou, China. 19th world congress of soil science, soil solutions for a changing world Brisbane, Australia.
- Lu, Y., Zhu, F., Chen, J., Gan, H.H., Guo, Y.B., 2007. Chemical fractionation of heavy metals in urban soils of Guangzhou, China. *Environ. Monit. Assess.* 134 (1-3), 429-439.
- Luo, X.S., Yu, S., Li, X.D., 2011. Distribution, availability, and sources of trace metals in different particle size fractions of urban soils in Hong Kong: Implications for assessing the risk to human health. *Environ. Pollut.* 159 (5), 1317-1326.
- Luo, X.S., Yu, S., Li, X.D., 2012a. The mobility, bioavailability, and human bioaccessibility of trace metals in urban soils of Hong Kong. *Appl. Geochem.* 27 (5), 995-1004.
- Luo, X.S., Yu, S., Zhu, Y.G., Li, X.D., 2012b. Trace metal contamination in urban soils of China. *Sci. Total Environ.* 421-422, 17-30.
- Luo, X.S., Ip, C.C.M., Li, W., Tao, S., Li, X.D., 2014. Spatial-temporal variations, sources, and transport of airborne inhalable metals (PM₁₀) in urban and rural areas of northern China. *Atmos. Chem. Phys. Discuss.* 14 (9), 13133-13165.
- Luo, X.S., Ding, J., Xu, B., Wang, Y.J., Li, H.B., Yu, S., 2012c. Incorporating bioaccessibility into human health risk assessments of heavy metals in urban park soils. *Sci. Total Environ.* 424, 88-96.
- Luo, X.S., Xue, Y., Wang, Y.L., Cang, L., Xu, B., Ding, J., 2015. Source identification and apportionment of heavy metals in urban soil profiles. *Chemosphere* 127, 152-157.
- Ma, Y.B., Lombi, E., Oliver, I.W., Nolan, A.L., McLaughlin, M.J., 2006. Long-term aging of Copper added to soils. *Environ. Sci. Technol.* 40 (20), 6310-6317.
- Madrid, F., Biasioli, M., Ajmone-Marsan, F., 2007. Availability and bioaccessibility of metals in fine particles of some urban soils. *Arch. Environ. Con. Tox.* 55 (1), 21-32.
- Madrid, L., Diaz-Barrientos, E., Ruiz-Cortes, E., Reinoso, R., Biasioli, M., Davidson, C.M., Duarte, A.C., Grčman, H., Hossack, I., Hursthouse, A.S., Kralj, T., Ljung, K., Otabbong, E., Rodrigues, S., Urquhart, G.J., Ajmone-Marsan, F., 2006. Variability in concentrations of potentially toxic elements in urban parks from six European cities. *J. Environ. Monit.* 8 (11), 1158-1165.

- Magge, H., Sprinz, P., Adams, W.G., Drainoni, M., Meyers, A., 2013. Zinc protoporphyrin and iron deficiency screening: Trends and therapeutic response in an urban pediatric center. *JAMA Pediatrics* 167 (4), 361-367.
- Manta, D.S., Angelone, M., Bellanca, A., Neri, R., Sprovieri, M., 2002. Heavy metals in urban soils: a case study from the city of Palermo (Sicily), Italy. *Sci. Total Environ.* 300 (1), 229-243.
- Martley, E., Gulson, B.L., Pfeifer, H.R., 2004. Metal concentrations in soils around the copper smelter and surrounding industrial complex of Port Kembla, NSW, Australia. *Sci. Total Environ.* 325 (1), 113-127.
- Martuzevicius, D., Kliucininkas, L., Prasauskas, T., Krugly, E., Kauneliene, V., Strandberg, B., 2011. Resuspension of particulate matter and PAHs from street dust. *Atmos. Environ.* 45 (2), 310-317.
- McIlwaine, R., Doherty, R., Cox, S.F., Cave, M., 2017. The relationship between historical development and potentially toxic element concentrations in urban soils. *Environ. Pollut.* 220, 1036-1049.
- Men, C., Liu, R., Xu, F., Wang, Q., Guo, L., Shen, Z., 2018. Pollution characteristics, risk assessment, and source apportionment of heavy metals in road dust in Beijing, China. *Sci. Total Environ.* 612, 138-147.
- Mendoza, C.J., Garrido, R.T., Quilodran, R.C., Segovia, C.M., Parada, A.J., 2017. Evaluation of the bioaccessible gastric and intestinal fractions of heavy metals in contaminated soils by means of a simple bioaccessibility extraction test. *Chemosphere* 176, 81-88.
- Mielke, H.W., Gonzales, C.R., Powell, E.T., 2017. Soil lead and children's blood lead disparities in pre- and post-hurricane Katrina New Orleans (USA). *Int J Environ Res Public Health* 14 (4).
- Miguel, E.D., Jiménez, d.G., M, Llamas, J.F., Martíndorado, A., Mazadiego, L.F., 1998. The overlooked contribution of compost application to the trace element load in the urban soil of Madrid (Spain). *Sci. Total Environ.* 215 (1-2), 113-122.
- Miner, D.K., 1993. Automotive hydraulic brake tube: the case for 90-10 copper-nickel tubing. SAE Technical Paper, Report No. SAE 931028.
- Ming, L.L., 2016. Fine atmospheric particles (PM_{2.5}) in large city clusters, China: Chemical compositions, temporal-spatial variations and regional transport, The Hong Kong Polytechnic University.

- MOHC, 2011. China health statistical year book in 2010. Peking union medical college press, Beijing. Ministry of Health, China.
- Mooi, E., Sarstedt, M., 2011. A concise guide to market research: The process, data, and methods using IBM SPSS statistics, Springer.
- Mossop, K.F., Davidson, C.M., 2003. Comparison of original and modified BCR sequential extraction procedures for the fractionation of copper, iron, lead, manganese and zinc in soils and sediments. *Anal. Chim. Acta.* 478 (1), 111-118.
- Nadal, M., Mari, M., Schuhmacher, M., Domingo, J.L., 2009. Multi-compartmental environmental surveillance of a petrochemical area: Levels of micropollutants. *Environ. Int.* 35 (2), 227-235.
- Nie, X.Q., 2012. Analysis on the relationship between industrial structure evolution and environmental quality of Guangzhou. Dissertation of academic degree of Jinan University
- Notten, M.J.M., Walraven, N., Beets, C.J., Vroon, P., Rozema, J., Aerts, R., 2008. Investigating the origin of Pb pollution in a terrestrial soil–plant–snail food chain by means of Pb isotope ratios. *Appl. Geochem.* 23 (6), 1581-1593.
- Nriagu, J.O., Pacyna, J.M., 1988. Quantitative assessment of worldwide contamination of air, water and soils by trace metals. *Nature* 333 (6169), 134-139.
- Oliva, S.R., Espinosa, A.J.F., 2007. Monitoring of heavy metals in topsoils, atmospheric particles and plant leaves to identify possible contamination sources. *Microchem. J.* 86 (1), 131-139.
- Ordóñez, A., Álvarez, R., De Miguel, E., Charlesworth, S., 2015. Spatial and temporal variations of trace element distribution in soils and street dust of an industrial town in NW Spain: 15years of study. *Sci. Total Environ.* 524-525, 93-103.
- Pan, L.B., Ma, J., Wang, X.L., Hou, H., 2016. Heavy metals in soils from a typical county in Shanxi Province, China: Levels, sources and spatial distribution. *Chemosphere* 148, 248-254.
- Pan, S., Lin, L., Zeng, F., Zhang, J., Dong, G., Yang, B., Jing, Y., Chen, S., Zhang, G., Yu, Z., Sheng, G., Ma, H., 2017. Effects of lead, cadmium, arsenic, and mercury co-exposure on children's intelligence quotient in an industrialized area of southern China. *Environ. Pollut.* 235, 47-54.
- Parra, S., Bravo, M.A., Quiroz, W., Moreno, T., Karanasiou, A., Font, O., Vidal, V., Cereceda, F., 2014. Distribution of trace elements in particle size fractions for contaminated soils by a

- copper smelting from different zones of the Puchuncaví Valley (Chile). *Chemosphere* 111, 513-521.
- Pelfrêne, A., Waterlot, C., Douay, F., 2013. Influence of land use on human bioaccessibility of metals in smelter-impacted soils. *Environ. Pollut.* 178, 80-88.
- Poggio, L., Vrščaj, B., Hepperle, E., Schulin, R., Marsan, F.A., 2008. Introducing a method of human health risk evaluation for planning and soil quality management of heavy metal-polluted soils—An example from Grugliasco (Italy). *Landscape Urban Plan.* 88 (2-4), 64-72.
- Poggio, L., Vrščaj, B., Schulin, R., Hepperle, E., Ajmone Marsan, F., 2009. Metals pollution and human bioaccessibility of topsoils in Grugliasco (Italy). *Environ. Pollut.* 157 (2), 680-689.
- Pueyo, M., Mateu, J., Rigol, A., Vidal, M., López-Sánchez, J.F., Rauret, G., 2008. Use of the modified BCR three-step sequential extraction procedure for the study of trace element dynamics in contaminated soils. *Environ. Pollut.* 152 (2), 330-341.
- Qin, J.H., Nworie, O.E., Lin, C.X., 2016. Particle size effects on bioaccessible amounts of ingestible soil-borne toxic elements. *Chemosphere* 159, 442-448.
- Qiu, Y., Guan, D.S., Song, W.W., Huang, K.Y., 2009. Capture of heavy metals and sulfur by foliar dust in urban Huizhou, Guangdong Province, China. *Chemosphere* 75 (4), 447-452.
- Ram, S.S., Kumar, R.V., Chaudhuri, P., Chanda, S., Santra, S.C., Sudarshan, M., Chakraborty, A., 2014. Physico-chemical characterization of street dust and re-suspended dust on plant canopies: An approach for finger printing the urban environment. *Ecol. Indic.* 36, 334-338.
- Ram, S.S., Majumder, S., Chaudhuri, P., Chanda, S., Santra, S.C., Chakraborty, A., Sudarshan, M., 2015. A review on air pollution monitoring and management using plants with special reference to foliar dust adsorption and physiological stress responses. *Crit. Rev. Env. Sci. Tec.* 45 (23), 2489-2522.
- Rasmussen, P.E., Beauchemin, S., Chénier, M., Levesque, C., MacLean, L.C.W., Marro, L., Jones-Otazo, H., Petrovic, S., McDonald, L.T., Gardner, H.D., 2011. Canadian house dust study: Lead bioaccessibility and speciation. *Environ. Sci. Technol.* 45 (11), 4959-4965.
- Reimann, C., Caritat, P.d., 2000. Intrinsic flaws of element enrichment factors (EFs) in environmental geochemistry. *Environ. Sci. Technol.* 34 (24), 5084-5091.

- Robertson, G.P., Klingensmith, K.M., Klug, M.J., Paul, E.A., Crum, J.R., Ellis, B.G., 1997. Soil resources, microbial activity, and primary production across an agricultural ecosystem. *Ecol. Appl.* 7 (1), 158-170.
- Rodríguez Martín, J.A., Arias, M.L., Grau Corbí, J.M., 2006. Heavy metals contents in agricultural topsoils in the Ebro basin (Spain). Application of the multivariate geostatistical methods to study spatial variations. *Environ. Pollut.* 144 (3), 1001-1012.
- Rodriguez-Barranco, M., Lacasana, M., Aguilar-Garduno, C., Alguacil, J., Gil, F., Gonzalez-Alzaga, B., Rojas-Garcia, A., 2013. Association of arsenic, cadmium and manganese exposure with neurodevelopment and behavioural disorders in children: a systematic review and meta-analysis. *Sci. Total Environ.* 454-455, 562-577.
- Rogge, W.F., Hildemann, L.M., Mazurek, M.A., Cass, G.R., Simoneit, B.R., 1993. Sources of fine organic aerosol. 3. Road dust, tire debris, and organometallic brake lining dust: roads as sources and sinks. *Environ. Sci. Technol.* 27 (9), 1892-1904.
- Root, R.A., 2000. Lead loading of urban streets by motor vehicle wheel weights. *Environ. Health Persp.* 108 (10), 937-940.
- Ruby, M.V., Lowney, Y.W., 2012. Selective soil particle adherence to hands: implications for understanding oral exposure to soil contaminants. *Environ. Sci. Technol.* 46 (23), 12759-12771.
- Ruby, M.V., Davis, A., Schoof, R., Eberle, S., Sellstone, C.M., 1996. Estimation of lead and arsenic bioavailability using a physiologically based extraction test. *Environ. Sci. Technol.* 30 (2), 422-430.
- Ruby, M.V., Schoof, R., Brattin, W., Goldade, M., Post, G., Harnois, M., Mosby, D.E., Casteel, S.W., Berti, W., Carpenter, M., 1999. Advances in evaluating the oral bioavailability of inorganics in soil for use in human health risk assessment. *Environ. Sci. Technol.* 33 (21), 3697-3705.
- Sahu, R., Elumalai, S.P., 2017. Identifying speed hump, a traffic calming device, as a hotspot for environmental contamination in traffic-affected urban roads. *ACS Omega* 2 (9), 5434-5444.
- Sawidis, T., Breuste, J., Mitrovic, M., Pavlovic, P., Tsigaridas, K., 2011. Trees as bioindicator of heavy metal pollution in three European cities. *Environ. Pollut.* 159 (12), 3560-3570.
- Schauer, J.J., Lough, G.C., Shafer, M.M., Christensen, W.F., Arndt, M.F., DeMinter, J.T., Park, J.-S., 2006. Characterization of metals emitted from motor vehicles. Research report (Health Effects Institute) (133), 1-76.

- Schreck, E., Foucault, Y., Sarret, G., Sobanska, S., Cécillon, L., Castrec-Rouelle, M., Uzu, G., Dumat, C., 2012. Metal and metalloid foliar uptake by various plant species exposed to atmospheric industrial fallout: Mechanisms involved for lead. *Sci. Total Environ.* 427-428, 253-262.
- Sgrigna, G., Sæbø, A., Gawronski, S., Popek, R., Calfapietra, C., 2015. Particulate matter deposition on *Quercus ilex* leaves in an industrial city of central Italy. *Environ. Pollut.* 197, 187-194.
- Shah, S.D., Cocker, D.R., Miller, J.W., Norbeck, J.M., 2004. Emission rates of particulate matter and elemental and organic carbon from in-use diesel engines. *Environ. Sci. Technol.* 38 (9), 2544-2550.
- Shahid, M., Dumat, C., Khalid, S., Schreck, E., Xiong, T., Niazi, N.K., 2017. Foliar heavy metal uptake, toxicity and detoxification in plants: A comparison of foliar and root metal uptake. *J. Hazard. Mater.* 325, 36-58.
- Shetaya, W.H., Marzouk, E.R., Mohamed, E.F., Elkassas, M., Bailey, E.H., Young, S.D., 2018. Lead in Egyptian soils: Origin, reactivity and bioavailability measured by stable isotope dilution. *Sci. Total Environ.* 618, 460-468.
- Shi, G.T., Chen, Z.L., Xu, S.Y., Zhang, J., Wang, L., Bi, C.J., Teng, J.Y., 2008. Potentially toxic metal contamination of urban soils and roadside dust in Shanghai, China. *Environ. Pollut.* 156 (2), 251-260.
- Siciliano, S.D., James, K., Zhang, G., Schafer, A.N., Peak, J.D., 2009. Adhesion and enrichment of metals on human hands from contaminated soil at an arctic urban brownfield. *Environ. Sci. Technol.* 43 (16), 6385-6390.
- Simon, E., Baranyai, E., Braun, M., Cserhádi, C., Fábíán, I., Tóthmérész, B., 2014. Elemental concentrations in deposited dust on leaves along an urbanization gradient. *Sci. Total Environ.* 490, 514-520.
- Smith, E., Kempson, I.M., Juhasz, A.L., Weber, J., Rofe, A., Gancarz, D., Naidu, R., McLaren, R.G., Gräfe, M., 2011. In Vivo–in Vitro and XANES spectroscopy assessments of Lead bioavailability in contaminated periurban soils. *Environ. Sci. Technol.* 45 (14), 6145-6152.
- Song, Y.S., Maher, B.A., Li, F., Wang, X.K., Sun, X., Zhang, H.X., 2015. Particulate matter deposited on leaf of five evergreen species in Beijing, China: Source identification and size distribution. *Atmos. Environ.* 105, 53-60.
- Sparks, D.L., 2003. *Environmental soil chemistry*, Academic press.

- Sutherland, R.A., Tack, F.M.G., Ziegler, A.D., 2012. Road-deposited sediments in an urban environment: A first look at sequentially extracted element loads in grain size fractions. *J. Hazard. Mater.* 225-226, 54-62.
- Tanner, P.A., Ma, H.L., Yu, P.K.N., 2008. Fingerprinting metals in urban street dust of Beijing, Shanghai, and Hong Kong. *Environ. Sci. Technol.* 42 (19), 7111-7117.
- Tanushree, B., Chakraborty, S., Bhumika, F., Piyal, B., 2011. Heavy metal concentrations in street and leaf deposited dust in Anand city, India. *Res. J. Chem. Sci.* 1 (5), 61-66.
- The Ministry of Environmental Protection, 2014. The ministry of land and resources report on the national soil contamination survey.
- Thompson, R.N., Nau, C.A., Lawrence, C.H., 1966. Identification of vehicle tire rubber in roadway dust. *Am. Ind. Hyg. Assoc. J.* 27 (6), 488-495.
- Thurston, G.D., Spengler, J.D., 1985. A quantitative assessment of source contributions to inhalable particulate matter pollution in metropolitan Boston. *Atmos. Environ.* 19 (1), 9-25.
- Thurston, G.D., Ito, K., Lall, R., 2011. A source apportionment of U.S. fine particulate matter air pollution. *Atmos. Environ.* 45 (24), 3924-3936.
- Tomašević, M., Vukmirović, Z., Rajšić, S., Tasić, M., Stevanović, B., 2005. Characterization of trace metal particles deposited on some deciduous tree leaves in an urban area. *Chemosphere* 61 (6), 753-760.
- Turer, D., Maynard, J.B., Sansalone, J.J., 2001. Heavy metal contamination in soils of urban highways comparison between runoff and soil concentrations at Cincinnati, Ohio. *Water Air Soil Poll.* 132 (3-4), 293-314.
- Turner, A., Ip, K.-H., 2007. Bioaccessibility of metals in dust from the indoor environment: Application of a physiologically based extraction test. *Environ. Sci. Technol.* 41 (22), 7851-7856.
- United Nations, 2014. World urbanization prospects: the 2014 revision, United Nations New York.
- Ure, A.M., Quevauviller, P.H., Muntau, H., Griepink, B., 1993. Speciation of heavy metals in soils and sediments. An account of the improvement and harmonization of extraction techniques undertaken under the auspices of the BCR of the Commission of the European Communities. *Int. J. Environ. An. Ch.* 51 (1-4), 135-151.
- USDOE, 2011. The risk assessment information system (RAIS). U.S. department of energy's Oak Ridge operations office (ORO).

- USEPA, 1989. Human health evaluation manual, risk assessment guidance for superfund, vol. I, office of soil waste and emergency response. EPA/540/1-89/002.
- USEPA, 1996. Soil screening guidance: technical background document, office of soil waste and emergency response. EPA/540/R-95/128.
- USEPA, 2011. Screening Levels (RSL) for chemical contaminants at superfund sites. U.S. Environmental Protection Agency.
- Vermette, S.J., Irvine, K.N., Drake, J.J., 1991. Temporal variability of the elemental composition in urban street dust. *Environ. Monit. Assess.* 18 (1), 69-77.
- VROM, 2000. Dutch target and intervention values, Dutch Ministry of Housing, Spatial Planning and Environment.
- Wackernagel, H., 2003. *Multivariate geostatistics*, Springer Science & Business Media.
- Walraven, N., Van Os, B.J.H., Klaver, G.T., Middelburg, J.J., Davies, G.R., 2014. The lead (Pb) isotope signature, behaviour and fate of traffic-related lead pollution in roadside soils in The Netherlands. *Sci. Total Environ.* 472, 888-900.
- Wang, C., Yang, Z., Zhong, C., Ji, J., 2016a. Temporal-spatial variation and source apportionment of soil heavy metals in the representative river-alluviation depositional system. *Environ. Pollut.* 216, 18-26.
- Wang, J., Li, S., Cui, X., Li, H., Qian, X., Wang, C., Sun, Y., 2016b. Bioaccessibility, sources and health risk assessment of trace metals in urban park dust in Nanjing, Southeast China. *Ecotoxicol. Environ. Saf.* 128, 161-170.
- Wang, Y., Luo, H., 1992. *The backgrounds of soil environment in Shanghai*. China Environmental Science Press, Beijing.
- Wei, B.G., Yang, L.S., 2010. A review of heavy metal contaminations in urban soils, urban road dusts and agricultural soils from China. *Microchem. J.* 94 (2), 99-107.
- Wei, B.G., Jiang, F.Q., Li, X.M., Mu, S.Y., 2009. Spatial distribution and contamination assessment of heavy metals in urban road dusts from Urumqi, NW China. *Microchem. J.* 93 (2), 147-152.
- Werkenthin, M., Kluge, B., Wessolek, G., 2014. Metals in European roadside soils and soil solution – A review. *Environ. Pollut.* 189, 98-110.
- Wijaya, A.R., Ouchi, A.K., Tanaka, K., Shinjo, R., Ohde, S., 2012. Metal contents and Pb isotopes in road-side dust and sediment of Japan. *J. Geochem. Explor.* 118, 68-76.

- Wiseman, C.L.S., Zereini, F., Püttmann, W., 2015. Metal and metalloid accumulation in cultivated urban soils: A medium-term study of trends in Toronto, Canada. *Sci. Total Environ.* 538, 564-572.
- Wong, C.S.C., Li, X.D., 2004. Pb contamination and isotopic composition of urban soils in Hong Kong. *Sci. Total Environ.* 319 (1-3), 185-195.
- Wong, C.S.C., Li, X., Thornton, I., 2006. Urban environmental geochemistry of trace metals. *Environ. Pollut.* 142 (1), 1-16.
- Wong, C.S.C., Li, X.D., Zhang, G., Qi, S.H., Peng, X.Z., 2003. Atmospheric deposition of heavy metals in the Pearl River Delta, China. *Atmos. Environ.* 37 (6), 767-776.
- Wong, F.M., 1975. Industrialization and family structure in Hong Kong. *J. Marriage Fam.* 37 (4), 985-1000.
- Wong, J.W.C., Mak, N.K., 1997. Heavy metal pollution in children playgrounds in Hong Kong and its health implications. *Environ. Technol.* 18 (1), 109-115.
- Wragg, J., Cave, M.R., 2003. In-vitro methods for the measurement of the oral bioaccessibility of selected metals and metalloids in soils: A critical review. Bristol: Environment Agency.
- Wuana, R.A., Okieimen, F.E., 2011. Heavy metals in contaminated soils: a review of sources, chemistry, risks and best available strategies for remediation. *ISRN Ecology* 2011, 1-20.
- Xu, X., Li, Y., Wang, Y., Wang, Y., 2011. Assessment of toxic interactions of heavy metals in multi-component mixtures using sea urchin embryo-larval bioassay. *Toxicol. in Vitro* 25 (1), 294-300.
- Yamamoto, N., Takahashi, Y., Yoshinaga, J., Tanaka, A., Shibata, Y., 2006. Size distributions of soil particles adhered to children's hands. *Arch. Environ. Con. Tox.* 51 (2), 157-163.
- Yang, C., 2004. From market-led to institution-based economic integration: the case of the Pearl River Delta and Hong Kong. *Issue & Studies* 40 (2), 79.
- Yang, Y., Christakos, G., Guo, M., Xiao, L., Huang, W., 2017. Space-time quantitative source apportionment of soil heavy metal concentration increments. *Environ. Pollut.* 223, 560-566.
- Young, T.M., Heeraman, D.A., Sirin, G., Ashbaugh, L.L., 2002. Resuspension of soil as a source of airborne lead near industrial facilities and highways. *Environ. Sci. Technol.* 36 (11), 2484-2490.

- Yu, Y., Li, Y.X., Li, B., Shen, Z.Y., Stenstrom, M.K., 2016. Metal enrichment and lead isotope analysis for source apportionment in the urban dust and rural surface soil. *Environ. Pollut.* 216, 764-772.
- Zahran, S., Laidlaw, M.A.S., McElmurry, S.P., Filippelli, G.M., Taylor, M., 2013. Linking source and effect: Resuspended soil lead, air lead, and children's blood lead levels in Detroit, Michigan. *Environ. Sci. Technol.* 47 (6), 2839-2845.
- Zhang, H., Wang, Z., Zhang, Y., Ding, M., Li, L., 2015. Identification of traffic-related metals and the effects of different environments on their enrichment in roadside soils along the Qinghai-Tibet highway. *Sci. Total Environ.* 521-522, 160-172.
- Zhang, H.B., Luo, Y.M., Wong, M.H., Zhao, Q.G., Zhang, G.L., 2007. Defining the geochemical baseline: a case of Hong Kong soils. *Environ. Geol.* 52 (5), 843-851.
- Zhang, W., 2002. SPSS11 statistical analysis (Advanced), Beijing: Hope Electronic Press.
- Zhao, F.J., Ma, Y.B., Zhu, Y.G., Tang, Z., McGrath, S.P., 2015a. Soil contamination in China: Current status and mitigation strategies. *Environ. Sci. Technol.* 49 (2), 750-759.
- Zhao, Z.Q., Zhang, W., Li, X.D., Yang, Z., Zheng, H.Y., Ding, H., Wang, Q.L., Xiao, J., Fu, P.Q., 2015b. Atmospheric lead in urban Guiyang, Southwest China: Isotopic source signatures. *Atmos. Environ.* 115, 163-169.
- Zheng, J., Tan, M., Shibata, Y., Tanaka, A., Li, Y., Zhang, G., Zhang, Y., Shan, Z., 2004. Characteristics of lead isotope ratios and elemental concentrations in PM₁₀ fraction of airborne particulate matter in Shanghai after the phase-out of leaded gasoline. *Atmos. Environ.* 38 (8), 1191-1200.
- Zheng, J.Y., Zhang, L.J., Che, W.W., Zheng, Z.Y., Yin, S.S., 2009. A highly resolved temporal and spatial air pollutant emission inventory for the Pearl River Delta region, China and its uncertainty assessment. *Atmos. Environ.* 43 (32), 5112-5122.
- Zheng, Y.M., Gao, Q.Z., Wen, X.H., Yang, M., Chen, H.D., Wu, Z.Q., Lin, X.H., 2013. Multivariate statistical analysis of heavy metals in foliage dust near pedestrian bridges in Guangzhou, South China in 2009. *Environ. Earth Sci.* 70 (1), 107-113.
- Zhu, B.Q., Chen, Y.W., Peng, J.H., 2001. Lead isotope geochemistry of the urban environment in the Pearl River Delta. *Appl. Geochem.* 16 (4), 409-417.
- Zurbrick, C.M., Gallon, C., Flegal, A.R., 2017. Historic and industrial lead within the Northwest Pacific Ocean evidenced by lead isotopes in seawater. *Environ. Sci. Technol.* 51 (3), 1203-1212.

Publications from the Research Project

Si-Yuan Liang, Jin-Li Cui, Xiang-Yang Bi, Xiao-San Luo, Xiang-Dong Li. Deciphering source contributions of trace metal contamination in urban soil, road dust, and foliar dust in Guangzhou, southern China. Submitted to *Science of the Total Environment* (under second round review).

Si-Yuan Liang, Jin-Li Cui, Xiang-Yang Bi, Xiang-Dong Li. Distribution, speciation, and bioaccessibility of trace metals in soil dust as a function of particle size. To be submitted.

Bi, X.Y., Liang, S.Y., Li, X.D., 2013. Trace metals in soil, dust, and tree leaves of the urban environment, Guangzhou, China. *Chin. Sci. Bull.* 58 (2), 222-230.

Bi, X.Y., Liang, S.Y., Li, X.D., 2013. A novel in situ method for sampling urban soil dust: Particle size distribution, trace metal concentrations, and stable lead isotopes. *Environ. Pollut.* 177, 48-57.

Database of Original Results from All Experiments in the Study

Raw data from this study has been provided in the CD, which includes all the results from every experiment involved in the thesis. The sampling information, GIS modeling results and cross validation results were also provided in the CD as appendix.